Innovation Report:
A Methodology for Estimating Gear Pump Wear-out Reliability Using Pump Pressure Ripple and an Extremely Small Sample Size - The Case Study of a Heavy-Duty Diesel Engine Lubrication Gear Pump

By
Edmund Zarzycki

A thesis submitted in partial fulfilment of the requirements for the degree of
Doctor of Engineering (International)

University of Warwick, Warwick Manufacturing Group
April 2020

Contents

List of Figures

List of Tables

Abbreviations

ADT	Accelerated Degradation Testing
ALT	Accelerated Life Testing
ANOVA	Analysis of Variance
ARMA	Autoregressive Moving Average
AMSAA	Army Material Systems Analysis Activity
BU	Bayesian updating
BM	Brownian Motion
BS	British Standards
CAB	ConcentricAB
CAE	Computer Aided Engineering
CBM	Condition Based Maintenance
Det05	Detailed Coefficient 5
DfR	Design for Reliability
DWT	Discrete Wavelet Transform
EMD	Empirical Mode Decomposition
ETC	European Transient Cycle
FTA	Fault Tree Analysis
FFT	Fast Fourier Transform
FTP	Federal Test Procedure
HAST	Highly Accelerated Stress Testing
HDE	Heavy Duty Engine
IEPE	Integrated Electronics Piezo-Electric
ISO	International Standards Organisation
MC	Monte Carlo
MLE	Maximum Likelihood Estimation
MODWT	Maximal Overlap Discrete Wavelet Transform
MOFT	Minimum Oil Film Thickness
NPD	New Product Development
OB	Objective Bayes
OE	Overall Efficiency
OEM	Original Equipment Manufacturer
PDF	Probability Distribution Function
P-F	Potential point of failure to Failure
PFT	Pseudo Failure Time
PHM	Prognostics and Health Management
PoF	Physics of Failure
Q	Flow
RCM	Reliability Centred Maintenance
RDE	Real Driving Emissions
RGP	Reliability Growth Plot
RGT	Reliability Growth Testing
RUL	Remaining Useful Life
SE	Standard Error
SOAP	Spectrometric Oil Analysis Procedure
SSADT	Step-stress Accelerated Degradation Test
T	Torque

UNECE	United Nations Economic Commission for Europe
WHTC	World Harmonised Transient Cycle

Notation

Q	Flow rate [m³/s]
Q_r	Flow rate [m³/rev]
D_o	Pumping gear outer diameter [m]
C_d	Pumping gear pair centre distance [m]
L	Pumping gear length [m]
R_0	Initial reliability
e_i	Random variation at observation i
y_i	Degradation at observation i
a_0	Initial performance
b_i	Degradation rate
C	Degradation threshold
t	Time [h], [s]
$\boldsymbol{\theta}$	Set of parameters
μ	Drift coefficient [Hz/h]
σ	Diffusion coefficient [Hz/h]
CI	Confidence Interval accuracy
α	Confidence Interval
$\hat{\sigma}_d$	Standard deviation of paired sample values
n_d	Number of pairs samples
$t_{\alpha,\nu}$	One tailed critical t value
ν	Degrees of freedom
d_j	Delta of values $x_{1,j}$ and $x_{2,j}$
$x_{1,j}$	j^{th} value of dataset 1
$x_{2,j}$	j^{th} valve of dataset 2
$\phi_w(x)$	Distribution of x wear particles from wear source w
q	Internal recirculation flow [m³/rev]
V	Volume of the sump [m³]
λ	Minimum oil film thickness to RMS surface finish ratio
P_j	Pump outlet pressure at stress level j [Pa]
A	Cost for sample hardware
B	Cost rate for testing
T	Total test time per sample
TC	Total Cost
$X(t)$	Time series data
ζ	Damping coefficient
w_n	Natural frequency [Hz]
$Z(t)$	Forcing function, white noise [s]
$Y(t)$	Degradation in performance [Hz]
y_0	Initial value of the performance [Hz]
$B(t)$	Brownian motion
Δy	Increment in degradation [Hz]

$\phi(\cdot)$	Probability density function
$\Phi(\cdot)$	Cumulative distribution function
k	Final step-stress level
$\Delta\bar{Y}_j$	Sample mean, increment in degradation at stress level *j*
S_j^2	Sample variance at stress level *j*
$\pi_j{}^{(0)}$	Prior distribution at stress level *j*
$\pi_j{}^{(1)}$	Posterior distribution at stress level *j*
L	Likelihood
m	Final observation
q	Observation
Γ^{-1}	Inverse-Gamma distribution
χ^2	Chi-squared distribution
$\mathcal{N}$	Normal distribution
$\beta_j^{(0)}$	Inverse gamma prior distribution shape parameter stress level *j*
$\beta_j^{(1)}$	Inverse gamma posterior distribution shape parameter stress level *j*
$\alpha_j^{(0)}$	Inverse gamma prior distribution scale parameter stress level *j*
$\alpha_j^{(1)}$	Inverse gamma posterior distribution scale parameter stress level *j*
$a_j^{(0)}$	Normal prior distribution location parameter stress level *j*
$a_j^{(1)}$	Normal posterior distribution location parameter stress level *j*
$\lambda_j^{(0)}$	Normal prior distribution scale parameter stress level *j*
$\lambda_j^{(1)}$	Normal posterior distribution scale parameter stress level *j*
$\varepsilon_{P_j \sim P_{j+1}}$	Accelerated stress coefficient
$\hat{y}_{\mu_j}$	Estimate of functional relationship, drift coefficient to stress level *j*
$\hat{y}_{\sigma_j^2}$	Estimate of functional relationship, coefficient to stress level *j*
a	Real number
ε_t	White noise error term
b	Complex number
d	Detailed coefficient
$\widetilde{D}_j$	MODWT detail coefficient
f	Frequency Fourier Transform
$g_{j,l}$	DWT scaling filter
$\widetilde{g}_{j,l}$	MODWT scaling filter
$h_{j,l}$	DWT wavelet filter
$\widetilde{h}_{j,l}$	MODWT wavelet filter
k	Scale parameter
m	Translation parameter
p	Order of the AR polynomial
q	Order of the MA polynomial
$\widetilde{S}_J$	MODWT approximation coefficient
s	Scale
t'	Time interval [s]

$\tilde{V}_{j,t}$	MODWT wavelet coefficient of level *j*
W	Continuous Wavelet Transform
$\tilde{W}_{j,t}$	MODWT wavelet coefficient of level *j*
$w(t)$	Windowing function
$x(t)$	Signal in the time domain
$X(f)$	Signal in frequency domain
$\psi(t)$	Mother wavelet
ϕ_i	Parameter of the AR model
σ_a	White noise variance
θ_j	Parameter of the MA model
*	Complex conjugate

Acknowledgements

This work would not have been possible without the funding of ConcentricAB, EPSRC and WMG to whom I am indebted. I would like to express my gratitude to my academic supervisors Dr Jane Marshall and Dr Jeffery Jones for their guidance. I am thankful to David Williams who offered me the opportunity to complete this research at ConcentricAB and to Paul Shepherd who continued the support through the project after David moved to pastures new. Finally, I appreciate the unwavering support of my family who kept me balanced and motivated.

Declaration

I, Edmund Zarzycki, declare that this partial fulfilment for the degree of Engineering Doctorate (International) titled, '*Innovation report: A Methodology for Estimating Gear Pump Wear-out Reliability Using Pump Pressure Ripple and an Extremely Small Sample Size - The Case Study of a Heavy-Duty Diesel Engine Lubrication Gear Pump*' and the work presented in it are my own.

I confirm that:

- This work was done wholly or mainly while in candidature for a research degree at this University.
- Where any part of this thesis has previously been submitted for a degree or any other qualification at this University or any other institution, this has been clearly stated.
- Where I have consulted the published work of others, this is always clearly attributed.
- Where I have quoted from the work of others, the source is always given. With the exception of such quotations, this thesis is entirely my own work.
- I have acknowledged all main sources of help.
- Where the thesis is based on work done by myself jointly with others, I have made clear exactly what was done by others and what I have contributed myself.

Signed: Ed Zarzycki

Date: 19th April 2019

To my wife Jude for her incredible patience, love and support.
And to my sons Daniel and Joseph with whom I will make up for lost time.

Abstract

Design for Reliability (DfR) encourages testing products early in the New Product Development (NPD) process to identify and resolve weaknesses quickly. An organisation can then track reliability growth and intervene to ensure the changes in product robustness are in line with a timely release to market. However, for products with long life spans (such as a Heavy-Duty engine (HDE) lubrication gear pump), the evaluation of reliability with an extremely small number of prototype samples is problematic. Budget constraints, product size, and test facilities can limit the possibilities of accurately assessing the initial reliability forming a test planning paradox. The research in this thesis proposes an innovate methodology to minimise this test planning paradox, specific to a gear pump.

The method uses step-stress accelerated degradation testing and Bayesian inference to estimate degradation parameters using only a sample size of two. Post-testing, numerical simulation is used to build a degradation model with larger sample sizes and produce a survival distribution at the quantile of interest. Increasing pump outlet pressure above normal usage accelerates the pump wear and pressure ripple measurements are used to monitor the performance degradation. On inspection, the pumps exhibit erosion on the housing and micro pitting of the gear flanks. The innovative use of a Maximal Overlap Discrete Wavelet Transforms (MODWT) with an Autoregressive Moving Average (ARMA 2,1) extracts a feature from the pressure ripple that provides a stochastic, linear and non-monotone degradation path that is appropriately modelled using a Brownian Motion simulation model. Regression analysis provides a drift and diffusion covariate functional relationship to pump outlet pressure. Given the stress-varying environment of an HDE, Monte Carlo simulations overcome the complexity of replicating vehicle drive cycle and produces a credible reliability estimate validated against a similarly designed high mileage pump.

The application of this original methodology offers the opportunity to minimise the test planning paradox and satisfies populating the reliability growth chart. It is foreseen the method can be adopted for a wide range of positive displacement pumps where is it possible to measure pressure ripple.

Preface

The structure of the Engineering Doctorate (International) (EngD) is a portfolio based research programme combined with taught modules and experience in an industrial setting overseas. The goal of the programme is the application of innovation used in an industry setting and the demonstration of knowledge considering the business context. The taught modules build varied competencies in an engineering business ranging from financial analysis and control to understanding strategic human resource. The development of competencies and learning outcomes are set out in a personal profile.

Portfolio Research Methodology

In terms of the research methodology and portfolio structure, the EngD is a series of theses that can be read in their own right; however, it is recommended they are read chronologically to appreciate the narrative. The theses cover the progression of the problems faced at the sponsoring company ConcentricAB Pumps Limited (CAB) (see Section 1.3) and identifying a gap in knowledge, to the development of an innovative solution that contributes to filling this gap. The Innovation Report is tasked with succinct dissemination of this new knowledge to the public domain, whereas the content of the submissions is not publicised.

The problem formation and identification of a gap in knowledge were specifically focused on the accelerated testing of pumps. The methodology was of experimental design and each submission held literature reviews using secondary source peer-reviewed journals, conference proceedings, standards, books and the internet. Regarding the case study, the lubrication gear pump was chosen based on a live NPD project. The idea was that a real situation and problem would sharpen the research output to be of value to CAB and the wider community. The primary gap in knowledge was identified in how to estimate product reliability at the earliest stage of NPD using extremely small sample sizes and little or no prior knowledge, especially for commercial HDE lubrication gear pumps. The gap has a wider reach to all positive displacement pumps. The personal motivation was to bring value to the project and ensure it was state-of-the-art and robust enough to set a new path in how CAB approaches validation and reliability.

Thesis Structure

In this report, the methodology for evaluating the reliability of a gear pump expediently assists in decision making which is necessary to satisfy the pressures in industry when developing a new product. The EngD project has progressed from little knowledge, experience and application of accelerated testing, to developing a methodology that is up-to-date and has the longevity to build a core competence and appease the strategic thinking of the business.

The Innovation Report structure follows a traditional experimental methodology in the sense there is an introduction, background, methodology, results and analysis, discussion and conclusions. The introduction sets the motivation of the research which is a classical reliability problem of budget and resource constraints that had not received a great deal of attention until the last decade. There are three main scenarios (or combination of scenarios) for an organisation to contend with; (1) products that are relatively expensive to prototype and therefore justifying a reasonable sample size for testing to destruction is difficult. (2) The products that are relatively cheap but struggle to justify the payback to address the question of estimating reliability, and (3) the products that required substantial test space and multiple test rigs to satisfy the statistical validity, which also requires a significant justifiable budget. With the motivation set, the introduction briefly states the structure of the EngD programme, summarises the portfolio structure and the innovation.

In Chapter 2 the background to the application and case study is reviewed and summarised in tables. The case study is of a NPD of a lubrication gear pump for a heavy-duty diesel engine, but it does not divulge any sensitive details. The studies of gear pump wear mechanisms, the detection of wear, the mission profiles and the degradation models available are reviewed before progressing to the innovative methodology that has been developed.

In Chapter 3 the methodology for estimating gear pump reliability can be followed and repeated by the reader which is where the value lies academically. It is foreseen the full method could be applied to hydraulic gear pumps and other positive displacement pumps with adjustment on the physics of failure. In this methodology, the industrial pump experience of the author recognises the value of simplicity. The test plan optimisation is a topic reviewed; however, these methods have pre-requisite of historical data which in part is the crux of the problem. If the data is not available to begin with, then there is no opportunity for optimisation.

In Chapter 4, the experimental results are presented. The test pumps are disassembled to confer that a realistic failure mechanism was produced. The test data was then analysed to output parameter estimates that fit into a simulation. The simulation then outputs the reliability estimate. The results discussed in Chapter 5 are critical of the methodology to show known and unknown weaknesses in the method and to reveal if the EngD research question has been answered and with what level of confidence. Chapter 6 concludes the analysis and research outcomes, and if the objectives have been met. Lastly, the limitations and recommendations to improve and increase the robustness of the methodology are given.

Chapter 1: Introduction

Through this chapter, the reader is introduced to the motivation behind the main research question. The problem identification is rooted in the fundamental reliability problem of how to increase product robustness and observe reliability growth using the most efficient and effective processes. The sponsoring company ConcentricAB Pumps Limited (CAB) (see section 1.3) are strategically motivated to trial better methods and best practices to gain a competitive advantage and thus, initiated a reliability project. A gap analysis in their product development process indicated their need to develop a test methodology to estimate reliability rather than relying on warranty data or demonstration testing (which coincidentally yields little value). As the project progressed it became apparent there was a need to solve a classical test planning paradox; to precipitate latent wear-out defects, to compress test times and to estimate the reliability using extremely small sample sizes at the earliest stage of the programme, ideally without a significant budget increase. On further exploration of state-of-the-art techniques in reliability, it was apparent that there was little publicised information on how to accelerate the wear-out of gear pumps concerning estimating lifetime reliability. The accumulation of problems requires the application of innovative solutions as given in this Innovation Report.

This chapter begins with the rationale for an organisation to develop reliability test capabilities and the strategies employed to implement them. The discussion then applies context to the research problem with the status of the pump and commercial vehicle industries and the associated challenges faced regarding the reliability of pumps, leading to the problem identification and the gap in knowledge. The research aims and objectives are stated within the penultimate subsection, summarising the innovation and contribution of knowledge to academia and industry.

1.1 Strategic Rationale for Reliability and Robustness

When a company is developing new innovative products or existing products to commercialisation, it is widely agreed that the New Product Development (NPD) process is a key strategic activity that aligns with the business process (Yeh, Pai and Yang, 2010; Ericsson and Lillieskold, 2012). The NPD process comprises of a series of phases that increase in the level of detail as the project progresses to "*reduce key project uncertainties and risks*" (Cooper, 2008). Sandwiched between each phase are so-called gates where stakeholders, typically senior level management, are presented with evidence to aid decisions whether the project should pass through the gateway to the next phase and be assigned the necessary budget and resource (Rainey, 2005; Cooper, 2008). The early involvement of senior management can prevent interventions at a later date that result in a significant delay or redesign (Rainey, 2005). A typical seven phase NPD process is presented in Figure 1-1. The focus of the EngD project

is in Phase 4 and Phase 5, concerned with estimating reliability as early as possible using prototype hardware.

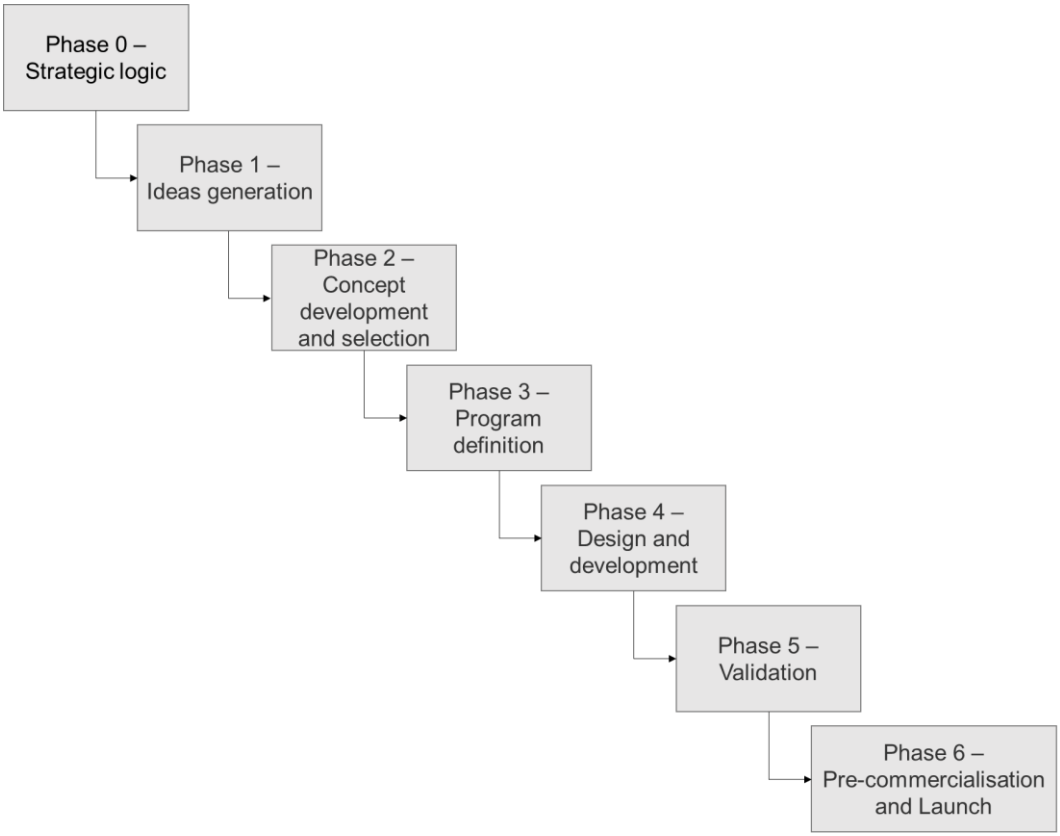

Figure 1-1 New Product Development process (Rainey, 2005).

At the start of the NPD, the requirements of a product are driven by its function, market demand and business strategy (Rainey, 2005). A standard practice for setting the strategic rationale of a business is to use a marketing mix model that considers the product, the balance of sales, price point, and profit margins reflected in the cost to design, develop, manufacture and distribute the product (Dibb, Simões and Wensley, 2014; Dibb *et al.*, 2016; Jobber and Ellis-Chadwick, 2016; Kotler *et al.*, 2016). The level of *reliability* and *robustness* the user expects from a product is influenced by its price (Rainey, 2005). To understand these two characteristics, it is necessary to define them. The definition of reliability for a product or system is the "*ability to perform as required, without failure, for a given time interval, under given conditions*" (British Standards Institution, 2014a). Whereas the definition of robustness is "*the ability to withstand or overcome adverse conditions or rigorous testing*" (Oxford English Dictionary, 2010). The two characteristics are linked in such a way that improving product robustness is expected to improve reliability (Spanó, 2008). Robustness is described by the stress-strength concept where the safety margin is increased by reducing the variation in stress or strength, and/or by increasing the component strength (Spanó, 2008). It is also

reasonable to assume increasing robustness incurs a cost penalty to do so (King and Jewett, 2010b, pp. 121–145). For example, adding more material or selecting a higher-grade material will increase the product/manufacture price (Dowlatshahi, 1994). The decision when to increase robustness in the NPD phase carries a cost penalty too as amplified by the *factor of ten rule* concept (Bertsche, 2008; Carlson *et al.*, 2010), (see Figure 1-2). Investing as early as possible in the design and development phases will reduce the risk of expensive tooling changes after the start of production and better still, reduce the risk of a product recall or warranty campaign once the products are in the field (Bertsche, 2008; King and Jewett, 2010b). The cost to retrospectively resolve the problem is compounded by a factor of ten and thus, the most opportune time to change is in design and development phase 4, which is a philosophy of Design for Reliability (DfR) (Huang, 1996; Strutt *et al.*, 2003; Childs, 2012).

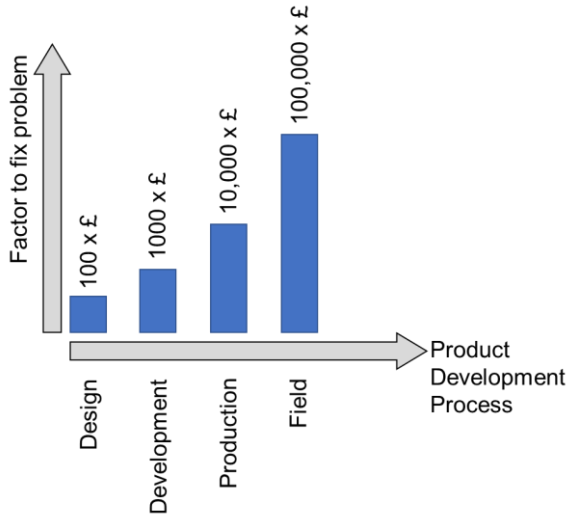

Figure 1-2 Factor of ten rule (Bertsche, 2008).

The approach of *design right first time* is analogous to the DfR principles (Huang, 1996). DfR aims to use a suite of tools to identify as early as possible the aspects of a proposed design that may fail, intending to minimise costly and time-consuming redesigns (Huang, 1996). Sarakakis, Gerokostopoulos and Mettas (2011) state that "*Designing for reliability is becoming the only way to quickly meet reliability goals and the new extreme time to market requirements*. Adopting the DfR approach leads to tangible reduced manufacturing costs and reduced service and warranty costs (Strutt *et al.*, 2003; Childs, 2012). Equally important are the intangible competitive differentiators that improve or maintain the company reputation (Huang, 1996; Stephenson and Wallace, 1996) and reward investors (Kotler, 1977; Kohli and Jaworski, 1990; Barney, 1991; Boxall and Purcell, 2016). In a world of innovation, the pressures and timing of product release influence the strategic rationale (Teece, Pisano and Shuen, 1997; Denrell and Powell, 2016). The race to be *first to market* receives the largest

publicity over rivals, often at the expense of reliability and robustness yet, the lesser thought of *right to market* usually wins the battle long term (King and Jewett, 2010b, p. 5).

One of the tools to assist senior management in the timely release of a product is Reliability Growth Testing (RGT) which is used to estimate reliability with planned hardware tests and timely product enhancements (National Research Council, 2015; Heydari and Sullivan, 2017). The Reliability Growth Plot (RGP) known as the Duane plot (Duane, 1964) is illustrated in Figure 1-3. With each design change the robustness of the product is expected to improve (King and Jewett, 2010a). Initially created for developing the reliability of repairable systems (Crow, 1974), the RGP can be used to predict and analyse the likelihood of achieving the target reliability before the target market entry date (King and Jewett, 2010a). The RGP contributes to the decision making of the project usually at gateway reviews (King and Jewett, 2010a). Delaying market entry threaten sales, competitive positioning and reputation (King and Jewett, 2010a). However, the risk of releasing an immature design to appease the target date magnifies the factor of ten rule (Bertsche, 2008), because of the increased risk of cost overruns (for example tooling modifications) and inventory consigned to the scrap (King and Jewett, 2010a). Substantial risk is when further improvements are not financially viable, leaving a substandard product in the market. (National Research Council, 2015).

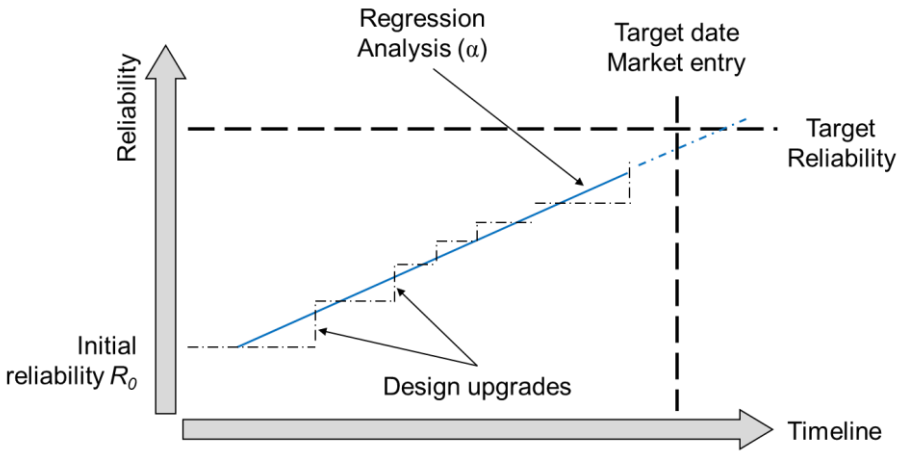

Figure 1-3 Conceptual reliability growth plot (King and Jewett, 2010a).

There are several strategies to manage the reliability growth and align the market entry date. Proactive robustness development methods such as design Failure Mode and Effects Analysis (FMEA),[1] Fault Tree Analysis (FTA),[2] Computer Aided Engineering (CAE),[3] and

[1] (O'Connor and Kleyner, 2012).
[2] (Main and McMurphy, 1999).
[3] (Spanó, 2008).

qualitative testing,[4] help enhance the initial reliability (R_0).[5] However, it is argued that reliability estimates through qualitative testing does not contribute to estimating R_0 due to the uncertainties of the test methodology, i.e. unrealistic failures from overstressing (Meeker, Sarakakis and Gerokostopoulos, 2013). Regardless, there are many advocates for the use of qualitative test methods and failure mode avoidance such as Highly Accelerated Stress Testing (HAST) (Hobbs, 2000; Davis, 2003; Clausing and Frey, 2005). The principle of these methods is to use extremely small sample sizes and overstress the samples to precipitate latent defects (Hobbs, 2000). The defects are analysed, and the case is made to justify the design change (Hobbs, 2000). Although HAST inevitably precipitates defects, the recommended design changes are frequently opposed because the overloads are not representative of the field (Hobbs, 2000; Davis, 2003; Clausing and Frey, 2005). Understandably, there is a great support for qualitative tests, suggesting it is better to invest in qualitative testing rather than *waste* time, resources and money on quantitative testing or predictions from warranty (Hobbs, 2000; Davis, 2003). After all, the theory of failure mode avoidance (increasing the stress-strength design margin) (Clausing and Frey, 2005) is rooted in DfR and capturing latent defects before the product reaches production is ideal (Huang, 1996; Stephenson and Wallace, 1996; O'Connor and Kleyner, 2012). However, given the subjectivity and the uncertainty in understanding where the product lies in respect to the reliability target (Meeker, Sarakakis and Gerokostopoulos, 2013) may result in an under or over-engineered product. The reliability estimates will be unknown until it becomes available later in the NPD process, at which stage the cost to change is significantly higher. Thus, there is a need to measure and estimate the initial reliability with the capability to update the reliability estimate with each design upgrade as quickly as possible.

Returning to the RGT, Duane (1964) first proposed an empirical reliability growth model for the development of hydro-mechanical aircraft devices, yet it was Crow (1974) that recognised Duane's proposal could be modelled with a parametric distribution and developed the Army Material Systems Analysis Activity (AMSAA). Over c.50 years the AMSAA model has been the foundation for developing RGT models due to its versatility (Heydari and Sullivan, 2017). However, there are known issues with RGT models primarily, impacted by management. For example, the budget and time allocation for each phase influences the uncertainty of the estimations (King and Jewett, 2010a; National Research Council, 2015). Producing expensive and/or large prototypes naturally restricts the sample size, and test capabilities limit the derivation of initial reliability estimates (and proceeding estimates for that matter). These limitations are is especially true for a NPD without a history (National Research Council, 2015; Awad, 2016).

[4] (Hobbs, 2000; Davis, 2003; Clausing and Frey, 2005).
[5] (King and Jewett, 2010a).

The efficiency of the reliability test depends on speed and accuracy which is directly connected to sample size (Nelson, 2005). The investment determines the test strategies employed, which alter the rate of reliability growth (α) (see Figure 1-3) and the prediction of meeting the target reliability before market entry (King and Jewett, 2010a, p. 47). Of course, there is a balance of investment, test capacity and human resource that restricts the rate of achieving reliability (King and Jewett, 2010a, p. 47). The most recent research has been focused on resolving the test planning issue through the modelling of efficient test plans, reducing test times, using smaller sample sizes and increasing or maintaining the accuracy of reliability, all within a constrained budget. For example optimise tests for sample size,[6] test duration,[7] the number of stressors,[8] the type of stress,[9] the application of stress,[10] and the test cost.[11] Dazer et al. (2016) describe this balance as a magic triangle but in the author's view it is better described as a *test planning paradox* (see Figure 1-4) as not all demands can be simultaneously met.

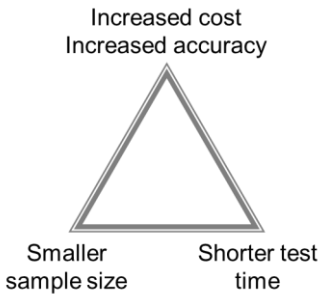

Figure 1-4 The test planning paradox, adapted from (Dazer et al., 2016).

With the test planning paradox, it is reasonable to assume that increasing the accuracy of estimation has a penalty of increased cost through higher sample sizes and extended test times (Dazer et al., 2016). The paradox is that not all three factors can be satisfied simultaneously and must compromise. Essentially, the desired output of this EngD project is to minimise the test planning paradox.

6 (Liao and Tseng, 2006; Ma, 2009; J.-R. Zhang et al., 2011; Sun et al., 2012; Yang, 2013; Pan and Sun, 2014; Weaver and Meeker, 2014; Ye et al., 2014; Lim, 2015; Zhang et al., 2016).
7 (Miller and Nelson, 1983; J.-R. Zhang et al., 2011; Yang, 2013; Lim, 2015).
8 (Khamis and Higgins, 1996; J.-R. Zhang et al., 2011).
9 (Nelson, 2005; Ye et al., 2014).
10 (Ma, 2009; Peng and Tseng, 2010).
11 (Liao and Tseng, 2006; J.-R. Zhang et al., 2011; Sun et al., 2012; Yang, 2013; Pan and Sun, 2014; Lim, 2015; Tsai et al., 2016; Zhang et al., 2016).

1.2 Simulation

Simulations can assist the possibility of minimising the test planning paradox. There are multiple approaches to studying a system (process), the choice of which depends on the objective and circumstances. The ideal situation is to experiment with the actual system in order to produce exact results (Law and Kelton, 2000, p. 4), however the cost and time to do so requires significant investment and it may not be practical or safe to test (Wu and Lewins, 1992; Law and Kelton, 2000, p. 4). For example, physical testing of nuclear power station systems in emergencies is not possible and must be simulated (Zio, 2013). Experimentation with system modelling is a cost-effective alternative that allows the evaluation of a system to be analysed under normal and extenuating conditions outside the possibility of an actual system test (Wu and Lewins, 1992; Law and Kelton, 2000, p. 4). Often, the complexity of the system model means exact analytical models are mathematically intractable; thus simulations are used to output estimates of interest (Law and Kelton, 2000, p. 4).

The type of simulation model depends on the system and properties of its state variables. A dynamic model represents a system that changes over time (Law and Kelton, 2000, p. 5) such as a mass-spring-damper, whereas a static model represents the system state at a discrete point in time (Law and Kelton, 2000, p. 5). The assumptions and properties of the state variables determine if the model should be deterministic or stochastic (Law and Kelton, 2000, p. 6). Monte Carlo (MC) simulations are widely used in industries to model the reality of randomness in a system (Kleijnen, 1974; Zio, 2013) and are commonplace in reliability assessments needing quantile estimates and confidence limits (Wu and Lewins, 1992; Zio, 2013; Liu and Meeker, 2014). The advantage of MC simulation lies in the flexibility to model a system with as much complexity and detail as needed, with scope to develop and improve the precision without intractable mathematics (Law and Kelton, 2000, pp. 90–91; Zio, 2013). The detail of the model can provide accuracy with a sufficiently large number of samples with relative simplicity (Hahn, 1972; Law and Kelton, 2000, pp. 90–93; Zio, 2013). The disadvantage as with all simulations is that the outputs are only as good as the input and the code can be computationally intensive (Law and Kelton, 2000, pp. 90–93; Zio, 2013) The balance between the program run time and the sample size can limit the precision required (Hahn, 1972; Zio, 2013). The benefits of simulations are balanced against the drawbacks found in the implementation of programming. The subject matter expert experience, the complexity of the program, the time to implement, the time to run, the debugging and heuristic process can all contribute to erroneous conclusions (Law and Kelton, 2000, pp. 265–290; Zio, 2013). These issues within the simulation need verification and validation to achieve credibility (Law and Kelton, 2000, pp. 265–290).

The use of simulation in reliability is prolific. For example, Lu and Meeker (1993) simulated the time to failure for fatigue-crack-growth using Monte Carlo simulations. Zaharia and Morariu (2015) used actual system data in a Monte Carlo simulation to estimate the reliability of gear bending fatigue from an accelerated life test. Similarly, Lin and Chung (2019) experimented with accelerated degradation testing on vehicle Lithium-ion batteries. The dual dynamic stressors of temperature and power thermal cycling output non-linear stochastic degradation. The degradation parameter estimates fed as inputs into a Monte Carlo simulation to estimate reliability representing real driving conditions (Lin and Chung, 2019). Simulations are also used for hypothetical solutions. Talafuse and Pohl (2017) recognised the realities of overcoming small sample size failure data and uncertainty in reliability growth plots (see Section 1.1) and used Monte Carlo simulation to demonstrate the advantage of Grey system theory (a colour scale of uncertainty) (Liu and Lin, 2006) to model reliability growth over the AMSAA model (Crow, 1974).

The use of simulation is a method of attaining greater certainty by methodically building up the complexity and randomness of the real world. It is a solution used to overcome restrictions over testing the actual system by making assumptions and outputting estimations. Further considerations to using simulations are presented in Section 3.8.

1.3 Industrial Sponsor ConcentricAB

The sponsoring organisation CAB is a global manufacturer of pumps operating in four key markets; Commercial Vehicles, Construction, Agriculture and Industrial Applications (COIC, 2017). In particular, the Engines Division designs and manufactures centrifugal coolant pumps, and positive displacement pumps for lubrication and fuel transfer in heavy-duty diesel engines (HDE), medium duty diesel engines and most recently hybrid commercial vehicles (COIC, 2017). CAB has a rich history in pumps and is a Tier 1 supplier to the major Original Equipment Manufacturers (OEM). CAB reports a total of c.1100 employees across eight sites worldwide (COIC, 2017). The lead technical centre sited at Birmingham UK is responsible for initiating the EngD project where the author is employed.

Each engine product is bespoke to the application, and unit sales per application range from 5,000/year to 200,000/year. CAB is an Investor in People, and the opportunity arose to sponsor an EngD through discussions on the best practices in reliability with Warwick Manufacturing Group's Dr Jane Marshall and Dr Jeffery Jones. The initial brief from CAB was open, in a sense the organisation knew that accelerated life testing and effective validation practices early in the NPD would be beneficial from a reputational, economic and learning perspective. A narrowing of the problem was first required as reported in Submission 1

(Zarzycki, 2015) and Submission 2 (Zarzycki, 2016) with an opportunity to test on a live NPD of an external gear pump intended to sharpen the contribution of the research.

1.4 The Pump Industry and Commercial Vehicle Markets

The make-up of the global pump market consists of sectors such as; oil and gas, aviation, automotive, heat pumps, households, water and waste management, industrial manufacture, chemical industries and HVAC (heating, ventilation and air conditioning) (Gerden, 2010) systems to name but a few. By the year 2022, the global pump market is expected to reach a value of US$84.4bn (Group, 2018). To position the pump market against more widely reported markets, the global mobile phones market reached a value of US$315.1bn (Marketline Industry Profile, 2018c) and the global automotive manufacturing industry reached a value of US$1,386.5bn (Marketline Industry Profile, 2018a). The truck market was valued at US$229.6bn in 2017 (Marketline Industry Profile, 2018b). Consider for a moment the commercial opportunities for pumps operating on an engine requiring fluids for three rudimental functions. A fuel pump is needed to deliver fuel from a tank to the combustion chamber/injectors (Xin, 2011). The combustion process generates heat, and therefore a coolant pump is required to transfer heat to a radiator for cooling (Xin, 2011). The combustion process is converted into power through a set of pistons and a crankshaft, which have relative motion and friction; thus without a lubrication pump the engine would seize (Xin, 2011). Generally, the coolant pump is of a centrifugal design whereas fuel transfer pumps and lubrication pumps are positive displacement pumps, i.e. piston pumps, ge-rotor pumps and gear pumps (Karassik, 2001) (see Section 2.1 for fundamental workings). In this regard, a Tier 1 supplier to this market has at least three opportunities per application to tender and demonstrate technical ability, quality and reputation.

In terms of the future, both the pump industry and vehicle industries are under pressure to make energy savings and boost pump efficiency, the benefit of which is reduced CO_2 and operating expenses for the end user (Giakoumis, 2016, pp. 1–10). Multiple factors are contributing to pump inefficiencies, such as pump design, operation, volumetric losses, hydraulic losses and friction losses (Manring, 2005). The solutions to improve efficiency are innovative with the prime solution of variable flow pumps tailored to the minimum requirements of the application (Rundo and Nervegna, 2015). Yet the challenge to bring these products to market are slowed by the "*energy efficiency paradox*" (Jaffe and Stavins, 1994) where there is a failure to adopt new technologies regardless of the payback and future operational savings because of associated risks (Jaffe and Stavins, 1994; Klemick *et al.*, 2015). The truck market is highly risk-averse because time off the road reduces the return on investment and damages reputation particularly regarding the delivery of goods (Klemick *et*

al., 2015). Therefore, the reliability and servicing of technology is one of the most significant barriers to its adoption (Roeth *et al.*, 2013; Klemick *et al.*, 2015)

The UK market is estimated to contribute US$1.46bn to the global pump market, and surprisingly, it is estimated that spares and repairs account for 39% of this value (World Pumps, 2016b). It is expected this figure to rise to 75% as a result of operators wanting to prolong the life of the pumps and improve the return on investment (World Pumps, 2016b). The downtime for unexpected repairs accounts for 70% of the pumps life-cycle cost, and so the latest developments in the industry are concerned with pump availability and condition-based maintenance (CBM) (World Pumps, 2016a). CBM aims to capture the onset of abnormal pump health and wear out using diagnostics and prognostics to schedule the ideal time to make repairs (British Standards Institution, 2018a). The studies of Greene and Casada (1995), Khoshzaban-Zavarehi (1997) and Martinez *et al.* (2000) propose several monitoring techniques for failure detection of hydraulic components. These primarily rely on a parameter deviating or crossing a threshold such as vibration levels against a lookup database with fault failure patterns (Liu *et al.*, 2015). Like all CBM activities these methods require extensive testing to generate a database of fault patterns (Heng *et al.*, 2009) and for this reason, the accelerated testing of pumps is less documented.

The risk-averse mindset of truck operators is not only reserved for new technologies. The commercial vehicle industry is also experiencing increased support for extended warranties. For example, Tata Motors Limited has recently offered an industry first with a driveline warranty option of six years which is double the industry standard (Auto Business News, 2018). These pressures are experienced at CAB where technical specifications now ask for double the life expectancy compared to ten years ago now requesting a 90% reliability of 40,000 hours (2,000,000km) and in some instances with tightened reliability targets such as 95% reliability. These challenges have not gone unnoticed at CAB and the commercial pressure to commit to extended warranty agreements results in a need to meet reliability targets as early in the NPD as possible.

1.5 Estimating the Lifetime of Pumps

This section highlights a gap in knowledge regarding the reliability estimation of gear pump wear-out. A warranty database can theoretically provide evidence to estimate the lifetime (Meeker and Hong, 2014) of a product (pump). However, the database can be laden with problems regarding the infrastructure, the collection of warranty information, and distribution of this information back to the supplier (Lawless, 1998; Sarakakis, Gerokostopoulos and Mettas, 2011; Lawless, Crowder and Lee, 2012). For example, an independent service station is not required to report replacement parts (Lawless, 1998) or in

some cases, replacing good parts is recommended practice (Sarakakis, Gerokostopoulos and Mettas, 2011). Such practice falsely increases the numbers of returns and the accompanying data, for example, time to failure, mileage and root causes are not recorded correctly (Lawless, 1998; Sarakakis, Gerokostopoulos and Mettas, 2011; Lawless, Crowder and Lee, 2012). Other problems assume that vehicles out of warranty are surviving and thus skew the estimations to be optimistic (Lawless, 1998; Sarakakis, Gerokostopoulos and Mettas, 2011; Meeker and Hong, 2014). Even if the database is well managed the reliability estimations from warranty data are post NPD. An alternative is to make initial reliability estimates using handbook calculations.

Part of the challenge is that vast amounts of literature on reliability originate from the creation of electronics standards and handbooks, for example, US MIL-HDBK-217F (1991). Thus, few state-of-the-art reliability techniques exist for pumps when compared to Light Emitting Diodes, for instance. The most recent non-electric component handbook created for the military is NSWC-11 (NSWC Carderock, 2011). The NSWC-11 includes the failure rate estimation of pump reliability, which is particularly useful at the earliest stages of design where there is no historical information. The handbooks use the parts count method to predict product reliability at the system level (NSWC Carderock, 2011). Essentially the base failure rate of a pump is modified by a set of empirical factors, depending on the operating conditions (NSWC Carderock, 2011). The handbooks do have major criticism and low credibility as they are renowned for being inaccurate and misleading (McLinn, 2008; Elerath and Pecht, 2012). Contrary to this McLinn (2005) published a paper validating the life testing of hydraulic gear motors. However, because the hazard rates are modelled as constant random failures, this does not capture the wear-out and is of limited value to CAB.

The ideal situation requires investment in reliability as early as possible to learn if the reliability targets are satisfied which invariably involves hardware testing (National Research Council, 2015). The long life and high-reliability requirements of the gear pump means testing must be accelerated or include large sample quantities to satisfy both reducing the test time and accurately estimating the reliability (Meeker, Escobar and Lu, 1998; Nelson, 2004; Meeker, Sarakakis and Gerokostopoulos, 2013; Guo and Liao, 2015; Pulido, 2015).

On the estimation of gear pump lifetime, the primary focus in the literature of gear pumps has been solving the sensitivity to the contamination that is often cited for contributing to 70% of failures (Eaton-Vickers, 2002; Dias, 2012; Singh, Lathkar and Basu, 2012). Many studies have used contamination to accelerate the wear of pumps and referred to this as Accelerated Life Testing (ALT) (Maroney, 1976; Milwaukee Fluid Power Institute, 1980; Frith and Scott, 1993). However, there is no prediction of lifetime and reliability estimates. The challenge is relating several debris characteristics such as shape, size and hardness, the distribution of quantity, the interaction with components, the wear mechanisms, and the timely

release of debris over the pump life (Frith and Scott, 1993) (see Section 2.2.4 for further discussion).

The most encouraging and recent study by Ranganathan and Mohanram (2005) used conventional accelerated wear testing on the journal bearing of a lubrication pump at a fixed speed and pressure for 1000h. Abrasive dust is added into the oil to accelerate the journal wear. Through the measurement of oil flow reduction, journal wear and pump clearances, the rig test time of 60h was correlated to an equivalent 100,000km field use (Ranganathan and Mohanram, 2005) however, this was based on a small sample size of 3 without considering the statistical implications. Additionally, the study does not consider the pitfalls as previously mentioned by Frith and Scott (1993) (also see Section 2.2.4).

The most relevant study without contamination is the accelerated life testing of a high-pressure hydraulic piston pump where the failure mechanism is the wear-out of the cylinder to plate valve and the piston-to-cylinder interfaces (Wang and Shi, 2006). The objective was to develop an accelerated test to shorten a 425 hour production qualification test (Wang and Shi, 2006). Five pumps were cyclically overstressed by 125% in terms of pressure, velocity and temperature (oil viscosity) to yield three failures ranging 2225 hours to 3750 hours and two suspensions at 3750 hours (Wang and Shi, 2006). Using a cumulative exposure model (Nelson, 2004) and a hybrid Weibull model (Nelson, 2004), the 425 hour qualification test was shortened to 61.5 hours, saving significant time and cost (Wang and Shi, 2006). In the case of Wang and Shi (2006), the pump is already in the field as the work is for a production test, not the earliest possible stage in the NPD as desired by CAB.

Additionally, five samples are statistically reasonable (Li and Meeker, 2014; Guan, Tang and Xu, 2016) whereas to reduce test costs with a smaller sample size raises issues with statistical validity (Zhang, Yuan and Li, 2015). The acceleration factor is not sufficiently high enough considering a HDE pump lifetime target of 40,000 hours. Furthermore, the test plan in Wang and Shi (2006) requires a rig capable of running five samples simultaneously or several test rigs. To satisfy improving the rate of reliability growth during a NPD the test time needs to be significantly shorter.

1.6 Accelerated Testing

Conventional lifetime analysis methods require the failure of products to populate the failure time distribution (Nelson, 2004). If the product has high reliability and lifetime (such as 40,000 hours for an HDE pump), the likelihood is that an insufficient number of failures will satisfy the lifetime models (Nelson, 2004). The situation is that normal stress levels will not precipitate failures and so the data becomes censored to the right and challenging to analyse (William Q Meeker and Escobar, 1998; Nelson, 2004). The likelihood is that the product will

not fail under normal usage for a very long time and requires an Accelerated Life Test (ALT) to reduce the time it takes to fail (Escobar & Meeker 2007). The time to failure can shorten by increasing the frequency of operations, by running continuously and raising stress levels (Nelson, 2004; Escobar and Meeker, 2006; Yang and Zaghati, 2006).

In the case of over-stressing, a stress-to-failure relationship is necessitated to extrapolate and estimate reliability at normal stress levels (Nelson, 2004). Conventionally the ALT model needs failures within the data to provide predictions. For example, Onsoyen (1991) accelerated the wear of a hydraulic gear pump by increasing the temperature and hence reducing oil viscosity. However, none of the pumps deteriorated enough to cross a failure threshold based on efficiency, and so the data is censored, and the ALT reliability model is incomplete.

Another risk is that overstressing will induce unrelated field failures (William Q Meeker and Escobar, 1998; Nelson, 2004) in similar principles to HAST and this will amplify the error in extrapolation (Sarakakis, Gerokostopoulos and Mettas, 2011). Errors are more likely when testing on a system or product because of competing failure modes (Meeker, Sarakakis and Gerokostopoulos, 2013) and the limiting accelerated factor is only as high as the weakest component (Meeker, Sarakakis and Gerokostopoulos, 2013). Furthermore, the methods require a reasonable sample size to provide statistical validity and precision (William Q Meeker and Escobar, 1998; Nelson, 2004) as mentioned for the test planning paradox (Section 1.1).

When considering the mechanism(s) of failure, generally products degrade beforehand (Meeker, Escobar and Lu, 1998). Having the capability to measure the degradation offers the possibility for Accelerated Degradation Testing (ADT). ADT is a powerful technique in estimating reliability (Meeker, Escobar and Lu, 1998; Nelson, 2004; Meeker, Sarakakis and Gerokostopoulos, 2013; Guo and Liao, 2015; Pulido, 2015).

The advantage of ADT is that the degradation of the product is measured over time and does not require the products to fail (Meeker, Escobar and Lu, 1998). A pseudo-failure threshold is set and, when the monitored degradation parameter crosses the threshold, the product is judged to be unacceptable (Guo and Liao, 2015). An advantage is realised by producing information in terms of the physics of degradation rather than the binary pass or fail of the ALT (Meeker, Escobar and Lu, 1998; Nelson, 2004; Meeker, Sarakakis and Gerokostopoulos, 2013; Guo and Liao, 2015; Pulido, 2015). Accordingly, an opportunity to resolve the root cause and instigate an effective design change is more likely (Meeker, Escobar and Lu, 1998; Nelson, 2004; Meeker, Sarakakis and Gerokostopoulos, 2013; Guo and Liao, 2015; Pulido, 2015). A significant advantage is that ADT studies are proven to lead to more accurate reliability estimates using fewer samples (Meeker, Escobar and Lu, 1998; Nelson, 2004, p. 521; Meeker, Sarakakis and Gerokostopoulos, 2013; Guo and Liao, 2015). The

disadvantage is that a regression model is required for the degradation and extrapolation back to normal usage levels (Meeker, Sarakakis and Gerokostopoulos, 2013). The model selection and assumptions increases complexity (Meeker, Escobar and Lu, 1998) and usually a closed form expression for reliability is mathematically intractable requiring simulation tools such as Monte Carlo to analyse the reliability (Meeker, Escobar and Lu, 1998; Ming and Meeker, 2014) (see Section 1.2 and 3.8).

A hidden factor in the test planning paradox is the application of stress. Stress is intrinsic to the sample size and test duration (Meeker, Escobar and Lu, 1998; Ming and Meeker, 2014). There are multiple stress application methods; constant stress, progressive step-stress, regressive step-stress, ramp stress, profile stress, stochastic stress and non-repeating pattern stress (Nelson, 2004, p. 49; René Van Dorp and Mazzuchi, 2004). As with any regression, a minimum of three data points (or in this case stress levels) are required to extrapolate back to normal usage levels. Constant stress tests use new samples for each stress (Nelson, 2004, p. 493) whereas a step-stress test uses a cumulative exposure model to pass the same sample through all the stress levels (Nelson, 2004, p. 493). The step-stress test is effective at precipitating failure quicker than constant stress tests at the expense of accuracy (Nelson, 2004, p. 493). The loss of accuracy is also the case for alternative stress methods, however, with varying-stress, it is the error and repeatability in setting the stress that becomes the prominent error especially for products with low degradation (Nelson, 2004, p. 493).

The balance of using the correct stresses with competing failure modes are reviewed in Chapter 2 as to how they contribute to the systemic wear of a pump. In Section 1.5 the estimation of pump life time was concluded with mixed success. The objectives of previous work has been focused on contamination sensitivity (Frith and Scott, 1993) and the correlation of contamination to the field (Ranganathan and Mohanram, 2005) however, contamination is too unpredictable (Frith and Scott, 1993). Alternatively, Wang and Shi (2006) successfully used three stressors to fail piston pumps and Onsoyen (1991) used temperature as an stressor to degrade a gear pump without complete failure. Thus, it is possible to use load and with a suitable wear detection method the use of accelerated degradation testing for the gear pump is possible. The challenge of competing failure modes and replication of field wear is key through carefully designed experimental methods that do not overstress the pump.

1.7 The Research Question

To summarise the preceding subsections, the classic industry-wide issues of reliability are; the requirements to achieve extended reliability targets, the doubling of the warranty agreement and, pressures to compress development time in the NPD process. The balance of timing, rig availability and using extremely small sample sizes are also industry-wide concerns. An idealistic solution is the philosophy of failure mode avoidance through qualitative test methods, but the outputs do not contribute to satisfactorily answering if the reliability target will be achieved and leaves questions whether to add cost to enhance robustness. In essence, the conceptual aim is to make the test planning paradox triangle as small as possible. An ideal solution is a form of accelerated degradation testing. However, a gap in knowledge exists in the testing of highly reliable gear pumps to estimate life without introducing overstressed failure modes.

The EngD project case study is on an HDE lubrication gear pump. It is expected that a methodology addressing these issues will be of value to an organisation in the market of positive displacement pumps. Thus, the overarching research question is:

"How to estimate the wear-out reliability of a gear pump using an extremely small sample size?"

1.8 Research Aim and Objectives

This research aims to create a methodology that manufacturers can follow in pursuing the estimation of gear pump reliability during a NPD. The value lies not only in the output but also in demonstrating the benefits of a DfR and reliability growth mindset. Three overarching objectives are set:

(1) To understand the competing gear pump failure modes and the internal physics of failure. How can these failure modes be measured and what resources are required in establishing an accelerated test.
(2) To understand the implications and solutions of using an extremely small sample size in an accelerated test. To develop a method of accelerated testing and validate gear pump life expectancy. The validation of the testing should be representative of field experience.
(3) To demonstrate the value of balancing the philosophy of failure mode avoidance with outputting reliability estimations early in the NPD process.

1.9 Summary of the Innovation

The innovation of the project to academia and the pump industry as a whole is summarised:

(A) An innovative methodology is developed to estimate the reliability of a gear pump using an extremely small sample size, thus adding value to the reliability growth management of NPD. This methodology uses the physics of failure (PoF) (Snook, Marshall and Newman, 2003) for journal-bush seizure and pumping gear fatigue to set test limits for a step-stress accelerated degradation test which has not been reported in the literature to date. This innovation relates explicitly to using pump pressure ripple monitoring in combination with the MODWT-ARMA(2,1) feature extraction method to provide a degradation path that can be modelled. The use of Bayesian inference methods using preceding test data as the prior was proposed by Viertl (1981) and Wan *et al.* (2014); however, this method was used in a simulated step-down stress degradation test and has not been applied to the step-up stress degradation test of a gear pump before. The application of inputting a transient driving pattern into a Brownian Motion (BM) model with covariate drift and diffusion coefficients (extracted from pressure ripple) to estimate the reliability of an engine lubrication gear pump has never been reported before. The generality of this original methodology can be widely adapted to positive displacement pumps in other industries.

(B) An innovative method using MODWT-ARMA(2,1) to monitor gear pump degradation using pump pressure ripple is developed and validated. Previously, the degradation monitoring of pump pressure ripple with the intention to estimate reliability has had mixed success. A method proposed by Silva (1986) linked pump pressure ripple to pump degradation using a second order model (ARMA 2,1). However, through experimentation in this project, the method did not output a suitable degradation model to estimate reliability. Alternative methods exhibited a similar outcome, for example, Fast Fourier Transforms (FFT) could distinguish a change in health, but this is suitable for diagnostics and not prognostics. Reviewing methods and applications outside the field of pumps the author recognised the work of Zhu, Wang and Fan (2014) that passed weather rainfall times through a MODWT to decompose the time series and used ARMA to forecast into the future. Given pump pressure ripple is time series data, the methodology was adapted to filter the pump pressure ripple signal using MODWT and extract the second order system features from the decomposed signals using ARMA(2,1). The original intention to relate the degradation to a second order system was lost because the MODWT essentially filtered the fundamental signal to give a pure sinusoidal wave, thus rendering the damping coefficient impractical. Still, the innovative method allows precise detection of degradation in pump health using the natural frequency.

The technique is ideally suited for laboratory conditions in this case step-stress accelerated degradation testing, which assisted in deciding to cease testing early. It is foreseen the innovative technique applies to all positive displacement pumps that generate pressure ripple.

(C) The innovative gear pump wear concept model (see Figure 3-18) is an application specific illustration of lubrication gear pump wear. The simple model by Frith and Scott (1996) is expanded to consider the complexity and variety of wear debris sources and the environment in which the gear pump operates. In this case, the wear concept is remodelled specifically for the lubrication pump of a HDE which has not been considered before in literature. The model is more effective through the identification of ten key contributors of abrasive wear particles (including cavitation wear, erosive wear and gear tooth wear) that degrade the pump. The significance of the model is understanding the competing wear mechanisms that are influenced by the operation factors and design factors. The systemic wear is presented with simplicity and allows the key covariates of the pump degradation to be conveyed diagrammatically.

1.10 Innovation Report Structure

Several sections that contribute to the innovation report are structured in a sequence building up to the wear detection and modelling methods. Figure 1-5 provides a visual overview where the sections fit into the report structure. Having already defined the research question in Chapter 1, the background to the pump wear mechanisms are provided in Section 2.2. In understanding the stresses that generate wear the sources of application load are reviewed in Section 2.3. It is worthwhile first understanding the context of the wear detection methods available as discussed in Section 2.4 before understanding the available degradation models and parameter estimation methods in Section 2.5 and 2.6, respectively.

With background knowledge there are several aspects that the methodology provides structure to in Chapter 3. The design of the step stress accelerated test is first defined by the vehicle mission profile as discussed in Section 3.1. Knowing the wear detection method and simulating the application the pump is experimentally set up according to Section 3.2. The understanding of all contributing sources of wear is summarised in Section 3.3 to aid the design of a test that is theoretically equivalent to the life of the pump in Section 3.4. The degradation is detected using a novel pressure ripple analysis method defined in Sections 3.5 and 3.6. Given no historical knowledge and using preceding test data, the parameter estimation of a Brownian Motion model is detailed in Section 3.7 with the Monte Carlo simulation algorithm demonstrated in Section 3.8.

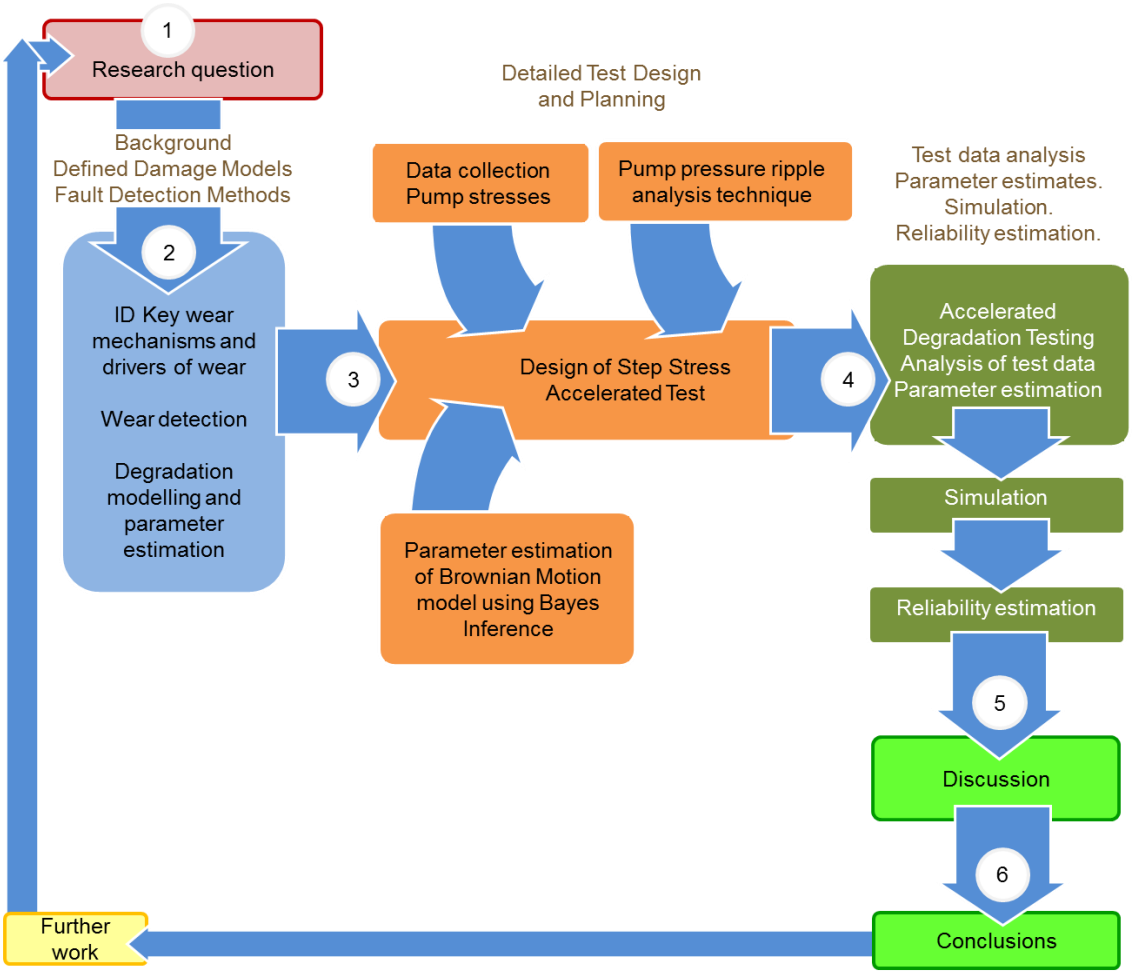

Figure 1-5 Methodology and organisation of portfolio

Post testing analysis and simulations are carried out in Chapter 4. The post-test examination of the pump confirms degradation in Section 4.1 and test data analysis in Section 4.2. The contributions of Section 4.3 and 4.4 output the covariate relationships for the Brownian motion model which are input into the simulations and reliability estimations are reported in Section 4.5. Ultimately, the outcomes from the methodology are discussed in Chapter 5 and concluded in Chapter 6 with further recommendations.

Chapter 2: Background

To propose an accelerated degradation test that meets the project objectives requires holistic consideration of the applicable theories, the pump design and characteristics, the environmental stressors, the test setup and its constraints and the analysis of data. The purpose of this Chapter is to; (1) Detail the basic operation and performance characteristics an external gear pump for a HDE. (2) Review the mechanisms of pump degradation as these decide which stressors to use in accelerated testing. (3) Explain the environmental stressors for a HDE pump because this will influence the life length of the pump. (4) Review the methods of condition-based monitoring and pump failure detection since this determines the instrumentation test setup and their limitations. (5) Review the available degradation models and explore how a stress-varying environment can be incorporated to estimate field reliability with the use of simulation accurately.

2.1 The Gear Pump

A positive displacement pump uses a change in volume to impart mechanical energy on a fluid causing it to displace and flow (Karassik, 2001). The method of displacing the fluid is diverse with an external gear pump amongst alternative designs such as ge-rotor pumps, sliding vane pumps, piston pumps and internal gear pumps (Karassik, 2001; Cudina, 2007). As this case study is focused on an external lubrication gear pump for the remainder of the thesis, *gear pump* will refer to an *external lubrication gear pump*.

The basic operation of a gear pump as illustrated in Figure 2-1 requires the following minimum components; a housing, cover, pumping drive gear, pumping idler gear, drive shaft and an idler shaft. The operation of a gear pump uses the volume change in the gear mesh zone to displace the fluid (AIChE, 2007). As the gear rotates, the increase in volume on the inlet side creates a suction pulling the fluid in (AIChE, 2007). The fluid then travels between the gear teeth in an enclosed space formed by the gear housing pocket, sealed by tight clearances radially between the tips of the gear teeth and the housing gear pocket and, axially between the pumping gear end faces and the housing and cover (Karassik, 2001, p. 3.81). On the outlet side, the decrease in volume at the gear mesh zone displaces the fluid causing it to discharge and flow (Naunheimer *et al.*, 2011).

The flow rate is proportional to the speed, and the theoretical flow rate Q_r per revolution is a function of the outer gear diameter D_o, the gear centre distance C_d and the gear length L.

$$Q_r = \frac{\pi}{2} \times \left(D_o^2 - C_d^2\right) \times L \tag{2.1}$$

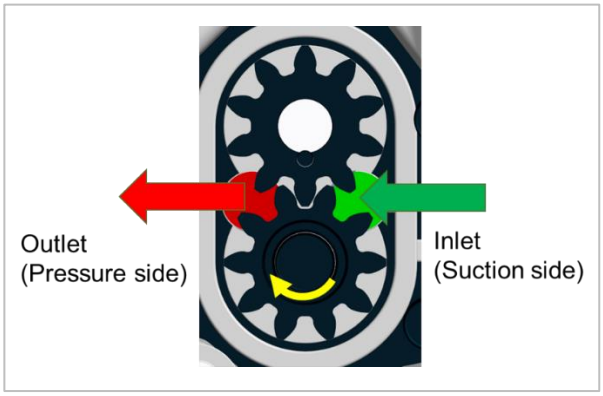

Figure 2-1 Basic operation of a gear pump.

With a fixed restriction on the outlet side, such as a pipe or the engine block, a pressure rise is generated proportional to flow squared as per Bernoulli's equation (Karassik, 2001, p. 4.2). The components are designed with fine clearances to allow access for lubrication, reduce wear (Karassik, 2001, p. 3.79-3.127). Under high pressure, these clearances are leak paths allowing fluid to recirculate back to the inlet, also referred to as slippage (Karassik, 2001, p. 3.79-3.127). Another source of leakage is the intentional clearances in the journal bearings and the design of the sealing land in the gear mesh zone (Karassik, 2001, p. 3.79-3.127). The total slippage causes a reduction in volumetric efficiency and thus a reduction in theoretical output (Karassik, 2001, p. 3.79-3.127). The slippage and clearances are not constant and are a function of pressure differentials, fluid viscosity, gear tip velocity, disc friction between gear faces to the housing, absorption of clearances during operation, thermal expansion of dissimilar material and misalignment (Karassik, 2001, p. 3.79-3.127). The largest influencing factor is viscosity (Karassik, 2001, p. 3.79-3.127) which determines backpressure through a fixed restriction, dependent on the type of fluid and the fluid temperature (see Section 2.3.2 for HDE details). The characteristics of a pump are typically defined by performance variables such as flow rate, pressure generation, speed, volumetric efficiency, hydraulic power, drive power and overall efficiency (Stapelberg, 2009), as illustrated in Figure 2-2 and Figure 2-3.

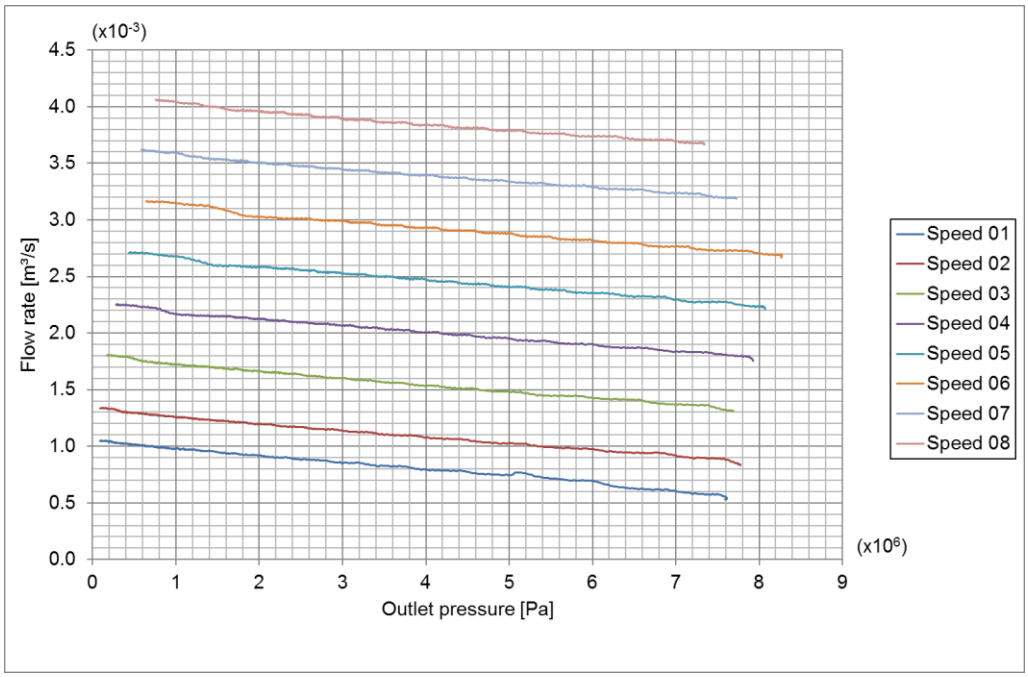

Figure 2-2 Performance curve for a HDE lubrication pump, SAE10W30 test oil @ 100°C.

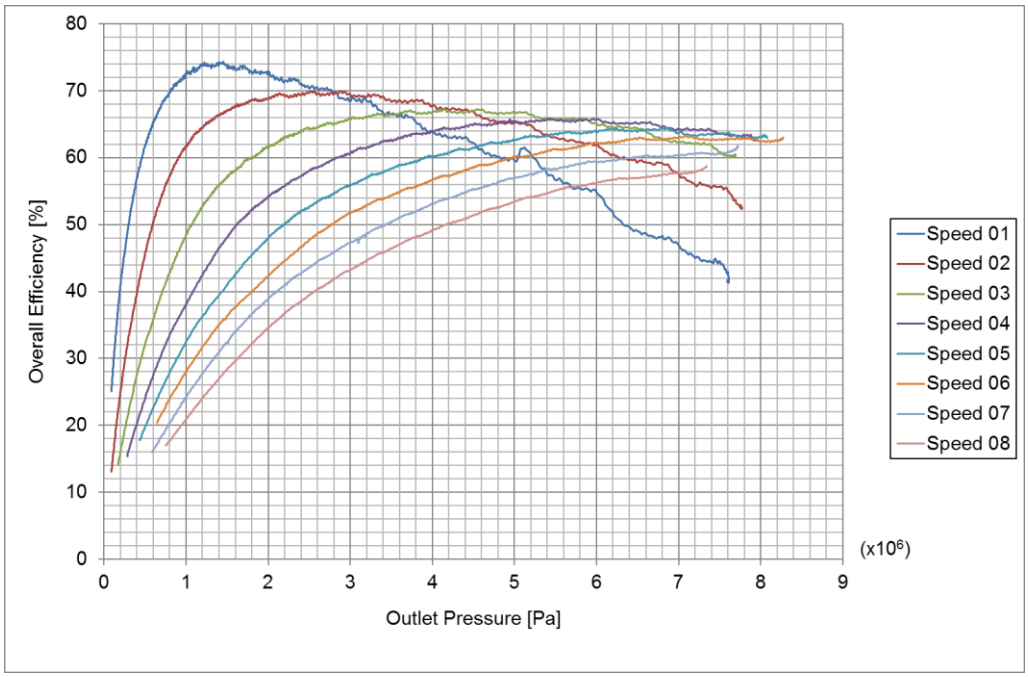

Figure 2-3 Overall efficiency performance curve for a HDE lubrication pump, SAE10W30 test oil @ 100°C.

The speeds in Figure 2-2 and Figure 2-3 are removed for confidentiality. As observed in Figure 2-2, the pump outlet pressure drives an increase in slippage and a reduction in flow, whereas Figure 2-3 illustrates the complexity of balancing volumetric efficiency, hydraulic efficiency and mechanical efficiency, which all interact as speed, flow and pressure alter. In terms of degradation, a pump can continue to operate, but it may degrade in performance and

fail to provide the correct flow or pressure for the application (Frith and Scott, 1993). In the case of a HDE, the consequences could be as severe as seizing the engine (Vencl and Rac, 2014). The primary mechanism for degradation in performance is wear, from opening up the clearances that allow greater slippage with the expectation to see a deterioration in flow output (Koç, 1989). However, these are not the only mechanisms that contribute to degradation in performance.

2.2 Gear Pump Wear Mechanisms

In this section, the primary contributing sources of gear pump wear are reviewed to understand what stressors are most applicable to the accelerated test design. Putting into context the severity of the problem, it is stated that 80% of aviation fuel pump failures are due to wear (Wang *et al.*, 2016), and the rule of thumb from the hydraulic pump industry estimates that contamination contributes 70% of pump wear failures (Eaton-Vickers, 2002; Dias, 2012; Singh, Lathkar and Basu, 2012). Firstly, it is necessary to define the meaning of *wear*. To classify a component as worn, it must have resulted in a loss of volume (Godet *et al.*, 1991; Williams and Hyncica, 1992; Glaeser, 2001). In a hydraulic pump, the primary modes of wear are reviewed as follows.

2.2.1 Contact Wear

Essentially *contact wear* is observed at any mechanical interface with relative sliding velocity (Godet *et al.*, 1991). In the gear pump the contact interfaces are at the journal bearing, the pumping gear to casing (diameter and end faces) and the gear teeth mesh zone (Fitch, 1986; Silva, 1986; Eaton-Vickers, 2002; Niu, 2002; NSWC Carderock, 2011; Dias, 2012; Singh, Lathkar and Basu, 2012). The severity of wear is a multi-faceted field of study. The primary factors influencing contact wear are based on load, velocity, surface roughness, material type, material hardness and two-body wear (see Figure 2-4) (Fitch, 1986; Godet *et al.*, 1991; Williams and Hyncica, 1992; Glaeser, 2001).

From the perspective of designing an accelerated test, the objective is to avoid seizure and unrealistic failures when overstressing the pump. Since the project is focused on extremely small sample sizes for a NPD, it will be necessary to find the pump limits using PoF. Using standard design methods is a practical solution in this respect of which standard journal bearing calculations and standard gear contact fatigue are stipulated in BS ISO 4378-1:2009 (British Standards Institution, 2009) and BS ISO 6336-2:2006 (British Standards Institution, 2006b) respectively. Recent research in this field is focused on the mechanism of contact wear. For example Dhar and Vacca (2015) propose state-of-the-art modelling for the

lubricating film thickness generation of pumping gears to the casing; however, the prediction of asperity contact requires further development (Dhar and Vacca, 2015).

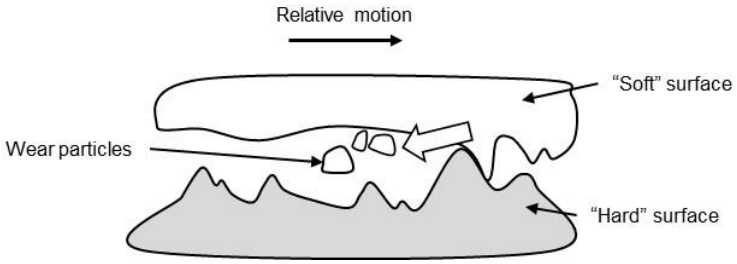

Figure 2-4 Two-body wear adapted from (Dias, 2012).

2.2.2 Worn Journal Bearings

The function of a journal bearing is to support loads transmitted through the rotational sliding motion of the journal (British Standards Institution, 2009). Conventionally, the design intent of a journal bearing is to generate a hydrodynamic lubrication regime where lubricant fully separates the journal from the plain bearing to prevent asperity contact, and in the process reduces friction and removes heat (Khonsari and Booser, 2008). The Stribeck curve (Jacobson, 2003) describes the lubrication regime in the form of a parameter lambda λ. Lambda is a function of viscosity, component surface roughness, load and velocity (Jacobson, 2003; Khonsari and Booser, 2008). The rule of thumb to achieve hydrodynamic lubrication is to set lambda to >3.0 (Xin, 2011, pp. 665–667). Operating below this figure risks entering the mixed lubrication regime where asperity contact and wear begins (Xin, 2011).

In the context of finding the loading limit for testing a short-bearing approximation is used (DuBois and Ocvirk, 1953) since the HDE pump is designed with a journal bearing length to diameter ratio of 1. In this approximation method, the interpolation of Sommerfield charts determines the Minimum Oil Film Thickness (MOTF) as a function of journal speed, the load spread over the projected bearing area, the journal radius, the radial clearance and the viscosity of the fluid (Khonsari and Booser, 2008). Used in conjunction with the Stribeck curve and lambda criteria the load and speed limits can be estimated. Of course, these methods are steady-state and, assuming the conditions are met; the journal bearings should not wear (Khonsari and Booser, 2008). The mechanisms of wear, in reality, are caused by misalignment and edge loading,[12] starvation by design or blockage,[13]cavitation erosion,[14] and transient operations.[15] The wear model from Dufrane, Kannel and McCloskey (1983) is progressed to

[12] (Sander *et al.*, 2015).
[13] (Akagaki and Kato, 1992).
[14] (Rafique, 1963; Brewe, 2001; Wedeven and Ludema, 2012).
[15] (Khonsari and Booser, 2008).

consider lift-off speeds relating to start-stop,[16] or alternatively model the wear through a second order system,[17] although these models need further validation.

2.2.3 Worn Pumping Gears

The conventional use of gears is for the transmission of power where BS ISO 6336-1:2006 (British Standards Institution, 2006a) details the procedures for the design and application of gears. The primary function of a gear pump is not the transmission of power, but the fundamental design is the same as a gearbox (Shen *et al.*, 2018). The main concern for accelerated testing purposes is once again to set the test limits. The wear modes of gears are a function of load, sliding velocity, material, hardness, temperature and viscosity (British Standards Institution, 2006a). Generally, the primary failure modes contributing to pump flow degradation are those that alter the gear form over time such as macro-pitting, scuffing and abrasive wear (Maroney and Tessmann, 1977) as observed in a high mileage HDE gear pump returned at the request of CAB (2013), see Figure 2-5. The pumping gear exhibits an uneven flank wear pattern and significant advancement of spalling.

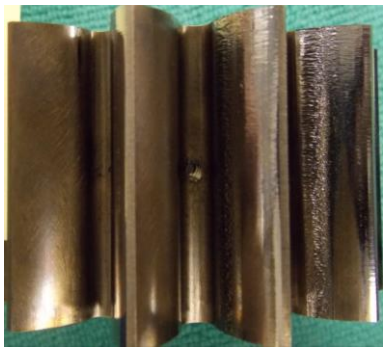

Figure 2-5 Report CI – 1357: 1,000,000 mile pump strip down, degradation of gear tooth surface (CAB, 2013).

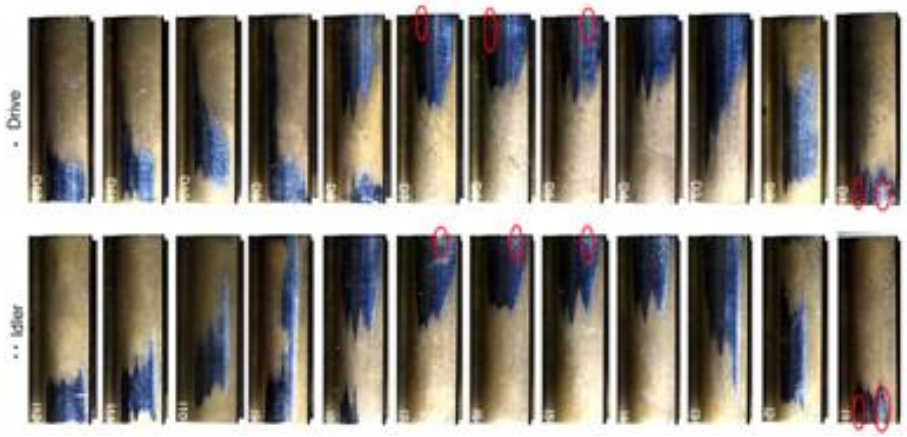

Figure 2-6 Report 61212 – uneven gear flank contacts and pitted (red region) pumping gears from a 226,000 mile vehicle application during in a NPD (Hannan, 2012).

[16] (Duckworth and Forrester, 1957; Harnoy, 1995; Khonsari and Booser, 2008).
[17] (Papadopoulos, Nikolakopoulos and Gounaris, 2008; Machado and Cavalca, 2015).

In terms of the HDE application, the formation of pitting is intolerable because there is a risk that the pit becomes an origin of a crack, ultimately leading to tooth failure. The risk of wear emanating at the tooth flanks is calculated from the theory of contact fatigue resulting in the form of macro and/or micro pitting (British Standards Institution, 2014b) which can progress into macro pitting, spalling and seizure (British Standards Institution, 2006a). The pumping gear flank images in Figure 2-6 illustrate the uneven wear pattern and pitted regions of a NPD after 226,000 miles. Another mechanism is scuffing caused by the highly localised temperature at the tooth flanks breaking down the lubrication (Anderson, 1982; Cheng, 2001; Höhn and Michaelis, 2004; NSWC Carderock, 2011).

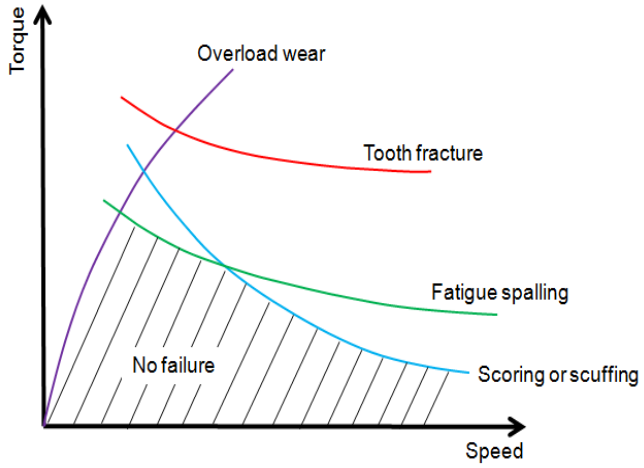

Figure 2-7 Operating regimes for a gear system and the expected failure mechanism (Anderson, 1982).

Using the standards BS ISO 6336-1:2006 (British Standards Institution, 2006a), the limits of the gear form, the pump operation and material can be set as illustrated in Figure 2-7 (Anderson, 1982). In this figure, there is a hatched "no failure" zone (Anderson, 1982) for the accelerated test to operate. The standards also demonstrate how to estimate the contact and bending fatigue life of the gear based on a steady-state duty cycle and Palmgren-Miner's cumulative damage model (British Standards Institution, 2006a). It is standard practice to validate the gear life through accelerated fatigue testing assuming the accelerated test is equivalent to the cumulative damage model of the normal usage duty cycle (Oda, Koide and Mizune, 1985; Kumar, Hirani and Agrawal, 2017). The acceleration factor is achieved by increasing the drive power using increased load, speed or both, providing the no failure zone thresholds, for example the limit of where fatigue spalling can occur (as in Figure 2-7), are not exceeded. Most recently Shen *et al.*, (2018) used computational fluid dynamics to estimate the outlet pressure in the gear mesh zone of an aviation fuel pump and input this stress into a gear contact fatigue model. In doing so, the fatigue prediction estimated the contacts to fail (Shen *et al.*, 2018) and is expected to help with increasing the initial reliability (R_0) before procuring hardware.

2.2.4 Contamination

As previously mentioned in Sections 1.4 and 2.2, the hydraulic pump industry states that 70% of pump failures are due to contamination (Eaton-Vickers, 2002; Dias, 2012; Singh, Lathkar and Basu, 2012). A typical source of contamination is external to the pump through the ingress of particles through seals, poor deburring and cleanliness methods of the pump and/or the application components (Eaton-Vickers, 2002; Dias, 2012; Singh, Lathkar and Basu, 2012). There are multiple sources of contamination generated internally through abrasion, adhesion, fretting, erosion and cavitation (Silva, 1990), from which the analysis of the lubricant and particles will reveal the likely source (Day, 1996; Singh, Lathkar and Basu, 2012). The fundamental mechanism of wear from contamination is described as three-body wear (Dias, 2012) which can happen in two ways. The first mechanism is when a contamination particle with higher hardness than the two component materials tumbles between the clearances of two components with relative motion as shown in Figure 2-8 (Dias, 2012). In doing so, the particle abrades and removes the softer material creating a wear particle (Dias, 2012).

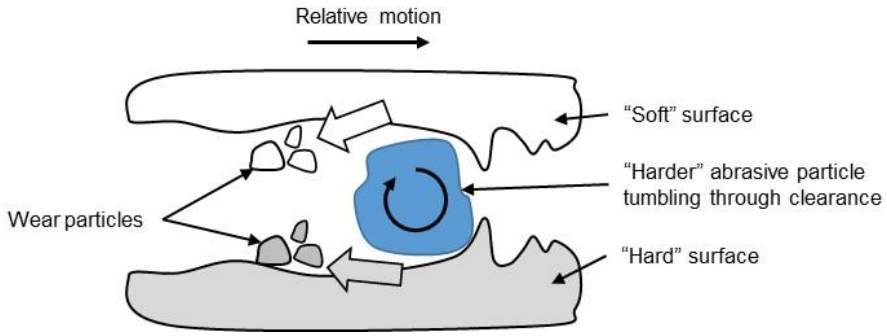

Figure 2-8 Three-body wear with tumbling contamination particle adapted from Dias (2012)

The alternative mechanism is when the contamination particle becomes embedded in the softer particle, as illustrated in Figure 2-9 (Dias, 2012). The wear particle is generated from the harder component (Dias, 2012).

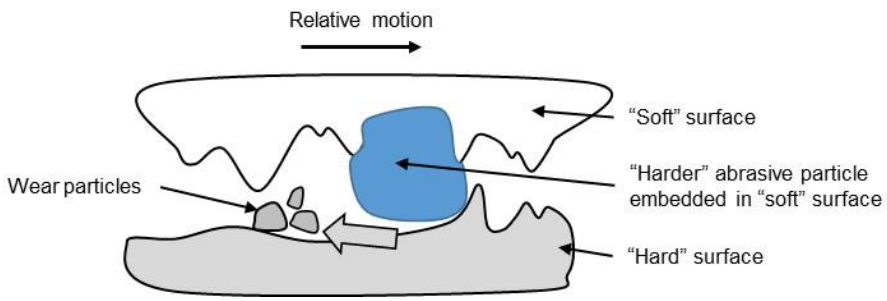

Figure 2-9 Three-body wear with embedded contamination particle adapted from Dias (2012)

There were extensive efforts in the late 1970s and through the 1990s to standardise and grade the sensitivity of a pump to contamination. By introducing contamination, the wear of the pump was accelerated; however, on review, the theory leaves unanswered questions (Tabor, 1977; Frith and Scott, 1993). The first phenomena observed from the specific pump study is an exponential wear activity with a time constant of approximately 9 minutes that had large variability (Frith and Scott, 1994). It is thought the reason for this is a diminishing ability of the introduced particles to abrade (Frith and Scott, 1994). A second phenomenon is that the blockage of clearances can increase volumetric efficiency (Frith and Scott, 1993). A third phenomenon is when the contamination acts as a bearing surface without generating wear (Frith and Scott, 1993). The probability of a wear particle generation, the size and shape of the contributing particle, hardness, geometry and the properties of lubrication with additives all add to the complexity of modelling wear (Fitch, 1986; Godet *et al.*, 1991; Williams and Hyncica, 1992; Glaeser, 2001).

In terms of reliability, there appears to be little in the way of correlating accelerated wear testing to pump life. The ge-rotor pump journal bush wear studies by Ranganathan, Hillson and Ram (2004) and, Ranganathan and Mohanram (2005) attempt to correlate an accelerated wear test to field mileage without considering these phenomena nor statistical testing or errors.

2.2.5 Cavitation Erosion

The definition of cavitation erosion is "*a form of damage to the surface of a solid body in liquid caused by implosion (violent inward collapse) of cavities or vapour bubbles*" (British Standards Institution, 2008). Cavitation is a phenomenon where the static local pressure of the fluid is below the vaporisation point of the fluid at a given temperature essentially allowing the fluid to evaporate and form micro-bubbles of vapour (British Standards Institution, 2008). The high-energy micro-bubbles flow to a higher local pressure, typically at a surface of the component, and then implode on impact causing very high-pressure shock waves and material removal (British Standards Institution, 2008; Buono et al., 2017). Four types of cavitation erosion are classified (British Standards Institution, 2008): (1) high velocities at sharp edges of geometry, (2) impact from the abrupt changes in flow such as opening and closing of ports, (3) suction causing a low pressure, (4) the fluid inertia from a sudden change in direction causes a local depression. This phenomena alters the vibration frequency (Buono et al., 2017) and adjusts the airborne noise emitted from a pump (Edge and Johnston, 1990). The prediction of cavitation has been successfully modelled using computational fluid dynamics (Frosina et al., 2014) however the sequence of damage and severity of wear is yet to be fully developed (Franc, 2009; Buono et al., 2017).

2.2.6 Gear Pump Wear Mechanism Summary

The field of wear is multi-faceted and co-dependent, particularly with respect to gear pumps. The mechanisms of gear pump wear are categorised into three sections; (1) Relative motion between contacting interfaces, (2) contamination and (3) cavitation erosion. With factors such as particle hardness, particle size, shape, distribution, wear particle generation, loss of abrasion, the blockage of clearance and the particles acting as bearings (to name but a few) it is acknowledged that a systematic pump wear model would be paradoxical (Godet *et al.*, 1991). The attempts to accelerate the wear using contamination is a practical method to degrading pumps quickly, but the correlation to life requires an extensive study to understand the factors as mentioned above. A summary of pump wear mechanisms and their effects on the pump is given in Table 2-1.

Table 2-1 Failure modes of wear for external gear pumps.

Failure Mode	Failure Effect	Failure Cause(s)
Journal bush wear	Pump seizure. Increased pump noise and vibration.	Contact of journal and bush from misalignment and/or overload.[18, 19, 20, 21, 22] Stop-start application not generating sufficient fluid film.[18, 19, 21, 23, 24,25, 26] System operates in boundary or mixed lubrication regime.[18, 20, 21, 24, 27, 28, 29] Adhesive wear from contacting journal and bush.[18, 27, 28, Abrasive wear from contamination.[18, 19, 22, 27, 28, 30] Cavitation wear.[18, 19, 20, 21, 28] Insufficient lubrication.[18 21, 27, 28, 29] Starvation from soot blocking feed holes and clearances.[18, 21, 24, 28]
Worn pumping gears	Reduced flow and efficiency. Increased pump noise and vibration.	Pumping gears from misalignment and/or overloaded.[31, 32, 33, 34] Contact fatigue.[27, 31, 33, 34, 35, 36] Scuffing.[27, 32, 34, 35] Abrasive wear from contamination.[34, 37, 38] Insufficient lubrication.[27, 31, 34]

(*Continued*)

[18] (British Standards Institution, 2008).
[19] (Rafique, 1963).
[20] (Szeri, 1978).
[21] (Khonsari and Booser, 2008).
[22] (Papadopoulos, Nikolakopoulos and Gounaris, 2008).
[23] (Mokhtar, Howarth and Davies, 1977).
[24] (Green, Lewis and Dwyer-Joyce, 2006).
[25] (Machado and Cavalca, 2015).
[26] (Chun and Khonsari, 2016).
[27] (Wedeven and Ludema, 2012).
[28] (Vencl and Rac, 2014).
[29] (Childs, 2014).
[30] (Duckworth and Forrester, 1957).
[31] (British Standards Institution, 2006a).
[32] (Anderson, 1982).
[33] (Zaretsky, 1987).
[34] (Cheng, 2001).
[35] (British Standards Institution, 2000).
[36] (British Standards Institution, 2014b).
[37] (Maroney and Tessmann, 1977).
[38] (Dudley, 1980).

Table 2-1 Failure modes of wear for external gear pumps (*Continued*).

Failure Mode	Failure Effect	Failure Cause(s)
Worn pump casing	Reduced flow and efficiency. Pump seizure. Wear debris generation. Increased pump noise and vibration.	Contact from pumping gears from misalignment and/or overload.[39, 40, 41, 42] Adhesive wear from contacting pumping gears.[43, 44] Abrasive wear from contamination.[43, 44, 45, 46, 47] Cavitation wear.[39, 40, 41, 42, 43, 44, 46, 47] Erosive wear.[43, 44, 48]
Pump cavitation	Erosion of pumping elements and casing. Reduced flow and efficiency. Increased pump noise and vibration.	Pump fill limits reached.[49, 50, 51] Fluid vaporisation pressure reached.[49, 51, 52, 53, 54] High velocities from small areas or changes in cross-section.[49, 51, 52]

[39] (Koç, 1989).
[40] (Koç, 1994).
[41] (Koç, 1991).
[42] (Koç and Hooke, 1997).
[43] (Smrdel and Clason, 2012).
[44] (NSWC Carderock, 2011).
[45] (Frith and Scott, 1993).
[46] (Frith and Scott, 1994).
[47] (Frith and Scott, 1996).
[48] (Niu, 2002).
[49] (Franc, 2009).
[50] (Buono *et al.*, 2017).
[51] (Kazama and Totten, 2012).
[52] (Edge and Johnston, 1990).
[53] (Greene and Casada, 1995).
[54] (Bose, 1966).

2.3 Case Study Application, Commercial Truck Engine

The purpose of this section is to state the complexities and considerations of a HDE platform that can be used for a variety of applications. The importance of understanding the HDE application becomes apparent in terms of the stress-varying environment and the implications on pump life, particularly regarding the vehicle driving habits and the associated factors. The final sub-section provides insight into the stress extremities the pump needs to function within.

2.3.1 Driving Patterns

An Original Equipment Manufacturer (OEM) will design an engine model (platform) to suit a range of vehicle applications, for example to power on-highway trucks, tankers, vehicle transporters, tipper trucks and crane trucks, city buses and coaches (Giakoumis, 2016, p. 194). The type of application will determine the different usage profile in terms of the engine's duty, the payload and the environmental conditions in which they operate (Giakoumis, 2016, p. 3). For example, a city bus will have a significantly larger number of accelerations as a consequence of increased stopping and starting than an on-highway truck (Giakoumis, 2016, p. 194). A vehicle on mountainous terrain in Switzerland will have a higher engine load than one operating in the Netherlands plains, and a vehicle in northern Sweden will experience freezing weather in winter as opposed to a vehicle in southern Spain in the peak of their winter.

With such diversity of applications and environments, the OEMs and suppliers face the challenge to pass regulatory vehicle emissions and fuel economy tests set by governing bodies such as the Federal Environmental Protection Agency (EPA), the California Air Resources Board (CARB), the European Union (EU), or the United Nations Economic Commission for Europe (UNECE) (Giakoumis, 2016, p. 194). For diesel engines, the transient tests are the most arduous from a NOx and particulate matter viewpoint (Rakopoulos and Giakoumis, 2009). The definition of a transient cycle uses a sequence of test points to represent the vehicle speed, engine speed and engine torque characterised for a time period (Rakopoulos and Giakoumis, 2009). The engine speed and torque are normalised to reflect the difference in transmissions and power. Several transient cycles exist to simulate the various driving patterns and vehicle speeds, usually segmented by urban, rural and motorway driving typically in the space of 1800 seconds. (For an example see Figure 2-10).

The three widely adopted transient cycles are the European Transient Cycle (ETC), the Federal Test Procedure (FTP) and the World Harmonised Transient Cycle (WHTC). The difference between duty cycles is represented in the histogram in Figure 2-11. The WHTC is the most recent cycle released in 2001 that replaces the ETC. The WHTC reflects the trend

for heavy-duty vehicles to spend their time at peak torque, whereas the FTP cycle was developed in the late 1970s and reflects a very high duty at idle and high engine speed.

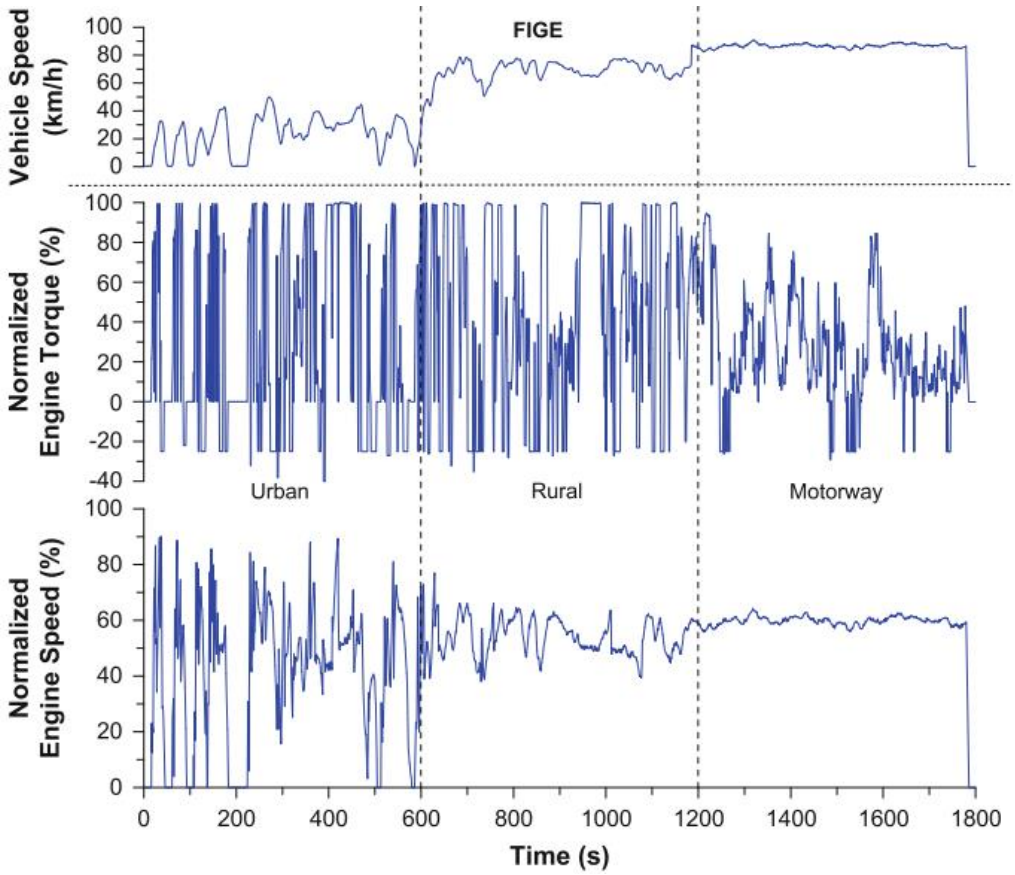

Figure 2-10 ETC, normalised engine speed and torque profile (Giakoumis, 2016, p. 208) Copyright © 2017, Springer International Publishing AG.

From a reliability perspective, these duty cycles allow calculations based on the assumption that each damage cycle has a constant degradation rate throughout the speed range and that Palmgren-Miners rule of cumulative damage is applicable (Bertsche, 2008), and this is a typical approach for bearing and gear fatigue calculations (British Standards Institution, 2006c). The OEMs will also provide suppliers with their estimated duty cycles specific to their applications. However, a new trend is emerging for OEMs to share the transient vehicle data, particularly for all electric and electric hybrid vehicles where accurate vehicle range is critical (Kumar Pathak *et al.*, 2016; Lee *et al.*, 2018). This data is primarily for the use of estimating fuel-saving technologies and strategies, yet the author recognises a gap in knowledge in applying these transients to reliability estimations for stress-varying degradation rate modelling. This gap is analysed in Submission 6 (Zarzycki, 2018b) where the standard transient cycles are compared to customer specific data.

The methodology for collecting custom driving patterns is influenced by several factors categorised into (Ericsson, 2000):

- Driver factors (attitudes, experience, gender, age and physical condition).
- Vehicle factors (vehicle type, engine power, mass, age, size, application).
- Weather factors (road surface conditions, precipitation, visibility, humidity, temperature, wind speed, wind direction).
- Traffic factors (traffic mix, speed, direction, flow, time of day).
- Street environment factors (street design, street function, traffic management).
- Travel behaviours (the type of journey, distance, time, choice of route).

The quality of a drive cycle depends on its data collection, the analysis, cycle construction and the cycle validation. Regarding data collection methods, two primary options are available. A reasonably low resource method is to instrument one vehicle (called a chase vehicle) to follow target vehicles. This method has been criticised for inconsistencies (Morey, Limanond and Niemeier, 2000). The better option (providing resource is available) is to add instrumentation to multiple vehicles that record the global positioning and all the engine control unit variables that are readily available. The quality of the collection is reflected in the sample size, the trip length, the variation and interdependencies between factors, and the volume of data (Ericsson, 2000; André, 2004).

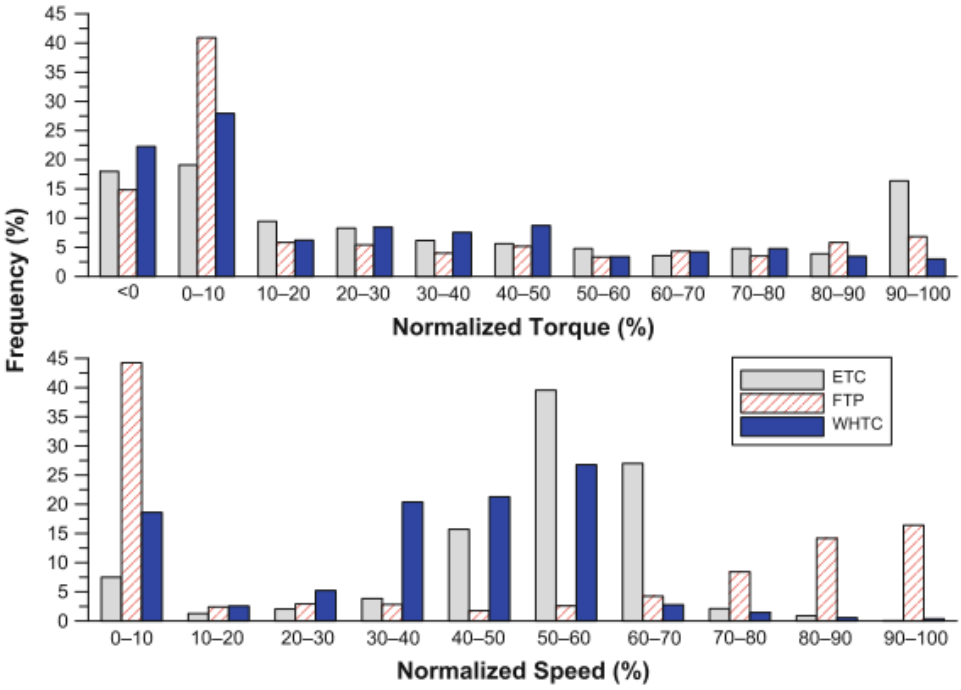

Figure 2-11 Histogram of normalised speed and torque for ETC, FTP and WHTC (Giakoumis, 2016, p. 277)

After data collection, the characterisation and dependencies of factors are analysed. The most recent methods use Principle Component Analysis to characterise the patterns such as in the ARTEMIS project (André, 2004) or stochastic modelling as developed by Lin and Niemeier (2003). The advantage is an improved resemblance to the driving cycle in exchange for only local applicability. The final step is the validation of the cycle on an engine dynamometer.

The future of transient driving cycles is already present. In March 2016, the European Commission introduced the Real Driving Emissions (RDE) legislation (EU) 2016/427 (EC, 2016) requiring vehicle manufacturers to publish the data collected during real driving set within real driving boundaries to improve quality and accuracy in reporting emissions and fuel economy. There is an opportunity to exploit this for reliability estimations as vehicle connectivity grows and the challenges of Big Data are overcome (Meeker and Hong, 2014).

A future consideration is given on the impact of hybridisation for ancillaries such as oil and coolant pumps. The reduction in ancillary parasitic loses is achieved by driving the pumps with electric motors allowing independent speed control from the engine or traction motor (Gao *et al.*, 2015). This independence brings increased complexity for a duty cycle where a pump's operation is governed by control strategies for heat rejection as a function of the driving pattern and vehicle speed rather than solely where the engine speed lies (Redfield *et al.*, 2006).

2.3.2 HDE Installation and Stressors

Additional to the typical engine speeds and loads, the gear pump for a HDE must survive in a hostile environment. The combination of the oil temperature and engine speed are the most significant contributors to pump load because as the viscosity changes this influences the power required to pump through the restriction and alters the outlet pressures. The OEM specification will state the environmental limits of operation typically entailing:

- Steady-state duty cycle, as previously mentioned.
- Oil temperatures:
  - Continuous: + 90° C to + 120° C
  - Transient (2 min): - 40° C to + 135° C
- Ambient temperatures:
  - Continuous: -40° C to + 130° C
  - Transient (2 min): up to + 140° C
- The number of cold starts at -40°C
- The pump must withstand oil aeration without any damages with max 10% volume

- Withstand a max internal oil pressure up to 25E5 Pa
- Vibrations
- The lubrication and the mix of contamination e.g. as 45% used engine oil 44.5% new engine oil 10 % diesel fuel (FAME) 0.5% coolant/water mixture.

However, the authors' experience recognises these ranges to be extremes and help to increase the pump robustness. An additional stressor not understood for gear pumps is the degradation of engine oil and the impact of extremely hard and small soot particles from the combustion process. Soot particles have a 988 to 1302 Vickers hardness (kgf/mm^2) and a typical size 50nm to 2μm (Li *et al.*, 2002) which are likely to contribute to 3-body wear through the pump clearances (Section 2.2.1). Wear is evident as soot has been shown to increase wear rates in pistons (McGeehan *et al.*, 1998; Li *et al.*, 2002; Kaneta *et al.*, 2006). Regarding accelerated testing, the ideal is to use real engine oil; however, the repeatability is challenging to control. The next best is to simulate the soot with carbon black to control its level and distribution (Green and Lewis, 2008).

When the objective is to verify that the lifetime requirements can be met, the importance of knowing the application and how the duty cycles were derived is critical. For example, the same HDE can be installed in a bus, which may have a high number of transients from stop-starts or a truck that has steady-state cruising on a highway. The review highlights the complexity of capturing this data and signifies the shift from standardised test cycles to real life driving reports. The advantage of this is yet to be taken in terms of improving the accuracy of correlating laboratory lifetime tests to the field.

2.4 Wear Detection

Machine condition monitoring is a process described in BS ISO 13381-1:2015 (British Standards Institution, 2015) as having five phases. The first phase is the detection of a problem (British Standards Institution, 2015) in this case study the desire is to capture the onset of gear pump wear-out before the pump has a catastrophic failure. In doing so there is an improved chance of diagnosing the fault and the fault mechanism (phase two) before the problem manifests to create consequential damages (British Standards Institution, 2015). The remaining three phases are concerned with prognosis, recommended actions and post-mortems (British Standards Institution, 2015). The objective of this section is to report the detection methods of pump health and the reasoning for developing a pressure ripple monitoring method. The standard BS ISO 17359:2018 (British Standards Institution, 2018a) lists examples of condition monitoring parameters for common machine types, such as an electric motor, compressors and pumps. A summary of advantages and disadvantages for pump monitoring methods are listed in Table 2-2. Fluid temperature, static pressure, fluid flow, drive power,

and overall efficiency are standard practice in measuring pump performance and are assumed to be readily available without additional funding, as such these are excluded from the remaining discussion.

The cost of instrumentation. The initial investment to acquire pressure ripple monitoring is comparable to vibration monitoring. Both techniques require data acquisition ideally with 24-bit resolution anti-aliasing and Integrated Electronics Piezo-Electric (IEPE) sensors (International Organization for Standardization, 2015). Whereas the alternative of wear debris analysis methods such as Spectrometric Oil Analysis Procedure (SOAP) (Jones, 1979; Glaeser, 2001) and Ferrography (Barwell *et al.*, 1977; Macián *et al.*, 2006; Wu *et al.*, 2008) requires specialist equipment that merits outsourcing. The following considerations propose why pressure ripple is the preferred choice for detecting pump degradation.

The ease of installation, setup and repeatability. The installation of dynamic pressure transducers into the pipework is standardised and straightforward as detailed in ISO 10767-1:2015 (International Organization for Standardization, 2015) with the sensors installed downstream of the pump. Unlike vibration testing, there is no concern about the casting and fixture stiffness nor the position of the accelerometer on the pump, especially with a design change. Nor is pressure ripple concerned with the external environment regarding reflected surfaces unlike acoustic measurement methods (Crocker, 2007) making it reasonably practicable in the test cell.

Sensitivity to change in pump health. The vibration and acoustic noise measurements are standardised practices of rotary machines that are proven to detect abnormalities (Carden and Fanning, 2004). Vibration is commonly used to detect bearing degradation and tooth damage and cavitation (Carden and Fanning, 2004; Robert B Randall, 2007). Although not often cited for condition monitoring, pressure ripple is the direct measurement of the interior pump condition that accounts for slippage and gear profile (Eaton, Keogh and Edge, 2006; Yang, Edge and Johnston, 2008) and casing wear, including cavitation (Eaton, Keogh and Edge, 2006) whereas contamination monitoring has the potential advantage to identify which components are degrading (Jones, 1979; Glaeser, 2001).

The response time of the method. Real-time capability is available for vibration, acoustic noise, pressure ripple and particle counting. Off-the-shelf in-line particle counters can only detect ferrous sources of wear debris (Bowen, 1981; Fitch, 2012) whereas with state-of-the-art techniques, such as online visual ferrography, the characterisation of the source is possible in-line (Cao *et al.*, 2015). However, these methods are not readily available, fully validated nor commercialised.

The use of pressure ripple has the added advantage that the instrumentation is likely to be readily available as a requirement from the OEM to characterise the pressure ripple primarily in terms of amplitude. The relative simplicity of the installation of pressure ripple

and its insensitivity to the external environment helps with the setup repeatability in a test cell that continually switches products (Liu and Hung, 1991). The disadvantage is the development of the feature extraction to make use of the signal as a degradation parameter and its relation to a failure mechanism which is proposed in this report. The development of a feature extraction method is reported in Chapter 3.6.

Table 2-2 Summary of wear detection methods.

Parameter	Method	Advantages	Disadvantages
Acoustic noise	Sound power measurement.[55]	Direct. [55] Sensitive depending on setup and instrumentation accuracy. [55]	Cost of hardware.[56] Sensitive to the repeatability of set up and exterior environment.[55, 56, 57] Ideally needs anechoic chamber.[55, 57]
Vibration	Accelerometer installed on pump casing.[59]	Direct.[58, 59, 60] Sensitive.[58, 59, 60] Multiple feature extraction methods.[58, 60]	Careful design and installation of accelerometer.[58, 59, 60] Sensitive to the repeatability of set up and exterior environment.[58, 59, 60] Output is a function of fixture and casing stiffness.[58, 60] Cost penalty for high resolution and data acquisition rates.[58,61]

(*Continued*)

[55] (British Standards Institution, 1992).
[56] (Fanti *et al.*, 2002).
[57] (Jacobsen, 2007).
[58] (Harris, 1996).
[59] (British Standards Institution, 2018b).
[60] (Robert B Randall, 2007).
[61] (Hansen, 2007).

Table 2-2 Summary of wear detection methods (*Continued*).

Parameter	Method	Advantages	Disadvantages
Contamination monitoring and wear debris analysis	Particle counting.[62, 63] Spectrometric Oil Analysis Procedures.[62, 63, 64, 65,] Ferrography.[62, 63, 64, 65, 66, 67, 68, 69]	Wear debris characterisation.[62, 63, 64, 65, 66, 67, 68, 69, 70] Ease of installation for particle counting.[62, 63]	Specialised equipment required.[62, 64, 63, 65, 66, 67, 70] Outsourcing the analysis is time-consuming.[62, 66, 70] Repeatability of sampling.[70] Control of cleanliness.[62, 65, 70] In direct.[62, 64, 65, 70]
Dynamic pressure	Piezo-electric pressure sensor for dynamic pressure ripple measurement.[71]	Direct.[71, 72, 73, 74, 75] Multiple feature extraction methods.[76] Insensitive to exterior environment.[73, 76, 75] Ease of installation.[72, 73, 76,75]	Cost of instrumentation.[72] Cost penalty for high resolution and data acquisition rates.[72]

[62] (Day, 1996).
[63] (Glaeser, 2001).
[64] (Hofman and Johnson, 1977).
[65] (Anderson, 1982).
[66] (Seifert and Westcott, 1972).
[67] (Jones, 1979).
[68] (Wu *et al.*, 2008).
[69] (Cao, Wang and Wang, 2012).
[70] (Fitch, 2012).
[71] (Edge and Johnston, 1990).
[72] (International Organization for Standardization, 2015).
[73] (British Standards Institution, 1999).
[74] (Liu and Hung, 1991).
[75] (Liu and Hung, 1991).
[76] (Silva, 1986).

2.5 Degradation Modelling

The ability to predict the timing of inevitable failures is highly desirable for the management of maintenance operations and safety-critical applications (Goode, Roylance and Moore, 2000). Decisions to balance operating expenses can be made to avoid unplanned downtime or to extend the remaining useful life (RUL) of a machine, aided by detecting and modelling the potential failure (Moubray, 1997, pp. 146–147; Goode, Roylance and Moore, 2000). The P-F curve in Figure 2-12 is generally used to assist in all maintenance models, including the management of reliability centred maintenance (RCM).

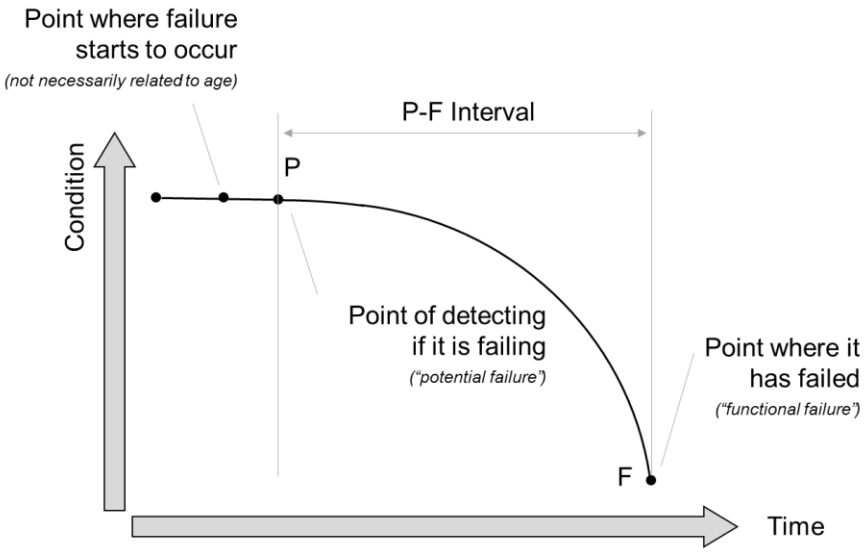

Figure 2-12 The P-F interval curve (Moubray, 1997, pp. 144–145).

The P-F curve illustrates the failing condition of a machine over time where the deterioration is detected at point 'P'. If left to degrade without intervention the hazard rate generally accelerates until there is a catastrophic failure at point 'F' (Moubray, 1997, pp. 144–145). The P-F interval indicates how often the deterioration should be checked, which sets the reaction rate of the maintenance schedule depending on the risk of safety, downtime and repair costs (Moubray, 1997, pp. 146–147). To optimise this methodology, the field of Prognostics and Health Monitoring (PHM) is a rapidly expanding subject in providing the solutions (Xia *et al.*, 2018; Zhang *et al.*, 2018; Hu *et al.*, 2019). BS ISO 13381-1:2015 (British Standards Institution, 2015, p. 4) states the principles of prognosis are to define the end of life, set the expected degradation rate, estimate the current state and the time to failure with a satisfactory confidence level. The choice of degradation modelling is wholly circumstantial on the machine and the desired objective (Heng *et al.*, 2009). Figure 2-13 from Tsui *et al.* (2015)

illustrates an example of Lithium-ion battery capacity as a function of charging cycles. Using an algorithm based on particle filtering Tsui *et al.* (2015) are able to predict the RUL accurately, particularly towards the batteries end of life where there is a notable change in performance. In the context of NPD, the field of PHM is a valuable source in learning about the choice of models to use in an ADT.

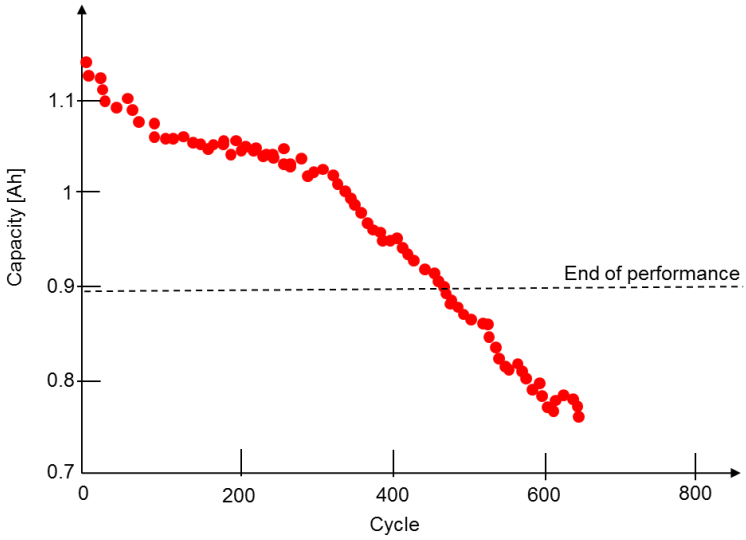

Figure 2-13 Example of real life performance degradation of Li-ion battery (Tsui *et al.*, 2015).

As previously mentioned in Section 1.6, the ADT is designed to deteriorate the product over time to a predefined threshold (in this project defined as the pseudo-failure threshold) where the degradation (or performance) is unacceptable (Meeker, Escobar and Lu, 1998). The time it takes for the degradation path to cross the threshold C is used to construct a time to failure (or pseudo-failure) distribution (Lehmann, 2010, pp. 157–180). Tomsky (1982) gives three criteria to define unacceptable degradation; (1) the hypothesis of a zero gradient is statistically rejected, (2) the confidence band of the regression mean drifts out of a predetermined pseudo failure level in a specified time, (3) the tolerance band for the population drifts out of the specification in a specified time. How quickly the parameter drift reaches the threshold is a function of the failure mechanism (Moubray, 1997, pp. 144–145). By monitoring the deterioration, a model can be fitted to the degradation path, the choice of which depends on the objective and level of required complexity.

Several models are available to describe the behaviour, increasing in complexity and representation of the physical phenomena of degradation. For instance, *Curve fitting* which smooths the data and often inadequately represents the physical mechanism (Khamis and Higgins, 1996; Nelson, 2004, pp. 527–534). The advantageously simple *constant rate* model is a linear function of degradation against constant stress but assumes all samples are identical

such as Palmgren's equation for bearing life (Nelson, 2004, p. 87,527-534). The *Bosch* (Bosch, 1979) model is simply an extension of the linear model that uses a first-order differential to model the degradation rate, but it requires significant sample size to be statistically confident (Jones, 1999). The *random coefficients model* includes variation for each test unit's starting point and constant degradation rate (Kim and Bae, 2013; Weaver and Meeker, 2014).

The *random walk process* (see Figure 2-14) more adequately describes a degradation path of the randomness of actual systems. In the simple case of a linear relationship, a drift parameter represents the random variation $e_i(t)$ of degradation around a trend line as illustrated in Figure 2-14 and described by equation (2.2).

$$y_i(t) = a_0 - b_i t + e_i(t) \tag{2.2}$$

Where $y_i(t)$ is the cumulative degradation, a_0 is the initial parameter, b_i is the rate of degradation and i is the ith value in time t. The point at which the degradation is unacceptable is defined as is the threshold C, illustrated in (see Figure 2-14) .

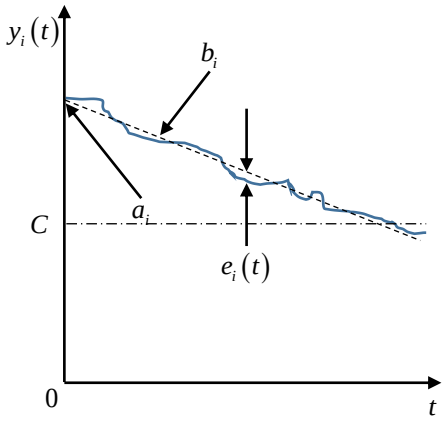

Figure 2-14 Random walk process model around a linear degradation relationship.

Within the random walk process, there are many variations. Mercer and Smith (1959) developed a model for the life of a conveyor belt with a random walk and cumulative degradation as a continuous mean abrasion and compared this to more damaging but less frequent discrete blows. The *Mercer* model works best assuming constant stress throughout the degradation. It is mathematically intractable but only requires a minimum of two data points making it ideal for small data set or early life predictions (Jones, 1999). The *Møltoft* (1980) model is a random walk process model with two thresholds that calculates the

probability the drift rate will cause failure in a known time. However, it only works with drift rates independent of their initial values and failure mode (Møltoft, 1980; Jones, 1999).

The *Majima* (1965) model only requires two measurements (start and end) to model degradation as a monotone random walk with a singular threshold. Two normal distributions are assumed for the initial distribution of the measurements and one for the drift rate, making the mathematics complex (Jones, 1999). The *Loughborough* model (Jones and Hayes, 1987) is an adaption of the Majima model that considers the intermediate data points using the Least Squares Method to estimate the drift and diffusion parameters.

In Jones and Hayes (1987) the four models of Linear, Majima, Møltoft and Loughborough were tested using capacitance degradation data. The drift behaviour for all models was compared with how precisely the early data points predict the actual degradation (Jones and Hayes, 1987). Their findings indicate the standard error for the Linear and Møltoft models to be significantly larger than the Majima and Loughborough counterparts but improved as the time increased (Jones and Hayes, 1987). Whereas the Majima model has the lowest standard error, it took twice as long to converge and output a marginally conservative estimate compared to the Loughborough model which was marginally optimistic (Jones and Hayes, 1987). Generally, the Møltoft model is most useful with the availability of early data (Jones, 1999).

A further subset of random walk process is the *Wiener* process (also known as the *Brownian motion* process model with drift) which is widely studied for modelling non-monotonic degradation assuming a normal distribution (Tian, Wu and Chen, 2014; Wang *et al.*, 2016). When the degradation is a strictly increasing, and a non-negative independent process, then modelling with the *Gamma* process can be used as an alternative to a deterministic model (Park and Padgett, 2006; Pan and Sun, 2014; Lim, 2015; Tsai *et al.*, 2016). If the degradation path is strictly monotone, the *Inverse Gaussian* process has better properties in coping with covariates and random effects than the Gamma Process (Ye *et al.*, 2014) as illustrated in a situation of competing failure modes (Li and Jiang, 2009).

In an application measuring the wear of roller bearings, although the overall trend was material loss as modelled by Mercer (1961), the measurement error was significant enough to influence the results and indicate the addition of material rather than the removal (Hersant *et al.*, 2012). In this situation, a deterministic model or Gamma process model is inadequate because the data must be strictly increasing. The Brownian Motion (BM) process can model such a problem of independent incremental randomness and non-monotonic degradation (Liao and Tseng, 2006; Peng and Tseng, 2010; J.-R. Zhang *et al.*, 2011; Hu, Lee and Tang, 2015). Uses include estimating the useful life of vehicle batteries (Wang *et al.*, 2017) or the RUL of pump bearings using vibration data (Tian, Wu and Chen, 2014). The most related study to the

gear pump is in the estimation of remaining useful life of an axial piston pump with significant variation in the leakage measurements (Wang *et al.*, 2016).

It should be noted the assumption that the BM process has a strong Markovian property (Zhang *et al.*, 2016). The principle of a Markov property is that the next state of a process is dependent on its current state and cumulative damage, not on the history of stress (Bogdanoff and Kozin, 1985, p. 74), making the BM model suitable for step-stress testing (Zhang *et al.*, 2018).

The *random increments* model is an extension of the random walk process model and is useful for modelling positive correlations (Tomsky, 1982). For instance, where test unit initial measurements (a_0) are high and remain high and where the test unit initial measurements are low and remain low (Tomsky, 1982). The random increments mode is typically chosen for wear fatigue and crack growth (Zaludova and Zalud, 1985; Owen and Padgett, 2000; Nelson, 2004; Sun *et al.*, 2012). The *proportional hazards* model (Cox, 1972) is a multiple regression technique that can be used to determine the baseline hazard rate (Bendell, 1985). The proportional hazards model assumes that stress acts multiplicatively on the hazard rate and that the hazard rate does not vary over time (Bendell, 1985). The advantage of this model is it only depends on stress; thus it was applied to optimise an ALT plan for a simple step-stress test (Elsayed and Zhang, 2007; Elsayed, 2012). The PHM is increasingly being used in accelerated testing (Huber, 2010; Chiquet and Limnios, 2013, p. 2), although its use is restricted to the Weibull distribution (Tobias and Trindade, 2012, pp. 320–321).

Finally, in a dynamic stress environment where the rate of degradation is dependent on the stress, researchers have developed the BM model to include covariates that vary with drift and diffusion coefficients (Singpurwalla, 1995; Gebraeel and Pan, 2008; Liao and Tian, 2013; Bian and Gebraeel, 2014; Bian, Gebraeel and Kharoufeh, 2015; Zhang *et al.*, 2018). For example, the drift coefficient of bearing degradation related to the temperature was modelled as an exponential covariate (Jin *et al.*, 2013). The paper by Singpurwalla (1995) was perhaps the first to review the state-of-the-art development regarding random walk process-based models for survival analysis, focusing on the inclusion of dynamic environments that change the hazard rate of a component or system. The first consideration of time-dependent wear was modelled as a stochastic process by Mercer (1961) and, recognising its importance, Singpurwalla (1995) steered the reliability community further in this field. The most current review of the BM model development is given by Zhang *et al.* (2018) including nonlinear models, age and state-dependent models, multi-source variability, covariates and multivariate degradation.

To summarise, detecting the start of potential failure and modelling the point of failure is highly desirable from a RCM and PHM perspective. These fields provide a plethora of

degradation models that can be used in the context of NPD. Generally, a model features a performance threshold where the product is considered to have failed once it has been crossed. The objective of the model is to achieve precision in the reliability estimate accounting for the stochastic degradation mechanism(s) and unit-to-unit variability. The random walk models continue to develop in complexity, considering competing failure modes and stress-varying environments. The loads on a HDE gear pump are also dynamic; therefore BM model with drift and diffusion covariates is preferred, as reported in Submission 4 (Zarzycki, 2017b), Submission 5 (Zarzycki, 2018a) and Submission 6 (Zarzycki, 2018b).

2.6 Parameter Estimation

As previously discussed in Section 2.5 the stress-varying environment and stochastic state variables can be modelled as a Brownian motion model with drift and diffusion covariates (Zhang *et al.*, 2018). This model has two unknown parameters $\boldsymbol{\theta} = (\mu, \sigma^2)$, the drift coefficient μ and the diffusion coefficient σ^2 (Kahle, Mercier and Paroissin, 2016). These parameters need to be estimated, and two approaches are recommended (providing the events have already occurred); the Maximum Likelihood Estimation (MLE) (Meeker, Escobar and Lu, 1998) and/or Bayesian methods (Li and Meeker, 2014).

The *likelihood* is a frequentist approach using statistics to estimate the probability of a specific outcome providing an event has already occurred (William Q. Meeker and Escobar, 1998; Nelson, 2004, p. 233). This frequentist approach is data-driven and objective (O'Hagan and Oakley, 2004). The MLE is a method for estimating the maximum value(s) of a parameter for a known likelihood distribution (Stapelberg, 2009, pp. 193–198) for example, a Gaussian (Normal) distribution. This method is consistently proven successful in reliability for sample sizes above five (Tseng, Balakrishnan and Tsai, 2009).

An alternative to the frequentist methods is Bayesian methods. Bayes Theorem allows the likelihood to be adjusted with a prior distribution reflecting a belief (Li and Meeker, 2014) as illustrated in Figure 2-15. Due to the incorporation of bias this method is the subject of strong debate (Box and Tiao, 1973; Bernardo and Smith, 1994), however it has been demonstrated that objective (non-bias) priors (Robert, Chopin and Rousseau, 2009) output similar outcomes as the MLE (Berger, Bernardo and Sun, 2009; Xu and Tang, 2012b). The advantage is that once the sample size is below five the statistical validity of MLE is in question, and Bayes theorem is a technique proven to improve the accuracy of small sample sizes and adjust the outcome closer to the measured data (Meeker, 2010; Li and Meeker, 2014; Guan, Tang and Xu, 2016).

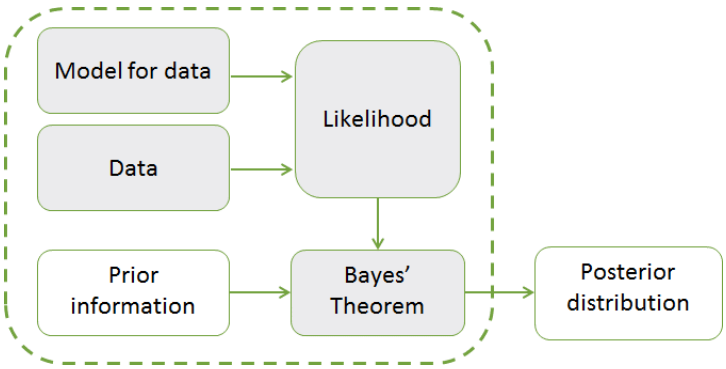

Figure 2-15 Bayesian concept (Li and Meeker, 2014).

The choice of prior distribution can have a profound influence on the outcome (Kass and Wasserman, 1996; Berger, Bernardo and Sun, 2009; Wang and Zhou, 2009). If there is no knowledge or confidence in the prior distribution, then the prior should be modelled with *ignorance* (Kass and Wasserman, 1996). Ignorance means to specify a prior that has as minimal impact on the likelihood as possible by using a non-informative (diffuse) prior (Kass and Wasserman, 1996). For example, the default for Bayesian statisticians is to apply Jefferys Prior (Jeffreys, 1946) as this is both invariant under re-parameterisation and proper (integrated to 1) (Kass and Wasserman, 1996). Providing confidence that the prior knowledge is not biased, the alternative is to apply reference priors (as used in simulating degradation testing of carbon film resistors) (Xu and Tang, 2012a; Guan, Tang and Xu, 2016). The downside of the reference prior is the difficulty of finding the closed form solution which strengthens the popularity of using Jefferys prior in the first instance (Kass and Wasserman, 1996).

A Bayesian methodology using Jefferys prior was used by Wan *et al.*, (2014) in a simulated step down accelerated degradation test. Wan *et al.*, (2014) used the preceding step test data as the prior and illustrated improved precision on the parameters' estimates for extremely small sample size 2 compared to the MLE.

In summary, parameter estimation using the MLE is less precise with extremely small samples sizes. Using Bayesian methods allows the option to adjust the likelihood based on prior knowledge. In the situation of NPD or no prior knowledge, the outputs using Bayes can remain objective and data-driven by using non-informative priors. To improve the estimate using extremely small sample size the Bayesian methodology of Wan *et al.*, (2014) illustrated increased precision by incorporating the preceding step test data. This methodology is developed in Section 3.7.

Chapter 3: Methodology for Estimating Reliability

In this chapter, an original methodology is developed for answering the main research question as illustrated in Figure 3-1. The justification of this methodology originates from estimating the reliability of gear pump wear-out from an extremely small sample size of two. To output a reliability estimation with confidence intervals the sample size needs to be increased. However without investment in more physical hardware and test time, then numerical simulations are a reasonably practicable alternative (Wu and Lewins, 1992; Law and Kelton, 2000, p. 4). The decision to use Monte Carlo simulation when modelling the degradation path of a measured parameter is given in Section 3.8.

Pump pressure ripple is chosen as the degradation parameter because it is a sensitive and direct measurement of pump health. The standard position of the sensor is remote from the pump. Therefore any design change (during the NPD) will not affect the validity of the test setup and the validity for comparing reliability growth as explained in Sections 3.5 and 3.6. The signal analysis is developed to extract a degradation parameter from the pressure ripple that can be modelled as justified in Sections 3.5 and 3.6.

The choice of degradation model is a function of a stress-varying environment from a HDE vehicle converted into pump pressure. The vehicle transients (accelerations) are critical in a cumulative damage model because it affects how quickly the damage reaches a pseudo-failure threshold (PFT), as reported in Submission 5 (Zarzycki, 2018a) and Submission 6 (Zarzycki, 2018b). The pump outlet pressure is used as a stressor because this is directly related to pump speed (and therefore flow), viscosity (and thus temperature) and the unit-to-unit variation between pumps and the application. Knowing that wear is the process of material removal, the degradation was expected to be monotone. However, the pressure ripple measurements indicate some recovery (negative increments). Thus the degradation process is stochastic and not strictly monotone (Zarzycki, 2017b). In this case, a BM model with covariates for drift and diffusion is justified.

A step-stress test accelerated degradation provides the data to estimate the drift and diffusion functional relationships to pump outlet pressure, see Section 3.4. These stresses are set using the PoF for the pumping gear contact fatigue and the seizure limits of the plain bearings. Because the test sample is extremely small, a Bayesian regression analysis is used to estimate the drift and diffusion parameters. This innovative method uses the preceding step test data to improve precision as detailed in the parameter estimation Section 3.7.

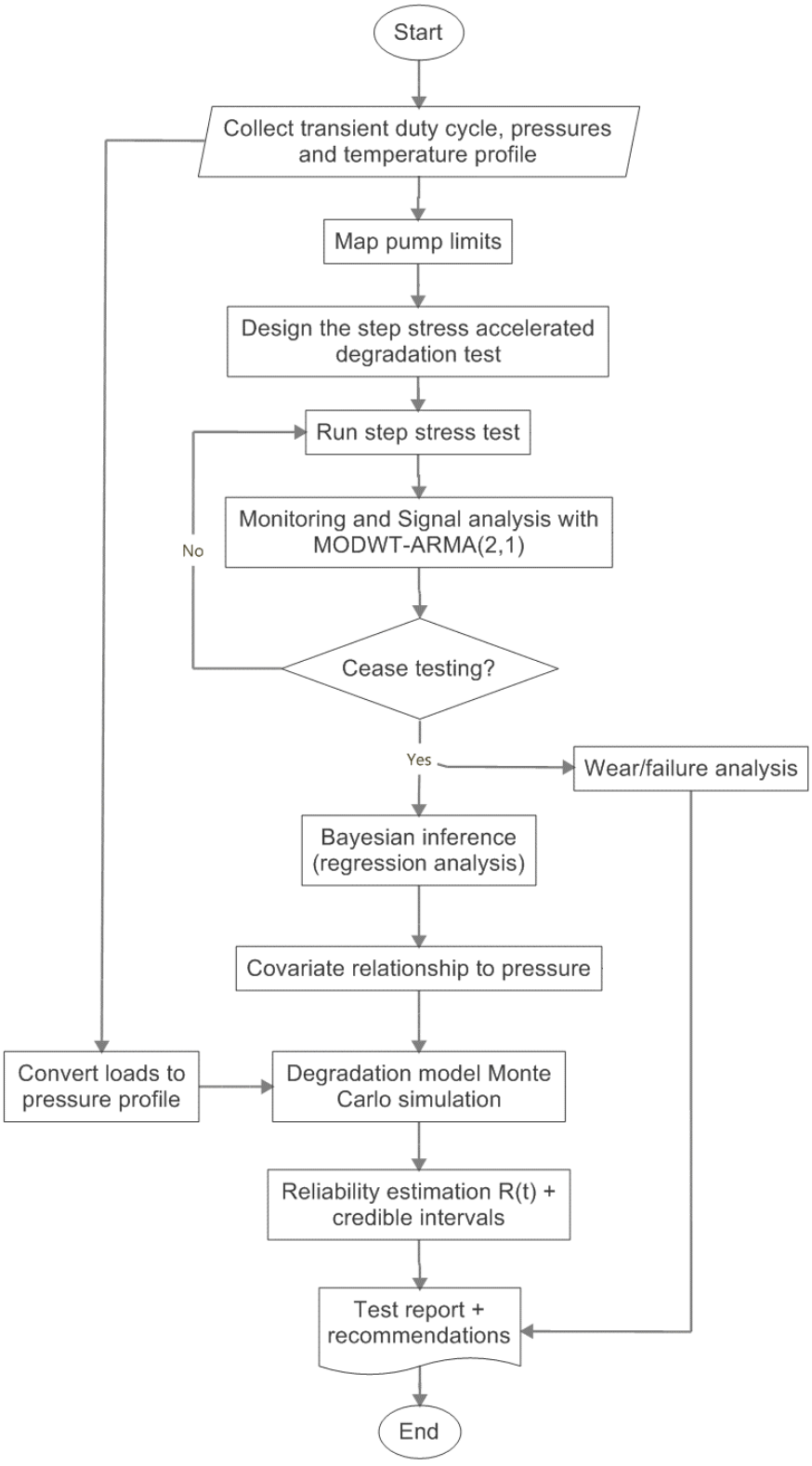

Figure 3-1 The proposed methodology for estimating lubrication gear pump reliability.

The flow of the methodology post-testing is demonstrated conceptually in Figure 3-2, Figure 3-3 and Figure 3-4. The raw pump pressure ripple signal in the time domain (1) is passed through the MODWT (2) which is then processed through the ARMA(2,1) to output the delta Omega over time (3). The data is regressed using the MLE or Bayesian analysis method to estimate the drift and diffusion coefficients (4). The functional relationship between the drift and diffusion coefficients to the stress is established (5).

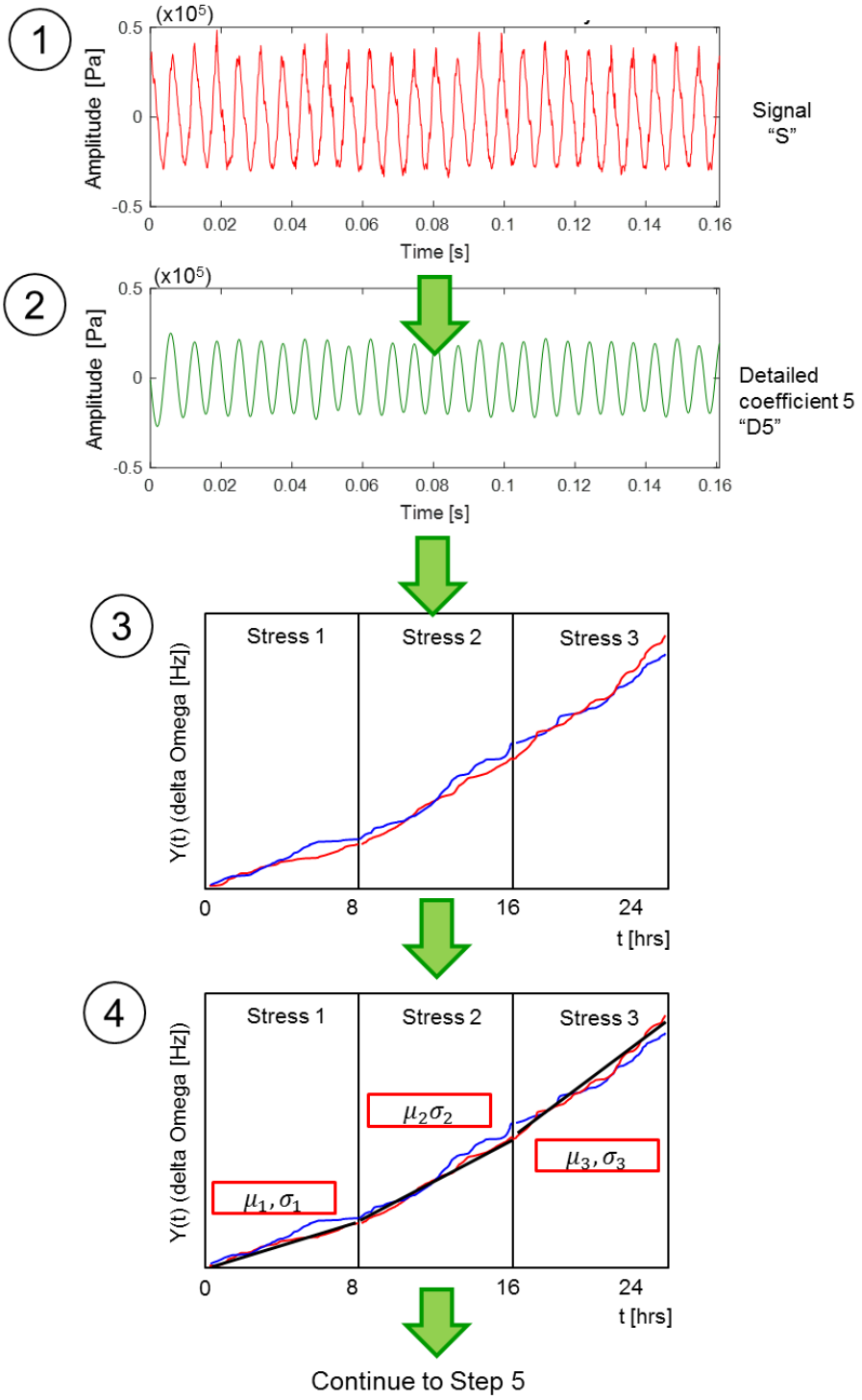

Figure 3-2 Steps 1 to 4: Flow of methodology post-testing for estimating lubrication gear pump reliability.

The simulation then input the pump mission profile (6) and converts this to stress (pressure) as a function of the application (7). In combination with the covariate relationships (5) and the stress (7) the MC simulation simulates the degradation for a significantly larger sample size (8). The first PFT for each sample is stored and a distribution is generated (9) from which the reliability CDF is created and the quantiles of interested are estimated (10).

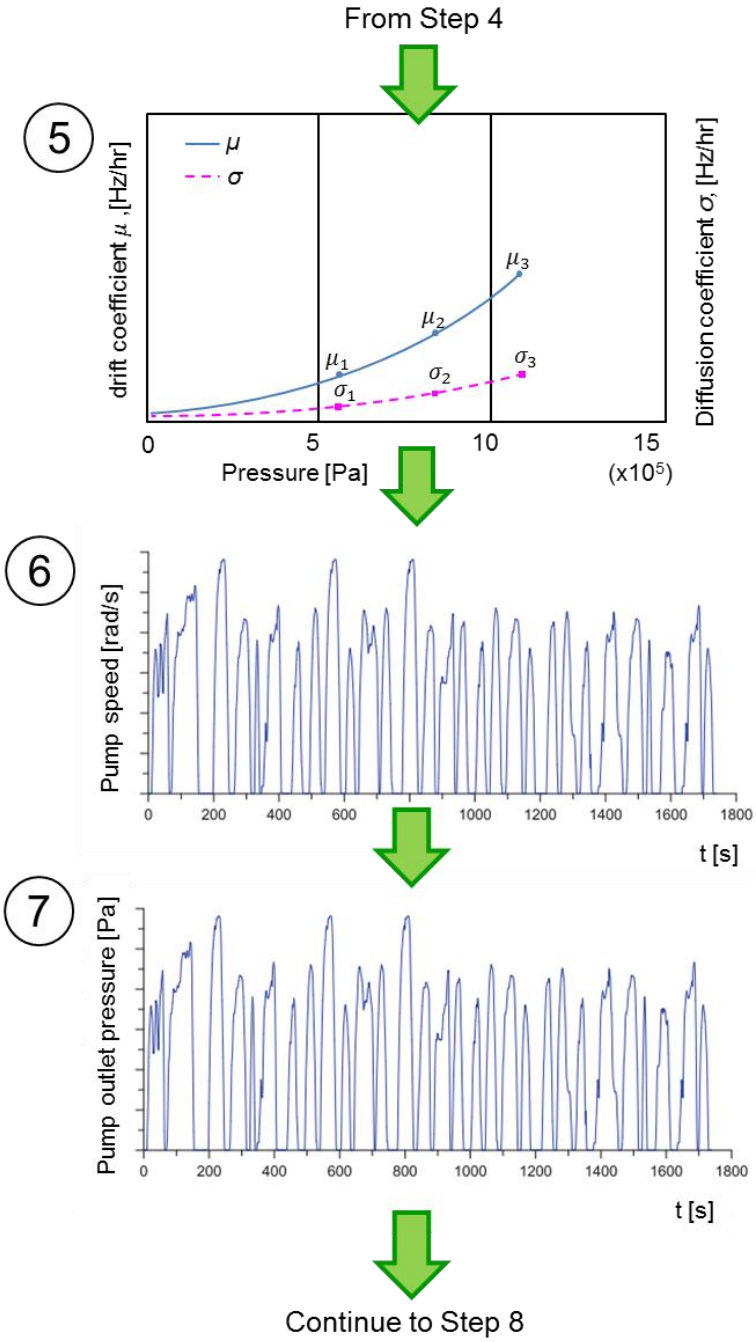

Figure 3-3 Steps 5 to 7: Flow of methodology post-testing for estimating lubrication gear pump reliability.

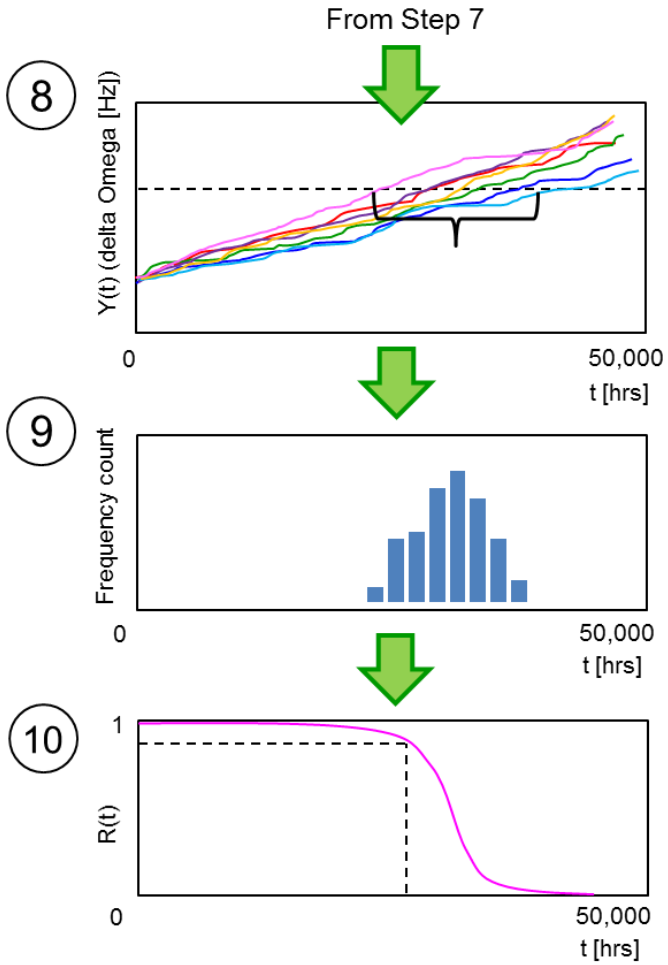

Figure 3-4 Steps 8 to 10: Flow of methodology post-testing for estimating lubrication gear pump reliability.

3.1 Drive Cycle Collection

The development of the degradation model requires engine transient cycle data representing the real driving pattern of the vehicle engine, rather than using the standard emissions testing cycles. The degradation rate is dependent on the stress-varying pressure set by the engine speed, and as previously investigated in Submission 5 (Zarzycki, 2018a) the emissions test are not designed to be wholly representative of the vehicle life. The primary data from a CAB customer was available from a single instrumented vehicle test with one driver, running back and forth on a single carriageway 61.4km micro-trip route. The purpose of the vehicle testing was understanding fuel consumption in the winter season, but for the case study, there is no discrimination because the pump is mounted inside the engine sump. Only 3 sequential recordings were made available each lasting c.3200s, the approximate trip duration. The 3 cycles captured are stitched together sequentially to create a fourth cycle labelled "C04" is shown in Figure 3-5 and the histogram in Figure 3-6. This is reasonable

because that data is from a single vehicle and driver. The benefit is including all data available to improve correlation to the field.

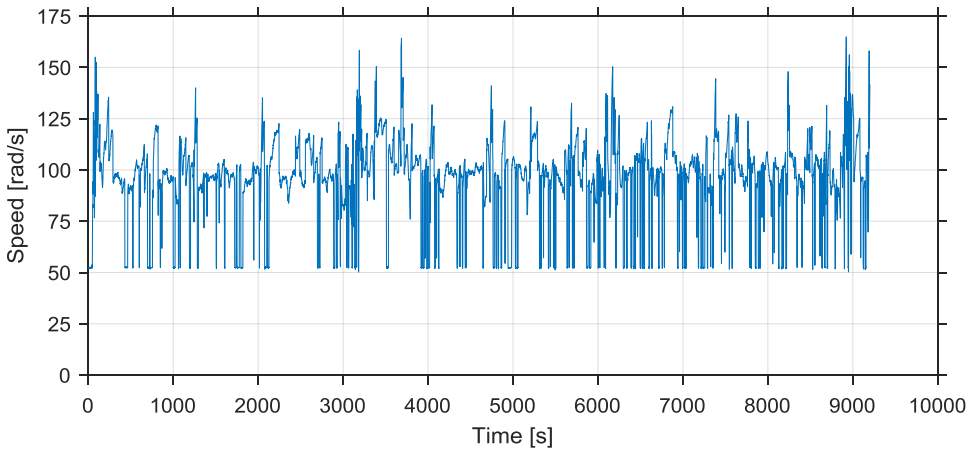

Figure 3-5 Engine speed, stitched transient cycles of 61.4km micro-trips, C04.

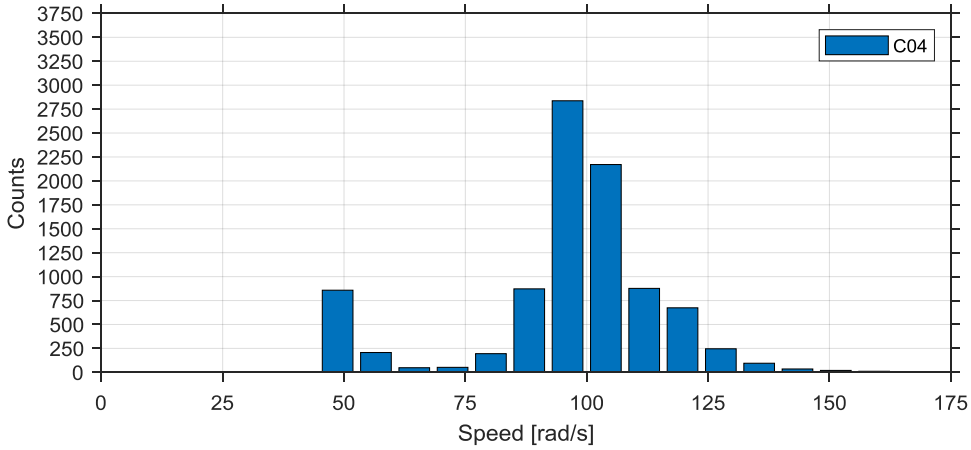

Figure 3-6 Engine speed histogram of stitched customer transient cycles, C04.

3.2 Experimental Setup

The ADT is performed on a test rig at CAB Birmingham Ltd on a new HDE lubrication pump development. The standard pump test, monitoring and recording procedures in BS ISO 4409:2007 (British Standards Institution, 2007) and BS ISO 17359:2018 (British Standards Institution, 2018a) apply. Beginning with the layout illustrated in Figure 3-7 and Figure 3-8, it adheres to the two pressure/two systems method ISO 10767-1:2015 (ISO, 2015) regarding the lengths and diameters of the stainless steel (10) reference pipe, (11) connecting pipe, (12) extension pipe and, the (3,5) piezoelectric transducer positions.

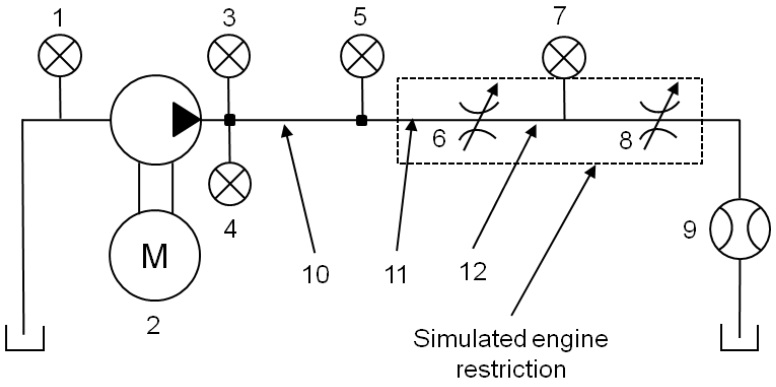

Key

1 Pressure transducer (Pump inlet)
2 Variable speed motor and pump
3 Piezoelectric pressure transducer no. 1 (Pump outlet)
4 Pressure transducer (Pump outlet)
5 Piezoelectric pressure transducer no. 2 (Pump outlet)
6 Loading valve (Engine inlet)
7 Pressure transducer (Engine gallery)
8 Loading valve (Engine gallery)
9 Flow meter
10 Reference pipe
11 Connecting pipe
12 Extension pipe

Figure 3-7 Test rig schematic.

The parameters in Table 3-1 are calculated specifically for the pump. Although it is recognised that ISO 10767-1:2015 is most useful for higher pressures >10E5 Pa (ISO, 2015) there are no alternatives for lower pressures.

Table 3-1 Discharge line description

Length of reference pipe	150[mm]
Inner diameter of reference pipe	Ø35 [m]
Length of extension pipe	200 [mm]
Method for changing standing wave mode in reference pipe (extension pipe or pressure vessel?)	Extension pipe
Wall thickness	2 [mm]
Material	Stainless steel 316L

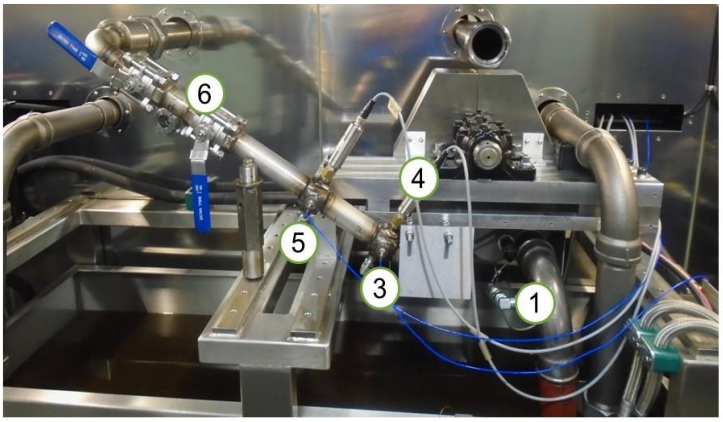

Key

1. Pressure transducer (Pump inlet)
2. Variable speed motor and pump
3. Piezoelectric pressure transducer #1 (Pump outlet)
4. Pressure transducer (Pump outlet)
5. Piezoelectric pressure transducer #2 (Pump outlet)
6. Loading valve (Engine inlet)
7. Pressure transducer (Engine gallery)
8. Loading valve (Engine gallery)
9. Flow meter
10. Reference pipe
11. Connecting pipe
12. Extension pipe

Figure 3-8 Test rig set up.

Cross-referencing with Figure 3-9, the rig simplifies the engine restriction using the loading valves (6 and 8). Valve (6) is the pressure drop across the engine filter, thermostat and oil cooler (Fenton, 1994; Arici, Johnson and Kulkarni, 1999) defined as boundary 8 in Figure 3-9, whereas valve (8) is the pressure drop across the engine bearings is defined as boundary 9 (Fenton, 1994; Arici, Johnson and Kulkarni, 1999) in Figure 3-9.

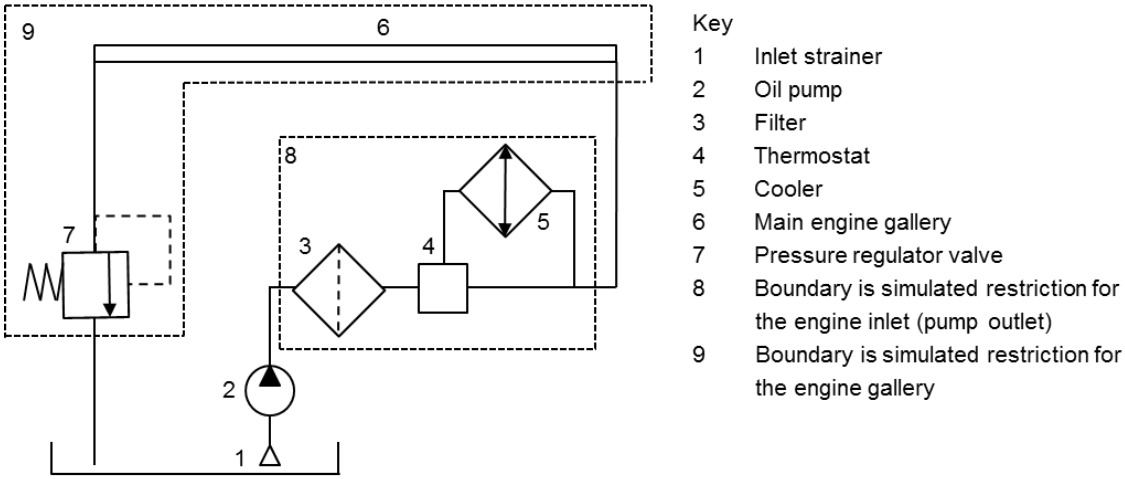

Figure 3-9 Engine Oil schematic adapted from Arici, Johnson and Kulkarni (1999).

An example of the setup test data demonstrating the pressure drop across the engine inlet (valve 6) and the engine gallery (valve 8) is provided in Figure 3-10 (CAB 2016).

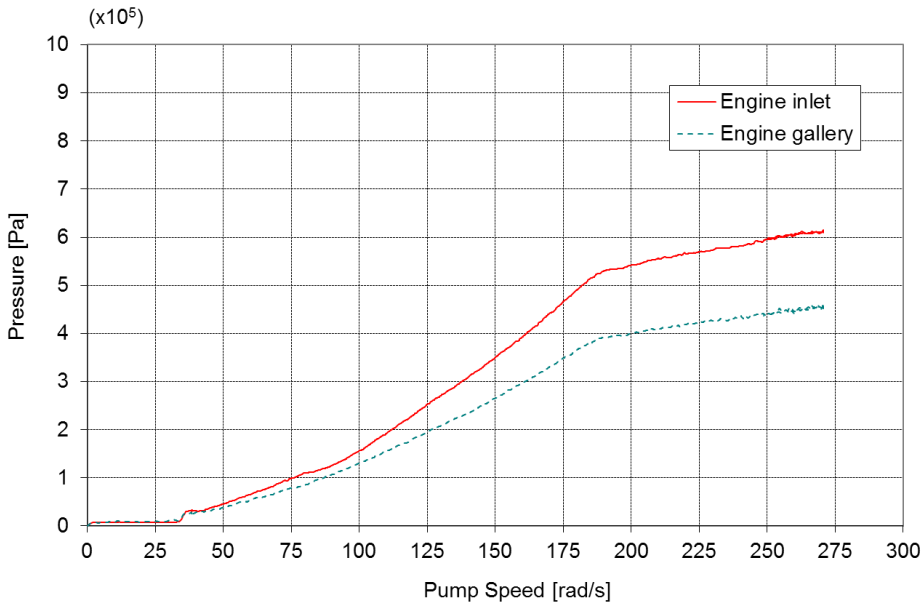

Figure 3-10 Example of pressure drop across the engine inlet and engine gallery for HDE (CAB 2016)

In this setup, the loading valves are manually operated because the hysteresis of the automated valves was too large to meet the repeatability requirements. The impact of using a manual valve is of no concern because once the orifice is set, it remains fixed for the duration of the test. The reproducibility in setting the valve and the measurement errors meet the BS ISO 4409:2007 (British Standards Institution, 2007) and ISO 10767-1:2015 (ISO, 2015) as documented in Appendix A.

The valve bore size is a standard size as close to the discharge pressure port of the test pump (refer to Table 3-2).

Table 3-2 Loading valves.

Manufacturer	NERO Pipeline Connections
Model	Three piece full bore ball valve socket weld
Range	1-1/4" internal diameter
Type	Full bore valve, stainless steel

Figure 3-11 Full bore valve

The inlet, outlet and gallery pressures (1, 4 and 7) are static pressure measurements used to set the restriction via the loading valves, as per the engine orifice settings. Usually, the more cost-effective transducers have temperature drift above 80°C, so as the typical operating temperature of HDE is 110°C, the chosen transducers are high temperature compensated to avoid non-linearity issues above 125°C, as per Table 3-3.

Table 3-3 Static pressure transducer.

Manufacturer	Roxspur Measurement & Control Ltd
Model	HPS - A Series 4-20mA Output Pressure Transmitter, temperature compensated to 125°C
Range	-1E5 to +1E5 [Pa] (Inlet) 0 to +25E5 [Pa] (Outlet)
Type	four active arm strain gauge bridge sensor, fused to a high-purity ceramic diaphragm
Accuracy	± 0.5 % of span (16mA) 0.00625E5 [Pa] (Inlet) 0.008E5 [Pa] (Outlet)
Repeatability	± 0.1 % of span (16mA)

Figure 3-12 Pressure transducer.

Piezoelectric transducers detect changes in pressure and are generally used for measuring the dynamic pressure above 1Hz because of limitations on the transducer construction and the charge amplifier (Gerges, Johnston and Rocha, 2012, p. 449). It is considered that miniature transducers are the most effective and robust because of the small sensor area and very high-frequency response (Gerges, Johnston and Rocha, 2012, p. 449). The transducer mounts flush on the pipework to avoid the risk of trapped air affecting the results.

The piezoelectric transducers require a charge amplifier and signal conditioning unit. For the model in Table 3-4, the amplifier is integrated into the sensor. The data acquisition and signal conditioning unit is a National Instruments NI 9234 (see Table 3-5) which has an

Integrated Electronics Piezoelectric (IEPE) signal conditioning at 2mA constant current. This unit features anti-aliasing filters and a 24-bit resolution as stipulated in ISO 10767-1:2015 (ISO, 2015). The sampling rate is up to 51.2 kHz, which is more than will be required because the 10th order maximum pump natural frequency is 8840 Hz. The pressure ripple is captured with commercial software developed by vibration and noise specialists M+P International, as this is already available at CAB.

Table 3-4 Dynamic pressure transducer.

Manufacturer	PCB Piezotronics MTS Systems Corporation
Model	Subminiature ICP® pressure sensor, 113B24
Range	0 to +68.95E5 [Pa]
Sensitivity	0.725 [mV/kPa]
Type	two quartz discs, a 2.5146mm diameter diaphragm and each with a built-in impedance-converting amplifier, two-wire, low-impedance operation
Accuracy	< 1.0% [FSD]
Frequency response	(-5%) 0.005Hz low-frequency response and (>=500 [kHz] resonant frequency)
Rise time	<1[μs]

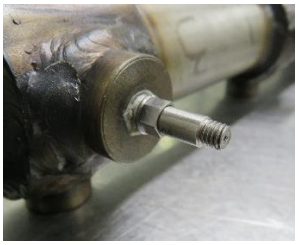

Figure 3-13 Piezoelectric pressure transducer.

The signal is recorded in the time domain, and it is conventional to analyse the signal in the frequency domain via a Fourier transform method ISO 10767-1:2015 (ISO, 2015). The decision for the author to develop the MODWT-ARMA(2,1) feature extraction method is discussed in Section 3.5.

Table 3-5 Pressure ripple data acquisition.

Details of data acquisition used to monitor pressure ripple	NI 9234 dynamic signal acquisition module.
Details of equipment used for frequency analysis (Commercial 24 bit analysing recorder and DFT on PC)	M+P Analyser, 24-bit analyser with anti-aliasing filters, maximum data rate 51.2kS/s. Original frequency analysis code MODWT-ARMA(2,1) by author
Bandwidth of frequency analyser	Maximum alias-free bandwidth 0.45 x f_s = 0.45 x 51.2kS/s = 23.04kS/s

Figure 3-14 NI9234 signal acquisition module .

The remaining test setup comprises of hardware previously commissioned on the rig. The 37kW motor (Table 3-6) is capable of running two pumps in parallel and is more than adequately sized to handle a single HDE pump.

Table 3-6 Drive motor.

Manufacturer	Siemens
Model	37 [kW]
Range	1500 [rpm] and 236 [Nm]
Accuracy	< 1% [rpm] and ±0.1 [Nm]

Equally, the torque meter (Table 3-7) is sized for 50Nm which under normal operation is adequate. This is a potential weakness in the setup if the accelerated test parameters require a torque above this setting.

Table 3-7 Torque meter.

Manufacturer	Magtrol Inc.
Model	TM310
Range	-50 to +50 [Nm]
Type	non-contact differential transformer
Accuracy	< 0.1 % of rated torque (<0.05 [Nm])

Figure 3-15 Torque transducer.

The flow meter specified in Table 3-8 is measured with an oval gear flow meter with a range large enough to handle the HDE lubrication pumps. The disadvantage is that the gear flow meter is susceptible to contamination and requires a filter upstream. This filter can create an undesired pressure drop that alters over time and adds doubt to the repeatability of the setup. The upstream filter was not used in the setup. The ideal choice would be to use a Coriolis flowmeter that does not require moving internal parts and is low maintenance.

Table 3-8 Flow meter.

Manufacturer	Titan Enterprises Ltd
Model	OG7-SS5-VHD-B
Range	5 to +500 [l/min]
Type	External oval gear, Hall effect sensing
Accuracy	± 0.5 % of reading with 30cSt Oil
Repeatability	± 0.1%

Figure 3-16 Oval gear flow meter.

The inlet, outlet and sump temperatures are measured in the fluid and pipework using conventional K-type thermocouples, Table 3-9. The reaction rates are typically within 2

seconds, but the primary function is to maintain the fluid temperature to achieve the correct viscosity throughout the test.

Table 3-9 Temperature measurement.

Manufacturer	RS Pro Type K Thermocouple
Model	RS397-1264
Range	-40°C to +1100°C
Type	Type 'K' (Nickel Chromium/Nickel Aluminium)
Accuracy	IEC 584 Class 1 -40 < t ≤375°C ±1.5

The system circuit is an open type with the 115-litre sump open to atmosphere as a function of the rig fabrication running two pumps. A typically HDE sump capacities are as large as 40 litres. During the experiment, the pumps will be run sequentially as the length of pipework required consumes the installation space. The test fluid is specified by the customer as SAE 10W30, the details of which are in Table 3-10.

Table 3-10 Test fluid properties.

Manufacturer	Fuchs
Model	SAE 10W30
Kinematic viscosity, in centistokes (cSt) (ASTM D445)	V40 = 85.76 [cSt] V100 = 10.58 [cSt]
Fluid density, in kilograms per cubic meter	V40 = 869.3 [kg/m3] V100 = 832.2[kg/m3]
Speed of sound in test fluid or effective isentropic tangent bulk modulus [bars]	1609 [ms-1] Calculated from ISO 10767-1:2015 (ISO, 2015)

The case study pump is a fixed displacement external lubrication gear pump for a HDE as described in Table 3-11 and shown in Figure 3-17. It is an underslung mount design that sits inside the engine sump and is fitted with a discharge pipe internal diameter of 32mm. The drive ratio of the engine to pump is masked for confidentiality. The pump contains a single set of pumping gears of 13 teeth each.

Table 3-11 Pump under test description.

Type of pump (e.g. axial piston, external gear) including any ancillary equipment	Gear
Type of displacement (e.g. fixed or variable)	Fixed
Type of displacement controller and setting	Driven by engine
Number of pumping elements	13 teeth gear pair
Diameter of discharge port	Ø32 [mm]
Type and power of pump drive	Engine crank gear driven (NA:1 drive ratio)
Type of pump mounting and details of any vibration isolation treatment	Sump mounted

Figure 3-17 Prototype pump no.1 used for SSADT.

In setting the quality of measurement recordings, the criteria for permissible variations in test conditions are set out BS ISO 4409:2007 (British Standards Institution, 2007) as speed (±0.5%), mean pressure (±2.0%), mean flow (±2.0%) and temperature (±2.0°C). These requirements are met as assessed in a Gauge Repeatability and Reproducibility study, see Appendix A.

The objective is to detect the point of potential failure (Moubray, 1997, pp. 144–145) by observing a significant change in the next monitoring point. Given the pump is not safety critical, a 95% confidence interval is acceptable ($\alpha = 0.05$). If an accuracy level of ±2.00% is required the sample size n needs to be at least 28:

$$CI = \pm t_{\alpha,\nu} \frac{\hat{\sigma}_d}{\sqrt{n_d}} \tag{3.1}$$

Where:

CI: Confidence Interval accuracy

$t_{\alpha,\nu} = t_{crit}$ One-tailed critical t value

ν: Degrees of freedom

n_d: The number of paired samples

$\hat{\sigma}_d$: The standard deviation of d_j values where

$$d_j = x_{1,j} - x_{2,j} \tag{3.2}$$

Where:

$x_{1,j}$ is the j^{th} value of dataset 1

$x_{2,j}$ is the j^{th} valve of dataset 2

Rearranging:

$$n = \left(\frac{t_{\alpha,\nu}\hat{\sigma}_d}{CI}\right) \tag{3.3}$$

Substituting values in

$$n = \left(\frac{1.6449 \times 0.3168}{0.1}\right)^2 = 27.15 \rightarrow 28$$

In summary, the test setup meeting BS ISO 4409:2007 (British Standards Institution, 2007) and ISO 10767-1:2015 (ISO, 2015) has been detailed, and the accuracy is documented in Appendix A.

3.3 The Gear Pump Wear Concept Model

The complexity of systemic wear is illustrated using the gear pump wear concept model in Figure 3-18 created by the author, that is a development from the debris distribution concept by Frith and Scott (1996) and mechanisms of wear from Silva (1987, 1990). The model is application specific and considers the sources of wear of a gear pump in the HDE and as such has not been illustrated in literature before (see Figure 3-18).

The volume of fluid V represents the HDE sump that holds a distribution of particles $\phi_1(x)$. It is conventional for an HDE lubrication pump to be mounted upstream of the HDE filter; thus it assumes the full distribution of particles will pass through the pump with flow $Q\ \phi_1(x)$. The wear debris generation from multiple sources adds to the distributions of particles that flows out of the pump with $Q\ \phi_2(x)$. The cumulative loss of material from the wear source(s) is characterised as abrasive particles $\phi_3(x)$ which is additive to the bulk particle distribution to described as $\phi_2(x) = \phi_1(x) + \phi_3(x)$. Internal recirculation and slippage denoted by q. It is assumed that the same distribution of particles in the main laminar flow out is also recirculated in turbulent flow $q\ \phi_2(x)$. The balance of flow is maintained with the internal recirculation flushing the wear debris $q\ \phi_3(x)$. The sources of wear are denoted with a w, for example, combustion soot wear contributes $q\ \phi_{w5}(x)$ to the total $\phi_3(x)$. The cumulative contribution of the wear source is $q\ \phi_3(x) = q\big(\phi_2(x) + \phi_{w1}(x) + \phi_{w2}(x) + \cdots \phi_{w10}(x)\big)$.

The purpose of this concept model is not to establish the contribution of particles from each wear source but to provide clarity for which operational factors will influence the wear source (as given in Table 3-12) and which should be targeted for accelerated testing.

The most useful control factors are the operational speed and load (using pump outlet pressure) as they will target six of the wear sources. These are gear tooth wear, cavitation wear (if there are localised low pressure), adhesion, bearing and casing wear (if the load is too high for the contact interface), and erosive wear (if there are areas of high velocity). The alternatives such as temperature and oil grade are intrinsically linked, but the normal operation of a HDE will specify the oil grade and typically operates at 110°C. The start-stop parameter is not the most significant influencing factor as it only targets contacts. The other groups of contamination are a function of the environment and not so easily controlled. It is therefore reasonably practicable to focus efforts on speed and load as acceleration factors.

Table 3-12 Influence of pump operation factors on wear source mechanisms (response factors).

Control Factor	Gear tooth wear	Cavitation wear	Adhesion wear	Corrosive wear	Combustion soot	Internal contamination	External contamination	Bearing wear	Casing wear	Erosive wear
Speed	☑	☑	☑					☑	☑	☑
Load	☑	☑	☑					☑	☑	☑
Temp	☑	☑	☑	☑				☑	☑	☑
Oil grade	☑	☑	☑	☑				☑	☑	☑
Start-stop	☑		☑					☑	☑	

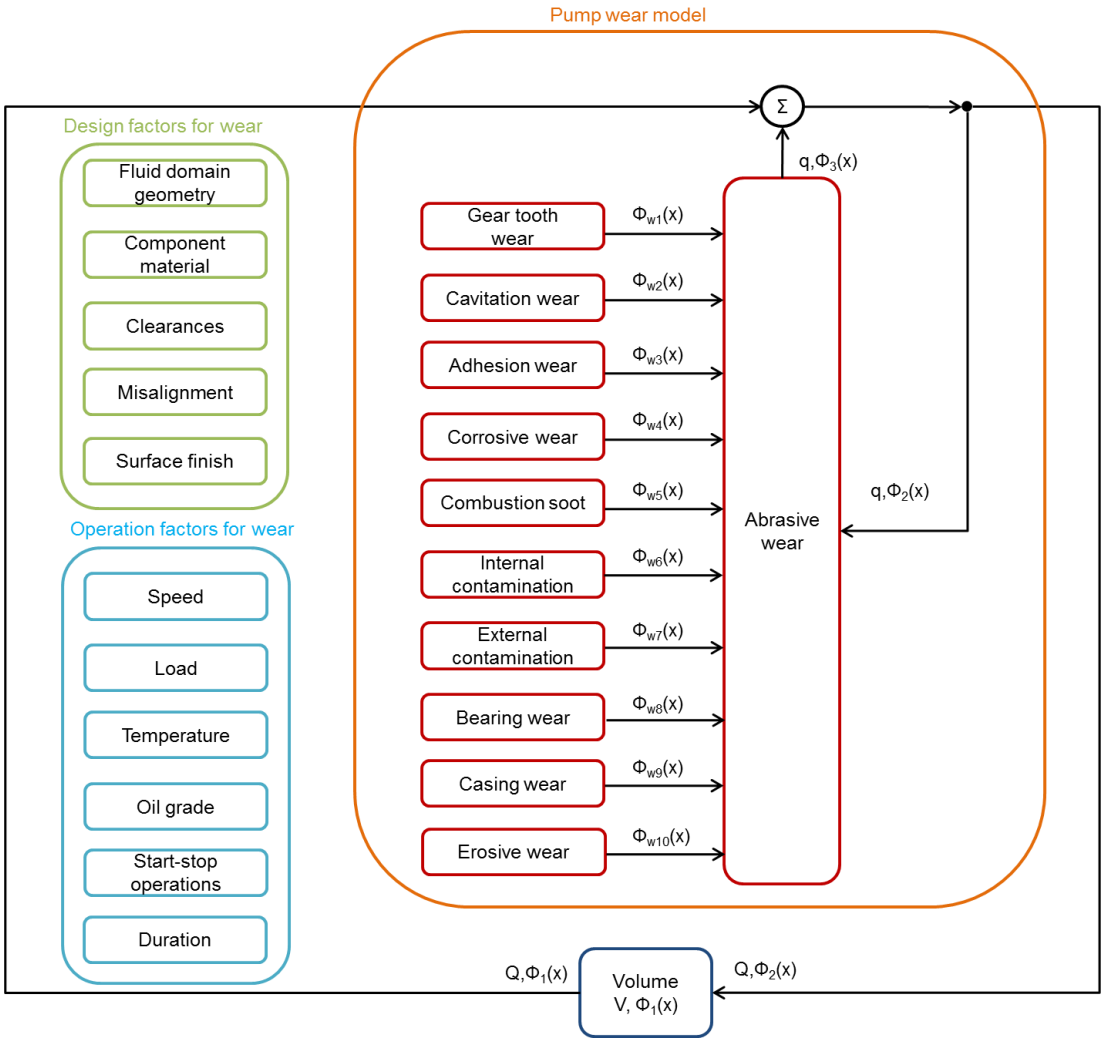

Figure 3-18 HDE lubrication gear pump wear concept model.

3.4 Step-stress Test Design

Consider the five systemic test control factors in Table 3-12, the ideal study of these factors and interactions merits the use of a full factorial Design of Experiment (DoE) (Montgomery, 2013). The DoE aids in understanding the response of a system when altering the control factor level. In a full factorial design, a five-factor (c) and two-level system with only one repetition (r) needs $2^c r = 2^5.1 = 32$ runs. For example, Guo and Mettas (2007) used a two-factor, two-level full factorial design with 150 samples to minimise the required measurement intervals for an accelerated degradation test; however, it must be noted that this method required pre-existing data for the degradation process. As the number of factors increases the required runs increases exponentially (Montgomery, 2013). Escobar and Meeker (1995) and Xu and Fei (2007) used DoE to plan an accelerated life test with more than two control factors however this was in an experiment knowing that there are no interactions between the factors. When the researcher needs to understand if a non-linear relationship exists, then three points are required to observe this. In a full factorial design, a five-factor and three-level system with only one repetition needs $3^c r = 3^5.1 = 243$ runs. The five control factors in Table 3-12 do not all require three levels; speed (3-level), pressure (3-level), temperature (3-level), oil grade (2-level), start-stop (2-level). The result is a full factorial design with 1 replicate requiring 108 runs. The number of runs is further compounded if a statistical understanding of the sample population is needed, then the number of replicates has to be greater than one. There are several DoE techniques to minimise the required number of runs such as the fractional factorial design,[77] blocking,[77] the Plackett-Burman design,[77] response surface methods,[77] the Latin square,[78] Latin hyper-cube,[79] and the Taguchi method.[80] The disadvantages of these minimal run techniques are concerned with aliasing,[77] and resolution that can mislead the inferences made.[77]

As a reminder, the objective is for the case study to emulate the early stage of a NPD, meaning the budget provides a sample size of two pumps to investigate reliability. Keeping this in mind, the use of DoE techniques are not viable because the pumps are single use. Hence, the decision to use one stressor is taken for the following reasons; (1) The extremely small sample size limits the availability of pumps to understand the driving mechanism(s) of wear. By using more than one stressor, it will inhibit understanding of which mechanism dominates systemic pump degradation and prevents a meaningful covariate relationship (which is essential for the BM model with covariate drift and diffusion coefficients). (2) If

[77] (Andreson and Whitcomb, 2000; Montgomery, 2013; Dean, Voss and Draguljić, 2017).
[78] (Montgomery, 2013; Dean, Voss and Draguljić, 2017).
[79] (Montgomery, 2013; Zhu and Elsayed, 2013; Dean, Voss and Draguljić, 2017).
[80] (Thaduri et al., 2012; Montgomery, 2013; Dean, Voss and Draguljić, 2017).

speed were the only stressor and the pump outlet is set to normal usage, then the primary acceleration of degradation is to run into excessive speeds. The outcome of this is the risk of unrealistic cavitation and erosion. (3) Using outlet pressure as the stressor carries higher value because it carries more uncertainties that can be modelled. For instance, under a constant engine speed the pressure varies from:

(A) The tolerances on pump performance. The tolerance on the flow rate (as a function of pump manufacturing variation) affects the pressure rise through a restriction. Lower flow means lower pressure as per Bernoulli's equation (Karassik, 2001, p. 4.2).

(B) The component operation and tolerances on the engine restriction affect the pressure rise. For example, pre-filter there is the oil cooler restriction and oil cooler thermostat. Post-filter, the load on the engine and piston cooling jets varies the load (Rundo and Nervegna, 2015). The filter is a consumable item that is periodically replaced with age. As the filter fills with debris, the pressure drop will also increase (Rundo and Nervegna, 2015).

(C) Conventionally, the pressure in the engine is regulated with a valve (in the pump or the engine block) to compensate for the variation. The breakpoint and valve characteristics of regulation are also assigned a tolerance (Rundo and Nervegna, 2015).

(D) The fluid temperature has an impact on the viscosity that not only alters pressure rise but also affects at which engine speed the pressure starts to regulate. For example, cooler fluid temperatures result in a higher viscosity, meaning the pressure rise through the engine will build earlier and regulates at a lower engine speed (Rundo and Nervegna, 2015).

Setting the single stressor as the pump outlet pressure offers scope to model the covariates mentioned above as stochastic or deterministic, time-invariant or time-varying, multivariate or univariate (Zhang *et al.*, 2018). It is practical to use the fixed speed where the engine spends the majority of its time throughout the SSADT. The whole duty cycle data from the customer is confidential, however as reported in the unpublicised Submission 2 (Zarzycki, 2016) the pump will fulfil 55.9% of its time at 1700 rpm. Equally, the fluid temperature will be set at 110°C as it is known this is where the engine will spend the majority of its time.

The process in Figure 3-19 assists in setting the test parameters, the order of which is not critical. It is possible to estimate the cavitation limit using computational fluid dynamics but once the hardware is available a dedicated performance pump should be used to validate the cavitation limit. The generation of head flow performance testing generally runs the pump into abnormal running conditions and can overstress the pump. Unused pumps are allocated for the SSADT to avoid different starting points of degradation and maintain the credibility of the degradation model.

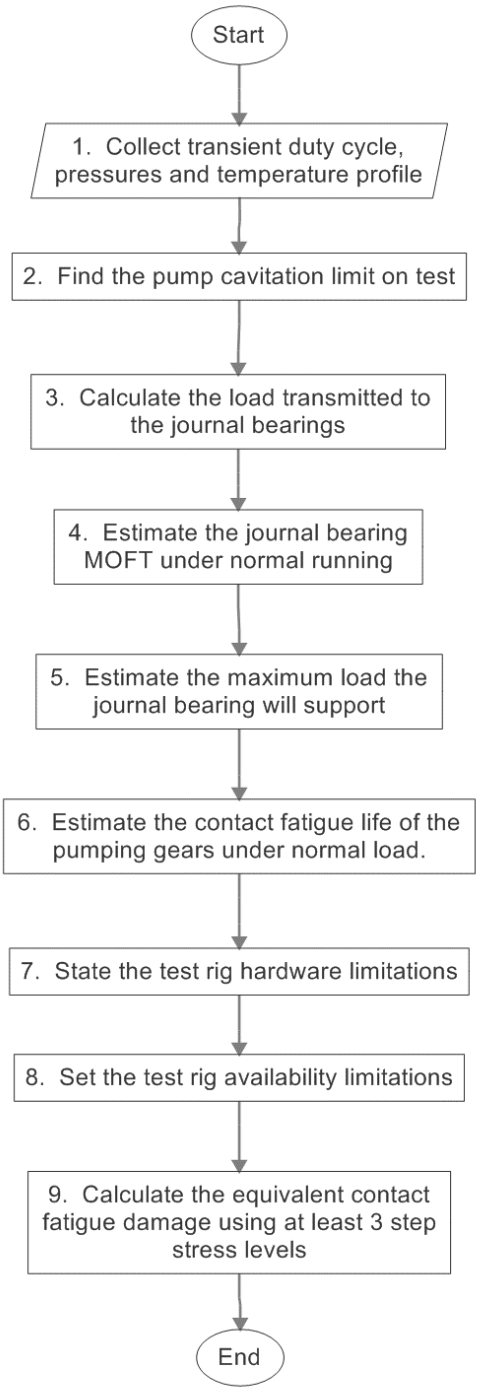

Figure 3-19 SSADT test design process for gear pump.

The test boundaries for the SSADT involve PoF calculations to ensure the parts are not overstressed. The journal bearing calculations BS ISO 4378-1:2009 (British Standards Institution, 2009) is used to establish the maximum pump outlet pressure vs pump speed assuming the risk of introducing mixed film lubrication is set by the criteria of $\lambda = 3.0$ (Xin,

2011, pp. 665–667). The capacity to overload the pump is highly dependent on the journal bearing clearances and surface finish, which are measured directly from the hardware.

The calculations as stipulated in BS ISO 6336-1:2006 (British Standards Institution, 2006a) are used to estimate the contact fatigue life under nominal duty and load. Although contact fatigue is only concerned with a set of gears and a single failure mode, it is a readily available cumulative damage model available for a gear pump. It is reasonable and convenient to design the test based on the gear contact fatigue model. In the accelerated testing of gears, the cumulative damage from the accelerated test is to be equivalent to or greater than the cumulative damage under normal running BS ISO 6336-1:2006 (British Standards Institution, 2006a). The largest restrictions in this case study are the outlet pressure limitations (to avoid journal bearing seizure and the available rig time). A further limitation is the need to fit a relationship to the drift and diffusion coefficients vs stress relationship which as a minimum requires three stresses/steps.

There are sophisticated possibilities to optimise the test design efficiency regarding pressure and the allocated step test duration; however, these require prior knowledge on the degradation model, which did not exist at the time. Additionally, in an industry setting, the simplification of the test makes it manageable from a test and analysis viewpoint (Weaver and Meeker, 2014). For this reason, the decision was taken to equally split the step time between three stressors so now all that remains is setting the stress. Given the time availability (after bedding in the pump) it is reasonable to assume that little or no detectable degradation will occur running under normal load within the allocated step time duration. Thus, the difference between normal usage pressure P_0 and allowable pressure limit P_k (at a fixed speed, temperature and oil grade), is split equally by k stress steps, in this case $k = 3$ levels.

$P_j = P_{j-1} + \Delta P$:	Stress at level j, ($j = 1,2 \dots k$).
P_0:	Normal usage stress.
P_k	Maximum allowable stress.
$\Delta P = \frac{P_k - P_0}{k}$:	Difference between stress levels.

The detailed calculations in estimating the pressure limits are in Submission 4 (Zarzycki, 2017b). The outcome of the SSADT is illustrated in Figure 3-20. At the pump speed 178 rad/s the nominal outlet pressure is $P_0 = 4.2E5\ [Pa]$. The prototype pump hardware measured with nominal journal bearing clearances, which is the limiting stress factor, allowing $P_3 = 10.50E5\ [Pa]$. The remaining steps are $\Delta P = (P_3 - P_0)/k = (10.50E5 - 4.2E5)/3 = 2.10E5\ [Pa]$. This sets $P_1 = 6.30E5\ [Pa]$ and $P_2 = 8.40E5\ [Pa]$.

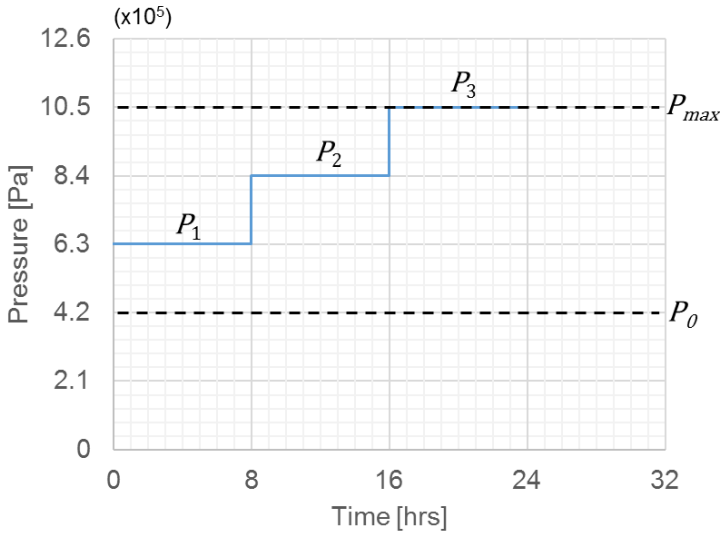

Figure 3-20 SSADT test plan.

Regarding the total test time, this is a trade-off between rig availability, as governed by live projects vying for the same resource and the hardware and test cost (a genuine case study of the test planning paradox, see Section 1.1). From a financial perspective, the cash expenditure for each pump sample size n costs "A" to procure. Even with a sample size of two, the SSADT is already twice as much as the conventional demonstration at CAB with a single sample. However, the test cost budget should assign a costing test rate B considering labour and overheads multiplied by the total test time T per sample. The total test cost TC, is:

$$TC = n\big((A) + (T \times B)\big) \tag{3.4}$$

The SSADT design can be governed by criteria, for instance, to make the SSADT total test cost equivalent to the cost of the conventional demonstration test. If this is the case, then the sample size could increase to improve confidence against the balance of test time (Dazer *et al.*, 2016). Alternatively, test budget cost savings, constraints on the test time and or sample size may be the criteria (Dazer *et al.*, 2016). In the case study, the test time availability was 2 working weeks excluding setup, with a sample size of 2. Compared to conventional demonstration testing at CAB, this resulted in a reduction of total test cost and increased the rig availability each by ~77%.

The disadvantage of this setup is that the pump pressure ripple is not automatically recorded, meaning supervision is required and limits the test to the working day. The manual collection also impedes the frequency of collecting data. Previous trials recorded the pressure ripple every eight hours only to find the resolution was not sufficient (Zarzycki, 2017a). The balance of using a manual process means the recording of at least 28 pressure ripple samples

(Section 3.2, Eqn. (3.1)) takes 15 minutes, and it seemed reasonably practicable to record every hour. Additionally, the test rig requires warming up each day, which takes approximately 1 hour. The result from a 37 hour working week soon becomes 6 hours/day actual SSADT running, meaning 26 hours of running the pump under the SSADT is available. The decision to use three stress levels splits 26 hours equally and a decision to round down to a whole hour meant a step test duration of 8 hours each, providing contingency and ease of management.

3.5 Monitoring Pump Pressure Ripple

The operation of positive displacement pumps use volume change to displace fluid causing it to flow (Karassik, 2001). If there were an instrument that could measure the dynamic flow rate this cyclical change would look like fluctuations superimposed over the mean flow rate, known as flow ripple (Edge and Johnston, 1990). The complex interactions of the pump components and circuit geometry create a counterpart called pressure ripple (Edge and Johnston, 1990). These interactions can generate airborne noise and vibrations that emanate through the circuit hardware causing component fatigue and failure (Edge and Johnston, 1990), particularly for hose pipes and radiators. For example, the modelling, prediction, and experimental evaluation of gear pump meshing pressures was critical in designing out cavitation erosion, with particular reference to aero-engine fuel pumps (Eaton, Keogh and Edge, 2006). The design, modelling and validation of flow ripple are important in this regard (Cudina, 2007; Johnston, 2007; Devendran and Vacca, 2012). However, the limitation of flow meter capture rates cannot directly measure flow ripple (Edge and Johnston, 1990).

The alternative is to measure pressure ripple using dynamic pressure transducers and subsequently calculate the flow ripple. There are three primary methods for recording pressure ripple as follows. The *secondary source* method BS 6335-1:1990 (British Standards Institution, 1990)**,** superseded by BS ISO 10767-1:1996 (British Standards Institution, 1996)**,** developed by Bath University's Fluid Power Centre uses a second pump to generate waves in the opposite flow direction to the test pump and calculate the complex wave coefficients. An alternative method with less accurate but more straightforward setup and processing technique uses a *two pressure/two systems* method ISO 10767-1:2015 (Kojima, Yui and Ichiyanagi, 2000; ISO, 2015; Bramley and Johnston, 2017) comprising of adjusting pipe lengths and hence wave travel with two loading valves. An even simpler method where flow ripple and accuracy are less of interest is the *blocked pressure ripple* technique using one dynamic pressure transducer BS ISO 10767-2: 1999 (British Standards Institution, 1999). The simpler methods are attractive from an installation and processing perspective, but the reproducibility, repeatability and reliability are not as robust as the secondary source (Yang, Edge and

Johnston, 2008; Johnston and Todd, 2010; Bramley and Johnston, 2017). These methods apply to higher-pressure applications typically above a minimum of 10E5 Pa, and the limitations on installation space make these methods suited to laboratory environments (International Organization for Standardization, 2015). In respect to the case study the two system methods have similitude with simulating the HDE circuit, thus it is reasonable to set pipe design lengths and pressure transducer positions set by ISO 10767-1:2015 (ISO, 2015), even though there is no need for flow ripple calculations or a second dynamic transducer.

In terms of utilising pressure ripple for condition monitoring, some of the earliest work appears in the 1970s when the availability of dynamic pressure transducers increased, as piezo-capacitive and piezo-resistive technologies became commercialised. Maroney (1976), and Maroney and Tessmann (1977) linked acoustical pump noise measurements to a noise wear index. The hypothetical link of the noise wear index to time and cumulative wear modelling was considered as a future development route. Later Silva (1986) proposed pump condition monitoring using pressure ripple. Silva devised a novel technique using the Auto-Regressive Moving Average (ARMA) method to convert a signal into a second order mechanical system (Silva, 1986). The characterisation of pump health is linked to membership functions to evaluate the pattern of failure, such as wear or cavitation (Silva, 1986). The prognostics time to failure models for cavitation and wear were hypothesised using regression (Silva, 1986); however, the degradation models were not explored any further. No other pump time to failure degradation models using pressure ripple could be found, but the detection methods exist.

The report of detection methods for pump degradation by Greene and Casada (1995) is insightful and covers pressure ripple, but there is no link to lifetime or feature extraction. Khoshzaban-Zavarehi (1997) agrees that the pressure ripple characteristics will change with the development of a fault, but suggests that the standard methods of frequency analysis and using lumped parameter model may not be sensitive enough to distinguish differences in severity (due to the dominant fundamental pumping frequencies). A similar conclusion was reached by Johnston and Todd (2010) for the condition monitoring of aircraft fuel pumps in attempting to distinguishing worn vs badly worn pumps.

The motivation continues to be focused on pump fault detection rather than modelling the time to failure. Yang, Edge and Johnston (2008), and Yang (2009) assessed a simplified flow ripple measurement to diagnose the health of a hydraulic power steering vane pump. Eltabach *et al.* (2011) used contamination to run an ALT and monitor the degradation of pressure ripple as a form of fault detection method however contamination was used to accelerate wear, and this does not link to the life of the pump nor the degradation modelled. Grasso, Pennacchi and Colosimo (2014) analysed pressure ripple for the health monitoring and fault classification of a waterjet cutting machine, however, once again there is no link to

degradation modelling. Buono *et al.* (2017), and Siano, Frosina and Senatore (2017) used pressure ripple to affirm the vibration signature for a light duty engine lubrication pump under cavitation, but the motivation was the consequence and severity of vibration levels under cavitation rather than estimating life. Thus, the gap in knowledge in developing a reliability degradation model based on pressure ripple was pursued.

3.6 Pressure Ripple Analysis Using MODWT-ARMA(2,1)

As previously reviewed in Section 3.5 there is an opportunity to explore the use of pressure ripple in prognostics regarding the estimation of time to failure. The methods already documented in literature have had mixed success in the manipulation and interpretation of the pressure ripple signal, with a focus on the detection and diagnosis rather than modelling the degradation. This section reviews the analysis and feature extraction methods leading the innovative development of using a Maximal Overlap Discrete Wavelet Transform (MODWT) combined with an ARMA(2,1).

A time domain signal can hold information which indicates the state of a system (Gertler, 1998) and there are multiple techniques available to extract the specific information of interest. The type of technique depends if the signal is classed as stationary or non-stationary, deterministic or non-deterministic (Herlufsen, Gade and Zaveri, 2007, p. 470). A stationary and deterministic signal can be a periodic signal approximated analytically usually by sinusoidal/composite functions (Herlufsen, Gade and Zaveri, 2007, p. 470). A non-deterministic signal is a random signal that cannot be expressed analytically but can be expressed statistically (Herlufsen, Gade and Zaveri, 2007, p. 471). A non-stationary signal can comprise of; (1) sine components that vary in amplitude and/or frequencies over time, (2) a random signal, and/or (3) transients (Herlufsen, Gade and Zaveri, 2007, p. 471). In condition monitoring, as a fault emerges, the signal(s) tend to become non-stationary (Fan and Zuo, 2006), which may be the case with gear pumps, for example detecting a fault in a tooth which will upset the periodicity (Liu *et al.*, 2015).

One simple technique that may observe a fault is to process the time domain signal using statistical methods such as standard deviation, and root mean square (Güemes and Sierra-Perez, 2013, p. 152); however, the fault is generally hidden in the frequency content (Jaber and Bicker, 2014). By using a Fast Fourier Transform (FFT) the time domain is transformed into a frequency domain from which the spectral content can be analysed and changes detected (Stark, 2005). For example, the FFT is used to analyse the vibration signature on electric motors to help diagnose its state of health (Robert Bond Randall, 2007, p. 549). The FFT will find frequencies, but it cannot associate the frequency with time and the non-stationary signal elements are output as "noise" between the frequency harmonics (Leavey *et al.*, 2003; Debnath

and Shah, 2015). To capture the transient characteristic, a time-frequency analysis is required (Leavey *et al.*, 2003; Debnath and Shah, 2015). There are three primary methods, the Short-time Fourier Transform (STFT) (Leavey *et al.*, 2003), the Discrete Wavelet Transform (DWT) (Leavey *et al.*, 2003) and Empirical Mode Decomposition (EMD) (Huang *et al.*, 1998).

The STFT uses a fixed windowing function with a fixed resolution that segments the signal and provides a band of the frequency spectrum in a band of time (Newland, 2007). The downside is that the exact time of the frequency component is lost in the bands and the resolution provides either high-frequency resolution or high time resolution but not both (Newland, 2007) this is also a consequence of Heisenberg's principle. This situation is improved with multi-resolution techniques such as DWT (Leavey *et al.*, 2003) or EMD (Huang *et al.*, 1998).

DWT can be thought of as an adjustable window Fourier analysis that uses sub-band coding on a dyadic grid (see Figure 3-21) to decompose the signal into banded frequencies (Huang *et al.*, 1998; Yan, Gao and Chen, 2014). The signal passes through a set of high and low bandpass filters that create the multi-resolution time-frequency spectrum (Leavey *et al.*, 2003; Yan, Gao and Chen, 2014). The control of the filters is through a mother wavelet function that is scaled to suit the frequency bands of interest (Leavey *et al.*, 2003). The selection of suitable mother wavelet and the number of levels is not a fixed procedure (Leavey *et al.*, 2003). With at least fifteen wavelet families to choose from the selection is through trial and error (Karthikeyan and Nagesh Kumar, 2013). A typical selection method passes the signal through a different number of wavelet families and calculates the highest Shannon-entropy figure for the detailed coefficients (Ngui *et al.*, 2013; Yang and Wang, 2015). After choosing the mother wavelet, the DWT process passes the original signal through a high pass filter to decompose it into a detailed coefficient (Det01) and a low pass filter to decompose it into an approximation coefficient (App01) (Huang *et al.*, 1998; Yan, Gao and Chen, 2014). The process is repeated on App01 to give Det02 and App02 and so forth until the desired level of coefficients is achieved (as shown in Figure 3-21). DWT is growing in popularity in CBM (Newland, 2007). For example, Gao and Zhang (2006) applied the method of pressure ripple to diagnose the health of a hydraulic piston pump on mobile machinery, although this was not linked to a degradation model.

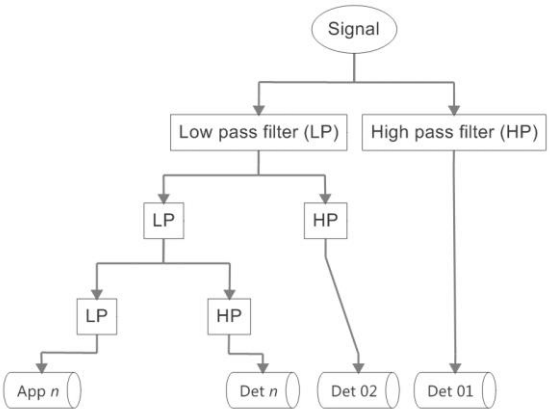

Figure 3-21 DWT signal decomposition adapted from Misiti and Poggi (2014, p. 1.48-1.53).

A downside to DWT is the resultant leakage or boundary distortion because the wavelets are limited in length. The solution for this is to apply a Maximal Overlap DWT (MODWT) (Cornish, Bretherton and Percival, 2006; Peng *et al.*, 2009; Zhang *et al.*, 2010).

An alternative to DWT is the empirical mode decomposition (EMD) technique which handles both non-linear and non-stationary time series data (Huang *et al.*, 1998). EMD is a data-driven method which is adaptive and provides higher accuracy of time discontinuities (Huang *et al.*, 1998). Similar to DWT, it too is particularly useful for diagnosis with vibration signals on gearboxes and bearings (Yu, Cheng and Yang, 2005; Grasso, Pennacchi and Colosimo, 2014; Hui *et al.*, 2014; Xue *et al.*, 2014; Ben Ali, Chebel-Morello, *et al.*, 2015; Ben Ali, Fnaiech, *et al.*, 2015). The issue is that it can over-decompose the signal (which is called mode mixing) (Huang *et al.*, 1998; Wu and Huang, 2009; Singh and Kumar, 2014; Liu *et al.*, 2015). EMDs self-adaptation can change the number of decompositions which is undesirable for prognostics in degradation (Grasso, Pennacchi and Colosimo, 2014).

Goyal and Pabla (2016) state feature extraction as one of the most challenging aspects of condition monitoring due to the fact there is multiple solutions and techniques, each individually tailored to the unique application. As previously mentioned in Section 3.5, there has been a mixed success in distinguishing the level of pump health using pressure ripple conventional statistical parameters such as RMS and amplitude (Johnston and Todd, 2010). An alternative feature extraction using Auto Regressive Moving Average on pressure ripple was proposed by Silva (1986). The advantage of the ARMA is there is no need to create a mathematical model to study the signal as a system (Junsheng, Dejie and Yu, 2006). As such, to be able to represent a dynamic system as a damping coefficient (Zeta) and natural frequency (Omega) allows greater inferences to be made rather than looking at statistical features alone (Junsheng, Dejie and Yu, 2006). Silva (1986) suggests pump health can be described as a second order system in terms of damping coefficient and natural frequency. A pump and its

components (i.e. the pumping gears and journal bearings) can be modelled to a second order system (Silva, 1986), which is particularly useful from a wear perspective because changes in clearance from wear will alter the system response. The following can represent a second order dynamic system:

$$\frac{d^2X(t)}{dt^2} + 2\zeta w_n \frac{dX(t)}{dt} + w_n^2\, X(t) = Z(t) \tag{3.5}$$

Where t is time, $X(t)$ is the time series data, ζ is the damping coefficient (Zeta), w_n is the natural frequency (Omega), and $Z(t)$ is a forcing function also known as the white noise function. Unlike a regression model which expresses a variable dependence on another variable, the Auto Regression (AR) expresses the dependence of a variable on itself at different times (Pandit and Wu, 1983). For instance, a second-order auto-regressive model AR(2) expresses the dependence of a variable on its two preceding datasets. The second element is the Moving Average (MA) which models the residual error based on its preceding value. For instance, a first-order moving average MA(1) bases its dependence on one preceding dataset. An ARMA(2,1) model can conveniently fit the second order system in Equation (3.5), and the lemma is documented by Pandit and Wu (1983, p. 249) provided in Section 3.6.2

Using ARMA(2,1) as Silva (1986) intended had not been successful in Submission 3 (Zarzycki, 2017a) and Submission 4 (Zarzycki, 2017b) because of the non-stationary time series pressure ripples measured. An innovative idea to develop ARMA as a feature extraction after passing the signal through a MODWT was developed from Zhu, Wang and Fan (2014) in their study of forecasting rainfall. The application in the gear pump case study is different. Using MODWT-ARMA(2,1) the damping coefficients and frequencies are extracted for each detailed coefficient, providing several monitoring features from one signal. The experimentation in later submissions successfully applied this innovative method (Zarzycki, 2017a, 2017b). The top-level algorithm and mathematical expressions of the MODWT-ARMA(2,1) are included as follows.

3.6.1 Maximal Overlap Discrete Wavelet Transform (MODWT)

The discrete wavelet transform produces dilation and translations of the wavelet filter and scaling filter. The maximal overlap time series $\{X = X_t,\ t = 0, 1, 2, \dots, N-1\}$ is an established transform. To appreciate the definition in mathematical terms the break down is repeated from Zhu, Wang and Fan (2014):

$$\tilde{h}_{j,l} = \frac{h_{j,l}}{2^{j/2}} \tag{3.6}$$

$$\tilde{g}_{j,l} = \frac{g_{j,l}}{2^{j/2}} \tag{3.7}$$

Where $h_{j,l}$ is the DWT wavelet filter and $\tilde{h}_{j,l}$ is the MODWT wavelet filter, and $g_{j,l}$ is the DWT scaling filter and $\tilde{g}_{j,l}$ is the MODWT scaling filter and The length of the filter $l = 1, \dots, L$ The MODWT wavelet coefficients of level j are defined as:

$$\widetilde{W}_{j,t} = \sum_{l=0}^{L_j - 1} \tilde{h}_{j,l}\, X_{t-l \bmod N} \tag{3.8}$$

$$\tilde{V}_{j,t} = \sum_{l=0}^{L_j - 1} \tilde{g}_{j,l}\, X_{t-l \bmod N} \tag{3.9}$$

Where $\{L_j = (2^j - 1)(L-1) + 1\}$. The MODWT can be expressed as a matrix as $\widetilde{W}_j = \widetilde{w}_j X$ and $\tilde{V}_j = \tilde{v}_j X$. The original time series X can be recreated from the MODWT by:

$$X = \tilde{v}_j^T \tilde{V}_J + \sum_{j=1}^{J} \widetilde{w}_j^T \widetilde{W}_j \tag{3.10}$$

The MODWT of X can be given in terms of the J level MODWT approximation $\tilde{S}_J = \tilde{v}_j^T \tilde{V}_J$ and the jth level MODWT details $\widetilde{D}_j = \widetilde{w}_j^T \widetilde{W}_j$:

$$X = \tilde{v}_j^T \tilde{V}_J + \sum_{j=1}^{J} \widetilde{w}_j^T \widetilde{W}_j = \tilde{S}_J + \sum_{j=1}^{J} \widetilde{D}_j \tag{3.11}$$

Thus:

$$X = \tilde{S}_J + \widetilde{D}_J + \widetilde{D}_{J-1} + \cdots \widetilde{D}_1 \tag{3.12}$$

For a discrete time series $\{X_t,\ t = 1, 2, \dots, N\}$:

$$X_t = \tilde{S}_{J,t} + \sum_{j=1}^{J} \widetilde{D}_{j,t}, \qquad t = 1, 2, \dots, N \tag{3.13}$$

This expands to give:

$$X_t = \tilde{S}_{J,t} + \tilde{D}_{J,t} + \tilde{D}_{J-1,t} + \cdots \tilde{D}_{1,t}, \qquad t = 1, 2, \ldots, N \tag{3.14}$$

Where $\tilde{S}_{J,t}$ is the approximation coefficient representing the smooth behaviour or slower dynamics at the coarser scale of X_t (Yang and Leu, 2008; Zhu, Wang and Fan, 2014) and $\tilde{D}_{J,t}$ is the detail coefficient representing the local details or faster dynamics at the finer scales (Yang and Leu, 2008; Zhu, Wang and Fan, 2014). The detailed coefficients can then be analysed, in this case using ARMA(2,1).

3.6.2 ARMA(2,1)

An ARMA(2,1) model can conveniently fit the second order system of Eqn (3.5). The general ARMA(*p*,*q*) model has the form:

$$X_t = \sum_{i=1}^{p} \varphi_i X_{t-i} + a_t + \sum_{r=1}^{q} \theta_r a_{t-r} \tag{3.15}$$

Where X_t is the observed data after subtraction from their average, p is the order of the AR polynomial, φ_i is the parameter of the AR model, a_t is the white noise error term which is normally and independently distributed residuals with mean zero and variance σ_a, θ_r is the parameter of the MA model and q is the order of the MA polynomial. An ARMA(2,1) expands out as follows:

$$X_t = \varphi_1 X_{t-1} - \varphi_2 X_{t-2} + a_t - \theta_1 a_{t-1} \tag{3.16}$$

The transform to output the model features ζ and w_n which are functionally related to the complex roots represented by the real part *a* and the complex part *b* (Pandit and Wu, 1983, p. 249). The natural frequency (Omega) w_n is calculated as:

$$w_n = \sqrt{(a^2 + b^2)} \tag{3.17}$$

The value of a is uniquely determined because φ_2 is a real number:

$$a = \zeta w_n = -\frac{\ln(-\varphi_2)}{2\Delta} \tag{3.18}$$

However, because the pressure ripple is periodic, the cosine function of the imaginary part will have multiple values. This multiplicity should be considered and checked under the condition that $\varphi_1^2 + 4\varphi_2 < 0$. If this is the case then:

(3.19)

$$b = a\sqrt{-(\varphi_1^2 + 4\varphi_2^2)}\left[\frac{2\varphi_1 - (1-\varphi_2)\left(\theta_1 + \frac{1}{\theta_1}\right)}{2(1-\varphi_2^2) - \varphi_1(1+\varphi_2)\left(\theta_1 + \frac{1}{\theta_1}\right)}\right]$$

Once b is calculated, the damping coefficient (Zeta) can be found after calculating the natural frequency:

$$\zeta = \frac{a}{w_n} \tag{3.20}$$

By combining this procedure with the MODWT the individual approximation and detail coefficients can be represented as damping coefficients and natural frequencies as follows.

3.6.3 MODWT-ARMA(2,1)

As eqn. (3.13) states the original signal is a summation of approximation and detail coefficients, the same ARMA(2,1) procedure given in section 3.6.2 can be applied to these coefficients individually. The detailed coefficient at level *j* decomposition is transformed into:

$$\widetilde{D}_j = \varphi_{\widetilde{D}_{j,1}}\widetilde{D}_{j,t-1} - \varphi_{\widetilde{D}_{j,2}}\widetilde{D}_{j,t-2} + a_{\widetilde{D}_{j,t}} - \theta_{\widetilde{D}_{j,1}}a_{\widetilde{D}_{j,t-1}} \qquad \begin{matrix} t = 1, 2, \dots, N \\ j = 1, 2, \dots, J \end{matrix} \tag{3.21}$$

The natural frequencies of the detailed coefficient at level *j:*

$$w_{n,\widetilde{D}_j} = \sqrt{\left(a_{\widetilde{D}_j}^2 + b_{\widetilde{D}_j}^2\right)} \qquad j = 1, 2, \dots, J \tag{3.22}$$

The real number of the detailed coefficient at level *j:*

$$a_{\widetilde{D}_j} = \zeta_{\widetilde{D}_j} w_{n,\widetilde{D}_j} = -\frac{\ln\left(-\varphi_{\widetilde{D}_{j,2}}\right)}{2\Delta} \qquad j = 1, 2, \dots, J \tag{3.23}$$

The complex number of the detailed coefficient at level j providing multiplicity is accounted for:

$$b_{\tilde{D}_j} = a_{\tilde{D}_j}\sqrt{-\left(\varphi_{\tilde{D}_{j,1}}^2 + 4\varphi_{\tilde{D}_{j,2}}^2\right)}\left[\frac{2\varphi_{\tilde{D}_{j,1}} - \left(1-\varphi_{\tilde{D}_{j,2}}\right)\left(\theta_{\tilde{D}_{j,1}} + \frac{1}{\theta_{\tilde{D}_{j,1}}}\right)}{2\left(1-\varphi_{\tilde{D}_{j,2}}^2\right) - \varphi_{\tilde{D}_{j,1}}\left(1+\varphi_{\tilde{D}_{j,2}}\right)\left(\theta_{\tilde{D}_{j,1}} + \frac{1}{\theta_{\tilde{D}_{j,1}}}\right)}\right] \qquad (3.24)$$

$$j = 1, 2, \ldots, J$$

The damping coefficient at the detailed coefficient level j:

$$\zeta_{\tilde{D}_j} = \frac{a_{\tilde{D}_j}}{w_{n,\tilde{D}_j}} \qquad j = 1, 2, \ldots, J \qquad (3.25)$$

This procedure will output J damping coefficients and natural frequencies. The same procedure applies for the approximation coefficient, only substituting $\tilde{D}_{j,t}$ with $\tilde{S}_{j,t}$:

$$\tilde{S}_{J,t} = \varphi_{\tilde{S}_{J,1}}\tilde{S}_{J,t-1} - \varphi_{\tilde{S}_{J,2}}\tilde{S}_{J,t-2} + a_{\tilde{S}_{J,t}} - \theta_{\tilde{S}_{J,1}}a_{\tilde{S}_{J,t-1}} \qquad t = 1, 2, \ldots, N \qquad (3.26)$$

3.6.4 MODWT-ARMA(2,1) Top-level Algorithm and Code

The top-level algorithm is shown in Figure 3-22 as the process for calculating the damping coefficient and natural frequency for the approximation and detailed coefficients. The structure follows the process and outputs the parameters as described in sections 3.6.1 and 3.6.3, namely $\varphi_{\tilde{D}_{j,1}}, \varphi_{\tilde{D}_{j,2}}, \theta_{\tilde{D}_{j,1}}, a_{\tilde{D}_j}, \zeta_{\tilde{D}_{j,1}}, w_{n,\tilde{D}_{j,1}}$ $j = 1, 2, \ldots, J$ and $\varphi_{\tilde{S}_{J,1}}, \varphi_{\tilde{S}_{J,2}}, \theta_{\tilde{S}_{J,1}}, a_{\tilde{S}_J}, \zeta_{\tilde{S}_J}, w_{n,\tilde{S}_J}$. The code has be written in MATLAB not only because it is a well validated program widely used in academia and industry, but also because it offers standard functions that can be manipulated with a degree of ease. The program requires the user to select the time series data and an appropriate wavelet filter and scaling filter for the analysis, after which the program automatically outputs and stores the parameters for post-test processing.

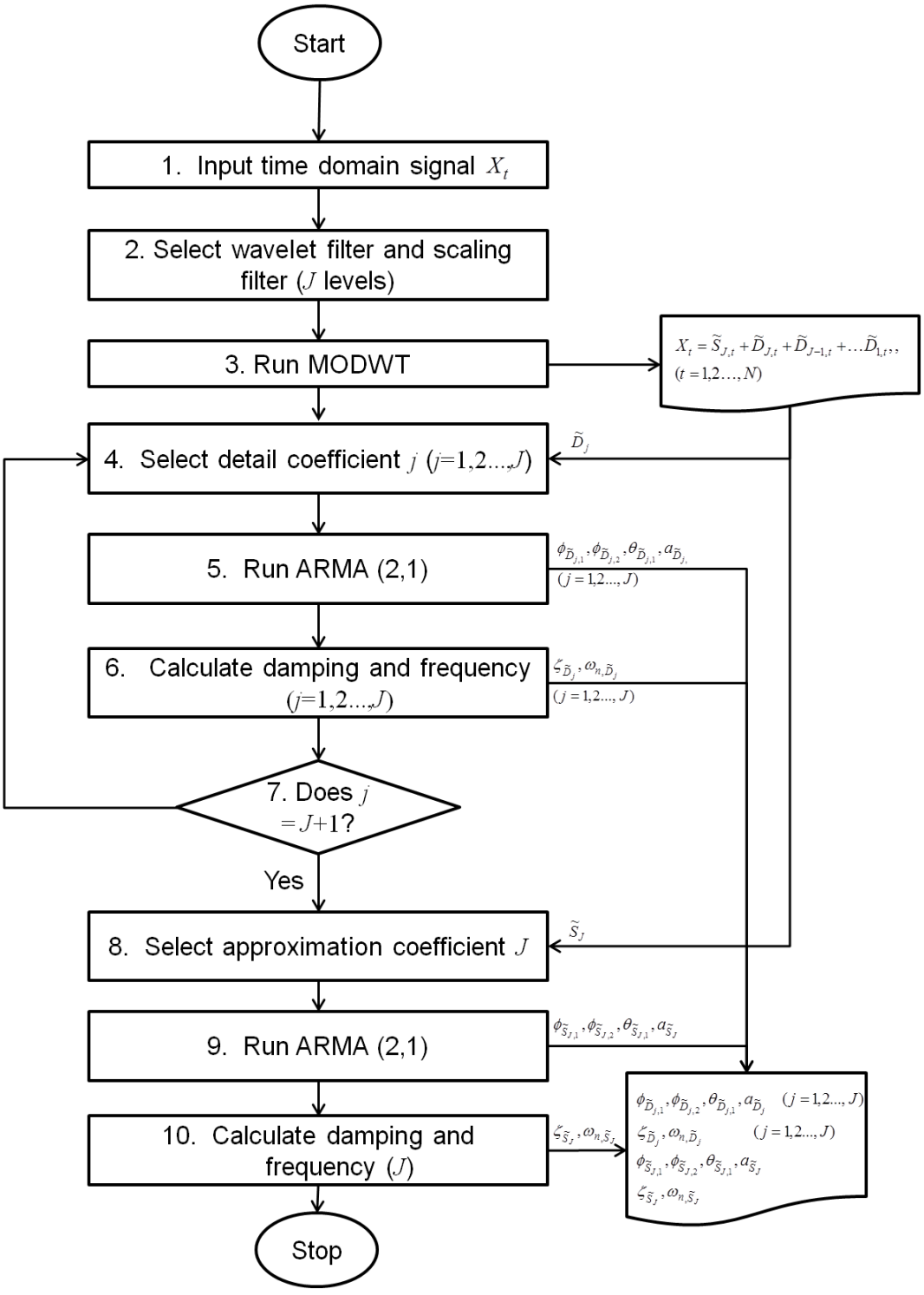

Figure 3-22 Top-level algorithm for MODWT - ARMA (2,1) analysis**.**

Some practical considerations for the case study as follows. The pump has 13 teeth on the pumping gears and operates from 748 rpm to 2924 rpm on the vehicle making the fundamental pumping frequency 162.1Hz and 633.5Hz respectively. The decision to record at the engine idle speed (pump speed of 748 rpm) stems from the potential convenience of recording in the field. ISO 10767-1:2015 (ISO, 2015) states the need to record up to the 10^{th} harmonic of the pumping frequency, in this case, the 10^{th} harmonic is 1621Hz. Accounting for Nyquist theorm the sampling frequency needs to be at least twice the frequency of interest to avoid aliasing (Piersol, 2007, p. 495). In this case, a sampling frequency above 3242Hz is required. To capture the 3242Hz in the wavelet frequency range, a 10kHz sampling rate is deemed sufficient in ISO 10767-1:2015 (ISO, 2015). 1 second of recorded data is practicable for achieving the frequency resolution as per ISO 10767-1:2015 (ISO, 2015). The frequency range sub-bands in the dyadic grid are shown in Table 3-13. The fundamental pumping frequency sits in level 5 (Det05).

Table 3-13 DWT frequency sub-bands.

	Level	Det01	Det02	Det03	Det04	Det05	Det06	Det07	Det08
Frequency range	Max [Hz]	5000.0	2500.0	1250.0	625.0	312.5	156.3	78.1	39.1
	Min [Hz]	2500.0	1250.0	625.0	312.5	156.3	78.1	39.1	19.5

Previous experimentation in Submission 3 (Zarzycki, 2017a) analysed several mother wavelets (Harr, Db, Sym, Coif and fk) and found the wavelet filter Fejér-Korovkin (fk22) (Nielsen, 2001) gave the highest Shannon-entropy ratio (Ngui *et al.*, 2013; Yang and Wang, 2015) under normal pump running conditions (748rpm 0.80E5 Pa, 110°C).

To summarise, the FFT is a conventional and widely used analysis technique of a time domain signal. The FFT has been reported to diagnose a change in pump health but not necessarily provide the condition level. Alternative methods such as STFT, DWT and EMD allow analysis in the time-frequency domain with a varying resolution to capture irregularity otherwise missed in the frequency domain alone. The decision to use MODWT was based on a compromise on the ability to fix the signal decomposition and minimise data loss (leakage) as reported from using STFT and DWT methods. MODWT is preferred over the adaptive EMD method for condition monitoring because there is no influence of mode mixing (which would distort the degradation parameter). The innovative feature extraction method of MODWT-ARMA(2,1) was therefore developed, and that has been experimentally shown to provide a degradation parameter (Zarzycki, 2017a, 2017b).

3.7 Parameter Estimation Using Bayesian Inference

Proceeding with a BM model with covariate drift μ and diffusion σ^2 coefficient, these parameters $\boldsymbol{\theta} = (\mu, \sigma^2)$ are estimated for each step-stress test using regression analysis and Bayesian inference. The completion of three step-stresses output drift and diffusion coefficients and provide the functional relationship to stress used to estimate the reliability. The use of Bayes is advantageous for two main reasons. Firstly, setting the prior distribution to be non-informative (Robert, Chopin and Rousseau, 2009) at each stress-step outputs approximately the same objective estimations as using MLE (Berger, Bernardo and Sun, 2009; Xu and Tang, 2012b), therefore operating in a Bayesian framework is not detrimental to the output. The use of non-informative priors is denoted Objective Bayes (OB) (Kass and Wasserman, 1996). Secondly, Bayes is reported to be more efficient and accurate with sample sizes below five compared to MLE (Meeker, 2010; Li and Meeker, 2014; Guan, Tang and Xu, 2016). The efficiency is dependent mainly on the prior distribution, which needs careful consideration not to be biased (Kass and Wasserman, 1996). In this case study and typically with innovative NPD there is little or no history to form a reference prior. The method proposed by Wan *et al.* (2014) resolves this problem by setting the step-stress prior based on the previous step-stress posterior. The step-stress coefficient or the accelerated stress coefficient (Viertl, 1981) is the ratio between step-stress drift coefficients used to shift the distribution mean of the previous step-stress posterior to create the current step-stress prior (Wan *et al.*, 2014). This methodology intuitively allows the data to speak for itself and brings objectivity to a situation where there is no prior data (Wang *et al.*, 2009). This method is denoted Bayesian Updating (BU) (Wang *et al.*, 2009; Peng *et al.*, 2013) as the prior is updated based on new data (Gebraeel *et al.*, 2005; Wang *et al.*, 2009; Li *et al.*, 2013). The process of the BU method for the three stress steps shown in Figure 3-23.

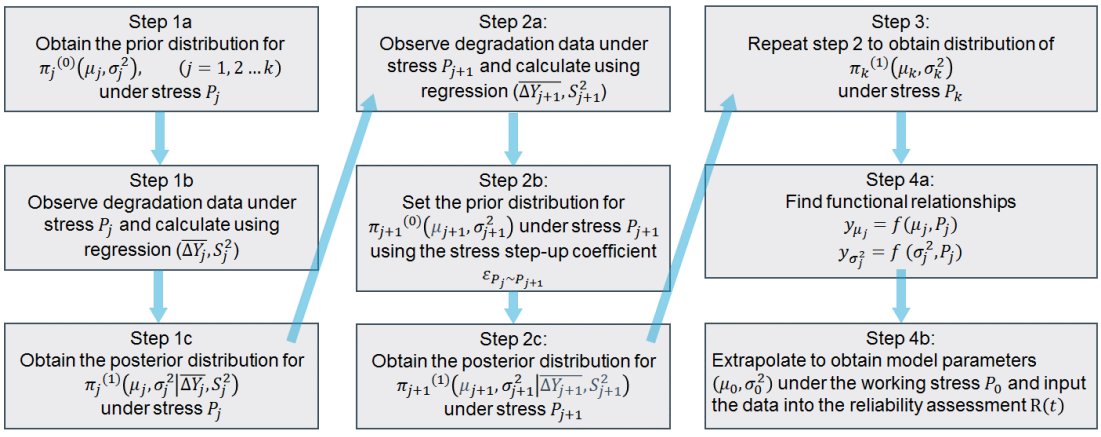

Figure 3-23 SSADT Bayesian updating process flow.

The BM process with the first passage of time to a threshold follows an inverse Gaussian distribution (Wang *et al.*, 2013). The degradation model is as follows:

$$Y(t) = y_0 + \mu t + \sigma B(t) \tag{3.27}$$

Where $Y(t)$ is the degradation in performance, y_0 is the initial value of the performance, μ is the drift coefficient (degradation rate) for a given stress ($\mu > 0$), σ is the diffusion coefficient ($\sigma > 0$) that describes the variation unit-to-unit and random errors, and $B(t)$ is the standard BM with a mean of 0 and a variance of t, $(B(t) \sim \mathcal{N}(0, t))$. The known property of the BM process is that the degradation increments Δy over time Δt follow a normal distribution:

$$\Delta y \sim \mathcal{N}(\mu \Delta t, \sigma^2 \Delta t) \tag{3.28}$$

Where the point in the degradation process exceeds a degradation threshold defined as a constant limit *C* at a time to failure t_0:

$$t_0 \equiv inf\{Y(t) \geq C\} = \{t | Y(t) \geq C, Y(t_0 \leq C), 0 \leq t_0 \leq t\} \tag{3.29}$$

Given the values of C, μ, σ, the distribution of t_0 follows the inverse Gaussian distribution for the probability distribution function (PDF) $Y(t)$ first passing the threshold C (Wang and Xu, 2010; Ge *et al.*, 2011; Yu Fan and Li, 2012; Wan *et al.*, 2014; Kahle, Mercier and Paroissin, 2016):

$$f\left(t; \mu, \sigma^2, C\right) = \frac{C - y_0}{\sigma \sqrt{t^3}} \cdot \phi\left(\frac{C - y_0 - \mu t}{\sigma \sqrt{t}}\right), \mu > 0, C > y_0 \tag{3.30}$$

$\phi(\cdot)$ is a standard normal Probability Density Function (PDF).

The reliability function $R(t)$ is given as (Park and Padgett, 2006; Li and Jiang, 2009; Ge *et al.*, 2011; Wan *et al.*, 2014):

$$R(t) = \Phi\left(\frac{C - y_0 - \mu t}{\sigma \sqrt{t}}\right) - \exp\left(\frac{2\mu (C - y_0)}{\sigma^2}\right) \Phi\left(-\frac{C - y_0 + \mu t}{\sigma \sqrt{t}}\right) \tag{3.31}$$

$\Phi(\cdot)$ is a standard normal cumulative density function (CDF).

To make reliability estimates using this closed-form requires parameter estimates for $\boldsymbol{\theta} = (\mu, \sigma^2)$. Using the Bayesian methodology the following describes the key stages. Where the superscript of (0) and (1) in $\pi_j^{(0)}$ and $\pi_j^{(1)}$ denote the prior and posterior distributions respectively under stress P_j , $(j = 0,1 \dots k)$, where *j* is the stress level with 0 defined as normal usage stress and k is the final step-stress. The sufficient statistics (Robert, Chopin and Rousseau, 2009) of the degradation sample mean $\Delta\bar{Y}_j$ and sample variance S_j^2 are used to estimate the population mean drift coefficient μ_j and diffusion coefficient (variance) σ_j^2 from a normal (linear) regression model.

3.7.1 Step 1a – Non-informative Prior for First Step-stress

For the first step-stress $j = 1$, at the beginning of the step-stress test with no history of test data (no prior data), specifically regarding pressure ripple monitoring. To keep the process objective, Jefferys prior is often used as a non-informative prior (He, He and Cao, 2016). In a situation of multidimensional parameters like the BM model Jefferys' rule stipulates that the parameters must be assumed independent *a priori*, otherwise the rules concerning the correct degrees of freedom for estimating parameters will not be met and this will generate disagreeable results (Bernardo and Smith, 1994; Syversveen, 1998). Therefore, it is assumed that the drift coefficient μ_1 is fixed and independent of the diffusion coefficient σ_1^2 under the pressure P_1 and Jefferys joint prior distribution ${\pi_1}^{(0)}(\mu_1, \sigma_1^2)$ is approximated:

$$ {\pi_1}^{(0)}(\mu_1, \sigma_1^2) \propto \frac{1}{\sigma_1^2} \tag{3.32} $$

3.7.2 Step 1b – Likelihood for Observed First Step-stress

After running the first stress P_1 where $j = 1$ the observations form a degradation data set $\Delta Y_1 = \left(\Delta y_{1,1}, \dots \Delta y_{1,m}\right), (m = 1, 2 \dots q)$, where m is the sample and q, is the last sample. The likelihood for the population mean drift coefficient μ_1 and diffusion coefficient σ_1^2 is generalised as:

$$ L\left(\mu_j, \sigma_j^2 \middle| \Delta Y_j\right) = \prod_{m=1}^{q} \pi\left(\Delta y_{j,m} \middle| \mu_j, \sigma_j^2\right), \quad (j = 0,1 \dots k) \tag{3.33} $$

The sufficient statistics for the sample mean $\Delta\bar{Y}_j$and variance S_j^2 are used to estimate the population mean for the drift coefficient μ_j and diffusion coefficient σ_j^2. Thus

$$ L\left(\mu_j, \sigma_j^2 \middle| \Delta Y_j\right) = L\left(\mu_j, \sigma_j^2 \middle| \Delta\bar{Y}_j, S_j^2\right) = \pi\left(\Delta\bar{Y}_j, S_j^2 \middle| \mu_j, \sigma_j^2\right), \quad ((j = 0,1 \dots k) \tag{3.34} $$

Where the sample mean $\Delta\bar{Y}_j$ is:

$$\Delta\bar{Y}_j = \frac{1}{q_j}\sum_{m=1}^{q_j}\Delta y_{j,m} \tag{3.35}$$

The sample variance S_j^2 is:

$$S_j^2 = \frac{1}{q_j - 1}\sum_{m=1}^{q_j}\left(\Delta y_{j,m} - \Delta\bar{Y}_j\right)^2 \tag{3.36}$$

The central limit theorem is applied to assume the distribution is normal:

$$\Delta\bar{Y}_j \sim \mathcal{N}\left(\mu_j, \sigma_j^2\right), \qquad \frac{q_j S_j^2}{\hat{\sigma}_j^2} \sim \chi^2\left(q_j - 1\right) \tag{3.37}$$

3.7.3 Step 1c – Posterior for First Step-stress

The standard parametric Bayesian inference adopts conjugate prior distributions for the joint posterior as normal inverse gamma (Jin, Matthews and Zhou, 2013; Yan *et al.*, 2013):

$$\mu_j \sim \mathcal{N}\left(a_j^{(1)}, \lambda_j^{(1)}\sigma_j^2\right), \qquad \sigma_j^2 \sim \Gamma^{-1}\left(\beta_j^{(1)}, \alpha_j^{(1)}\right) \tag{3.38}$$

$$\pi_j{}^{(1)}\left(\mu_j, \sigma_j^2 \middle| \Delta\bar{Y}_j, S_j^2\right) = \pi_j^{(1)}\left(\sigma_j^2\right) \cdot \pi_j^{(1)}\left(\mu_j \middle| \sigma_j^2\right) \tag{3.39}$$

Where:

$$\pi_j^{(1)}\left(\mu_j \middle| \sigma_j^2\right) \sim \mathcal{N}\left(a_j^{(1)}, \lambda_j^{(1)}\sigma_j^2\right) \tag{3.40}$$

$$\pi_j^{(1)}\left(\sigma_j^2\right) \sim \Gamma^{-1}\left(\sigma_j^2; \beta_j^{(1)}, \alpha_j^{(1)}\right) \tag{3.41}$$

3.7.4 Step 2a - Likelihood for Observed Second Step-stress

After acquiring the degradation data $\Delta Y_2 = \left(\Delta y_{2,1}, \ldots \Delta y_{2,m}\right), (m = 1, 2 \ldots q)$ under the second stress P_2 the sample mean and variance are used to estimate the population mean and variance from equation (3.34):

$$L\left(\mu_2, \sigma_2^2 \middle| \Delta\bar{Y}_2, S_2^2\right) = \pi\left(\Delta\bar{Y}_2, S_2^2 \middle| \mu_2, \sigma_2^2\right) \tag{3.42}$$

3.7.5 Step 2b - Informative Prior for Second Step-stress

Using the Bayesian updating and assuming conjugacy (Jin, Matthews and Zhou, 2013; Yan *et al.*, 2013), the second step-stress prior $\pi_2^{(0)}(\mu_2, \sigma_2^2)$ is set to the posterior from the first

step-stress $\pi_1^{(1)}(\mu_1, \sigma_1^2)$, which is assumed to be normal-inverse gamma,[81] Γ^{-1} representing the inverse gamma. Pragmatics reasons for this assumption include; (1) the normal distribution is used to model a mix of populations,[81] (2) the gamma distribution incorporates distributions such as the chi-square,[81] and (3) the posterior distribution produces a closed form equation for ease.[81] More generally:

$$\pi_{j+1}^{(0)}\left(\mu_{j+1}^{(0)}, {\sigma_{j+1}^2}^{(0)}\right) \sim \mathcal{N}\left(a_{j+1}^{(0)}, \lambda_{j+1}^{(0)} {\sigma_{j+1}^2}^{(0)}\right).\Gamma^{-1}\left({\sigma_{j+1}^2}^{(0)}; \beta_{j+1}^{(0)}, \alpha_{j+1}^{(0)}\right) \tag{3.43}$$

Where $\beta_{j+1}^{(0)}$ is the shape parameter and $\alpha_{j+1}^{(0)}$ is the scale parameter for the inverse gamma distribution of ${\sigma_{j+1}^2}^{(0)}$. The drift coefficient $\mu_{j+1}^{(0)}$ assumes a normal prior distribution conditional on ${\sigma_{j+1}^2}^{(0)}$. $a_{j+1}^{(0)}$ and $\lambda_{j+1}^{(0)}$ are introduced as values to calibrate the drift and diffusion coefficients by the accelerated stress coefficient $\varepsilon_{P_j \sim P_{j+1}}$ (Viertl, 1981; Wang *et al.*, 2013). By using $\varepsilon_{P_j \sim P_{j+1}}$ the prior estimations for the mean and variance can be calibrated to reflect the prior belief objectively based on test data (Wang *et al.*, 2013). As there is no data to suggest otherwise, it is assumed the diffusion coefficient remains constant, and the stress to drift coefficient has a relationship where the values of $\beta_{j+1}^{(0)}$ and $\alpha_{j+1}^{(0)}$ do not change. The accelerated stress coefficient is calculated from the drift coefficients in the step-stress data P_j and P_{j+1}.

$$\varepsilon_{P_j \sim P_{j+1}} = \frac{\mu_{j+1}^{(0)}}{\mu_j^{(1)}} \tag{3.44}$$

Thus the informative and objective prior for the P_{j+1} is:

$$\pi_{j+1}^{(0)}\left(\mu_{j+1}^{(0)}, {\sigma_{j+1}^2}^{(0)}\right) \sim \mathcal{N}\left(\varepsilon_{P_j \sim P_{j+1}}.a_{j+1}^{(0)}, \varepsilon_{P_j \sim P_{j+1}}^2.\lambda_{j+1}^{(0)} {\sigma_{j+1}^2}^{(0)}\right).\Gamma^{-1}\left({\sigma_{j+1}^2}^{(0)}; \beta_{j+1}^{(0)}, \alpha_{j+1}^{(0)}\right) \tag{3.45}$$

[81] (Bian and Gebraeel, 2014).

3.7.6 *Step 2c – Posterior for Second Step-stress*

Again, the standard parametric Bayesian inference adopts conjugate prior distributions for the joint posterior as normal inverse gamma (Jin, Matthews and Zhou, 2013; Yan *et al.*, 2013):

$$\mu_{j+1} \sim \mathcal{N}\left(a_{j+1}^{(1)}, \lambda_{j+1}^{(1)}\sigma_{j+1}^2\right),\ \sigma_{j+1}^2 \sim \Gamma^{-1}\left(\beta_{j+1}^{(1)}, \alpha_{j+1}^{(1)}\right) \tag{3.46}$$

$$\pi_{j+1}{}^{(1)}\left(\mu_{j+1}, \sigma_{j+1}^2 \middle| \Delta\bar{Y}_{j+1}, S_{j+1}^2\right) = \pi_{j+1}^{(1)}\left(\sigma_{j+1}^2\right) \cdot \pi_{j+1}^{(1)}\left(\mu_{j+1} \middle| \sigma_{j+1}^2\right) \tag{3.47}$$

Where:

$$\pi_{j+1}^{(1)}\left(\mu_{j+1} \middle| \hat{\sigma}_{j+1}^2\right) \sim \mathcal{N}\left(a_{j+1}^{(1)}, \lambda_{j+1}^{(1)}\sigma_{j+1}^2\right) \tag{3.48}$$

$$\pi_{j+1}^{(1)}\left(\sigma_{j+1}^2\right) \sim \Gamma^{-1}\left(\sigma_{j+1}^2; \beta_{j+1}^{(1)}, \alpha_{j+1}^{(1)}\right) \tag{3.49}$$

3.7.7 *Step 3 – Posterior Estimation for Third Step-stress*

Similarly, the proceeding next stress level P_3 repeats the procedure from step 2. To convert this methodology into an OB methodology then only use Jefferys prior would be used, i.e. in Step 2b the step-stress up coefficient is omitted and replaced with Jefferys prior (similar to Step 1a).

3.7.8 *Step 4 – Functional Relationships*

Having estimated the drift and diffusion coefficients, the functional relationships $\hat{y}_{\mu_j}$ and $\hat{y}_{\sigma_j^2}$ respectively are established using exploratory regression analysis (given the acceleration model is unknown). However, wear is expected to follow a power law according to Wang and Shi (2006) for a hydraulic piston pump. P_j is the accelerated stress level and $(\hat{\mu}_j, \hat{\sigma}_j^2)$ are the estimated model parameters:

$$\hat{y}_{\mu_j} = f(\hat{\mu}_j, P_j) \tag{3.50}$$

$$\hat{y}_{\sigma_j^2} = f\ (\hat{\sigma}_j^2, P_j) \tag{3.51}$$

In summary, given a degradation dataset, the closed form reliability assessment for a Brownian motion model has been shown to need parameter estimates regarding the degradation rate (drift coefficient) and the variability (diffusion coefficient). The top-level

view of the Bayesian updating methodology has been illustrated with the concept of beginning with non-informative priors indicating no prior knowledge before testing. The likelihood from test data is adjusted objectively, and the preceding test data is used to alter the shape and scale parameters via an accelerated stress coefficient. Finding the parameter estimates at each step-stress level forms the covariates used for the stress-varying environment in the Monte Carlo simulation which is then used to estimate the quantiles and credible limits of interest.

3.8 Degradation Simulation and Reliability Estimation

As reviewed in Section 1.2, the level of detail in the simulation model relates to the desired precision on the output. A consequence of testing with an extremely small sample size is the statistical uncertainty present in the parameter estimates for the simulation model (Talafuse and Pohl, 2017). The observation from the SSADT in Submission 4 (Zarzycki, 2017b) (as reported next in Chapter 4) indicates the degradation path to experience recovery in the pressure ripple measurement. It is not fully understood why the degradation path is not strictly monotone. Had it been possible to measure the physical wear of erosion then it is expected to have been strictly monotone, after all, material cannot be added. It is hypothesised that the wear of the components changes the fluid dynamics which is reflected in the pressure ripple. The degradation path trend is linearly increasing and the random change on the output is non-monotone. It is also observed that with only a sample size of two the degradation paths differ significantly, indicating a need to include unit-to-unit variability. All together these properties fit a BM model to suggest the system model is a continuous-time stochastic process (Ibe, 2013). Further complexity is added considering the random stress-varying environment of the vehicle and the power law relationships for the drift (Section 4.3) and diffusion coefficients (Section 4.4).

The inputs to these relationships are continuous; however, the time series data captured is discrete, i.e. every second. Therefore the drift and diffusion coefficients are modelled as deterministic state variables for simplicity. The simulation is classed to be stochastic and static because the state of the system is represented at a particular point in time. Such models are suited to Monte Carlo simulations. The primary advantage of MC simulations is the simplicity of detail required on the properties of interest. The primary disadvantage of MC simulation is that it computes approximations where the precision is dependent on the number of samples n (Fishman, 2006). This addition of sampling error to the overall error of approximation is undesirable (Fishman, 2006). As the number of samples increases the law of large numbers, independent and identically distributed data and the central limit theorem are satisfied and reduce the error rate by $n^{-1/2}$ (Fishman, 2006). To reduce the simulation error requires a large sample size and longer computation time, which holds irrespective on the number of

dimensions m needed for the model. Whereas for deterministic simulations the error rate is the function $n^{-1/m}$ and the complexity of detail required on the properties is increased (Fishman, 2006). To gain the extra detail is time-consuming and outweighs the benefit compared to MC Simulation(Fishman, 2006). For instance, at this stage, the level of detail does not require the inclusion of pump unit-to-unit variability regarding performance and downstream engine restrictions because the NPD is in its infancy. However, the scope should leave the capability to expand the model to include this data in the future and achieve greater precision in the reliability estimate. This scope may be easily implemented using MC simulation. For these reasons, a Monte Carlo (MC) simulation is pursued.

The system model is based on the Brownian motion model as defined in Section 3.7, eqn. (3.27) where $B(t)$ is the standard Brownian motion with a mean of 0 and a variance of t, $B(t) \sim \mathcal{N}(0, t)$. Thus, $B(t)$ is modelled as a continuous-time random normal parametric distribution using the MATLAB random number generator function `randn`. The issue with random number generators is that they are not exact and are pseudorandom numbers and deterministic (Moler, 2004; Zio, 2013). It is recommended to check the validity of the "black box" function available in proprietary software (Law and Kelton, 2000) and as expected MATLAB uses a validated algorithm developed by Marsaglia and Tsang (2015) called the *ziggurat* algorithm. The *ziggurat* algorithm quickly approximates from an exact normal distribution and as such the trade-off is a variance range available of at least 0.98 and a resolution of 2^{64} (Marsaglia and Tsang, 2015). This means the algorithm will generate 2^{64} random numbers before repeating itself. In the case study simulation, the transient vehicle data inputs are in seconds, so to simulate a degradation path to at least $40{,}000$h requires $144{,}000{,}000$s. Although the actual system is continuous, the inherent nature of the vehicle data input makes the simulation time discrete. Because the system model is static, this has no implications on the output. However, the drift and diffusion coefficients need to be time-scaled from hours to revolutions because the SSADT speed was held constant, leaving a simple scaling of the drift coefficient by the pump speed and the diffusion coefficient scaled by time only.

The sample size required for a simulation can be first estimated by the same methods as for a statistical experiment (Hahn, 1972), for example simulating lithium-ion battery degradation (Lin and Chung, 2019). Given that the Brownian motion model approximates to a normal distribution the equation (3.1) is used as a starting sample size. The allowable accuracy is arbitrarily set in line with standard precision on performance measurements as ±2.00%, and the confidence level is set by the reliability target of 90% ($\alpha = 0.10$). Thus, 28 samples are the first approximation; however it is common to increase the sample size until the quantity of interest converges (Hahn, 1972). This approach can be a costly methodology

depending on the duration to complete one sample simulation (Hahn, 1972), and was analysed in Submission 5 (Zarzycki, 2018a) where a closed-form expression was used to compare the simulation error. It was concluded that 1000 samples were sufficient enough to achieve the desired precision of ±2.00%. Additionally, in Submission 5 (Zarzycki, 2018a) and Submission 6 (Zarzycki, 2018b) several vehicle transients were input into the simulation. It was observed that the duration of simulation time increases as the survival rate improves with the longest simulation of 1000 samples taking approximately 15 minutes.

The top-level algorithm for the BM model with covariate drift and diffusion coefficient is shown in Figure 3-24. The left-hand side of the process loads the formulae for the drift and diffusion coefficients based on the pump outlet pressure. The transient cycle of the engine speeds are broken down into revolutions per second, and the total number of revolutions is calculated for the desired total simulation time. The right-hand side of the process is setting the pseudo-failure threshold and the number of random samples before proceeding to run the MC simulation with the Brownian motion model. For continuity in comparing the difference between simulations, the code uses a seeded random number from a Normal distribution. After the simulation of one sample degradation path $Y_t(i)$ according to Equation (3.27) and Figure 3-24, the first time to pseudo failure threshold is found and stored before proceeding to erase the path to free up the computer memory.

With the MC simulations complete, the first time to the pseudo-failure threshold is passed through a proprietary statistical package. In this case, Minitab 18 is used as it is more readily set up to generate the cumulative distribution function than coding in MATLAB. Using Minitab, the quantile and confidence limits can be extracted. The customer specific requirements were a B10 life of 40,000 hours with a 95% confidence limit.

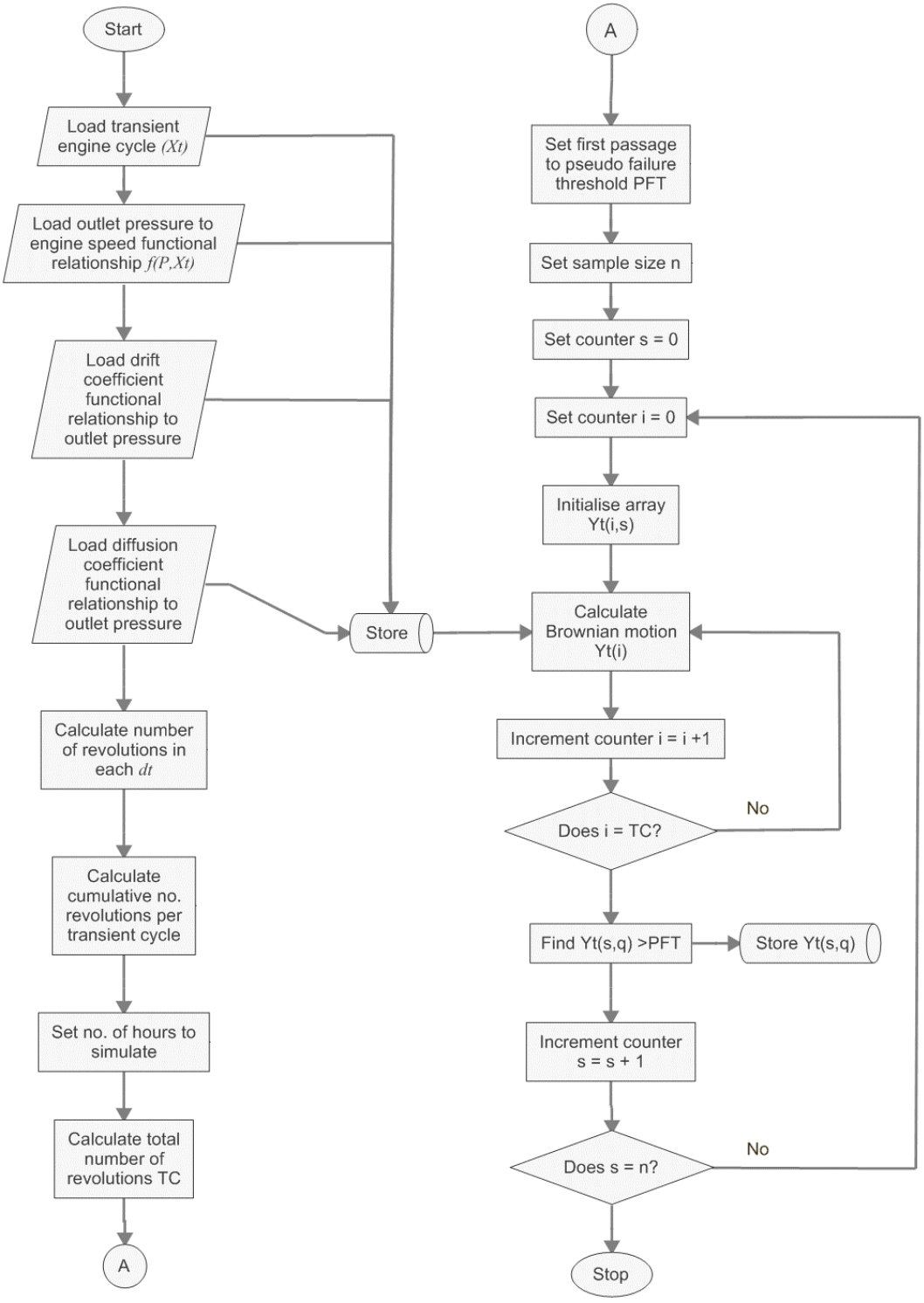

Figure 3-24 Brownian motion model with covariate drift and diffusion coefficient.

Chapter 4: Results, Analysis and Simulations

In this chapter, the key findings from the step-stress test and the analysis of results and simulations are presented. The post-test examination (Section 4.1) of the pumps reveals degradation captured in the analysis of the time domain signal (Section 4.2). The data is regressed, and the parameters estimated are used to describe the functional relationship of stress to the drift coefficients (Section 4.3) and diffusion coefficients (Section 4.4). These are input into the Monte Carlo simulation to extract pseudo failure time for the three parameter estimations methods (MLE, OB and B) (Section 4.5).

4.1 Post-Test Examination of Pump

Upon the pump disassembly, there are signs of two latent defects. The first observation (see Figure 4-1) captures erosion on the gear pocket end face, positioned on the edge of where the pumping gears open up to the outlet port. The erosion is more prominent on pump no.1 but equally visible is the bright polishing on pump no.2 in the same vicinity (see Figure 4-2). The erosion is a mechanism of the gear tooth pocket filled with low-pressure fluid suddenly opening up to a volume of high-pressure fluid BS ISO 7146-1:2008 (British Standards Institution, 2008), causing localised high velocities to erode the edge of the gear pocket face and or produce localised cavitation.

Figure 4-1 Pump no.1 after SSADT. Drive gear pocket exhibiting erosion.

Figure 4-2 Pump no.2 after SSADT. Drive gear pocket exhibiting erosion.

Pump cavitation erosion in this vicinity frequently occurs in NPD after long hour engine tests (Zarzycki, 2017a). The solution involves the addition of timing grooves to dampen the sudden opening of the gear cavity, although this is at the sacrifice of pump efficiency.

Secondly, an uneven tooth wear pattern is observed (see Figure 4-3) indicating either misalignment of the pumping gears or insufficient stiffness of the design. Similar to the erosion, pump no.1 (see Figure 4-3) has a larger area of macro pitting (Höhn and Michaelis, 2004) on the gear tooth flank whereas pump no.2 (see Figure 4-4) has developed micro pitting, indicated by the light grey shade (Höhn and Michaelis, 2004). The solution may be as simple as tightening up the tolerances to reduce misalignment. Alternatively, it may need a significant design change to stiffen the journal to reduce bending or require the selection of a different pumping gear material grade or surface treatment. The detection of degradation pump health was successful as discussed in the analysis of test data.

Figure 4-3 Pump no.1 after SSADT. Pumping drive gear exhibiting contact fatigue (pitting) and uneven wear.

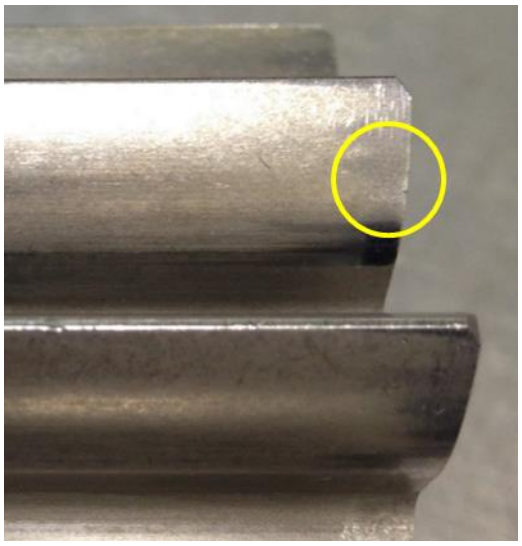

Figure 4-4 Pump no.2 after SSADT. Pumping drive gear exhibiting contact fatigue (micro-pitting) and uneven wear.

4.2 Analysis of Test Data

In terms of the experiment, the test duration was shortened from 24 hours to 21 hours because the pressure ripple measurements (Figure 4-6 to Figure 4-9) were successfully indicating a change in pump health. To validate the need for the pressure ripple MODWT-ARMS(2,1) a one-way analysis of variance (ANOVA) was conducted on (1) the conventional performance test data, (2) FFT of the pressure ripple, (3) the original ARMA method on pressure ripple and (4) the ARMA-MODWT(2,1). A one-way ANOVA is a statistical test to establish if there is

a common mean from a group of data (Montgomery, 2013). In essence, it is used to detect a significant change of the performance mean providing the data from incremental time and pressure is normally distributed (as already proven in the measurement error study). The summary of the findings is in Table 4-1.

The ANOVA on the performance test results measuring flow (Q) [m^3/s], torque (T) [Nm] and calculating overall efficiency (OE) [%] indicated no change in flow for both pumps, but a significant change in torque. Pump no.1 initially reduced in torque, yet after 7 hours of running it then experienced a jump in torque of 0.05Nm and continued to rise after that. The jump in torque coincides with the change in the step-stress at 8 hours. Conversely, pump no.2 initially reduced in torque and continued to do so. The outcome is mixed on the overall efficiency; pump no.1 lowered in OE only to recover to finish on the same OE, whereas pump no.2 experienced an increase in OE by 2.5%. The results are not wholly conclusive.

Similarly, the analysis of pressure ripple measurements using FFT and focusing on the first three harmonics also did not offer a clear degradation path. The pressure ripple signal and FFT for the start and finish of pump no.1 shown in Figure 4-6 and Figure 4-7 and pump no.2 shown in Figure 4-8 and Figure 4-9. There is a significant difference in the profile of the trace and the amplitude when comparing results from the two pumps. Generally the 2^{nd} harmonic collaborated (in the sense that the amplitudes were increasing for both pumps with distinguishable mean drift coefficients for each stress), however, the variance for each repeated measurement was too large to use for modelling degradation.

Referring to Figure 4-5, the pressure ripple analysis using ARMA(2,1) indicates an increase in damping coefficient Zeta suggesting the damping of the pump system has increased, most likely from the erosion of housing material (see Figure 4-1). The expected trajectory of the system natural frequency Omega, from increased damping, is to lower the natural frequency however; the analysis shows a progressive increase with a final significant jump. It is surmised that the gear contact fatigue (see Figure 4-3) is interacting and contributing to the increased noise of the pressure ripple signal and stiffness of the pump as a system. Overall, the ARMA(2,1) alone did not yield any revelations with the start and finish points of Omega and Zeta looping back and forth and leaving inconclusive degradation paths.

The pressure ripple analysis using ARMA(2,1) alone did not yield any revelations, with the start and finish points of the natural system frequency (Omega [Hz]) and the system damping coefficient (Zeta) looped back and forth and leaving inconclusive degradation paths.

The pre and post-test decomposed MODWT signals for pump no.1 are shown in Figure 4-10 and Figure 4-11 respectively. There is a noticeable change in the detailed coefficients D1 to D8. Further clarity is provided with images focused on the raw signal and the detailed

coefficient D5 are provided in Figure 4-12 and Figure 4-13 for pump no.1 at 0 and 21 hours respectively.

Similarly, the results for pump no.2 shown in Figure 4-14, Figure 4-15 and zoomed in images in Figure 4-16 and Figure 4-17 indicates a deviation from 0 hours. The raw signal indicates a larger amplitude however, the difference is less emphatic in detail coefficient 5, which correlates with the observations of less wear found in the physical post-test inspection.

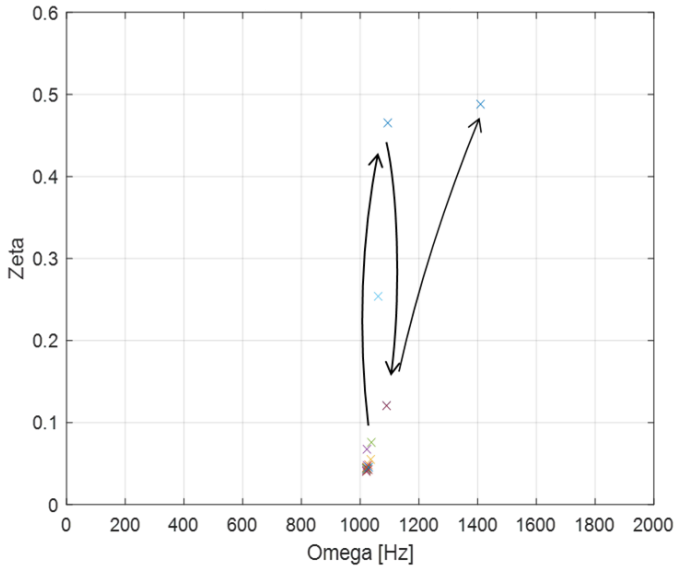

Figure 4-5 ARMA Outputs for pump no.1.

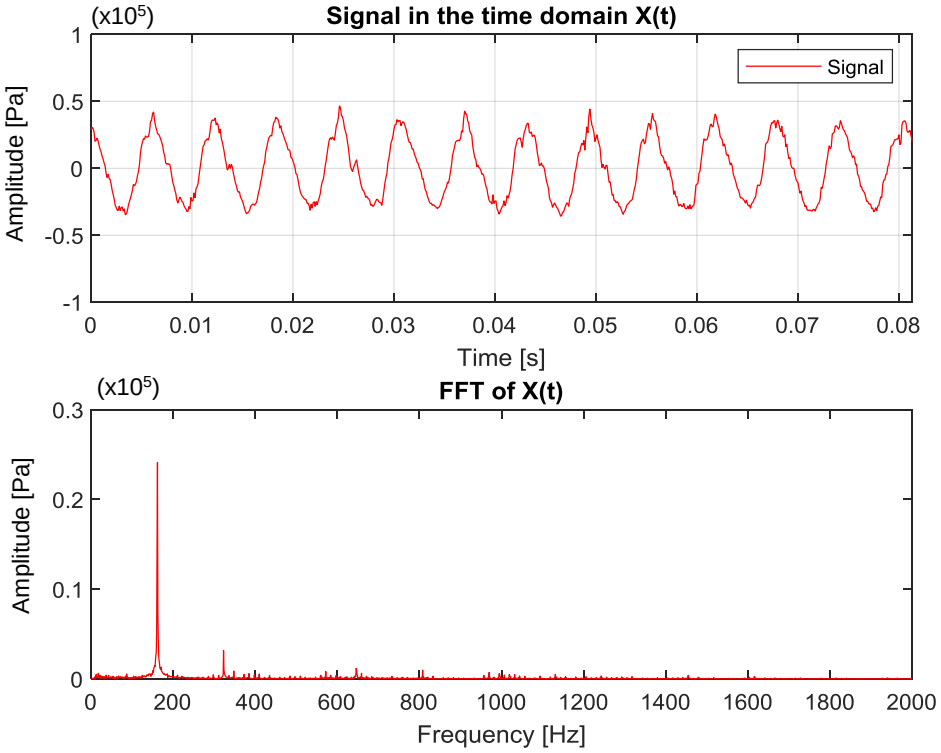

Figure 4-6 Pressure ripple signal for 1 rev, FFT for pump no.1, 0 hours, 746rpm.

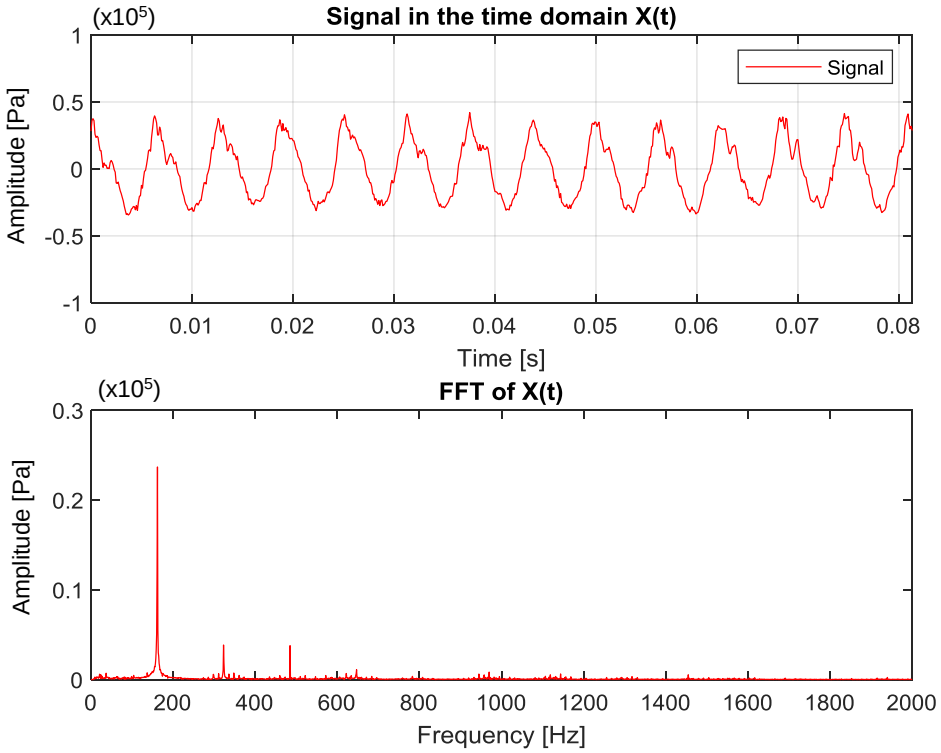

Figure 4-7 Pressure ripple signal for 1 rev, FFT for pump no.1, 21 hours, 746rpm.

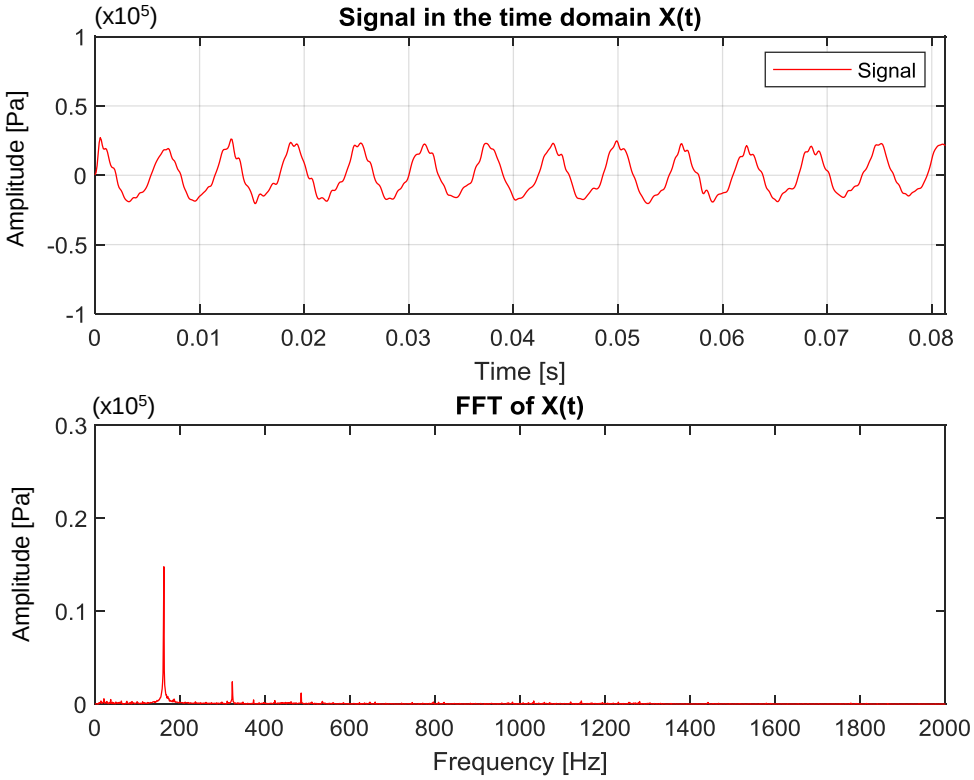

Figure 4-8 Pressure ripple signal for 1 rev, FFT for pump no.2, 0 hours, 746rpm.

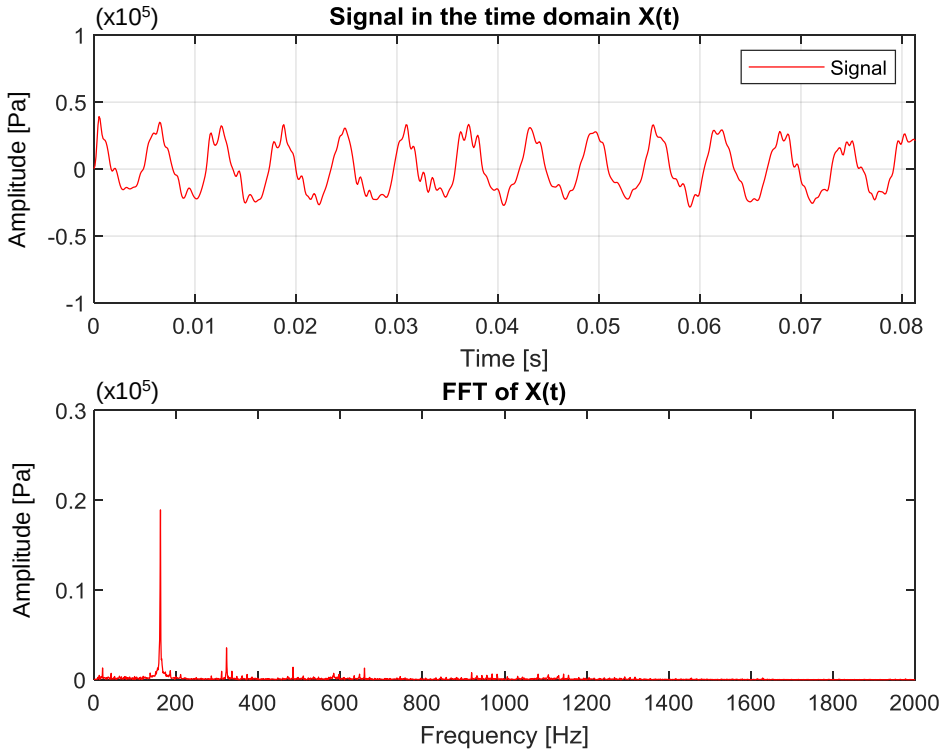

Figure 4-9 Pressure ripple signal for 1 rev, FFT for pump no.2, 21 hours, 746rpm.

Table 4-1 Summary, Analysis of degradation parameters.

Parameter	Analysis method	Pump no.1	Pump no.2	Comments
Pump flow	Mean (ANOVA)	No change	No change	Too insensitive to detect a change
Pump torque	Mean (ANOVA)	Increased by 0.05 Nm	Decreased by 0.15 Nm	Opposite degradation paths are inconclusive
Pump overall efficiency	Mean (ANOVA)	Decreased in efficiency but recovered to the same as the start	Increased by 2.5%	Opposite degradation paths are inconclusive
Pressure ripple	FFT (1st harmonic) (ANOVA)	A significant change in step-stress P_3 good for diagnostics	Stochastic reduction in magnitude over time	High variance and no visual degradation path
Pressure ripple	FFT (2nd harmonic) (ANOVA)	Increasing magnitude over time with distinguished drift coefficients	Increasing magnitude over time with distinguished drift coefficients	High variance
Pressure ripple	FFT (3rd harmonic) (ANOVA)	Increasing magnitude over time with distinguished drift coefficients	Decreasing magnitude over time with higher drift coefficients rates at lower stresses	High variance Opposite degradation paths are inconclusive
Pressure ripple	ARMA (2,1)	A significant change in step-stress P_3 good for diagnostics however significant recovery experienced	Significant changes throughout time with significant recovery experienced	Opposite start and finish points with multiple significant changes over time. The degradation paths are inconclusive
Pressure ripple	MODWT-ARMA(2,1) Det05 Omega	Increasing magnitude over time with distinguished drift coefficients	Increasing magnitude over time with less distinguished drift coefficients than pump no.1	Stochastic with 2 or 3 recoveries but overall degradation path is increasing for both
Pressure ripple	MODWT-ARMA(2,1) Det05 Zeta	Increasing magnitude over time with smaller distinguished drift coefficients compared to Det05 Omega	Increasing magnitude over time with smaller distinguished drift coefficients compared to Det05 Omega	Stochastic with 2 or 3 recoveries but overall degradation path is increasing for both. High variance.

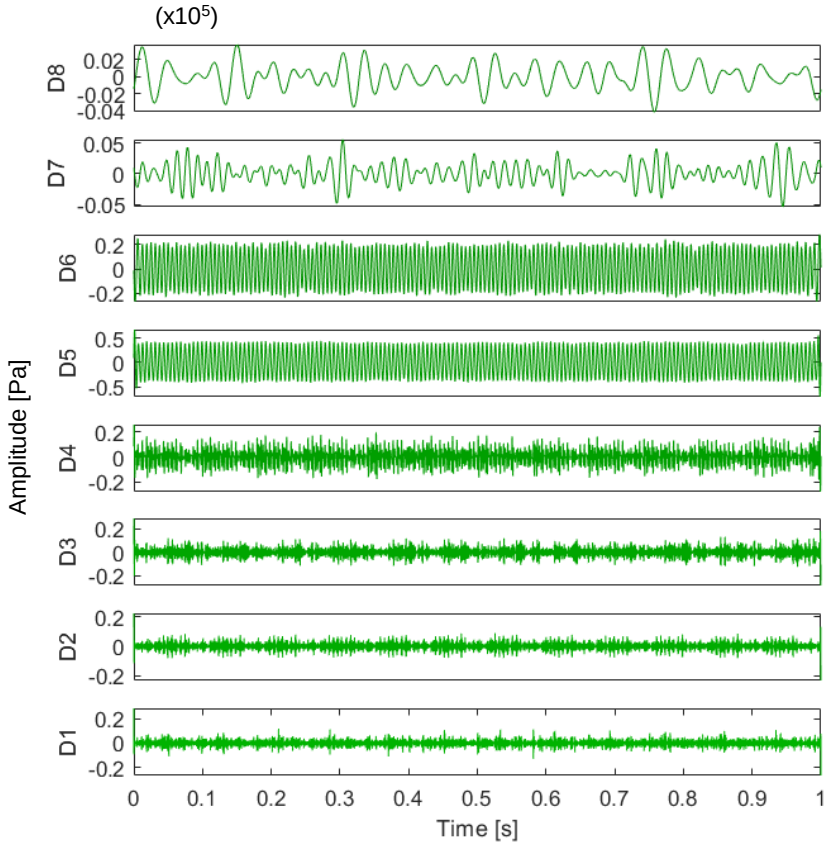

Figure 4-10 MODWT Signal decompositions (D1 to D8) for pump no.1, 0 hours.

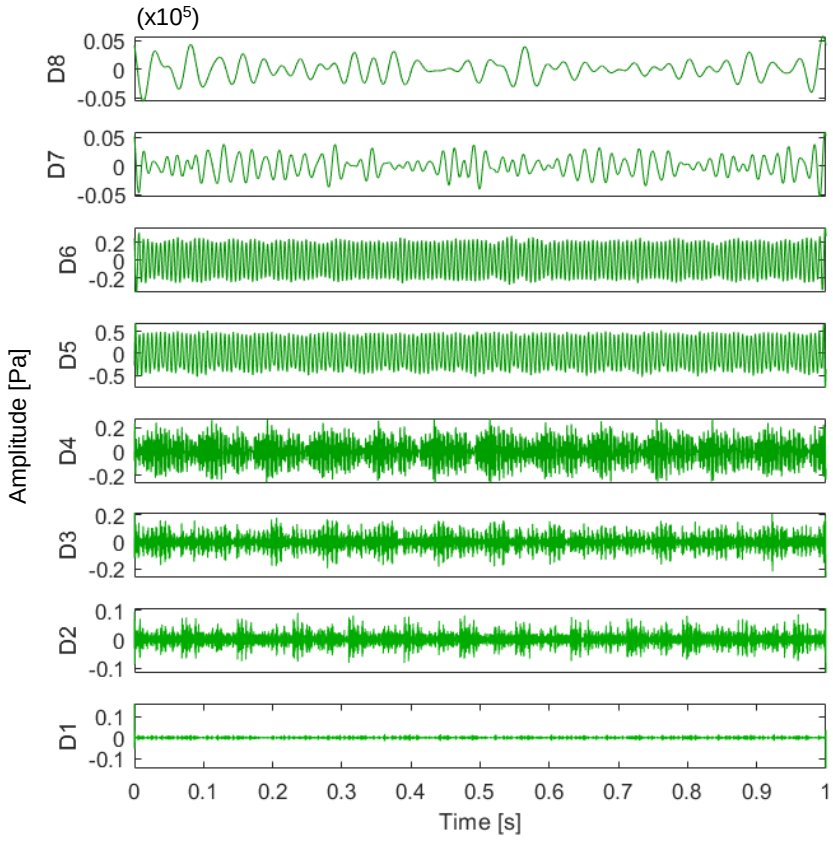

Figure 4-11 MODWT Signal decompositions (D1 to D8) for pump no.1, 21hours.

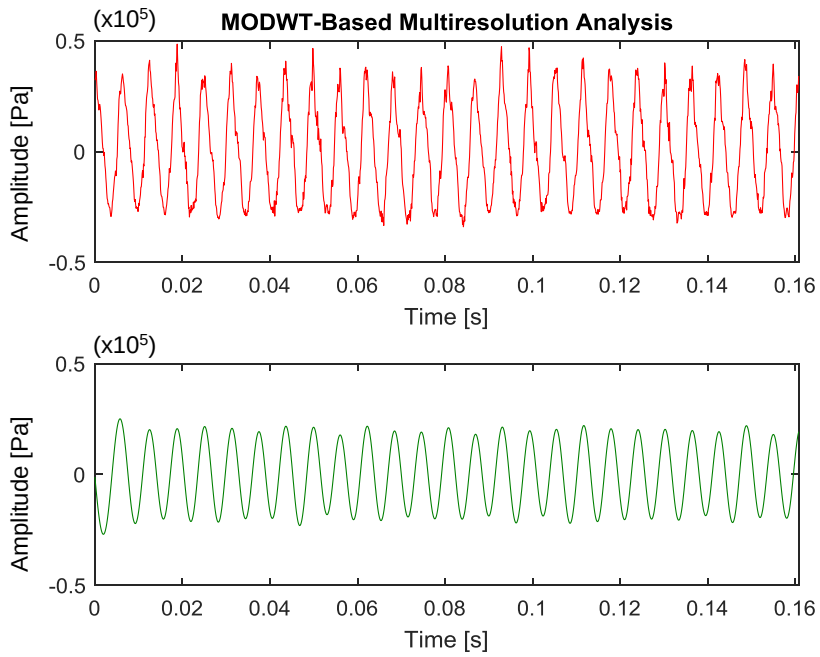

Figure 4-12 Closer image of raw signal "S" (Top) and MODWT Detail 5 "D5" coefficient (Bottom) for pump no.1, 0 hours.

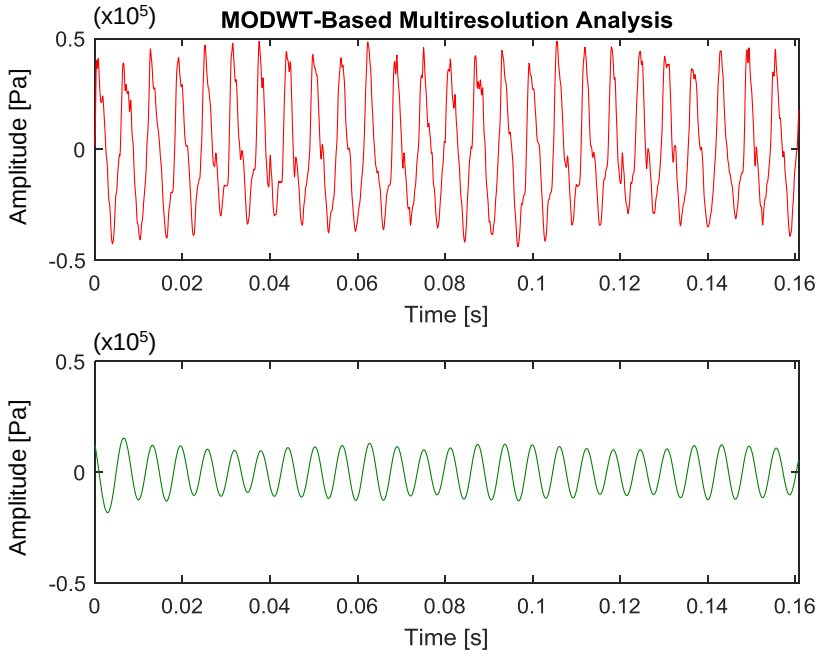

Figure 4-13 Closer image of raw signal "S" (Top) and MODWT Detail 5 "D5" coefficient (Bottom) for pump no.1, 21 hours.

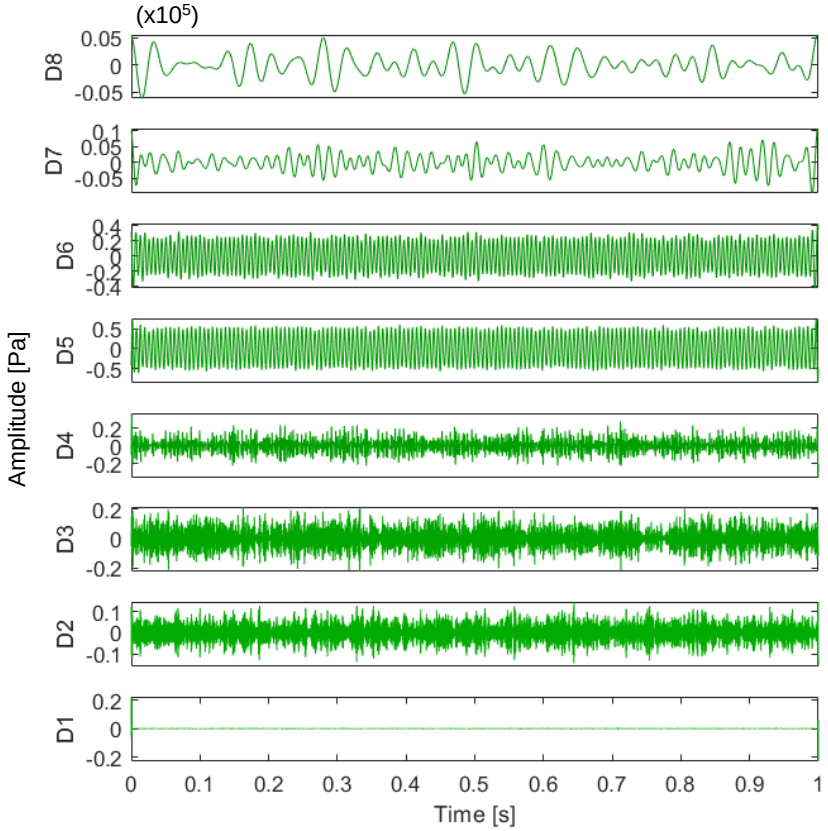

Figure 4-14 MODWT Signal decompositions for pump no.2, 0 hours.

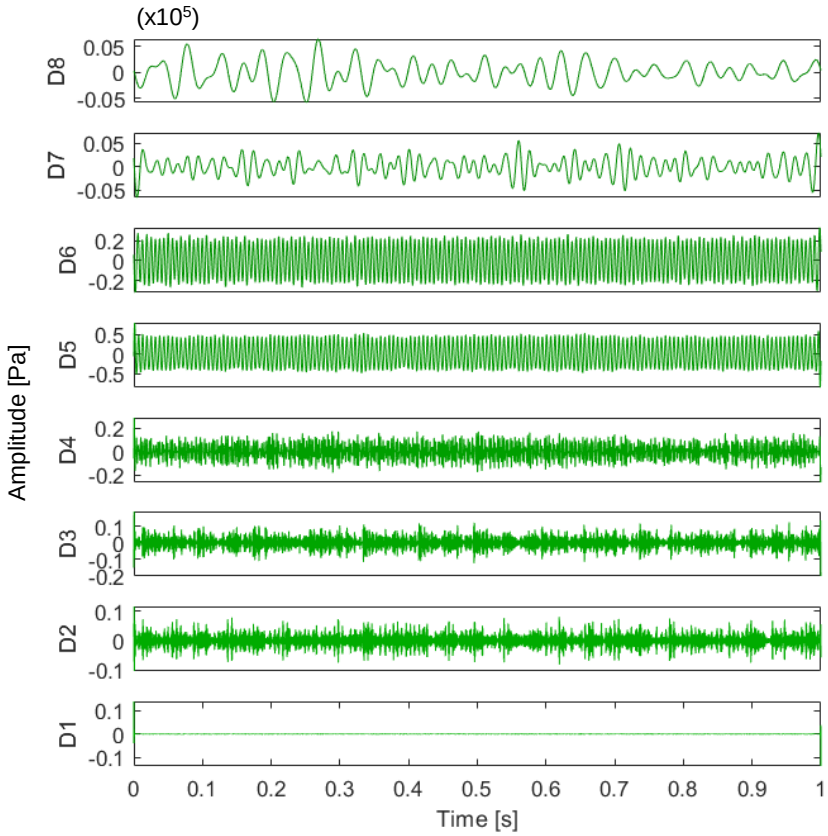

Figure 4-15 MODWT Signal decompositions for pump no.2, 21hours.

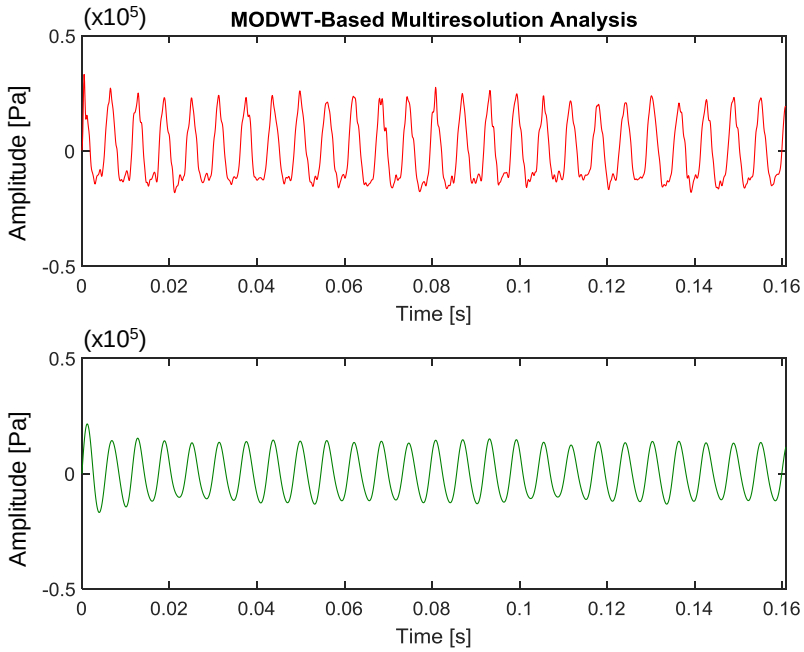

Figure 4-16 Closer image of raw signal "S" (Top) and MODWT Detail 5 "D5" coefficient (Bottom) for pump no.2, 0 hours.

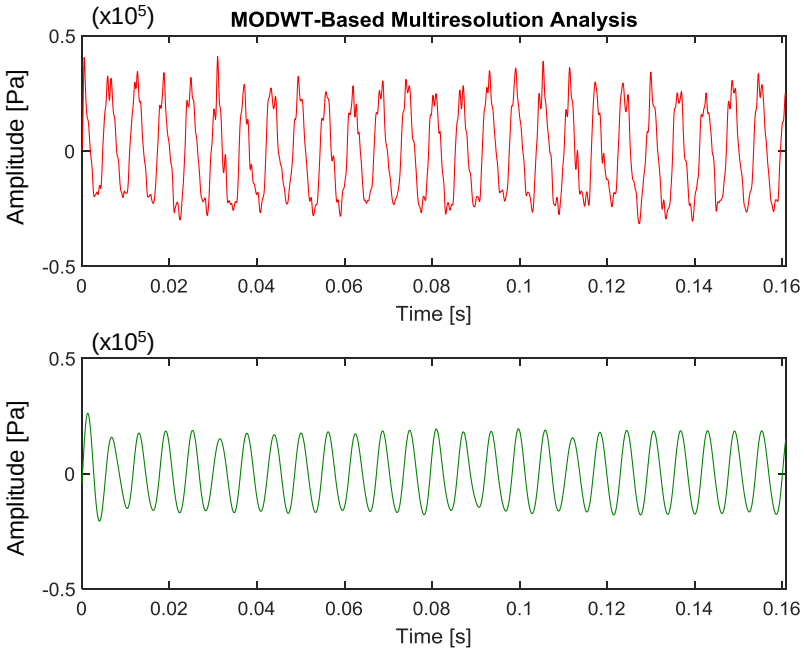

Figure 4-17 Closer image of raw signal "S" (Top) and MODWT Detail 5 "D5" coefficient (Bottom) for pump no.2, 21 hours.

The analysis indicates that combining MODWT with ARMA(2,1) for pressure ripple analysis provides a greater opportunity to model the degradation. Focusing on the fundamental frequency range in the detailed coefficient 5 (Det05) and Figure 4-18, the extracted parameter Omega indicates distinguished changes in the drift coefficient for each step-stress, with both pumps exhibiting an increase in Omega. Pump no.1 has a larger drift coefficient that coincides with the more considerable damage observed on the pump disassembly (see Figure 4-1). The hypothesis is that a lump of metal broke free during the third stress, which caused an erratic jump. The extracted parameter Zeta also follows a similar mean degradation path; however, the variance is larger, and it is realised that the MODWT technique essentially removes the damping from Det05 to create a sinusoidal wave, rendering it unusable. Thus, the remainder of the study uses Omega extracted from Det05. The repeated measurements at each data point demonstrate a low standard error (SE) in the measurements, indicating the sensitivity of the monitoring method.

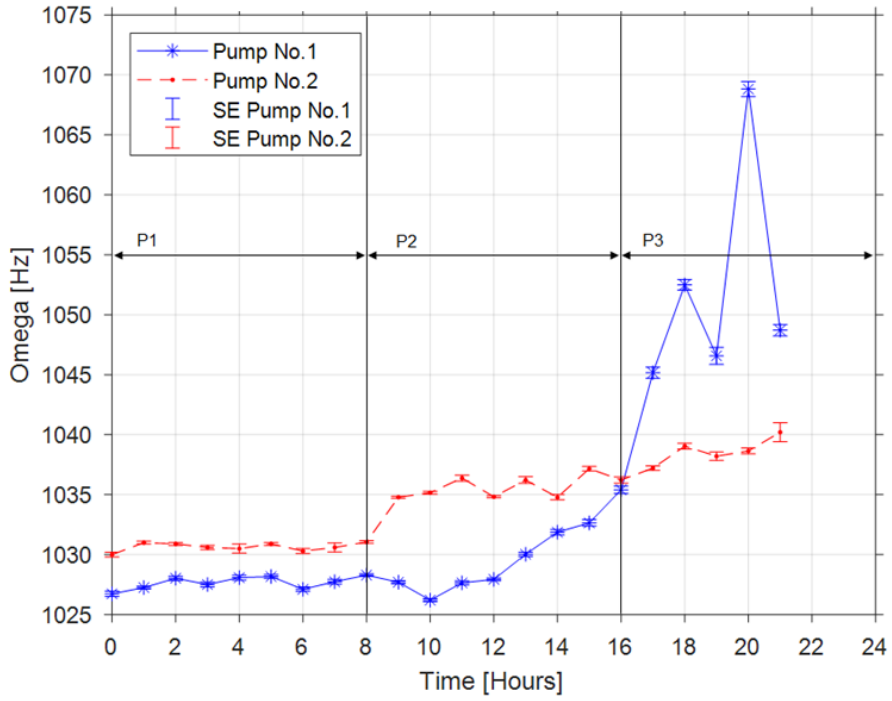

Figure 4-18 Det05, ARMA(2,1) mean Omega degradation path for pumps no.1 and no.2 with standard errors.

The next step is the regression analysis and parameter estimation where the differential change in Omega is of more use than the reported value because the interest is in detecting change. The individual degradation paths for each pump are split by the step-stress, P_1, $P_2$and P_3. Exploratory plotting (Figure 4-19, Figure 4-20 and Figure 4-21) indicate linear regression as a suitable method. The data points are not strictly monotonic because some recovery is observed; for instance, pump no.1 at 19 hours (Figure 4-21). This stochastic process is ideal for the Brownian motion model as no linear transformation is required.

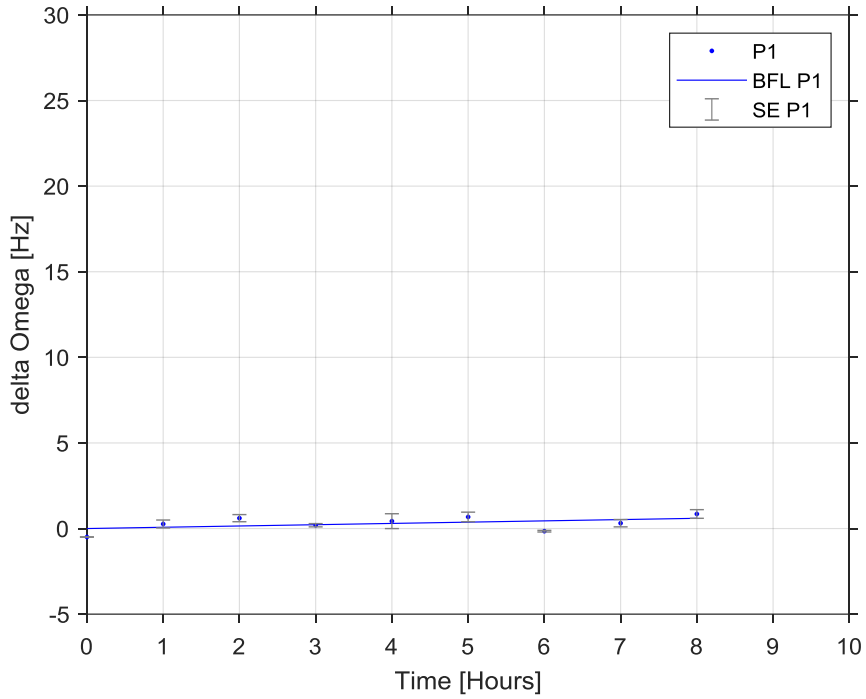

Figure 4-19 The averaged result of pumps no.1 and no.2, Omega degradation path for stress $\boldsymbol{P_1}$, Det05 (BFL = Best Fit Line).

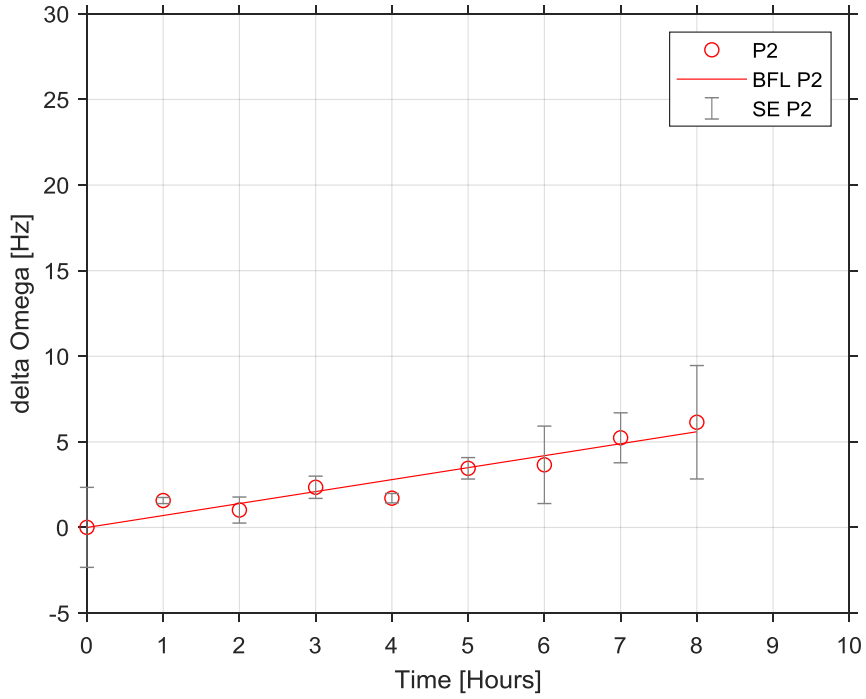

Figure 4-20 The averaged result of pumps no.1 and no.2, Omega degradation path for stress $\boldsymbol{P_2}$, Det05 (BFL = Best Fit Line).

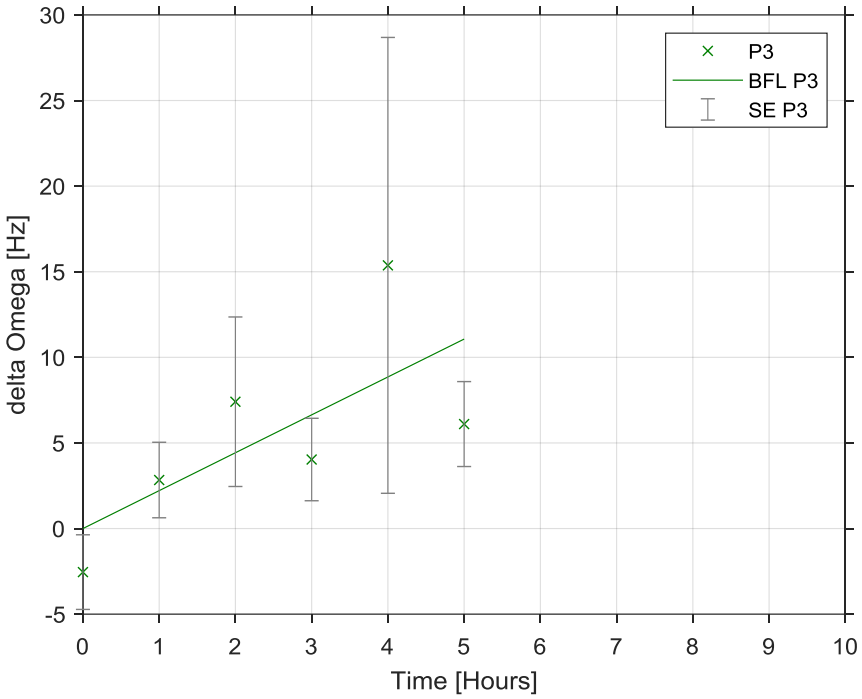

Figure 4-21 The averaged result of pumps no.1 and no.2, Omega degradation path for stress $\boldsymbol{P_3}$, Det05 (BFL = Best Fit Line).

In summary, the conventional performance parameters and feature extraction techniques reveal inconclusive evidence and inconsistent degradation paths for modelling. The MODWT-ARMA(2,1) illustrates a linear regression can be fitted for each stress, but the SE is significant for the higher stress P_3. The SE reflects the difference in degradation paths rather than the measurement error, which is insignificant. The validity of the regression analysis is discussed in the following section.

4.3 Drift Coefficient Parameter Estimation and Functional Relationship

In this section, the three-parameter estimation methods Maximum Likelihood Estimation (MLE), Objective Bayes (OB) and Bayesian Updating (BU) are compared for the drift coefficient. The mean parameter estimates for all three methods (refer to Table 4-2) are the same because the linear regression is no different between methods. However, the Standard Error (SE) differs between the methods and forms the majority of this discussion. Reporting the SE reveals the precision in the parameter estimation and its validity (Barford, 1985; Berendsen, 2011).

Table 4-2 MLE, OB and BU Drift parameter estimation with standard error.

	Pressure [Pa] ($x10^5$)	Drift coefficient [Hz/hr]	SE [Hz/hr]
MLE	6.30	0.0747	0.04027
	8.45	0.6990	0.17088
	10.60	2.2134	1.33731
OB	6.30	0.0747	0.04305
	8.45	0.6990	0.18268
	10.60	2.2134	1.49516
BU	6.30	0.0747	0.04305
	8.45	0.6990	0.12344
	10.60	2.2134	0.57494

A graphical presentation of Table 4-2 is provided in Figure 4-22. As expected, the diffuse prior of the OB method outputs similar precision compared to the MLE (Berger, Bernardo and Sun, 2009; Xu and Tang, 2012b) for the first and second stress (P_1 and P_2), that are typically 7% wider. The difference between the MLE and OB is that the SE widens to 11.8% as observed for the third stress (P_3), reflecting greater uncertainty. The precision when using an extremely small sample size and reasonably practicable measurement intervals is indicated in the SE because it is a direct function of the number of observations (Barford, 1985; Berendsen, 2011). In hindsight, stopping the test early to prevent the risk of overdeveloped wear meant the third stress (P_3) has fewer observations compounding the wider SE. Overall, the SE for all stresses are significantly large, and this does not provide sufficient confidence in the parameter estimates.

This situation is improved using the BU method. The solution of using the preceding test data as the prior improves the confidence in the mean parameter estimate. As observed, the SE narrows compared to the MLE as the sequence of building on existing data progresses. The SE in the BU method for the second (P_2) and third stress (P_3) is reduced by 27.8% and 43.0% respectively, compared to the MLE. It is expected that if more observations were taken in the third stress (P_3), this would be improved further.

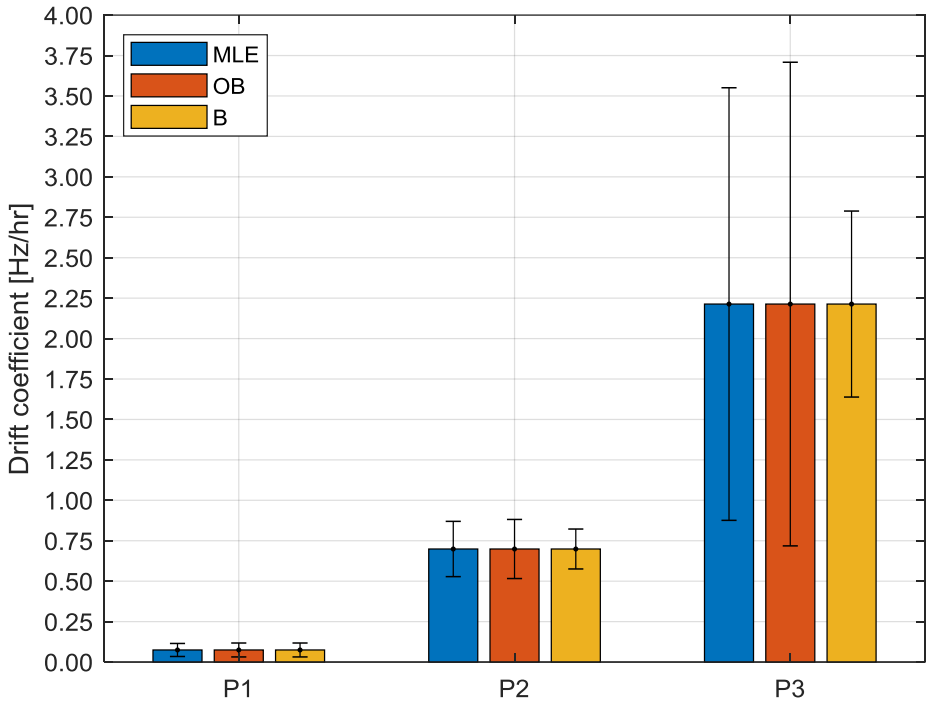

Figure 4-22 MLE, OB and BU drift parameter estimation with SE bars.

Nevertheless, acknowledging the lack of confidence in the parameter estimations but continuing to demonstrate the methodology, the functional relationship is analysed next. Visually the mean drift coefficient to stress relationship, as shown in Figure 4-23 and Figure 4-24, are no differences between the three parameter estimation methods, only differing in the SE. In this graphical summary is it clear that the functional relationship has significant uncertainty.

However, generally, a power law relationship is formed which is typical for mechanical failure mechanisms such as wear and fatigue (Wang and Shi, 2006) $\left(\hat{y}_{\mu} = (4.6237\text{E}-07) \times P^{6.56651}\right)$. Using natural logs gives the following linear relationship and simplifies analysing the goodness of fit:

$$\hat{y}_{\mu} = \text{e}^{(6.56652 \times \ln P) - 14.58690} \tag{4.1}$$

The log regression confirms the linearity and in Table 4-3 the goodness of fit R^2 = 0.988 validates the linearity further.

Table 4-3 Drift coefficient functional relationship to stress (MLE, OB and BU).

	Estimate	SE	R^2
Intercept *c*	-14.58690	1.51710	0.988
Gradient *m*	6.56652	0.71475	

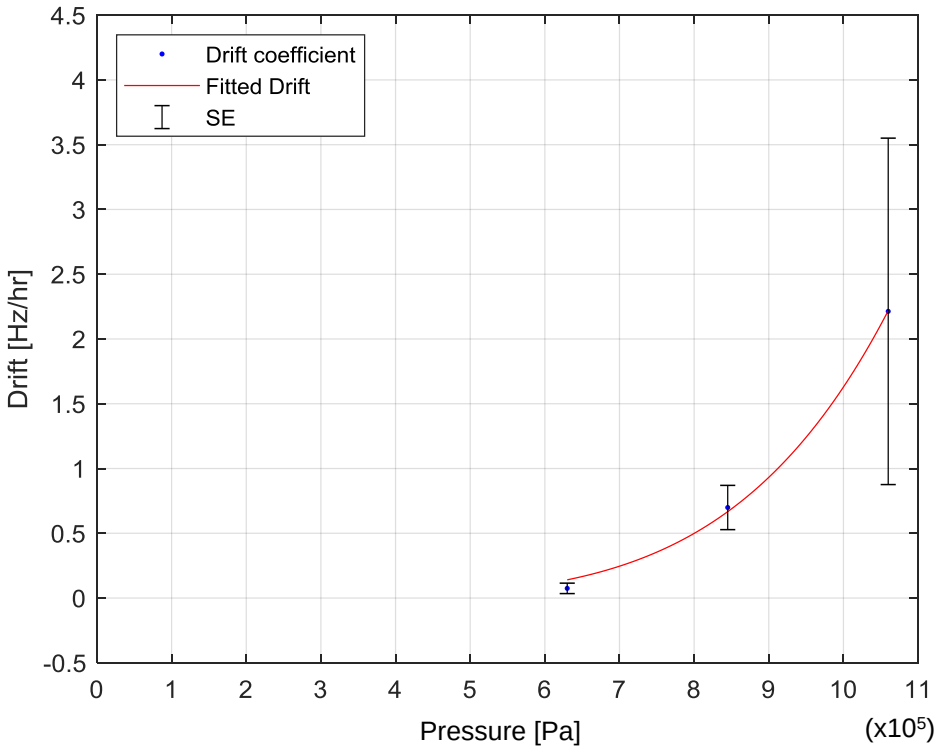

Figure 4-23 MLE parameter estimates, drift coefficient vs stress with SE bars.

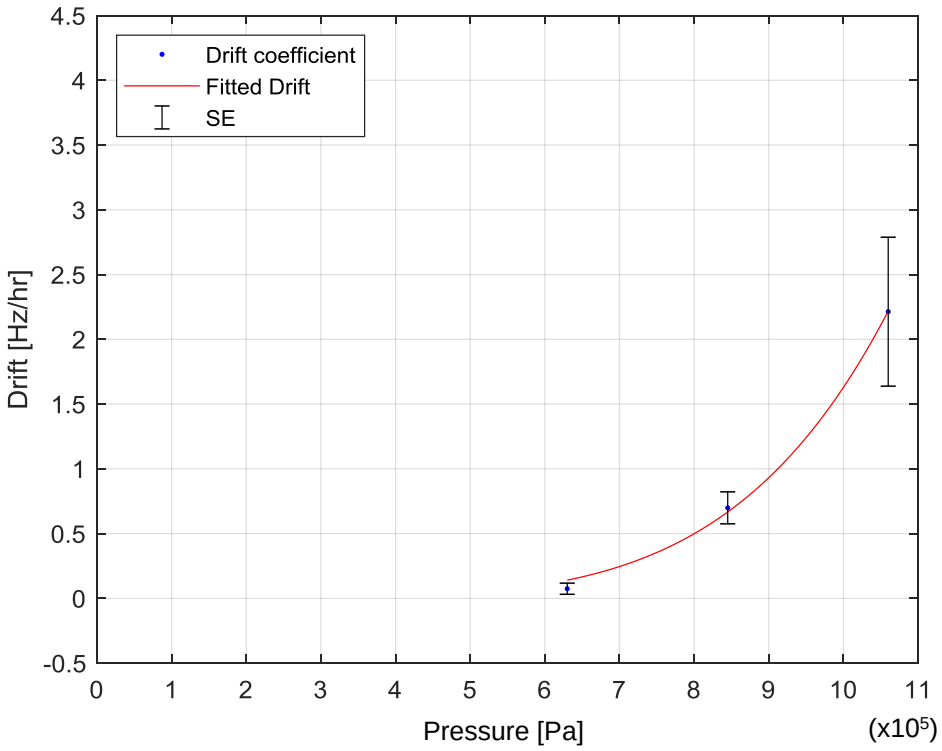

Figure 4-24 BU parameter estimates, drift coefficient vs stress with SE bars.

To summarise, the SE of the mean drift coefficient widens as the pump degrades under higher stress. Improvement is required in the test setup as the standard errors are too high, leading to insufficient confidence in the estimations. The precision can be improved by increasing the number of observations (Barford, 1985; Berendsen, 2011) ideally by reducing the interval between repeated measurements, which was not reasonably practicable using a manual measurement system.

Regarding the methods of parameter estimation, it was observed that the OB model outputted marginally wider SE compared to the MLE. Most importantly a positive outcome is observed because the BU methodology reduces the SE with extremely small sample sizes. The BU method is advantageous as it contributes to achieving the overall goal; however, this alone was not enough to improve confidence beyond doubt.

Irrespective of the SE, the resulting functional relationship of drift to stress is generally found to be a power law as expected with typical mechanical wear out failures such as fatigue (Wang and Shi, 2006). A similar set of observations is expected for the diffusion coefficient, which will be analysed next.

4.4 Diffusion Coefficient Parameter Estimation and Functional Relationship

In this section, the three parameter estimation methods MLE, OB and BU are compared for the diffusion coefficient. The diffusion coefficient is estimated from the sample standard deviation of the mean drift coefficient (see section 3.7). Thus, the diffusion coefficient varies depending on the method (refer to Table 4-4). Reporting the standard error (SE) reveals the precision in the parameter estimation and its validity (Barford, 1985; Berendsen, 2011).

Table 4-4 MLE, OB and BU diffusion parameter estimation with standard error.

	Pressure [Pa] (x10^5)	Diffusion coefficient [Hz/hr]	SE [Hz/hr]
MLE	6.30	0.4411	0.2584
	8.45	1.8719	1.0963
	10.60	7.9116	5.1662
OB	6.30	0.4716	0.3013
	8.45	2.0012	1.2786
	10.60	8.8455	6.7211
BU	6.30	0.4716	0.3013
	8.45	1.3599	0.6910
	10.60	3.9460	1.8433

Figure 4-25 shows the data in Table 4-4 as a graphical summary. Similarly to the drift coefficient, the OB method outputs parameter estimations close to the MLE with the same ratios, i.e. 7% larger for the first and second stress (P_1 and P_2) and 11.8% larger for the third stress (P_3). The difference in the SE is reflected in the drift coefficient (see Section 4.3). The precision of the diffusion parameter differs though, with a wider SE of 16.6% for both P_1 and P_2, and 30.1% for P_3. Once again, there is more significant uncertainty using the OB method. Similarly, the SE for all stresses are significantly large, and that does not provide sufficient confidence in the diffusion parameter estimates.

Conversely, the BU method reduces the diffusion coefficient parameter estimate for all stresses, but notably halves the estimate of the MLE from 7.9 Hz/hr to 3.9Hz/hr for stress P_3. The reduction is a consequence of using the preceding test data as the prior by increasing the number of observations and reduces the standard deviation for the drift parameter estimate. Equally, the SE narrows significantly compared to the MLE as the sequence of building on existing data progresses. The SE for the BU method for the P_2 and P_3 stresses are reduced by 37.0% and 64.3% respectively, compared to the MLE. However, in terms of increasing confidence in the diffusion parameter estimate, the ratio to the SE does not improve

significantly. It is expected that if more observations were taken in the third stress (P_3), this would be improved further.

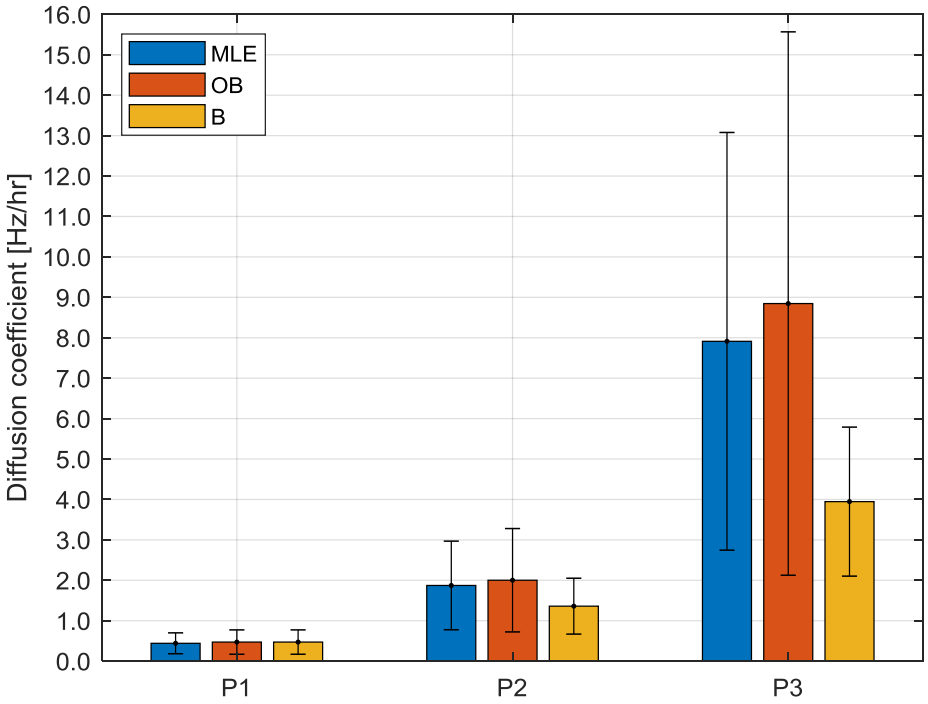

Figure 4-25 MLE, OB and BU diffusion parameter estimation with SE bars.

Figure 4-26,

Figure 4-27 and Figure 4-28 all indicate a power law dependence of the diffusion coefficient to outlet pressure for the MLE, OB and the BU methods respectively. The power law is significant in confirming the need to incorporate the diffusion as a covariant in the degradation model. In these graphical summaries is it clear that the functional relationship has considerable uncertainty, which is improved with the BU method.

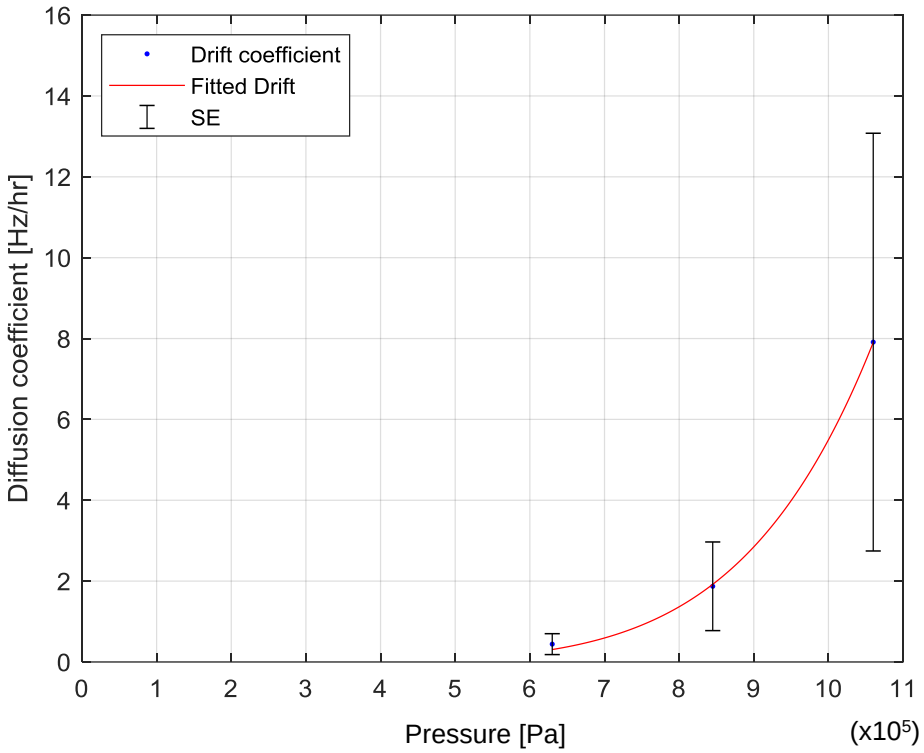

Figure 4-26 MLE parameter estimates, diffusion coefficient vs stress with SE bars.

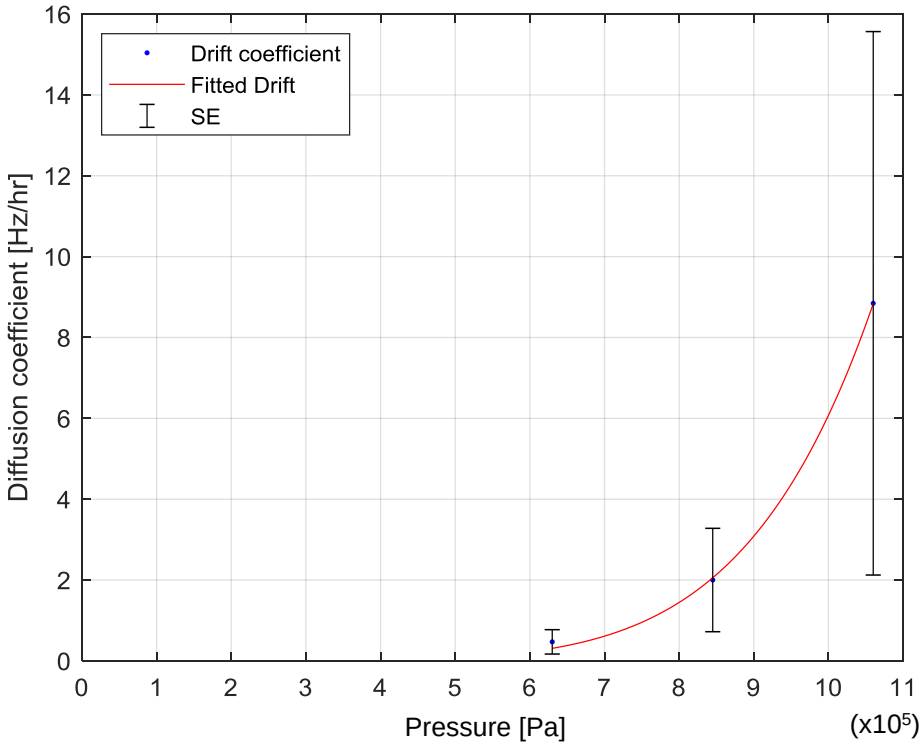

Figure 4-27 OB parameter estimates, diffusion coefficient vs stress with SE bars.

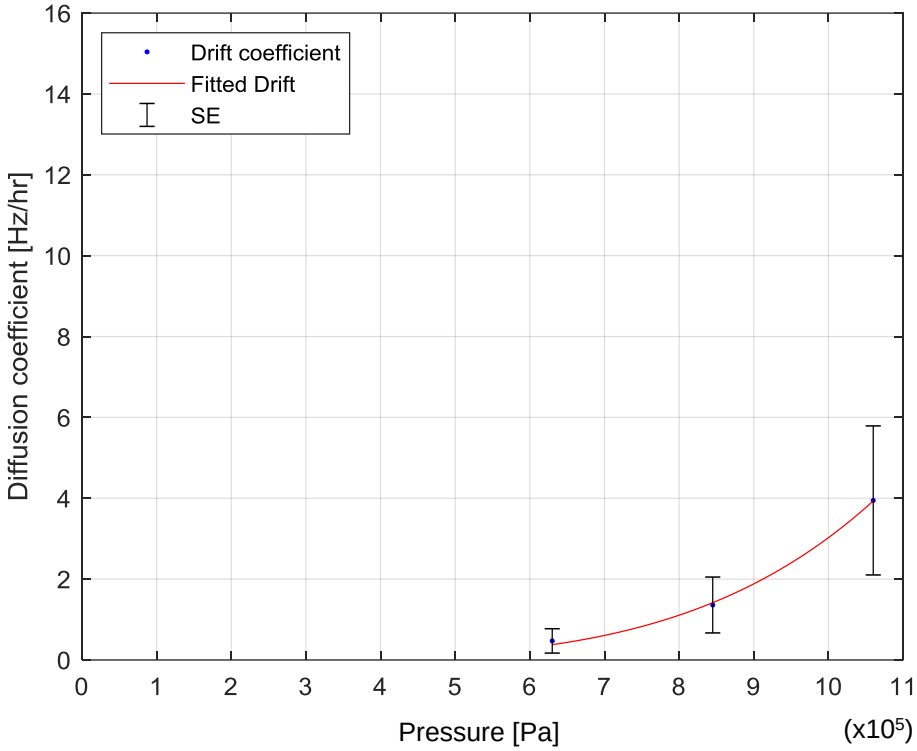

Figure 4-28 BU parameter estimates, diffusion coefficient vs stress with SE bars.

Using natural logs gives the following linear relationship and simplifies the analysis of the relationship:

For the MLE:

$$\hat{\sigma} = \mathrm{e}^{(5.51801 \times \ln P) - 11.02762} \tag{4.2}$$

For the OB method:

$$\hat{\sigma} = \mathrm{e}^{(5.59998 \times \ln P) - 11.11902} \tag{4.3}$$

For the BU method:

$$\hat{\sigma} = \mathrm{e}^{(4.05992 \times \ln P) - 8.26447} \tag{4.4}$$

Table 4-5 indicates the goodness of fit R^2 = 0.994, 0.988 and 0.994 for all three methods validating the linearity. When considering the simulation at normal usage stress levels in the region of 2.2E5 to 5.0E5 Pa, the BU method will output a higher diffusion coefficient due to the lower gradient and higher intercept. As discussed in the following sections the higher diffusion coefficient outputs a greater spread in which the degradation path can walk.

Table 4-5 Diffusion coefficient functional relationship to stress (MLE, OB, B).

		Estimate	SE	R^2
MLE	Intercept *c*	-11.027620	0.860450	0.994
	Gradient *m*	5.518017	0.405381	
OB	Intercept *c*	-11.119028	0.978905	0.988
	Gradient *m*	5.599987	0.461188	
BU	Intercept *c*	-8.264473	0.654698	0.994
	Gradient *m*	4.059923	0.308446	

To summarise, the diffusion coefficient is essentially the standard deviation of the mean drift coefficient. Thus the diffusion coefficient is dependent on the parameter estimation method. The functional relationships follow a power law with increasing uncertainty at higher stresses. The MLE and OB methods output similar estimates compared to the BU method. Similarly to the drift coefficient, the SE indicates insufficient confidence in the estimates. The BU method demonstrates improved confidence by incorporating preceding test data. The learning outcome is that the diffusion coefficient is significant enough in magnitude that it requires modelling as a covariate depending on the stress.

4.5 Simulation and Pseudo Failure Times

In this section, the drift and diffusion parameters are modelled as covariates in the BM model using MC simulation. In conjunction with Figure 3-24, the input/output diagram in Figure 4-29 demonstrates the overview of the MC simulation. The dynamic environment of the gear pump degradation model is a function of the driving pattern. The trace of engine speed over time is an input that determines the mean pump outlet pressure which has a functional relationship to the drift and diffusion coefficient as processed in the simulation. Because the diffusion coefficient has a power law relationship to outlet pressure $P(t)$ it is modelled a covariate. The model expression is:

$$dY(t) = h(P(t);\gamma)dt + f(\sigma_B(t);\beta)dtdB(t) \tag{4.5}$$

Where $h(P(t);\gamma)dt = P(t)^{\gamma_1}$ is the power law relationship of the drift coefficient outlet pressure, and $f(\sigma_B(t);\beta) = \sigma_B(t)^{\beta_1}$ is the power law relationship of the diffusion coefficient to pressure.

Regarding Figure 4-29, program begins by loading the transient drive cycle with a constant time step of 1s. The length of the cycle only affects the number of repetitions throughout a pre-selected total number of hours in life. The next steps load the functional relationships for the drift and diffusion coefficients. In this case, the relationships are determinate and traced back to the engine speed. The assumption that each pump revolution

contributes to pump degradation requires the conversion from time to revolutions. The total number of revolutions is calculated assuming the transient cycle data point is fixed for the duration of the time step, regardless of the application is accelerating or decelerating. The simplification is reasonable as used by emissions testing procedures (Giakoumis, 2016). The user input sets the first passage to pseudo failure threshold based on the delta Omega that is determined experimentally. A sample size is input in order to output a distribution of PFT and the total simulation hours is set as a stop criteria to prevent the simulation over running, for example twice the required life time.

Once the total number of cycles have been calculated, the array $Y(t)$ is initialised to save on processing power after which the cumulative damage of the BM model runs until the total number of revolutions is complete. For each iteration the BM model calculate the degradation in delta Omega. At this stage, the process is to find where the degradation path first passes over the threshold, after which the number of hours is stored, and the next sample can begin. Computer processing power reduces by erasing the degradation paths from memory, and thus, only one sample runs at a time. Once the sample size condition has been met the code stops. The advantage of this code is the simplicity to load any cycle irrespective of length and adjust the covariates as required, for instance, switching between the Objective Bayes (OB) and Bayesian Updating (BU) parameter estimation methods. The disadvantage is the loss of the degradation path, but the primary interest is the PFT.

The pump system degradation has a relationship dependent on the pump outlet pressure which is a function of pump speed and the engine restriction (Rundo and Nervegna, 2015). For simplicity, the continuous distribution of pump outlet pressure from engine to engine (Rundo and Nervegna, 2015) is ignored. However, it is known that pumps towards the tail ends of the distribution will output higher flow rates which under Bernoulli's principle will generate higher pressures. Equally, the engines with smaller restrictions will generate higher pressures. At the beginning of a NPD this information is not available and is not necessary to understand the reliability growth. Although, later in the NPD process this data will assist in increasing the accuracy of estimations.

As previously mentioned in Section 3.8, the drift and diffusion relationships are time-scaled from hours to revolutions, this is because the SSADT speed was held constant (see Section 3.4), leaving a simple scaling of the drift coefficient by the pump speed and the diffusion coefficient scaled by time only. Such transformation is necessary because the transient drive cycle of the vehicle engine speed is recorded every second (Section 2.3). For clarity, the cumulative damage at a high speed under 1s, is greater than at a lower speed for the same time.

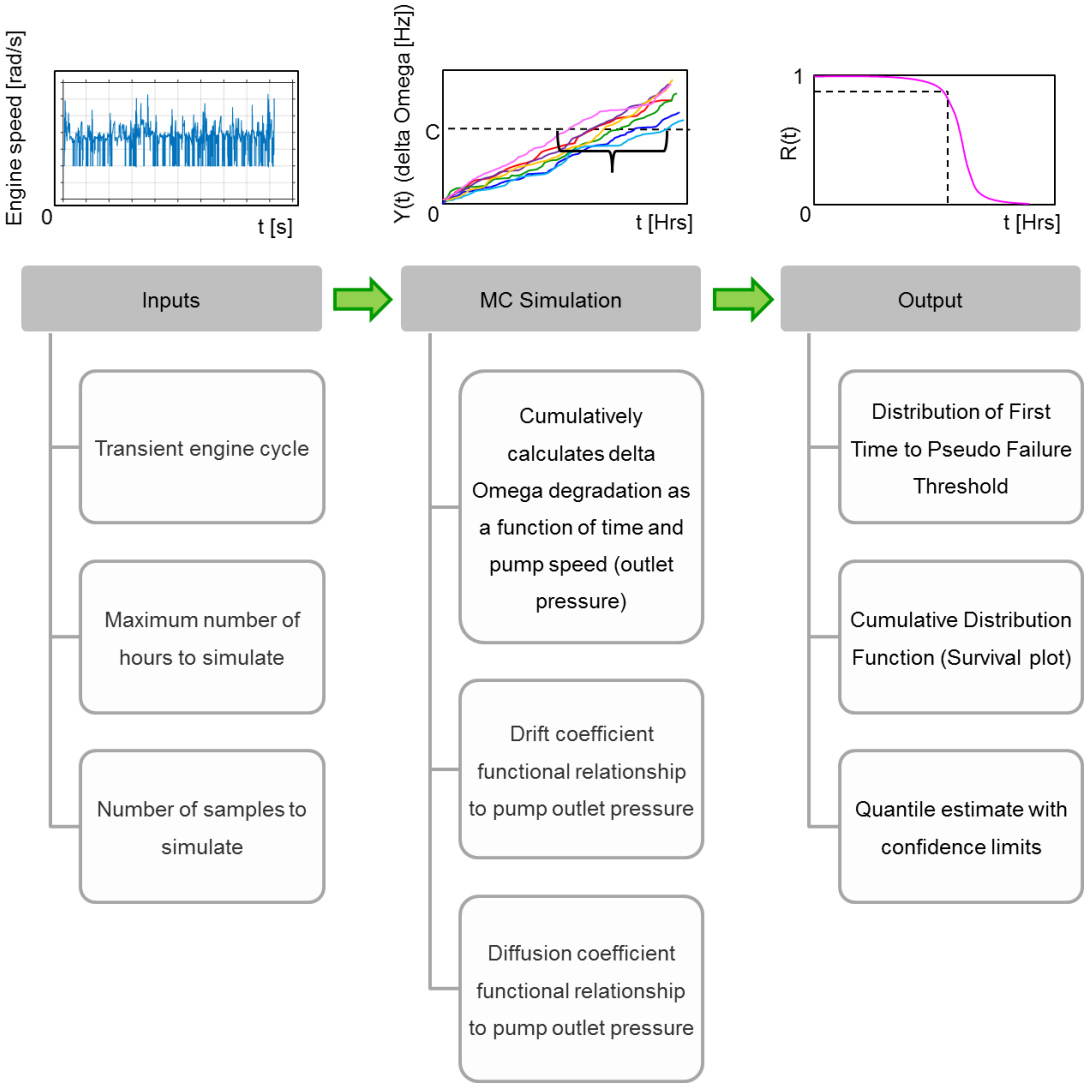

Figure 4-29 Inputs and output block diagram for MC Simulation

Inputting the stitched customer transient Cycle C04 and running the MC simulation, the typical degradation path for Omega is shown in Figure 4-30. All the computing memory is used to produce such a figure in excess of 16Gb, which is only for four degradation paths. Nonetheless, with only four samples the degradation paths indicate cumulative damage, it is stochastic, not strictly monotonic and experiences some recovery as observed in the step-stress test. Until future testing and receiving field returns on the project, it is not possible to comment directly on the validation of the model but it is possible to observe similitude with a secondary source. The CBM experimental work of Eltabach *et al.* (2011) used contamination to accelerate the wear of a hydraulic pump. Eltabach *et al.* (2011) monitored the pressure ripple for a hydraulic pump over time and exhibited a similar stochastic and non- monotonic trend in the amplitude of the pressure signal.

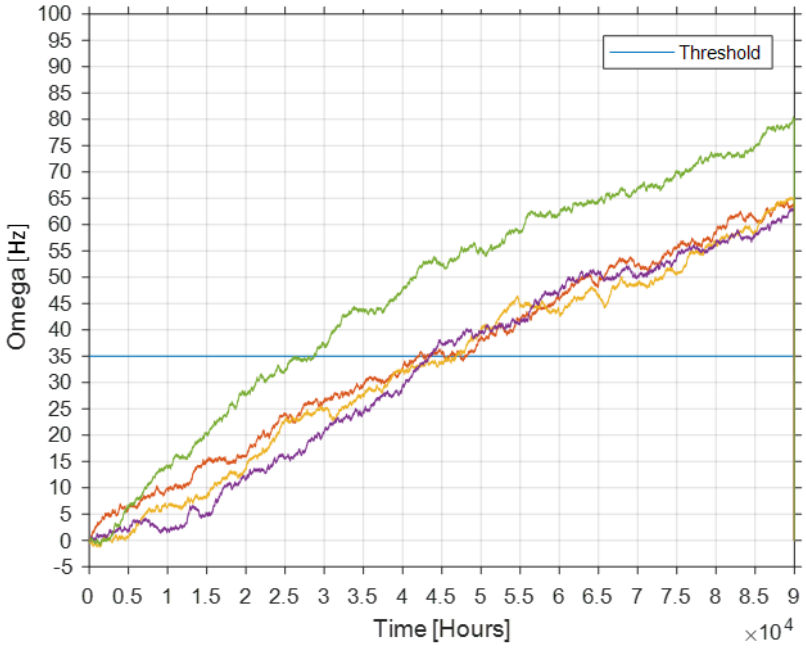

Figure 4-30 Omega, MC Simulation degradation path, Cycle C04, n = 4 samples, BU.

In Figure 4-30 the pseudo-failure threshold is set to 35Hz based on the decision to cease testing earlier at 21 hours instead of 24 hours. In order to increase the sample size and reduce the computational memory the simulation only stores the time of the first to pass to the threshold, as this is the point of interest. The pseudo failure time (PFT) is recorded once the degradation path first hits the threshold. Post processing using Minitab 16, the first passage to PFT is given in Table 4-6 that summarises the survival quantile R(0.9) with 95% credible limits for all three parameter estimation methods. A demonstration that the distribution is normal including the summary statistics is included in Appendix B for all three methods.

By erasing the degradation path, computer memory is freed, and a higher number of samples can be simulated. In this case, a sample size 1000 gave a reasonably practicable computation time c.15mins and narrowed the standard error 95% confidence limits typically by 11.6% for all three methods comparing 33 samples to 1000 samples (Zarzycki, 2018b).

As anticipated from the similar parameter estimates, the difference between the MLE and OB method is negligible, estimating that 10% of the pumps will reach the degradation threshold within 28145h ±107h (MLE) and 28089h ±109h (OB). Notably, although the BU parameter estimates have a lower diffusion coefficient (primarily on the higher stress P_3), 10% of pumps are estimated to reach the threshold a mean 4071h earlier and 2.2 times wider SE compared to the MLE. The wider SE is a function of a shallower power law relationship on the coefficient, resulting in higher diffusion at the lower normal usage stresses, thus a more conservative estimation.

Table 4-6 MC simulation, cycle C04, R(0.9) quantiles with Confidence Interval (CI).

Parameter Estimation method	Sample size n	R(0.9) Quantile [hrs]	Standard Error [hrs]	95% Normal CI Lower [hrs]	95% Normal CI Upper [hrs]
MLE	1000	28145	107	27934	28436
OB	1000	28089	109	27874	28303
BU	1000	24073	240	23603	24544

Reviewing the survival plots from Figure 4-31 to Figure 4-33, the distribution and spread around the mean context specific. Without the study of field data or comment from an industry perspective, as discussed in Section 1.5, it is unknown how representative the estimations are to the field. However, it is reasonable to comment on the differences between parameter estimation methods. The survival plots from Figure 4-31 and Figure 4-32 show the difference between MLE and OB is negligible, with the same mean of c.31376h and standard deviation c.2521h. The BU survival plot in Figure 4-33 also has the same mean due to the same drift coefficient estimates, yet a wider standard deviation of 5626h reflecting the shallower diffusion power law relationship to pump outlet pressure. From an engineering survival perspective the conservatism of the BU method is preferred because of the extra margin of safety.

In summary, a MC simulation has been developed to efficiently extract the PFT for a sample size of 1000 degradation paths. The simulations adhered to the expected characteristic of a BM model in observing a non-monotone, stochastic degradation path with cumulative damage and recovery. All three parameter estimate methods output the same mean PFT due to the same drift parameter estimations, with negligible difference between the MLE and OB methods. However, the BU method outputs a more conservative estimate.

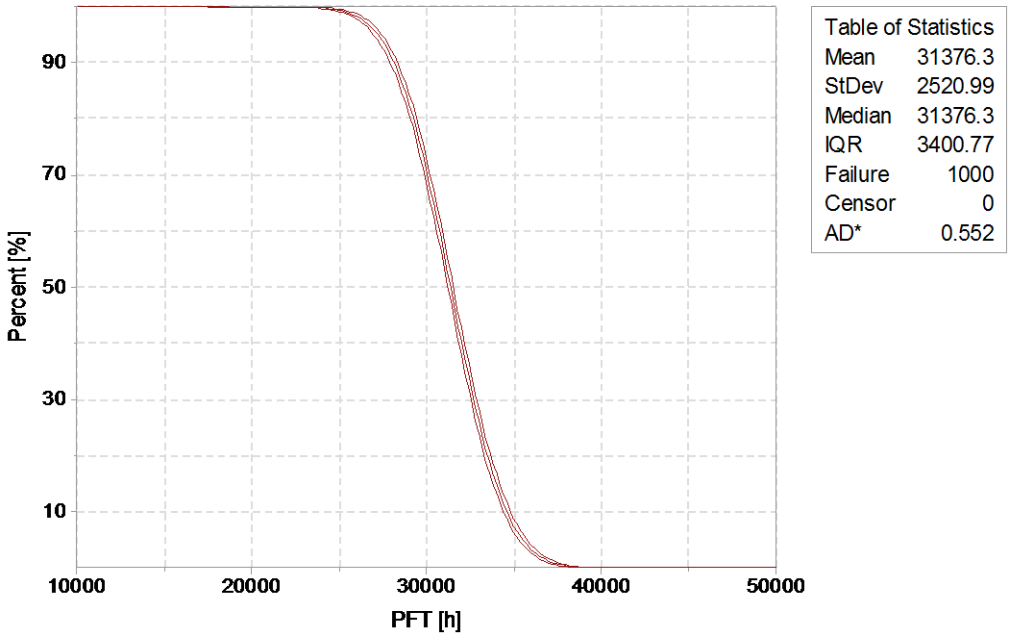

Figure 4-31 MLE, PFT, CDF Survival plot, n = 1000, Normal 95% CI.

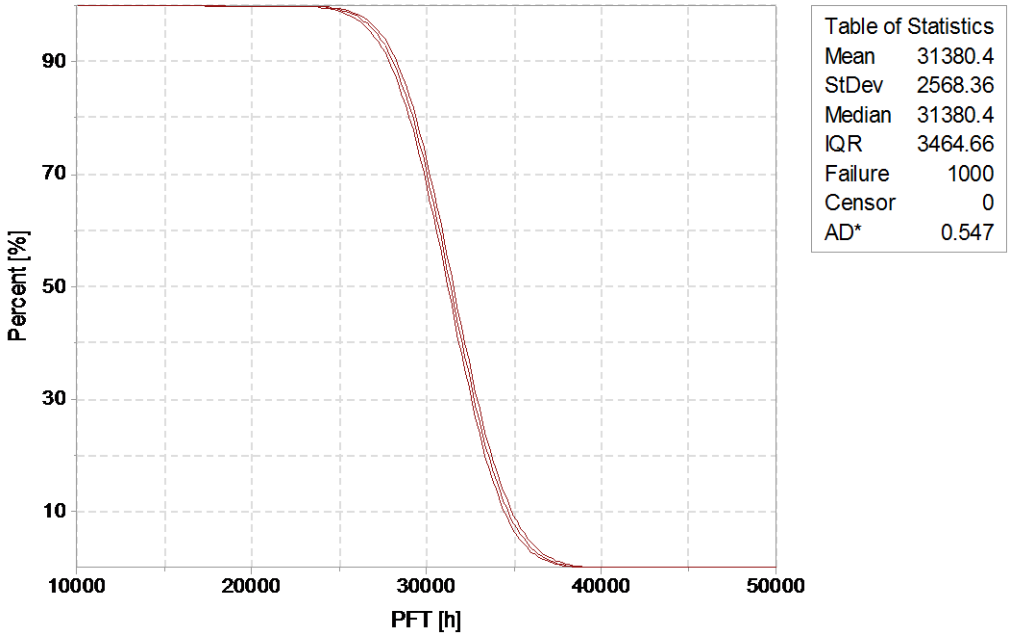

Figure 4-32 OB, PFT, CDF Survival plot, n = 1000, Normal 95% CI.

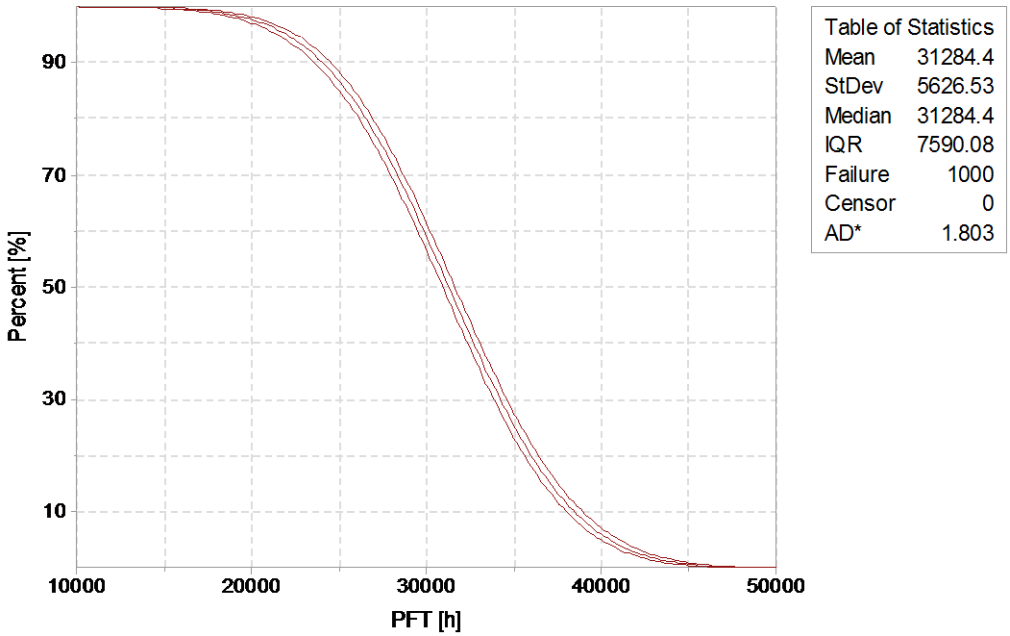

Figure 4-33 BU, PFT, CDF Survival plot, n = 1000, Normal 95% CI.

4.6 Summary of SSADT

Post-SSADT, the two pump samples were inspected internally and exhibited signs of erosion on the edge of the outlet pumping gear pocket face and early signs of micro pitting on the pump gear flanks. During the test, the MODWT-ARMA(2,1) pressure ripple technique successfully indicated a change in health where typical performance and conventional feature extraction methods did not. As a result, the decision to cease testing 3 hours early on the final step-stress was taken to prevent the risk of catastrophic failure. The pseudo failure threshold of $\Delta y = 35\ [Hz]$ was set based on this decision.

The analysis indicates that each step-stress has a different linear degradation rate, leading to the formulation of covariate drift and diffusion power law relationship. The analysis suggests insufficient precision on the parameter estimates that is most likely to be improved with an increased frequency of measurement intervals. In hindsight, more data on the final stress would have been beneficial to improving the precision on the parameter estimation too. The MLE and OB parameter estimation methods agreed with literature (Berger, Bernardo and Sun, 2009; Xu and Tang, 2012b) and output similar estimates. The precision of the parameter estimates was improved using the preceding test data as the prior in the BU method.

The MC simulations were developed to include covariate drift and diffusion relationships in the BM model. The result of the model output non-monotone, stochastic degradation paths indicating cumulative damage. As these paths crossed the pseudo failure threshold, the first hitting pseudo failure times were used to generate a cumulative distribution curve (survival plot) and the 90% quantile survival estimates with 95% confidence intervals where calculated. The BU method outputs a more conservative estimate of 24073h ±240h; some 4072h less than MLE and OB methods. The standard deviation of the BU method is also 2.2 times wider than the MLE.

Chapter 5: Discussion

In this chapter, the methodology and outputs from the testing and simulations are discussed. The research motivation (Section 1.1) comes from classic reliability problems in industry; (1) the need to provide evidence that the product life requirements will be met,[82] (2) The risk of increasing the warranty period,[83]To gain a competitive edge,[84]And (3) the pressures to compress development time for NPD.[85] The desire from stakeholders is to find latent defects quickly through testing (Hobbs, 2000; Davis, 2003; Clausing and Frey, 2005) before the design matures, however, the balance of needing to invest heavily in qualitative testing philosophy is firmly in favour of limiting the number of test samples to keep budget costs under control (King and Jewett, 2010b, pp. 121–145). The chance of finding defects is high, but this is at the expense of overstressing the components being tested (Hobbs, 2000; Davis, 2003; Clausing and Frey, 2005). It would also risk not populating the reliability growth chart to assist with the timely product release (Meeker, Sarakakis and Gerokostopoulos, 2013).

The HAST philosophy is to keep fixing the defect to increase robustness; however one argument is that the product will never experience those levels of stress in the field, thus it is difficult to justify the design change (Meeker, Sarakakis and Gerokostopoulos, 2013). Secondly, qualitative testing does not contribute to estimating reliability (Meeker, Sarakakis and Gerokostopoulos, 2013). Thirdly, although conventional quantitative testing contributes to estimating reliability, it also requires large samples sizes and long test times (Hobbs, 2000; Davis, 2003; Clausing and Frey, 2005). The above issues are problematic for products that are designed for high reliability and long life. The ideal solution is to gain insight into the reliability of a product very early on in the NPD process, performing the tests more quickly than conventional practices using an extremely small sample size. The methodology in this thesis proposes the solution and applies it to the case study of a real live NPD.

Based on the BU method, the estimated lower 95% credible limit at R(0.9) concludes the HDE gear pump will not meet the lifetime requirement of 40,000 hours yet when put into context, the physical degradation during the step-stress test was very mild, and the pumps continued to function perfectly well. The initial recommendation would be to initiate design changes, although it would also be prudent to review the inputs into the MC simulation to make a better judgement.

[82] (Klemick *et al.*, 2015; National Research Council, 2015).
[83] (Shuster *et al.*, 2002).
[84] (Huang, 1996; Stephenson and Wallace, 1996).
[85] (Ling and Wang, 2004; Komsan, 2009).

5.1 Pseudo Failure Threshold

A weakness in the methodology exists in setting the pseudo failure threshold for a completely new feature extraction method. The acceptable degradation threshold of 35Hz, set in Section 4.2, was subjectively judged to sit close to where the test was terminated. If the threshold is too high, the reliability will increase and potentially miss a critical design change required. Conversely, set the boundary too low and unnecessary design changes will be implemented adding cost. For instance, the erosion and micro-pitting on pump no.2 were minor enough that it would have been overlooked had pump no.1 not shown significant erosion first. This weakness is dependent on the type of product and monitoring parameters. For example, in the condition monitoring of induction motors, the threshold of current leakage is well defined (P. Zhang *et al.*, 2011), whereas pump degradation is typically determined by an acceptable decline in flow (Greene and Casada, 1995). The predicament reported in Section 4.2 is that there was no flow degradation and, although minor, there was conflicting evidence of change in torque measurement too. Those parameters offered no success for degradation or threshold settings. The knowledge that performance parameters do not adequately identify wear issues is interesting because conventionally, the indication of flow degradation relates to significant wear on the pump, and this is not the case. What this innovative methodology does is detect the potential point of failure "P" in the P-F curve (section 2.5) with precision before a decline in flow was registered. The methodology has potential application for other industries (such as the steel mills) where CBM of hydraulic pumps is a high priority (Goode, Moore and Roylance, 2000).

In this case study, there was no known data before testing, and the research considered eliciting the threshold from expert judgement within a proven framework, for example, the Reliability Enhancement Methodology and Modelling (Jones *et al.*, 2003; Bedford, Quigley and Walls, 2006). However, using the filtered Omega parameter Det05 (Section 4.2) is an unfamiliar concept in describing pump performance, and it was envisaged to cause some difficulty in eliciting the value. There is no easy resolve besides building a database of experience, which much of CBM relies on (Heng *et al.*, 2009).

Detecting a change in pump health (the potential point of failure "P") is a benefit for CBM, but not enough precision in the threshold setting leads to inaccurate reliability estimations. Setting a tolerance on the threshold is a reasonable solution (Isermann, 2011), although it may be better to apply a holistic perspective and spend less effort on finding the ideal limit and maintain the PFT threshold, to observe reliability growth. After all, the methodology is designed to assist in decision making, and taking the estimations at face value does not necessarily lead to the correct inferences.

5.2 Mission Profile

The mission profile has a profound influence on the reliability estimates too because of the stress-varying (Singpurwalla, 1995) engine speed and engine loads influencing the degradation rates. In this situation, a histogram of the duty cycle (supplied by the customer) is of little value because the rate of degradation determines how quickly the degradation path reaches the PFT threshold. Real usage transient mission profiles are required because the rate of cumulative damage is influenced by where the engine runs in time series. An observation 2.3.1was made in Submission 6 (Zarzycki, 2018b) (see section 2.3.1), where the standards used for the emission and fuel economy testing were not representative of the HDE application. For instance, a HDE for an on-highway vehicle is likely to spend more its life on the highway than in stop-start traffic (Rakopoulos and Giakoumis, 2009). Equally, in this case, the customer driving transients are only representative of one trip, one vehicle and one driver, which does not cover the demographic (Ericsson, 2000). It is recommended to pursue more customer transient data to refine the model.

On the other hand, a NPD will not necessarily be used in the same way, and so transient data collection on the application will lag behind the NPD. The value of this research is that the structure is developed and the methodology can easily and quickly (only 30 minutes to simulate ref. Section 4.5) test alternative mission profiles when they become available. The proposal applies the same reasoning as the pseudo failure threshold, to hold the same mission profile and observe reliability growth. The value lies in determining the risk of meeting reliability requirements for specific applications. For instance, the same HDE will be installed for inner-city buses and trucks. Inner-city buses are known to experience harsher operating conditions which is reflected in the lower lifetime requirements (Rakopoulos and Giakoumis, 2009). With the model established, new mission profiles can be assessed quickly to confirm if a design change is necessary.

5.3 Parameter Estimation

The covariate drift (Section 4.3) and diffusion (Section 4.4) coefficients for the BM model were estimated using linear regression analysis. However, the standard errors calculated increased with stress, particularly for the third stress P_3. It is unsurprising to observe low precision, given the difference in wear between only two pumps as this reflects the variability of stress-strength from unit to unit (Spanó, 2008). The simplicity of using linear regression resulted in the MLE, the OB and the BU methods outputting the same drift coefficients. The functional covariate relationship of drift coefficient to outlet pressure was a power law, eqn. (4.1), which is typical of mechanical wear-out or fatigue (Wang and Shi, 2006). The relationship had a good fit based on R^2, providing confidence in the relationship,

and the precision improved closer to normal operating stress as illustrated in Figure 4-23, providing further assurance. In terms of the parameter estimation, the BU method improved the precision at the higher stresses (see Figure 4-24), reflecting a benefit over the MLE and OB methods.

Conversely, the diffusion coefficient had different values for each parameter estimation method. It was expected that the MLE and OB methods would give the closest results (Berger, Bernardo and Sun, 2009; Xu and Tang, 2012b) in comparison to BU, and the results in Table 4-4 demonstrated this prediction. On closer inspection, the diffusion coefficients for each stress were different, with the third stress being significantly different. In the MC simulation (Section 4.5), the MLE and OB method output remarkably similar reliability estimations, even though the third stress was higher in value. As such, this builds confidence that the precision for the third stress has a low influence when simulating with normal usage stresses. However, the BU method had significantly lower diffusion coefficients, which influenced the function relationship (see Table 4-5). This BU functional relationship shape has a shallower rate of change, so the normal usage stresses have higher diffusion coefficients than the MLE and OB estimations. The result on the reliability estimations is a wider range on the confidence limits and a lower estimate on life as recorded in Table 4-6.

The literature recommends reporting the more conservative estimate to provide a higher safety margin in reliability (Luo *et al.*, 2014). Although the BU methodology outputs a more conservative estimate, simply choosing the more conservative result is unsubstantiated yet considering the context and background to the calculations, is it a proven approach for extremely small sample sizes in terms of statistical validity (Meeker, 2010; Li and Meeker, 2014; Guan, Tang and Xu, 2016). In this regard, the advantage of the BU method is favoured. It satisfies a degree of objectivity by utilising the preceding step-stress test data to alter the likelihood of the very small data set. By doing this, the variation from pump to pump, the wear degradation and measurement errors are cumulative for the next step and thus, improves the statistical confidence in the final step (as observed in Table 4-5).

Ultimately, the BU method contributes to smoothing the significant variation in estimating the diffusion coefficient parameter for the third step-stress. Hence, this is particularly useful where the 20^{th} hour for pump no.1 shows an unexplained jump in Omega, or conversely the unexplained recovery at the 21^{st} hour (see Figure 4-18). Of course, with only two samples, it is not possible to suggest if a result is an outlier. At this early stage, it merely requires more data, more knowledge and more experience as to which estimation is valid. Thus, it is recommended to report estimates from all three-parameter estimation methods until the methodology matures. It may be best to introduce a condition that all methods must achieve the lifetime requirements.

5.4 Pressure Ripple

In terms of the pressure ripple measurement, the two pressure/two systems method in ISO 10767-1:2015 (ISO, 2015) is highly representative of simulating the engine restriction, but the setup is not wholly necessary because calculating flow ripple is not of interest. The setup lends itself to maintaining a standardised approach to pressure ripple measurement that can be repeated when pumps return from the field after several years. The downfall of using the standardised methods is that the outlet pressures are not sufficiently high enough to meet the criteria in ISO 10767-1:2015 (ISO, 2015). To satisfy the precision and repeatability of using lower pressures requires a study outside the scope of the project. For future improvement, it would also be beneficial to install a sensor directly onto the pump which could then be fitted to an engine to test for correlation and achieve further validation.

The methods of pressure ripple measurement (Section 3.5) are established (Bramley and Johnston, 2017), although the choice of manipulation and feature extraction has had mixed success. Using FFT or ARMA(2,1) alone did not provide a viable degradation modelling opportunity (see Table 4-1). It is demonstrated that the innovative manipulation of pump pressure ripple by combining MODWT and ARMA(2,1) (Section 3.6) promises and viable condition monitoring technique. As discussed in the analysis of the results (Section 4.2), the method diagnosed a change in pump health causing the tests to cease early before further damage was accumulated. In doing so, this captured the beginning of wear-out from erosion and micro-pitting on the pumping gear flank edge (Figure 4-1to Figure 4-3). From the author's experience and CAB reports (Hannan, 2012; CAB, 2013) these failures are usually advanced and take thousands of hours in the field to emerge as observed from the high mileage pump in Figure 2-5 and Figure 2-6.

The downside of the technique is interpreting the extraction features. The attractiveness of the ARMA(2,1) method was being able to make inferences based on natural frequencies and damping coefficients and relating the changes to increasing wear (Silva, 1986). However, it was not until testing with ARMA(2,1) that this inference is lost once the signal is filtered with MODWT. For instance, this is particularly so for the detailed coefficient in the natural pumping frequency range, i.e. Det05. Essentially Det05 is a pure sinusoidal wave and hence the damping coefficient Zeta is zero. The value of the "natural" frequency Omega Det05 after filtering is also unintuitive, for example, c.1030Hz. Therefore, Omega holds no meaning but does provide a feature extraction for comparing timelines and pumps to pumps. In this sense, it makes no difference if Det05 is described with Hertz or a different unit, the trend of degradation is visible, and the measurements can be modelled with the BM model.

In terms of the pressure ripple measurement and manipulation, the case study was a manual process that was time-consuming and limited to supervised hours (as discussed in the

Step-stress test design in Section 3.4). It would be beneficial to quicken and automate this process to utilise the full 24 hours available per day. This advantage would speed up the step-stress test or allow for greater resolution by capturing the data every half hour for instance. It could also provide scope to increase the step-stress duration, yet remain within the allocated resource time constraints. In automating the process, the increased number of observations will aid in reducing the SE, particularly for the third stress (as illustrated in Figure 4-21).

5.5 Step-stress Testing

Generally, the conventional method of running long hour demonstration tests on one sample does not expose any weaknesses (Sarakakis, Gerokostopoulos and Mettas, 2011). At the other end of the spectrum, HAST can unrealistically cause the product to fail (Meeker, Sarakakis and Gerokostopoulos, 2013). The step-stress testing was designed as a result of understanding the PoF of key pump components such as the journal bearing (Section 2.2.2) and pumping gear contact fatigue (Section 2.2.3). The success of the step-stress is evident from the post-test examination of the pump (Section 4.1) as early signs of erosion and micro-pitting were observed. In this section, the original test methodology is justified further.

After the introduction of the test planning paradox and investigation of the optimal test plan (Section 1.1), it was realised that optimisation is a function based on experience and existing data, which was a missing key ingredient in this case study. Additionally, the existing accelerated wear methods for pumps use contamination as a stressor which did not relate to lifetime reliability calculations, only to sensitivity against contamination (Tabor, 1977; Frith and Scott, 1993). At the time a published methodology to estimate the reliability wear out of a HDE gear pump from the accelerated test was not found. The original method (Figure 3-1 and Figure 3-19) utilises existing PoF but in a pump application. For instance, using Miners cumulative damage rule for gear contact fatigue is a widely accepted method for power transmission BS ISO 6336-2:2006 (British Standards Institution, 2006b) and by assuming equivalent damage, the lifetime requirements of the gears can be validated quickly by increasing the load. In the pump, the increased load is limited by the risk of journal bearing seizure, which in this instance turned out to be the limitation of the whole pump. Using the step-stress design (and Miners equivalent cumulative damage rule) is rudimental and easy to follow, which is practical for test engineers.

The physical inspection post-testing (Figure 4-4 and Figure 4-3) was revealing and appears to capture the onset of wear-out before it advances to the state typically seen in the field. The contact fatigue calculations estimated sufficient design margin to avoid micro-pitting, yet it was discovered within a rapid space of time. The gear wear could be attributed to two things. Firstly, the contact fatigue properties of the pumping gear materials were not

available. Therefore the material properties were assumed, and then matched to database material properties BS ISO 6336-2:2006 (British Standards Institution, 2006b) based on their heat treatment and surface hardness. Assuming the properties is a reasonable practice without investing significantly to know the actual properties. Secondly, the calculations assumed perfect stiffness and no misalignment, both of which would adversely affect the design margin of contact fatigue (British Standards Institution, 2006b). The evidence of an uneven tooth wear pattern suggests misalignment is the most likely cause of pitting.

The most striking observation was the presence of erosion, particularly on pump no.1. From experience, this is a commonplace to discover erosion or cavitation erosion, and it is usually resolved by machining timing grooves to ease the sudden transition of the gear pocket volume to the pump outlet cavity. The downside is that the test design is missing the damage accumulation model from the fluid to predict this. It is possible to run computational fluid dynamics to locate the position and likelihood of cavitation or erosion (Frosina *et al.*, 2014), but it is the relation of these figures to damage that is undeveloped (Franc, 2009; Buono *et al.*, 2017).

In the step-stress test, the change in drift coefficient based on pressure is evident (see Figure 4-19 to Figure 4-21), and it is assumed the rate of erosion is related to the pressure. This assumption is not likely to be valid when concerned with stress-varying environments based on speed. The change in pump speed will alter the pump flow and radial velocity of the pumping gears, which in turn is likely to change the erosion rate and discharge pressure. Thus, it is a weakness in the model, but the decision to focus on a single speed is justified for practicality particularly when the engine is likely to spend over 55% of its time at this speed (as specified by the customer). An improvement in the step-stress test is to incorporate a change in pump speed. This proposal would need to repeat the SSADT at two other speeds (possibly under the same pressures) to create a covariate matrix. For two more speeds, it would take an additional four pumps to satisfy the model, which ultimately undermines the extremely small sample size requirement and reinforces the test planning paradox (Figure 1-4) (Dazer et al., 2016). In reality, the budget constraints could utilise the four pumps more effectively to assess reliability growth after a design change which is arguably higher value to industry and NPD projects (King and Jewett, 2010a).

5.6 The Degradation Model and Simulation

The validity of the degradation model first stems from the parameter estimations as previously discussed in Section 5.3. Critically the model has been developed to account for a stress-varying environment (Section 2.3) after recognising that the order of damage accumulation is vitally important in determining how quickly the time to the pseudo-failure threshold is first reached. It was clear to see in Submissions 5 and 6 (Zarzycki, 2018a, 2018b) that the transient data from the customer (Section 3.1) influences the first time to the pseudo-failure threshold, and thus, the transients are critical to the model.

The BM with covariate drift and diffusion coefficient model is beneficial in providing the flexibility to incorporate future covariate relationships. Currently the model assumes that the pressure drop across the engine population remains constant; however, in reality, multiple variations are influencing the pump load. As discussed in the step-stress test design (Section 3.4), the pump unit variability from manufacturing in combination with the application will bring variation to the pressure drop. Additional data collection is required from the customer; (1) the tolerance of pressure regulation, (2) the engine restriction variation influencing the pressure rise, (3) the wear of the engine affecting the pressure rise and (4) the service intervals (particularly the oil filter) that also change the pressure rise (Rundo and Nervegna, 2015). With this data collection, the covariate simulation model can incorporate this variation without further testing. Therefore, a key advantage of the MC simulations is the flexibility to increase the level of detail.

5.7 Summary of Discussion

The project has developed an innovative methodology and contributed to knowledge in several ways. Previously it was not known how to accelerate the degradation of a gear pump in such a manner that one could estimate reliability from it with an extremely small sample size.

The original solution relied on targeting the pumping gears' contact fatigue as the primary failure mechanism for pump degradation. Using Miners' cumulative damage model to assumed the equivalent damage could be compressed into a short space of time. If the gears were not damaged, it would be assumed the pumping gears would survive the lifetime requirements. The test offered further value because (in the short space of test time), competing failure mechanisms were detected that were representative of field returns.

In modelling the degradation, the research tested the feasibility of manipulating pressure ripple data. Previous studies focused on conventional methods that could detect a change in pump health, but they did not yield a degradation path (Greene and Casada, 1995; Khoshzaban-Zavarehi, 1997; Johnston and Todd, 2010). By investigating the combination of

MODWT-ARMA(2,1) this innovative approach essentially filtered the signal to leave a degradation path that could be modelled using the BM model.

While developing the degradation model further, it was concluded that engine transient cycles were required to represent the reliability estimate more accurately. For this, the BM model with covariate drift and diffusion coefficients is ideal because it provides the flexibility to incorporate stress-varying environments encountered in the engine.

Finally, the use of BU methods was explored. The literature stated that BU methods are more statistically efficient with small sample sizes (Meeker, 2010; Li and Meeker, 2014; Guan, Tang and Xu, 2016). It was not possible to fully validate, because it ideally requires a large sample size of field returns to be investigated (all of which have had their engine speed, oil temperature and outlet pressure recorded for the duration of its life). The compromise is to utilise the methodology as a contribution to understanding reliability growth. After making a design change and testing under the same conditions, it is expected the robustness and reliability will improve, thus providing information if the design change is worth the additional cost in a short space of time (King and Jewett, 2010a).

From an academic and industry perspective, this original methodology could be useful for other types of positive displacement pumps, and it is envisaged to provide a baseline from which to develop a prognostic tool for CBM.

Chapter 6: Conclusions

When investing in a NPD, it is highly desirable to judge if the reliability requirements can be achieved as early as possible in the project timeline. The benefit of early intervention is logical because making design changes during new product introduction becomes increasingly difficult and expensive and causes delay. Hence, the sooner a failure mechanism is discovered, the sooner a fix can be implemented (before committing to production tooling). In this respect, the approach of qualitative testing is attractive for quickly precipitating latent defects by overstressing the product on a few samples (at the expense of estimating the reliability). The philosophy continually makes design improvements to increase product robustness. However, it requires significant upfront investment and risks over-engineering the product and adding unnecessary cost. Equally, quantitative testing using accelerated life or degradation testing requires a substantial investment in sample sizes, test resource and test time to output reliability estimates. It is particularly challenging for mechanical products such as gear pumps designed and manufactured by small to medium enterprises, where budgets and test resources constrain the ideology of finding latent defects and estimating reliability with a design for reliability mind-set.

In this research, a combination of innovative methods addresses this challenge by estimating the reliability of a HDE lubrication gear pump for the first time. This research is the first example of manipulating pump pressure ripple using MODWT-ARMA(2,1) to monitor degradation and estimate reliability using step-stress accelerated degradation testing with an extremely small sample size of two.

The decision to use step-stress accelerated degradation testing is based on multiple advantages. In this case study, the interest was in detecting the point of wear-out rather than outright failure. Literature proved that degradation tests led to more useful inferences on the PoF rather than simply testing until the product fails. The benefit of ADT permits run the stresses at lower levels to understand the PoF. Otherwise, the justification for making a design change is in no better position than qualitative testing. The research also demonstrated that fewer samples were required to make reliability estimations when using ADT. The conclusion was to develop an ADT and a method of degradation monitoring that had at least three step-stresses to create a functional relationship.

The added complexity of testing a product rather than a component is the multiple competing failure mechanisms contributing to wear. The competing wear mechanisms are illustrated for the first time, specifically for the HDE gear pump, by adapting and expanding on the wear concept model by Frith and Scott (1996). It was concluded that introducing contamination to accelerate wear had too many unknowns. Even if the distribution of particles from the life of the engine is known, the phenomenon of contamination losing abrasion,

embedded contamination in the components acting as bearings and, particles blocking leak paths to increase volumetric efficiency, was too superficial to solve using an extremely small sample size. The application-specific concept wear model is the first documented model highlighting several controllable stressors namely the engine speed, pump load, fluid viscosity, fluid temperature and the oil grade, all of which could be used for an accelerated test. Based on two field examples of 1,000,000 mile gears pumps (CAB, 2013) and failure report during a NPD (Hannan, 2012), the conclusion was to target two primary failure modes; the cavitation erosion and pumping gear contact fatigue. The damage accumulation models of cavitation erosion were not found, but the gear contact fatigue could be modelled using the gear design standard. The calculations estimate the gear contact fatigue over the duty cycle of the engine. The standard practice to validate gear life is to assume equivalent damage from normal usage can be generated with an accelerated test by increasing the load. Thus, this is the primary reason for using a single stressor, but it is also used for simplicity. The other reasons are that the oil grades for the engine are mostly the same and selected for the worst-case viscosity and that the oil temperature spends the majority of its time is constant.

The chosen method for condition monitoring was validated through a feasibility study and the case study. The analysis of pressure ripple using conventional FFT did not result in a degradation path that could be modelled. Additionally, the use of ARMA(2,1) was also inconclusive. The idea to essentially filter the signal and extract a feature using MODWT-ARMA(2,1) is a first for pump pressure ripple analysis, and the outcome was successful. The pump health could be monitored, and testing ceased early to capture the beginning of wear-out on the pump casing and pumping gears.

The degradation model was developed based on the pressure ripple measurements. The parameter estimations through linear regression concluded that the Brownian motion model satisfactorily simulated the degradation path. The functional relationships of degradation to outlet pressure fitted well to the power law. However, further, development was required to output a reasonable reliability estimate. The stress-varying environment required the development of a BM model with covariate drift and diffusion coefficients. It was concluded that the reliability estimates weigh heavily on HDE transient cycles because of the power law relationships and the rate of degradation is dependent on engine speed and the order of its appearance.

Equally important is the setting of the pseudo-failure threshold. With only two samples available and one sample experiencing more advanced wear than the other, it was challenging to set and elicit a threshold, particularly with an unfamiliar degradation parameter extracted with MODWT-ARMA(2,1). The pseudo-failure threshold requires future development which may only evolve with the maturity and experience of using the methodology. During the early

development of this methodology, it is recommended to fix a threshold and observe the reliability growth as design changes are made.

This conclusion is also true in taking the reliability estimates at face value. Literature is consistently proving that Bayesian methods are more statistically "efficient" with small sample sizes less than five, yet frequentists disapprove of the potential bias involved. The ideal solution when using Bayesian methods is to make the prior distribution objective by using Jefferys prior. The other innovative idea is to use the preceding step-stress posterior distribution as the next step-stress prior distribution, described as a BU methodology. The advantage is the inclusion of variance regarding pump-to-pump variability and measurement error, which is attractive in a situation of extremely small sample sizes. From the simulations, the MLE and the OB reliability estimations match each other, whereas the BU method was more conservative. The estimates could not be validated because the study is representative of a current NPD project and relies on the successful tender and in the region of 6 years to mature. Hence, this inconclusiveness forces the decision that it is no hardship to report all three methods and set a rule that all three estimations must be equal to or greater than the reliability target.

The methodology proposed in this research is applicable to the wider gear pump industry because of the fundamentals in gear pump design. The outcome of this research is an innovative methodology for estimating the reliability of gear pumps using an extremely small sample size within an extremely short period. It achieves a balance of the qualitative testing philosophy with the benefit of aiding decisions for future design changes which may prevent over-engineering and adding the cost into the product. Coupled with the precipitation of latent defects, a compressed development and potentially a lower upfront investment, this methodology provides a competitive edge.

These findings have resulted in the development of an innovate methodology which considers the holistic and systematic wear of a gear pump. The main innovations are:

(A) An application specific gear pump wear concept for a HDE reported in Section 3.3 (see Figure 3-18) considering several sources of wear. Although this is a development from Frith and Scott (1996), the concept model for a lubrication gear pump of a HDE is new and has not been reported before in literature. It is foreseen that the top-level model will be used in sessions at CAB regarding FMEA and design reviews to promote discussions about failure mode avoidance and, used in validation planning. The impact is already observed as the concept offers an alternative perspective in terms of contributing sources of wear and specific projects targeting wear modes are planned, for instance wear in journal bearings for stop-start applications.

(B) An innovative pressure ripple feature extraction method was developed using MODWT-ARMA(2,1) to monitor gear pump degradation, as discussed in Section 3.6. This method was validated in the analysis of test data in Section 4.2 and proven to output a degradation path where finer differences in pump health could be distinguished (Figure 4-18). This precision of wear detection has not been documented before using pressure ripple measurements as reviewed in Section 3.5. The application of this monitoring method can be applied to both ADT and CBM of positive displacement pumps. The impact is the dissemination of using pressure ripple as a viable an alternative or as a supplement for monitoring methods, which another research may continue to investigate if it is benefit from higher precision in detecting changes in pump health. This may improve safety critical applications.

(C) Overall an innovative methodology (summarised in Figure 3-1) is developed to estimate the reliability of a gear pump using an extremely small sample size. The method uses the PoF of journal bearings (Section 2.2.2) and gear fatigue (Section 2.2.3) to set the test limits for a step-stress accelerated degradation. As already mentioned, the methodology uses an innovative pressure ripple monitoring technique to provide a degradation path that can be modelled. In Section 3.7, the use of an existing BU inference method is developed to improve the confidence in parameter estimate over frequentist methods. The use of preceding step-stress test data helps to address the test planning paradox (Section 1.1) by increasing the number of observations and improve the precision of parameter estimates. In Section 2.3 the findings indicate a gap in knowledge using transient vehicle data for estimating gear pump degradation. The simulation work concluded the use of stress-varying environment was necessary to improve the precision of field reliability estimates. The application of the methodology is specific to positive displacement pump manufactures. It is particularly effective for the reliability growth of NPD and can be equally effective on quickly assessing the risk of wear issues in the field. The impact is significant for CAB in changing their mind-set to NPD and new high potential projects are planned to further verify the method, see Section 6.1.4.

In summary, this EngD aimed to understand how to estimate the point of potential failure regarding the wear-out of a HDE lubrication gear pump, specifically within the context a NPD where only an extremely small sample size and there is little, or no pre-existing data was available. On the whole, this aim has been met although with limitations and scope for future work as discussed next.

6.1 Limitations and Future Work

To progress and strengthen the validity of the methodology several aspects are recommended. The first is validating the accuracy and repeatability of pressure ripple measurements for low-pressure pump applications such as the engine lubrication pump. The other is partnering with an engine OEM for a long term study regarding the NPD of their engine lubrication pumps.

6.1.1 Pressure Ripple Repeatability for Low-Pressure Applications

Compared to hydraulic pump applications, the pump outlet pressures required for a HDE are significantly lower (in the region of 1E5 to 6E5 Pa). In other words, the impedance is small, and in such cases, the pressure ripple measurement techniques are known to lose accuracy ISO 10767-1:2015 (ISO, 2015). Therefore it is recommended to study in greater detail if it is advantageous to measure the pressure ripple at higher pressures while investigating the impact on the pump in doing so. There is a balance to be found. After all, it has been established that outlet pressure degrades the pump and the monitoring method should not be overstressing the pump.

6.1.2 Automation and Test Plan Optimisation.

The step-stress test design (Section 3.4) was limited by a manual process and working hour restrictions. The methodology would benefit from automated pressure ripple monitoring, where the pump speed and loading valves automatically adjust for the pressure ripple measurement. Automation would provide the benefit of being able to test for 24 hours every day, which would contribute to resolving the test planning paradox by shortening the test window. It also allows improving the accuracy of the parameter estimates by maintaining the same test window (testing for longer at the lower stresses). As more data becomes available the opportunity to optimise the test duration and stress levels improves (Miller and Nelson, 1983; Khamis and Higgins, 1996; Nelson, 2005; Ma, 2009; Peng and Tseng, 2010; J.-R. Zhang *et al.*, 2011; Yang, 2013; Ye *et al.*, 2014; Lim, 2015).

6.1.3 Validation from the Field and Prognostics

An ideal situation is to validate the methodology and reliability growth for a NPD on an engine OEM program. This risk is finding an OEM prepared to see the value and invest in such a study. An opportunity exists to share a prognostics model with the OEM and collate the necessary data as an input into the simulation, such as time series data containing engine speed, oil temperature and pump outlet pressure. The prognostics model would activate a service light on the cabin dashboard once a pseudo-failure threshold was crossed. The

dashboard would inform the service technician to replace and return the pump for pressure ripple measurement and inspection. The benefit further develops and validates the degradation model for the field. With the advent of big data and connectivity (Meeker and Hong, 2014) this may even become possible offline. The competitive benefit is a prognostics model to reduce the risk of catastrophic field failures that the pump manufacturer compensates for, and it may prevent reputational damage for both Tier 1 suppliers and OEM.

6.1.4 Planned Implementation

To implement and sustain the uptake of the methodology requires a vision and target timeline. When considering the business model of ConcentricAB the timeline for a NPD can involve up to 3 years design phase including validation followed by 1 to 2 years of ramping up in production (COIC, 2012). A similar implementation timeline is required to design, develop and validate an automated monitoring system whilst in parallel initiating the current methodology to gain field experience, as illustrated in Figure 6-1 starting from Q1 2020.

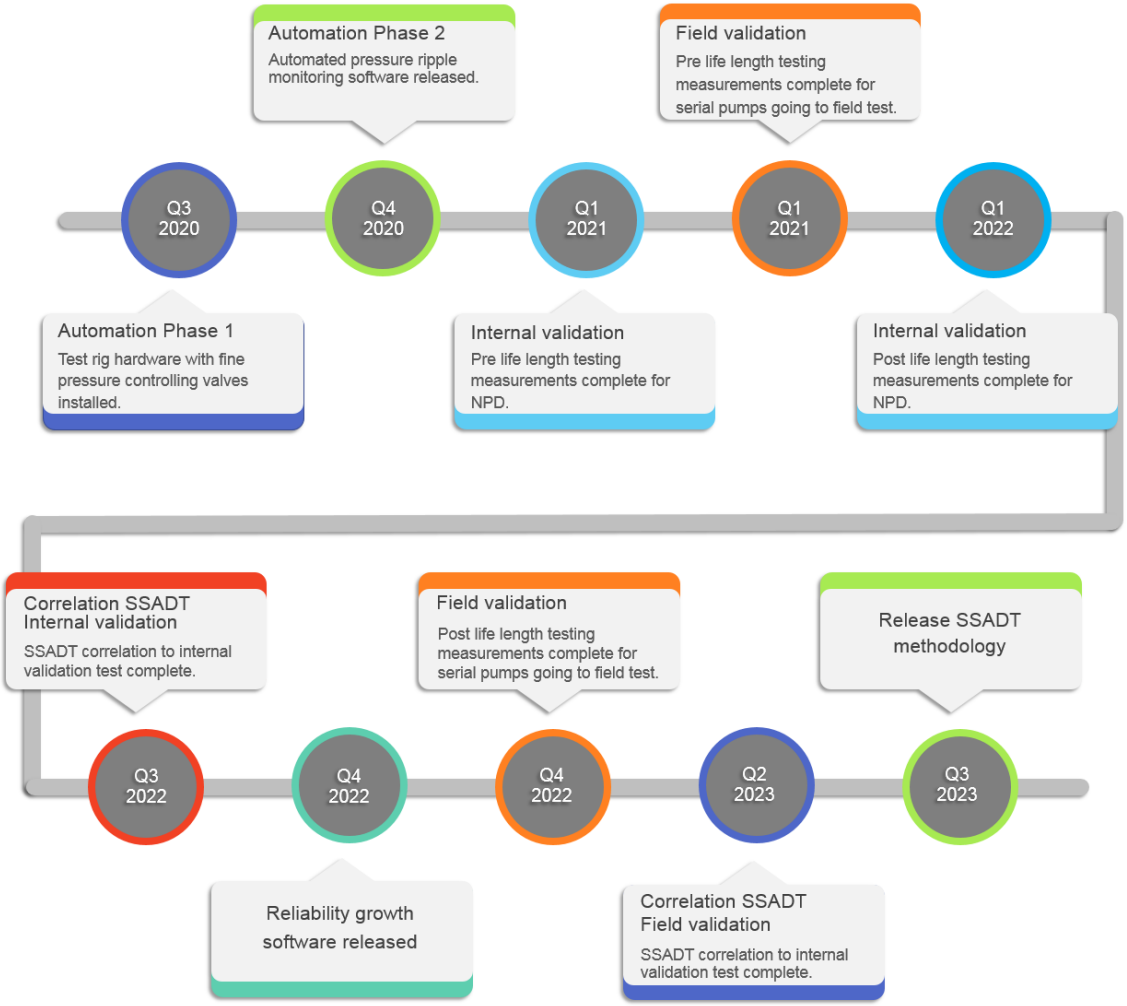

Figure 6-1 Roadmap for the introduction of gear pump SSADT methodology at CAB.

The Automation Phase 1 requires the capital expenditure approval, procurement and commission of pressure control valves that provide significantly improved control resolution, low hysteresis and improved repeatability. The valves are critical to automating the SSADT, and speeding up the physical constraints of needing personnel.

In parallel to the procurement of control valves, the Automation Phase 2 can begin with designing, testing and commissioning the pressure ripple monitoring software. The process of integrating the control valves and automatically capturing and processing least 28 pressure ripple signals every 15 minutes (for example) is expected to significantly improve the confidence in regression analysis.

Once the automation hardware and software have been commissioned, several stages of verification and validation are planned. The Internal Validation begins in Q1 2021 by periodically measuring the degradation from life length testing on a NPD which typically takes up to 3000 hours per pump, and is expected to take up to a year to complete in Q1 2022. In parallel, the pumps are measured before entering a customer field test in Q1 2021. The field tests cannot be accelerated in time compared to a test rig and therefore the completion date is at within two years finishing in Q4 2022.

The purpose of the Internal and Field Validation is to take the baseline degradation data to improve the correlation of the SSADT methodology to be completed in Q3 2022 for the internal validation comparison and Q2 2023 for the field validation comparison.

The overall aim is to demonstrate reliability targets will be achieved. The reliability growth software fed by the SSADT method is designed, tested and commissioned by Q4 2022 in preparation for release of the whole SSADT methodology in Q3 2023 to benefit in future projects.

References

AIChE (2007) Positive Displacement Pumps: A Guide to Performance Evaluation, Center for Chemical Process Safety of the American Institute of Chemical Engineers and John Wiley & Sons, Inc. Edited by R. P. O'Connor et al. John Wiley & Sons, Inc.

Akagaki, T. and Kato, K. (1992) 'Ferrographic analysis of failure process in a full-scale journal bearing', Wear, 152, pp. 241–252.

Ben Ali, J., Chebel-Morello, B., et al. (2015) 'Accurate bearing remaining useful life prediction based on Weibull distribution and artificial neural network', Mechanical Systems and Signal Processing. Elsevier, 56–57, pp. 150–172.

Ben Ali, J., Fnaiech, N., et al. (2015) 'Application of empirical mode decomposition and artificial neural network for automatic bearing fault diagnosis based on vibration signals', Applied Acoustics. Elsevier Ltd, 89, pp. 16–27.

Anderson, D. P. (1982) Wear Particle Atlas (Revised), Naval Air Engineering Center (Lakehurst, N.J.).

André, M. (2004) 'The ARTEMIS European driving cycles for measuring car pollutant emissions', Science of the Total Environment, 334–335, pp. 73–84.

Andreson, M. J. and Whitcomb, P. J. (2000) DOE Simplified: Practical Tools for Effective Experimentation. Productivity, Inc.

Arici, O., Johnson, J. H. and Kulkarni, A. J. (1999) 'The Vehicle Engine Cooling System Simulation Part 1 - Model Development', SAE Technical Paper Series.

Auto Business News (2018) 'Tata to offer six-year warranty for entire range of medium and heavy commercial vehicles', Auto Business News, January.

Awad, M. (2016) 'Economic allocation of reliability growth testing using Weibull distributions', Reliability Engineering and System Safety. Elsevier, 152, pp. 273–280.

Barford, N. C. (1985) Experimental Measurements: Precision, Error and Truth. 2nd edn. John Wiley & Sons Ltd.

Barney, J. (1991) 'Firm Resources and Sustained Competitive Advantage', Journal of Management, 17(1), pp. 99–120.

Barwell, F. T. et al. (1977) 'The use of temper colors in ferrography', Wear, 44(1), pp. 163–171.

Bedford, T., Quigley, J. and Walls, L. (2006) 'Expert Elicitation for Reliable System Design', Statistical Science, 21(4), pp. 428–450.

Bendell, A. (1985) 'Proportional hazards modelling in reliability assessment', Reliability Engineering, 11(3), pp. 175–183.

Berendsen, H. J. C. (2011) A Student's Guide to Data and Error Analysis. Cambridge University Press.

Berger, J. O., Bernardo, J. M. and Sun, D. (2009) 'The formal definition of reference priors', The Annals of Statistics, 37(2), pp. 905–938.

Bernardo, J. M. and Smith, A. F. M. (1994) Bayesian Theory. John Wiley & Sons, Ltd.

Bertsche, B. (2008) 'Chapter 1: Introduction and Chapter 2: Fundamentals of Statistics and Probability Theory', in Reliability in Automotive and Mechanical Engineering. Springer-Verlag Berlin Heidelberg, pp. 1–83.

Bian, L. and Gebraeel, N. (2014) 'Stochastic modeling and real-time prognostics for multi-component systems with degradation rate interactions', IIE Transactions (Institute of Industrial Engineers), 46(5), pp. 470–482.

Bian, L., Gebraeel, N. and Kharoufeh, J. P. (2015) 'Degradation modeling for real-time estimation of residual lifetimes in dynamic environments', IIE Transactions, 47, pp. 471–486.

Bogdanoff, J. L. and Kozin, F. (1985) Probabilistic Models of Cumulative Damage. John Wiley & Sons, Inc.

Bosch, G. (1979) 'Model for failure rate curves', Microelectronics Reliability, 19(4), pp. 371–375.

Bose, R. E. (1966) The effect of cavitation on particulate contamination generation. Oklahoma State University.

Bowen, E. R. (1981) Real Time Ferrograph Development, Report #80015, Naval Air Propulsion Center.

Box, G. E. P. and Tiao, G. C. (1973) Bayesian inference in statistical analysis. Addison-Wesley Publishing Company.

Boxall, P. and Purcell, J. (2016) Strategy and Human Resource Management. 4th edn. Edited by G. Burrell, M. Marchington, and P. Thompson. Palgrave and Macmillan.

Bramley, C. and Johnston, N. (2017) 'Comparison of methods for measuring pump flow ripple and impedance', in Proceedings of the ASME/BATH 2017 Symposium on Fluid Power and Motion Control FPMC2017. Sarasota, Florida, USA: ASME, pp. 1–11.

Brewe, D. E. (2001) 'Chapter 27: Slider Bearings', in Bhushan, B. (ed.) Modern Tribology Handbook, Volume Two, Materials Coatings, and Industrial Applications. 1st edn. CRC Press LLC.

British Standards Institution (1990) BS 6335-1:1990 Methods for determining pressure ripple levels generated in hydraulic fluid power systems and components. Part 1. Secondary source methods for pumps. 2nd edn. BSI Standards Limited.

British Standards Institution (1992) BS 5944-1:1992 Measurement of airborne noise from hydraulic fluid power systems and components - Part 1: Method of test for pumps. 2nd edn. BSI Standards Limited.

British Standards Institution (1996) BS ISO 10767-1: 1996 Hydraulic fluid Determination of pressure ripple levels generated in systems and components — Part 1 : Precision method for pumps. BSI Standards Limited.

British Standards Institution (1999) BS ISO 10767-2: 1999 Hydraulic fluid power - Determination of pressure ripple levels generated in systems and components - Part2: Simplified method for pumps. 1st edn. BSI Standards Limited.

British Standards Institution (2000) ISO/TR 13989-1 Calculation of scuffing load capacity of cylindrical, bevel and hypoid gears - Flash temperature method. BSI Standards Limited.

British Standards Institution (2006a) BS ISO 6336-1:2006 Calculation of load capacity of spur and helical gears - Part 1: Basic principles, introduction and general influence factors. 2nd edn. BSI Standards Limited.

British Standards Institution (2006b) BS ISO 6336-2:2006 Calculation of load capacity of spur and helical gears - Part 2: Calculation of surface durability (pitting). 2nd edn. BSI Standards Limited.

British Standards Institution (2006c) BS ISO 6336-6:2006 Calculation of load capacity of spur and helical gears - Part 6: Calculation of service life under variable load. BSI Standards Limited.

British Standards Institution (2007) BS ISO 4409:2007 Hydraulic fluid power - Positive displacement pumps, motors and integral transmissions - Methods of testing and presenting basic steady state performance. 2nd edn. BSI Standards Limited.

British Standards Institution (2008) BS ISO 7146-1:2008 Plain bearings - Appearance and characterization of damage to metallic hydrodynamic bearings. Part 1: General. 1st edn. BSI Standards Limited.

British Standards Institution (2009) BS ISO 4378-1:2009 Plain bearings - Terms, definitions, classification and symbols. Part 1: Design, bearing materials and their properties. 3rd edn. BSI Standards Limited.

British Standards Institution (2014a) BS 5760-0:2014 Reliability of systems, equipment and components – Part 0: Guide to reliability and maintainability. 2nd edn. BSI Standards Limited.

British Standards Institution (2014b) PD ISO/TR 15144-1:2014 Calculation of micro-pitting load capacity of cylindrical spur and helical gears. Part 1: Introduction and basic principles. 2nd edn. BSI Standards Limited.

British Standards Institution (2015) BS ISO 13381-1:2015 Condition monitoring and diagnostics of machines - Prognostics. Part 1: General guidelines. 2nd edn. BSI Standards Limited.

British Standards Institution (2018a) BS ISO 17359:2018 Condition monitoring and diagnostics of machines - General guidelines. 3rd edn. BSI Standards Limited.

British Standards Institution (2018b) BS ISO 20816-5:2018 Mechanical vibration - Measurement and evaluation of machine vibration. Part 5: Machine sets in hydraulic power generating and pump-storage plants. 1st edn. BSI Standards Limited.

Buono, D. et al. (2017) 'Gerotor pump cavitation monitoring and fault diagnosis using vibration analysis through the employment of auto-regressive-moving-average technique', Simulation Modelling Practice and Theory. Elsevier B.V., 71, pp. 61–82.

CAB (2013) 1,000,000 mile pump report CI-1357.

CAB (2016) Report 3287 (Conventional PRV Oil Pump Performance).

Cao, W. et al. (2015) 'Multisensor information integration for online wear condition monitoring of diesel engines', Tribology International. Elsevier, 82, pp. 68–77.

Cao, W., Wang, W. and Wang, R. (2012) 'Wear Trend Prediction of Gearbox Based on Oil Monitoring Technology', Advanced Materials Research, 411, pp. 576–579.

Carden, P. and Fanning, P. (2004) 'Vibration Based Condition Monitoring: A Review', Structural Health Monitoring, 3(4), pp. 355–377.

Carlson, C. et al. (2010) 'Best practices for effective reliability program plans', in 2010 Annual Reliability and Maintainability Symposium. IEEE, pp. 1–7.

Cheng, H. S. (2001) 'Chapter 29: Gears', in Bhushan, B. (ed.) Modern Tribology Handbook, Volume Two, Materials Coatings, and Industrial Applications. 1st edn. CRC Press LLC.

Childs, J. A. (2012) 'Reliability Design Tools', in Raheja, D. and Gullo (eds) Design for Reliability. John Wiley & Sons, Inc, pp. 15–35.

Childs, P. R. N. (2014) 'Chapter 5: Journal Bearings', in Mechanical Design Engineering Handbook. 1st edn. Elsevier, pp. 139–200.

Chiquet, J. and Limnios, N. (2013) 'Dynamical Systems with Semi-Markovian Perturbations and Their Use in Structural Reliability', in Dohi, T. and Nakagawa, T. (eds) Stochastic Reliability and Maintenance Modeling. Springer-Verlag London, pp. 191–218.

Chun, S. M. and Khonsari, M. M. (2016) 'Wear simulation for the journal bearings operating under aligned shaft and steady load during start-up and coast-down conditions', Tribology International. Elsevier Ltd., 97, pp. 440–466.

Clausing, D. and Frey, D. D. (2005) 'Improving system reliability by failure-mode avoidance including four concept design strategies', Systems Engineering, 8(3), pp. 245–261.

COIC (2012) Annual Report 2012. ConcentricAB, LINKÖPING.

COIC (2017) ConcentricAB Annual Report 2017. ConcentricAB, LINKÖPING.

Cooper, R. G. (2008) 'Perspective: The Stage-Gate ® Idea-to-Launch Process -Update, What's New, and NexGen Systems', Journal of Product Innovation Management, 25, pp. 213–232.

Cornish, C. R., Bretherton, C. S. and Percival, D. B. (2006) 'Maximal Overlap Wavelet Statistical Analysis With Application to Atmospheric Turbulence', Boundary-Layer Meteorology, 119(2), pp. 339–374.

Cox, D. R. (1972) 'Models and Life-Tables Regression', Journal of the Royal Statistical Society. Series B (Methodological), 34(2), pp. 187–220.

Crocker, M. J. (2007) 'Chapter 2: Theory of sound - Predictions and Measurement', in Fundamentals of Acoustics and Noise. John Wiley & Sons, Inc.

Crow, L. H. (1974) 'Reliability Analysis for Complex, Repairable Systems', Reliability and Biometry, pp. 379–410.

Cudina, M. (2007) 'Chapter 73: Pumps and pumping system noise and vibration prediction and control', in Crocker, M. J. (ed.) Handbook of Noise and Vibration Control. John Wiley & Sons, Inc., pp. 897–909.

Davis, T. P. (2003) 'Chapter 4: Reliability Improvement in Automotive Engineering', in Strutt, J. E. and Hall, P. L. (eds) Global Vehicle Reliability - Prediction and Optimization Techniques. Professional Engineering Publishing Limited, p. 140.

Day, M. J. (1996) 'Chapter 10: Condition Monitoring of Hydraulic Systems', in Rao, B. K. N. (ed.) Handbook of Condition Monitoring. 1st edn. Elsevier Science Ltd, pp. 209–252.

Dazer, M. et al. (2016) 'Planning of reliability life tests within the accuracy, time and cost triangle', in 2016 IEEE Accelerated Stress Testing & Reliability Conference (ASTR). Florida: IEEE, pp. 1–9.

Dean, A., Voss, D. and Draguljić, D. (2017) Design and Analysis of Experiments. 2nd edn. Springer International Publishing (Springer Texts in Statistics).

Debnath, L. and Shah, F. A. (2015) Wavelet Transforms and Their Applications. 2nd edn. Boston, MA: Birkhäuser Boston.

Denrell, J. and Powell, T. C. (2016) Dynamic Capability as a Theory of Competitive Advantage. Edited by D. J. Teece and S. Heaton. Oxford University Press.

Devendran, R. S. and Vacca, A. (2012) 'Optimal Design of Gears and Lateral Bushes of External Gear Machines', in Johnston, D. N. and Plummer, A. R. (eds) 2012 Conference Proceedings of Fluid Power and Motion Control, pp. 292–50.

Dhar, S. and Vacca, A. (2015) 'A novel FSI-thermal coupled TEHD model and experimental validation through indirect film thickness measurements for the lubricating interface in external gear machines', Tribology International. Elsevier Ltd., 82, pp. 162–175.

Dias, A. (2012) 'Chapter 12: Failure Analysis', in Totten, G. E. and De Negri, V. J. (eds) Handbook of Hydraulic Fluid Technology. 2nd edn. Taylor and Francis Group, LLC, pp. 461–529.

Dibb, S. et al. (2016) Marketing : concepts and strategies. 7th edn. Andover, Hampshire, United Kingdom : Cengage Learning.

Dibb, S., Simões, C. and Wensley, R. (2014) 'Establishing the scope of marketing practice: insights from practitioners', European Journal of Marketing, 48(1–2), pp. 380–404.

Dowlatshahi, S. (1994) 'A morphological approach to product design in a concurrent engineering environment', International Journal of Advanced Manufacturing Technology, 9, pp. 324–332.

Duane, J. T. (1964) 'Learning Curve Approach To Reliability Monitoring', IEEE Transactions on Aerospace, 2(2), pp. 563–566.

DuBois, G. E. and Ocvirk, F. W. (1953) Analytical derviation and experimental evaluation of short-bearing approximation for full journal bearings. Washington, DC.

Duckworth, W. E. and Forrester, P. G. (1957) 'Wear of lubricated journal bearings', in Proceedings of the Institute of Mechanical Engineers Conference on Lubrication and Wear. IMechE, pp. 713–719.

Dudley, D. W. (1980) 'Gear wear', in Peterson, M. B. and Winer, W. O. (eds) Wear Control Handbook. American Society of Mechanical Engineers, pp. 755–830.

Dufrane, K. F., Kannel, J. W. and McCloskey, T. H. (1983) 'Wear of Steam Turbine Journal Bearings at Low Operating Speeds', Transactions of the ASME, Journal of Lubrication Technology, 105(July), pp. 313–317.

Eaton-Vickers (2002) The Systemic Approach to Contamination Control - A Complete Guide for Maximum System Performance, Eaton Corporation.

Eaton, M., Keogh, P. S. and Edge, K. A. (2006) 'The Modelling, Prediction, and Experimental Evaluation of Gear Pump Meshing Pressures with Particular Reference to Aero-Engine Fuel Pumps', Proceedings of the Institution of Mechanical Engineers, Part I: Journal of Systems and Control Engineering, 220(5), pp. 365–379.

EC (2016) 'Regulation 2016/427', Official Journal of the European Union, (692).

Edge, K. A. and Johnston, D. N. (1990) 'The "secondary source" method for the measurement of pump pressure ripple characteristics. Part 1 : description of method', Proceedings of Institute of Mechanical Engineers Part A: Journal of Power and Energy, 204, pp. 33–40.

Elerath, J. G. and Pecht, M. (2012) 'IEEE 1413: A standard for Reliability Predictions', IEEE Transactions on Reliability, 61(1), pp. 125–129.

Elsayed, E. A. (2012) 'Overview of Reliability Testing', IEEE Transactions on Reliability, 61(2), pp. 282–291.

Elsayed, E. A. and Zhang, H. (2007) 'Design of Optimum Simple Step-Stress Accelerated Life Testing Plans', in Dohi, T., Osaki, S., and Sawaki, K. (eds) Recent Advances in Stochastic Operations Research. World Scientific Publishing Co Pte Ltd., pp. 23–38.

Eltabach, M. et al. (2011) 'Monitoring volumetric gear pumps using cyclostationarity of the downstream pressure signals', CETIM.

Ericsson, E. (2000) 'Variability in urban driving patterns', Transportation Research Part D, pp. 337–354.

Ericsson, E. and Lillieskold, J. (2012) 'Identifying weaknesses in the design for six sigma concept through a pedagogical structure', in Proceedings of PICMET: Technology Management for Emerging Technologies. IEEE, pp. 3379–3386.

Escobar, L. A. and Meeker, W. Q. (1995) 'Planning Accelerated Life Tests with Two or More Experimental Factors', Technometrics, 37(4), pp. 411–427.

Escobar, L. A. and Meeker, W. Q. (2006) ‘A Review of Accelerated Test Models’, Statistical Science, 21(4), pp. 552–577.

Fan, X. and Zuo, M. J. (2006) ‘Gearbox fault detection using Hilbert and wavelet packet transform’, Mechanical Systems and Signal Processing, 20(4), pp. 966–982.

Fanti, G. et al. (2002) ‘An innovative technique for quality control of gear pumps’, International Journal of Reliability, Quality and Safety Engineering, 09(04), pp. 383–392.

Fenton, M. B. M. (1994) Flow and Heat Transfer Modelling of an Automative Engine Lubrication Syste. University of Warwick.

Fishman, G. S. (2006) A First Course in Monte Carlo. Belmont, CA: Thomson Brooks/Cole.

Fitch, J. C. (1986) ‘Systems and Methods for Real-Time Condition Monitoring of Mechanical Machinery’, SAE Transactions. SAE International, 95(5), pp. 184–192.

Fitch, J. C. (2012) ‘Chapter 5: Control and Management of Particle Contamination in Hydraulic Fluids’, in Handbook of Hydraulic Fluid Technology. 2nd edn. Taylor and Francis Group, LLC.

Franc, J.-P. (2009) ‘Incubation Time and Cavitation Erosion Rate of Work-Hardening Materials’, Journal of Fluids Engineering, 131.

Frith, R. H. and Scott, W. (1993) ‘Control of solids contamination in hydraulic systems - An overview’, Wear, 165(1), pp. 69–74.

Frith, R. H. and Scott, W. (1994) ‘Wear in external gear pumps: a simplified model’, Wear, 172, pp. 121–126.

Frith, R. H. and Scott, W. (1996) ‘Comparison of an external gear pump wear model with test data’, Wear, 196, pp. 64–71.

Frosina, E. et al. (2014) ‘A tridimensional CFD analysis of the oil pump of an high performance motorbike engine’, Energy Procedia. Elsevier B.V., 45, pp. 938–948.

Gao, Y. and Zhang, Q. (2006) ‘A Wavelet Packet and Residual Analysis Based Method for Hydraulic Pump Health Diagnosis’, Proceedings of the Institution of Mechanical Engineers, Part D: Journal of Automobile Engineering, 220(6), pp. 735–745.

Gao, Z. et al. (2015) ‘Exploring Fuel-Saving Potential of Long-Haul Truck Hybridization’, 2502(1), pp. 99–107.

Ge, Z. et al. (2011) ‘Optimal design for step-stress accelerated degradation testing based on D-optimality’, in 2011 Proceedings - Annual Reliability and Maintainability Symposium. Lake Buena Vista, FL, USA: IEEE.

Gebraeel, N. et al. (2005) ‘Residual-life distributions from component degradation signals: A Bayesian approach’, IIE Transactions, 37, pp. 543–557.

Gebraeel, N. and Pan, J. (2008) ‘Prognostic degradation models for computing and updating residual life distributions in a time-varying environment’, IEEE Transactions on Reliability, 57(4), pp. 539–550.

Gerden, E. (2010) ‘The pump market’, World Pumps. Elsevier Ltd, 2010(10), pp. 24–27.

Gerges, S. N. Y., Johnston, D. N. and Rocha, L. Z. (2012) ‘Chapter 11: Noise and Vibration of Fluid Power Systems’, in Crocker, M. J. (ed.) Handbook of Hydraulic Fluid Technology. 2nd edn. Taylor and Francis Group, LLC.

Gertler, J. J. (1998) Fault detection and diagnosis in engineering systems. New York: Marcel Dekker.

Giakoumis, E. G. (2016) Driving and engine cycles. 1st edn. Springer International Publishing.

Glaeser, W. (2001) ‘Chapter 8: Wear Debris Classification’, in Bhushan, B. (ed.) Modern Tribology Handbook, Volume One, Principles of Tribology. CRC Press LLC.

Godet, M. et al. (1991) ‘Wear Modeling - Using Fundamental Understanding or Practical Experience’, Wear, 149, pp. 325–340.

Goode, K. B., Moore, J. and Roylance, B. J. (2000) ‘Plant machinery working life prediction method utilizing reliability and condition-monitoring data’, Proceedings of the Institution of Mechanical Engineers, Part E: Journal of Process Mechanical Engineering, 214(2), pp. 109–122.

Goode, K. B., Roylance, B. J. and Moore, J. (2000) ‘Development of model to predict condition monitoring interval times’, Ironmaking & Steelmaking, 27(1), pp. 63–68.

Goyal, D. and Pabla, B. S. (2016) 'The Vibration Monitoring Methods and Signal Processing Techniques for Structural Health Monitoring: A Review', Archives of Computational Methods in Engineering. Springer Netherlands, 23, pp. 585–594.

Grasso, M., Pennacchi, P. and Colosimo, B. M. (2014) 'Empirical mode decomposition of pressure signal for health condition monitoring in waterjet cutting', The International Journal of Advanced Manufacturing Technology, 72(1–4), pp. 347–364.

Green, D. A. and Lewis, R. (2008) 'The effects of soot-contaminated engine oil on wear and friction: a review', Proceedings of the Institution of Mechanical Engineers, Part D: Journal of Automobile Engineering, 222(9), pp. 1669–1689.

Green, D. A., Lewis, R. and Dwyer-Joyce, R. S. (2006) 'Wear effects and mechanisms of soot-contaminated automotive lubricants', Proceedings of the Institution of Mechanical Engineers, Part J: Journal of Engineering Tribology, 220(3), pp. 159–169.

Greene, R. H. and Casada, D. A. (1995) Detection of Pump Degradation, Oak Ridge National Laboratory.

Group, T. F. (2018) Global Pump Market to Grow 5.6% Annually Through 2022. Available at: https://www.freedoniagroup.com/Content/News/2018/06/15/Global-Pump-Market-to-Grow-56-Annually-Through-2022 (Accessed: 22 March 2019).

Guan, Q., Tang, Y. and Xu, A. (2016) 'Objective Bayesian analysis accelerated degradation test based on Wiener process models', Applied Mathematical Modelling. Elsevier Inc., 40(4), pp. 2743–2755.

Güemes, J. A. and Sierra-Perez, J. (2013) New Trends in Structural Health Monitoring. Edited by W. Ostachowicz and J. A. Güemes. Vienna: Springer Vienna (CISM International Centre for Mechanical Sciences).

Guo, H. and Liao, H. (2015) 'Practical Approaches for Reliability Evaluation Using Degradation Data', in 2015 Annual Reliability and Maintainability Symposium. Palm Harbor, Florida, USA: IEEE.

Guo, H. and Mettas, A. (2007) 'Improved Reliability Using Accelerated Degradation & Design of Experiments', IEEE, pp. 446–450.

Hahn, G. J. (1972) 'Sample Sizes for Monte Carlo Simulation', IEEE Transactions on Systems, MAN, and Cybernetics, (November), pp. 678–680.

Hannan, E. (2012) Report No C61212 Metallurgical Examination Oil Pump Gears.

Hansen, C. H. (2007) 'Types of Vibration Transducers', in Crocker, M. (ed.) Handbook of Noise and Vibration Control. John Wiley & Sons, Inc.

Harnoy, A. (1995) 'Model-Based Investigation of Friction During Start-Up of Hydrodynamic Journal Bearings', Transactions of the ASME, Journal of Tribology, 117(Oct), pp. 667–673.

Harris, T. J. (1996) 'Artificial Neural Networks in Condition Monitoring', in Rao, B. K. N. (ed.) Handbook of Condition Monitoring. 1st edn. Elsevier Science Ltd, pp. 341–348.

He, L., He, D. and Cao, M. (2016) 'Objective Bayesian analysis of degradation model with respect to a Wiener process', Journal of Systems Science and Complexity, 29, pp. 1737–1751.

Heng, A. et al. (2009) 'Rotating machinery prognostics: State of the art, challenges and opportunities', Mechanical Systems and Signal Processing, 23, pp. 724–739.

Herlufsen, H., Gade, S. and Zaveri, H. K. (2007) 'Chapter 40: Analyzers and signal generators', in Crocker, M. (ed.) Handbook of Noise and Vibration Control. John Wiley & Sons, Inc.

Hersant, J. et al. (2012) 'Reliability estimation from test data using two different approaches', in 2012 Proceedings Annual Reliability and Maintainability Symposium. Reno, NV, USA: IEEE, pp. 1–7.

Heydari, M. and Sullivan, K. M. (2017) 'Robust allocation of testing resources in reliability growth', Reliability Engineering and System Safety. Elsevier Ltd, pp. 1–16.

Hobbs, G. K. (2000) Accelerated Reliability Engineering: HALT and HASS. John Wiley & Sons Ltd.

Hofman, M. V. and Johnson, J. H. (1977) 'The development of ferrography as a laboratory wear measurement method for the study of engine operating conditions on diesel engine wear', Wear, 44(1), pp. 183–199.

Höhn, B. R. and Michaelis, K. (2004) 'Influence of oil temperature on gear failures', Tribology International, 37(2), pp. 103–109.

Hu, C.-H., Lee, M.-Y. and Tang, J. (2015) 'Optimum step-stress accelerated degradation test for Wiener degradation process under constraints', European Journal of Operational Research, 241(2), pp. 412–421.

Hu, Y. et al. (2019) 'Remaining Useful Life Model and Assessment of Mechanical Products: A Brief Review and a Note on the State Space Model Method', Chinese Journal of Mechanical Engineering. Springer Singapore, 32(1), p. 15.

Huang, G. Q. (1996) 'Introduction', in Huang, G. Q. (ed.) Design for X: Concurrent engineering imperatives. Chapman & Hall, pp. 1–17.

Huang, N. E. et al. (1998) 'The Empirical Mode Decomposition and the Hilbert Spectrum for Nonlinear and Non-Stationary Time Series Analysis', Proceedings of Royal Society of London A, 454(1971), pp. 903–995.

Huber, C. (2010) 'Chapter 21: Robust Versus Nonparametric Approaches and Survival Data Analysis', in Nikulin, M. S. et al. (eds) Advances in Degradation Modeling: Applications to Reliability, Survival Analysis, and Finance. Birkhäuser Boston, pp. 323–337.

Hui, K. H. et al. (2014) 'Time-Frequency Signal Analysis in Machinery Fault Diagnosis: Review', Advanced Materials Research, 845, pp. 41–45.

Ibe, O. C. (2013) 'Brownian Motion', in Markov Processes for Stochastic Modeling. Elsevier, pp. 263–293.

International Organization for Standardization (2015) ISO 10767-1:2015 Hydraulic fluid power - Determination of pressure ripple levels generated in systems and components Part 1 : Method for determining source flow ripple and source impedance of pumps. 2nd edn. BSI Standards Limited.

Isermann, R. (2011) Fault-Diagnosis Applications. Springer Berlin Heidelberg.

Jaber, A. A. and Bicker, R. (2014) 'A Simulation of Non-stationary Signal Analysis Using Wavelet Transform Based on LabVIEW and Matlab', in UKSim-AMSS 8th European Modelling Symposium. IEEE, pp. 138–144.

Jacobsen, F. (2007) 'Chapter 45 Sound Intensity Measurements', in Crocker, M. J. (ed.) Handbook of Noise and Vibration Control. John Wiley & Sons, Inc., pp. 534–548.

Jacobson, B. (2003) 'The Stribeck memorial lecture', Tribology International, 36(11), pp. 781–789.

Jaffe, A. B. and Stavins, R. N. (1994) 'The energy-efficiency gap. What does it mean?', Energy Policy, 22(10), pp. 804–810.

Jeffreys, H. (1946) 'An Invariant Form for the Prior Probability in Estimation Problems', Proceedings of the Royal Society of London. Series A, Mathematical and Physical Sciences, 186(1007), pp. 453–461.

Jin, G. et al. (2013) 'Physics of failure-based degradation modeling and lifetime prediction of the momentum wheel in a dynamic covariate environment', Engineering Failure Analysis. Elsevier Ltd, 28, pp. 222–240.

Jin, G., Matthews, D. E. and Zhou, Z. (2013) 'A Bayesian framework for on-line degradation assessment and residual life prediction of secondary batteries in spacecraft', Reliability Engineering and System Safety. Elsevier, 113(1), pp. 7–20.

Jobber, D. and Ellis-Chadwick, F. (2016) Principles and practice of marketing. 8th edn. London: McGraw-Hill Education.

Johnston, N. (2007) 'Chapter 76: Hydraulic system noise prediction and control', in Crocker, M. J. (ed.) Handbook of Noise and Vibration Control. 1st edn. John Wiley & Sons, Inc., pp. 946–955.

Johnston, N. and Todd, C. (2010) 'Condition Monitoring of Aircraft Fuel Pumps using Pressure Ripple Measurements', in 2010 Conference Proceedings of Fluid Power and Motion Control. Bath, pp. 161–174.

Jones, J. A. (1999) 'A toolkit for parametric drift modelling of electronic components', Reliability Engineering and System Safety, 63, pp. 99–106.

Jones, J. A. et al. (2003) 'Development of an expert system for reliability task planning as part of the REMM methodology', in 2003 Annual Reliability and Maintainability Symposium. IEEE, pp. 423–428.

Jones, J. A. and Hayes, J. A. (1987) 'The parametric drift behaviour of aluminium electrolytic capacitors: an evaluation of four models', in Proceedings of the 1st Capacitor and Resistor Technical Symposium. Brighton, England: Components Technology Institute, pp. 171–179.

Jones, M. H. (1979) 'Ferrography applied to diesel engine oil analysis', Wear, 56(1), pp. 93–103.

Junsheng, C., Dejie, Y. and Yu, Y. (2006) 'A fault diagnosis approach for roller bearings based on EMD method and AR model', Mechanical Systems and Signal Processing, 20, pp. 350–362.

Kahle, W., Mercier, S. and Paroissin, C. (2016) Degradation Processes in Reliability.

Kaneta, M. et al. (2006) 'Effects of soot on wear in elastohydrodynamic lubrication contacts', Proceedings of the Institution of Mechanical Engineers, Part J: Journal of Engineering Tribology, 220(3), pp. 307–317.

Karassik, I. J. (2001) Pump Handbook. 3rd edn. Edited by I. J. Karassik et al. New York; London: McGraw Hill.

Karthikeyan, L. and Nagesh Kumar, D. (2013) 'Predictability of nonstationary time series using wavelet and EMD based ARMA models', Journal of Hydrology. Elsevier B.V., 502, pp. 103–119.

Kass, R. E. and Wasserman, L. (1996) 'The Selection of Prior Distributions by Formal Rules', Journal of the American Statistical Association, 91(435), pp. 1343–1370.

Kazama, T. and Totten, G. E. (2012) 'Physical Properties and Their Determination', in Handbook of Hydraulic Fluid Technology. 1st edn. Taylor and Francis Group, LLC.

Khamis, I. H. and Higgins, J. J. (1996) 'Optimum 3-Step Step-Stress Tests', IEEE Transactions on Reliability, 45(2), pp. 341–345.

Khonsari, M. M. and Booser, E. R. (2008) 'Chapter 8: Journal Bearings', in Applied Tribology: Bearing Design and Lubrication. 2nd edn. John Wiley & Sons, Ltd, pp. 201–261.

Khoshzaban-Zavarehi, M. (1997) On-line condition monitoring and fault diagnosis in hydraulic system components using parameter estimation and pattern classification. The University of British Columbia.

Kim, S.-J. and Bae, S. J. (2013) 'Cost-effective degradation test plan for a nonlinear random-coefficients model', Reliability Engineering and System Safety. Elsevier, 110, pp. 68–79.

King, J. P. and Jewett, W. S. (2010a) 'Chapter 3: Strategies for Reliability Development', in Robustness Development and Reliability Growth. Pearson Education Limited, p. 47.

King, J. P. and Jewett, W. S. (2010b) Robustness Development and Reliability Growth. Pearson Education Inc.

Kleijnen, J. P. C. (1974) Statistical techniques in simulation Part 1. New York; Dekker.

Klemick, H. et al. (2015) Heavy-duty trucking and the energy efficiency paradox: Evidence from focus groups and interviews, Transportation Research Part A. Elsevier Ltd.

Koç, E. (1989) 'Analytical and experimental investigation into the sealing and lubrication mechanisms of the gear ends in pumps', Wear, 135(1), pp. 79–94.

Koç, E. (1991) 'An investigation into the performance of hydrostatically loaded end-plates in high pressure pumps and motors: movable plate design', Wear, 141(2), pp. 249–265.

Koç, E. (1994) 'Bearing misalignment effects on the hydrostatic and hydrodynamic behaviour of gears in fixed clearance end plates', Wear, 173(1–2), pp. 199–206.

Koç, E. and Hooke, C. J. (1997) 'An experimental investigation into the design and performance of hydrostatically loaded floating wear plates in gear pumps', Wear, 209(1–2), pp. 184–192.

Kohli, A. K. and Jaworski, B. J. (1990) 'Market Orientation: The Construct, Research Propositions, and Managerial Implications', Journal of Marketing, 54, pp. 1–18.

Kojima, E., Yui, J. and Ichiyanagi, T. (2000) 'Experimental Determining and Theoretical Predicting of Source Flow Ripple Generated by Fluid Power Piston Pumps', SAE Technical Papers Series.

Komsan, S. (2009) 'Managing new producct development performance: A process-based automotive product realization', Proceedings - International Conference on Management and Service Science, MASS 2009.

Kotler, P. (1977) 'From Sales Obsession to Marketing Effectiveness', Harvard Business Review, 55(6), pp. 67–75.

Kotler, P. et al. (2016) Principles of Marketing European Edition. 7th edn. Pearson Education Limited.

Kumar, P., Hirani, H. and Agrawal, A. (2017) 'Fatigue failure prediction in spur gear pair using AGMA approach', Materials Today: Proceedings. Elsevier Ltd, 4(2), pp. 2470–2477.

Kumar Pathak, S. et al. (2016) 'Real world vehicle emissions: Their correlation with driving parameters', Transportation Research Part D: Transport and Environment. Elsevier Ltd, 44, pp. 157–176.

Law, A. M. and Kelton, W. D. (2000) Simulation Modeling and Analysis. 3rd edn. McGraw Hill Higher Education.

Lawless, J. F. (1998) 'Statistical Analysis of Product Warranty Data', International Statistical Review, 66(1), pp. 41–60.

Lawless, J. F., Crowder, M. J. and Lee, K.-A. (2012) 'Monitoring Warranty Claims With Cusums', Technometrics, 54(3), pp. 269–278.

Leavey, C. M. et al. (2003) 'An introduction to wavelet transforms: A tutorial approach', Insight: Non-Destructive Testing and Condition Monitoring, 45(5), pp. 344–353.

Lee, D. Y. et al. (2018) 'Life-cycle implications of hydrogen fuel cell electric vehicle technology for medium- and heavy-duty trucks', Journal of Power Sources. Elsevier, 393, pp. 217–229.

Lehmann, A. (2010) 'Failure Time Models Based on Degradation Processes', in Nikulin, M. S. et al. (eds) Advances in Degradation Modeling. Birkhäuser Boston, pp. 209–233.

Li, B. et al. (2013) 'A gamma Bayesian exponential model for computing and updating residual life distribution of bearings', Proceedings of the Institution of Mechanical Engineers, Part C: Journal of Mechanical Engineering Science, 227(11), pp. 2620–2633.

Li, M. and Meeker, W. Q. (2014) 'Application of Bayesian Methods in Reliability Data Analyses', Journal of Quality Technology, 46(1), pp. 1–23.

Li, S. et al. (2002) 'Wear in Cummins M-11/EGR Test Engines', SAE Technical Paper Series.

Li, X. and Jiang, T. (2009) 'Optimal design for step-stress accelerated degradation testing with competing failure modes', in Proceedings of Annual Reliability and Maintainability Symposium. Fort Worth, Texas: IEEE, pp. 64–68.

Liao, C. M. and Tseng, S. T. (2006) 'Optimal design for step-stress accelerated degradation tests', IEEE Transactions on Reliability, 55(1), pp. 59–66.

Liao, H. and Tian, Z. (2013) 'A framework for predicting the remaining useful life of a single unit under time-varying operating conditions', IIE Transactions, 45(9), pp. 964–980.

Lim, H. (2015) 'Optimum accelerated degradation tests for the gamma degradation process case under the constraint of total cost', Entropy, 17(5), pp. 2556–2572.

Lin, J. and Niemeier, D. A. (2003) 'Estimating Regional Air Quality Vehicle Emission Inventories: Constructing Robust Driving Cycles', Transportation Science, 37(3), pp. 330–346.

Lin, Y. and Chung, K. (2019) 'Lifetime Prognosis of Lithium-Ion Batteries Through Novel Accelerated Degradation Measurements and a Combined Gamma Process and Monte Carlo Method', Applied Sciences, 9(3), p. 559.

Ling, J. and Wang, J. (2004) '2004-01-1539 Mega Trends of Automotive Industry and Evolution of Reliability Engineering', in SAE Technical Paper Series.

Liu, S. and Hung, J. C. (1991) 'Pulsating Parameter Method for Fault Diagnosis for a Hydraulic Pump', in Proceedings of International Conference on Industrial Electronics, Control and Instrumentation. Kobe, Japan: IEEE, pp. 2145–2150.

Liu, S. and Lin, Y. (2006) Grey Information. Edited by L. Jain and X. Wu. London: Springer-Verlag (Advanced Information and Knowledge Processing).

Liu, S. and Meeker, W. Q. (2014) 'Using Degradation Models to Assess Pipeline Life', Statistics Preprints, (Paper 127).

Liu, Z. et al. (2015) 'A Fault Diagnosis Methodology for Gear Pump Based on EEMD and Bayesian Network', PLoS One, 10(5).

Lu, C. J. and Meeker, W. Q. (1993) 'Using Degradation Measures to Estimate a Time-to-Failure Distribution', Technometrics, 35(2), pp. 161–174.

Luo, W. et al. (2014) 'Accelerated reliability demonstration under competing failure modes', Reliability Engineering and System Safety. Elsevier, 136, pp. 75–84.

Ma, H. (2009) New Developments in Planning Accelerated Life Tests. Iowa State University.

Machado, T. H. and Cavalca, K. L. (2015) 'Modeling of hydrodynamic bearing wear in rotor-bearing systems', Mechanics Research Communications. Elsevier Ltd., 69, pp. 15–23.

Macián, V. et al. (2006) 'Applying analytical ferrography as a technique to detect failures in Diesel engine fuel injection systems', Wear, 260, pp. 562–566.

Main, B. W. and McMurphy, K. J. (1999) '1999-01-0421 Safety Through Design: The State of the Art in Safety Processes', in SAE Technical Paper Series.

Majima, K. (1965) 'An application of random drift to reliability analysis', in 11th Proceedings of The National Symposium on Reliability and Quality. Anaheim, CA, pp. 506–509.

Manring, N. D. (2005) 'Measuring Pump Efficiency: Uncertainty Considerations', ASME Journal of Energy Resources Technology, 127, pp. 280–284.

Marketline Industry Profile (2018a) 'Global Automotive Manufacturing', (June), pp. 1–39.

Marketline Industry Profile (2018b) 'Global Medium & Heavy Trucks', (April), pp. 1–40.

Marketline Industry Profile (2018c) 'Global Mobile Phones', (April), pp. 1–40.

Maroney, G. E. (1976) Acoustical signature analysis of high pressure fluid pumping phenomena. Oklahoma State University.

Maroney, G. E. and Tessmann, R. K. (1977) 'Non-intrusive acoustical diagnostics for appraising pump contaminant wear', in 1977 SAE National Off-Highway Vehicle Meeting. Milwaukee, WI: SAE International.

Marsaglia, G. and Tsang, W. W. (2015) 'The Ziggurat Method for Generating Random Variables', Journal of Statistical Software, 5(8), pp. 1–7.

Martinez, F. et al. (2000) 'Dynamic monitoring for early failure diagnosis and modern techniques for design of positive displacement pumping systems', in Proceedings of the 17th International Pump Users Symposium. Texas A&M University: Turbomachinery Laboratories.

McGeehan, J. A. et al. (1998) '981371 New Diesel Engine Oil Category for 1998: API CH-4', SAE Technical Paper Series.

McLinn, J. A. (2005) 'Life testing hydraulic gear motors', in 2005 Proceedings of Annual Reliability and Maintainability Symposium. Alexandria, VA, USA: IEEE, pp. 245–249.

McLinn, J. A. (2008) 'Reliability predictions - More than the sum of the parts', in 2008 Proceedings of Annual Reliability and Maintainability Symposium. Las Vegas, Nevada USA: IEEE, pp. 446–451.

Meeker, W. Q. (2010) 'Chapter 1: Trends in the Statistical Assessment of Reliability', in Advances in Degradation Modeling. Boston, MA: Birkhäuser Boston, pp. 3–16.

Meeker, W. Q. and Escobar, L. A. (1998) 'Pitfalls of accelerated testing', IEEE Transactions on Reliability, 47(2), pp. 114–118.

Meeker, W. Q. and Escobar, L. A. (1998) Statistical Methods for Reliability Data. 1st edn. John Wiley & Sons, Inc.

Meeker, W. Q., Escobar, L. A. and Lu, C. J. (1998) 'Accelerated Degradation Tests: Modeling and Analysis', Technometrics, 40(2), pp. 89–99.

Meeker, W. Q. and Hong, Y. (2014) 'Reliability Meets Big Data: Opportunities and Challenges', Quality Engineering, 26(1), pp. 102–116.

Meeker, W. Q., Sarakakis, G. and Gerokostopoulos, A. (2013) 'More Pitfalls of Accelerated Tests', Journal of Quality Technology, 45(3), pp. 213–222.

Mercer, A. (1961) 'Some Simple Wear-Dependent Renewal Processes', Journal of the Royal Statistical Society, Series B (Methodological), 23(2), pp. 368–376.

Mercer, A. and Smith, C. S. (1959) 'A Random Walk in Which the Steps Occur Randomly in Time', Biometrika, 46(1/2), pp. 30–35.

Miller, R. and Nelson, W. (1983) 'Optimum Simple Step-Stress Plans for Accelerated Life Testing', IEEE Transactions on Reliability, R-32(1), pp. 59–65.

Milwaukee Fluid Power Institute (1980) A final report on the investigation into hydraulic gear pumps efficiencies in the first few hours of their lives and a comparative study of accelerated life test methods on hydraulic fluid power gear pumps. Milwaukee, WI.

Ming, L. and Meeker, W. Q. (2014) 'Application of Bayesian Methods in Reliability Data Analyses', Journal of Quality Technology, pp. 1–23.

Misiti, M. and Poggi, J. (2014) Wavelet Toolbox ™ Getting Started Guide R2014a. MathWorks.

Mokhtar, M. O. A., Howarth, R. B. and Davies, P. B. (1977) 'Wear Characteristics of Plain Hydrodynamic Journal Bearings During Repeated Starting and Stopping', ASLE Transactions, 20(3), pp. 191–194.

Moler, C. B. (2004) 'Random Numbers', in Numerical Computing with Matlab. Society for Industrial and Applied Mathematics, pp. 255–267.

Møltoft, J. (1980) 'The failure rate function estimated from parameter drift measurements', Microelectronics Reliability, 20(6), pp. 787–802.

Montgomery, D. C. (2013) Design and Analysis of Experiments. 8th edn. John Wiley & Sons, Inc.

Morey, J. E., Limanond, T. and Niemeier, D. A. (2000) 'Validity of chase car data used in developing emissions cycles', Journal of Transportation and Statistics, 3(2), pp. 15–28.

Moubray, J. (1997) Reliability Centred Maintenance. 2nd edn. Elsevier Ltd.

National Research Council (2015) Reliability Growth: Enhancing Defense System Reliability. Panel on Reliability Growth Methods for Defense Systems, Committee on National Statistics, Division of Behavioral and Social Sciences and Education. Washington, DC: The National Academies Press.

Naunheimer, H. et al. (2011) 'Design and Configuration of Further Design Elements', in Automotive Transmissions. 2nd edn. Berlin, Heidelberg: Springer-Verlag Berlin Heidelberg, pp. 420–478.

Nelson, W. B. (2004) Accelerated Testing, Statistical Models, Test Plans, and Data Analysis. John Wiley & Sons, Inc.

Nelson, W. B. (2005) 'A bibliography of accelerated test plans', IEEE Transactions on Reliability, 54(2), pp. 194–197.

Newland, D. E. (2007) 'Chapter 49: Wavelet Analysis of Vibration Signals', in Crocker, M. (ed.) Handbook of Noise and Vibration Control. John Wiley & Sons, Inc., pp. 585–597.

Ngui, W. K. et al. (2013) 'Wavelet Analysis: Mother Wavelet Selection Methods', Applied Mechanics and Materials, 393(August), pp. 953–958.

Nielsen, M. (2001) 'On the Construction and Frequency Localization of Finite Orthogonal Quadrature Filters', Journal of Approximation Theory, 108(1), pp. 36–52.

Niu, C. (2002) 'Accelerated testing in hydraulic component operational life test', in Proceedings of the 5th Japan Fluid Power System International Symposium on Fluid Power. Nara, pp. 125–130.

NSWC Carderock (2011) NSWC-11 Handbook of reliability prediction procedures for mechanical equipment. Carderock Division, Naval Surface Warfare Center.

O'Connor, P. D. T. and Kleyner, A. (2012) Practical Reliability Engineering. 5th edn. John Wiley & Sons, Ltd.

O'Hagan, A. and Oakley, J. E. (2004) 'Probability is perfect, but we can't elicit it perfectly', Reliability Engineering and System Safety, 85(1–3), pp. 239–248.

Oda, S., Koide, T. and Mizune, M. (1985) 'Study on Bending Fatigue Strength of Helical Gears', Japan Society of Mechanical Engineers, 28(244), pp. 2429–2433.

Onsoyen, E. (1991) 'Chapter 1.3: Accelerated Testing of Components Exposed to Wear', in Holmberg, K. and Folkeson, A. (eds) Operational Reliability and Systematic Maintenance. Elsevier Applied Science London and New York, pp. 51–77.

Owen, W. J. and Padgett, W. J. (2000) 'A Birnbaum-Saunders accelerated life model', IEEE Transactions on Reliability, 49(2), pp. 224–229.

Oxford English Dictionary (2010) Oxford Dictionary of English. 3rd edn. Edited by A. Stevenson. Oxford University Press.

Pan, Z. and Sun, Q. (2014) 'Optimal Design for Step-Stress Accelerated Degradation Test with Multiple Performance Characteristics Based on Gamma Processes', Communications in Statistics - Simulation and Computation, 43(2), pp. 298–314.

Pandit, S. M. and Wu, S.-M. (1983) 'Chapter 7: Second order system and random vibration', in Time Series and System Analysis with Applications. John Wiley & Sons, Inc, pp. 248–293.

Papadopoulos, C. A., Nikolakopoulos, P. G. and Gounaris, G. D. (2008) 'Identification of clearances and stability analysis for a rotor-journal bearing system', Mechanism and Machine Theory, 43(4), pp. 411–426.

Park, C. and Padgett, W. J. (2006) ‘Stochastic degradation models with several accelerating variables’, IEEE Transactions on Reliability, 55(2), pp. 379–390.

Peng, C.-Y. and Tseng, S.-T. (2010) ‘Progressive-stress accelerated degradation test for highly-reliable products’, IEEE Transactions on Reliability, 59(1), pp. 30–37.

Peng, W. et al. (2013) ‘Life cycle reliability assessment of new products—A Bayesian model updating approach’, Reliability Engineering & System Safety. Elsevier, 112, pp. 109–119.

Peng, Z. K. et al. (2009) ‘On the energy leakage of discrete wavelet transform’, Mechanical Systems and Signal Processing, 23(2), pp. 330–343.

Piersol, A. G. (2007) ‘Chapter 42: Signal Processing’, in Crocker, M. (ed.) Handbook of Noise and Vibration Control. John Wiley & Sons, Inc.

Pulido, J. (2015) ‘Life Data Analysis Using the Competing Failure Modes Technique’, in 2015 Proceedings of Annual Reliability and Maintainability Symposium. Palm Harbor, Florida, USA: IEEE, pp. 310–315.

Rafique, S. O. (1963) ‘Paper 15: Failures of Plain Bearings and Their Causes’, Proceedings of the Institution of Mechanical Engineers, Conference Proceedings, 178(14), pp. 180–195.

Rainey, D. L. (2005) Product Innovation: Leading Change through Integrated Product Development. Cambridge University Press.

Rakopoulos, C. D. and Giakoumis, E. G. (2009) ‘Chapter 1: Transient Operation Fundamentals’, in Diesel Engine Transient Operation, Principles of Operation and Simulation Analysis. 1st edn. Springer-Verlag London Limited.

Randall, R. B. (2007) ‘Chapter 46: Noise and vibration data analysis’, in Crocker, M. J. (ed.) Handbook of Noise and Vibration Control. John Wiley & Sons, Inc, pp. 549–564.

Randall, R. B. (2007) ‘Chapter 48: Machinery Condition Monitoring’, in Crocker, M. (ed.) Handbook of Noise and Vibration Control. John Wiley & Sons, Inc., pp. 575–584.

Ranganathan, G. and Mohanram, P. V. (2005) ‘2005-26-038 Development of Improved Test Practices - Case Study for a Critical Engine Component’, SAE Technical Paper Series.

Ranganathan, G., Raj, T. H. S. and Mohanram, P. V. (2004) ‘Wear characterisation of small PM rotors and oil pump bearings’, Tribology International, 37(1), pp. 1–9.

Redfield, J. et al. (2006) ‘Accessory Electrification in Class 8 Tractors’, SAE Technical Paper Series.

René Van Dorp, J. and Mazzuchi, T. A. (2004) ‘A general Bayes exponential inference model for accelerated life testing’, Journal of Statistical Planning and Inference, 119(1), pp. 55–74.

Robert, C. P., Chopin, N. and Rousseau, J. (2009) ‘Harold Jeffreys’s Theory of Probability Revisited’, Statistical Science, 24(2), pp. 141–172.

Roeth, M. et al. (2013) ‘Barriers to the Increased Adoption of Fuel Efficiency Technologies in the North American On-Road Freight Sector’, International Council on Clean Transportation, (July).

Rundo, M. and Nervegna, N. (2015) ‘Lubrication pumps for internal combustion engines: A review’, International Journal of Fluid Power, 16(2), pp. 59–74.

Sander, D. E. et al. (2015) ‘Edge loading and running-in wear in dynamically loaded journal bearings’, Tribology International. Elsevier, 92, pp. 395–403.

Sarakakis, G., Gerokostopoulos, A. and Mettas, A. (2011) ‘Special topics for consideration in a design for reliability process’, in 2011 Proceedings - Annual Reliability and Maintainability Symposium. Lake Buena Vista, Florida, USA: IEEE.

Seifert, W. W. and Westcott, V. C. (1972) ‘A method for the study of wear particles in lubricating oil’, Wear, 21(1), pp. 27–42.

Shen, H. et al. (2018) ‘A method for gear fatigue life prediction considering the internal flow field of the gear pump’, Mechanical Systems and Signal Processing. Elsevier Ltd, 99, pp. 921–929.

Shuster, M. et al. (2002) ‘2002-01-1172 Development of an Accelerated Testing Methodology of Rotary Oil Seals for Off-Highway Vehicles’, SAE Technical Paper Series.

Siano, D., Frosina, E. and Senatore, A. (2017) 'Diagnostic Process by Using Vibrational Sensors for Monitoring Cavitation Phenomena in a Getoror Pump Used for Automotive Applications', Energy Procedia. Elsevier Ltd, 126, pp. 1115–1122.

Silva, G. (1986) 'Pump Failure Mode Forecasting Through the Use of an Integrated Diagnostic Methodology, SAE 861307', SAE Technical Paper Series. SAE International.

Silva, G. (1987) A study of the synergistic effects of pump wear. Oklahoma State University.

Silva, G. (1990) 'Wear Generation in Hydraulic Pumps', SAE Technical Paper Series. SAE International.

Singh, M., Lathkar, G. S. and Basu, S. K. (2012) 'Failure Prevention of Hydraulic System Based on Oil Contamination', Journal of The Institution of Engineers (India): Series C, 93(3), pp. 269–274.

Singh, S. and Kumar, N. (2014) 'Combined rotor fault diagnosis in rotating machinery using empirical mode decomposition', Journal of Mechanical Science and Technology, 28(12), pp. 4869–4876.

Singpurwalla, N. D. (1995) 'Survival in Dynamic Environments', Statistical Science, 10(1), pp. 86–103.

Smrdel, D. and Clason, D. L. (2012) 'Chapter 10: Bench and Pump Testing Procedures', in Totten, G. E. and De Negri, V. J. (eds) Handbook of Hydraulic Fluid Technology. 2nd edn. Taylor and Francis Group, LLC, pp. 401–446.

Snook, I., Marshall, J. M. and Newman, R. M. (2003) 'Physics of failure as an integrated part of design for reliability', in Annual Reliability and Maintainability Symposium, 2003. IEEE, pp. 46–54.

Spanó, C. C. (2008) '2008-36-0005 Design for Reliability Application', SAE Technical Paper Series, pp. 1–11.

Stapelberg, R. F. (2009) 'Chapter 3: Reliability and Performance in Engineering Design', in Handbook of Reliability, Availability, Maintainability and Safety in Engineering Design. 1st edn. Spring-Verlag London Limited, pp. 158–160.

Stark, H.-G. (2005) Wavelets and Signal Processing. An Application-Based Introduction. Springer-Verlag Berlin Heidelberg.

Stephenson, J. and Wallace, K. (1996) 'Chapter 12: Design for Reliability for Mechanisms', in Huang, G. Q. (ed.) Design for X: Concurrent engineering imperatives. Chapman & Hall, pp. 245–267.

Strutt, J. E. et al. (2003) 'Progress Towards a "Design for Reliability" Methodology for Automotive Components and Systems', in Strutt, J. E. and Hall, P. L. (eds) Global Vehicle Reliability - Prediction and Optimization Techniques. Professional Engineering Publications, IMechE, London., pp. 5–24.

Sun, Q. et al. (2012) 'Optimization of step stress accelerated degradation test plans based on MSE', in 2012 International Conference on Quality, Reliability, Risk, Maintenance, and Safety Engineering. Chengdu, China: IEEE.

Syversveen, A. R. (1998) 'Noninformative Bayesian Priors. Interpretation and Problems with Construction and Applications', Preprint Statistics, 3, p. 11.

Szeri, A. Z. (1978) 'Thick-Film Lubrication', in Fluid Film Lubrication. 1st edn. Cambridge: Cambridge University Press, pp. 88–146.

Tabor, D. (1977) 'Wear - A Critical Synoptic View', Transactions of the ASME, Journal of Lubrication Technology, 99(4), pp. 387–395.

Talafuse, T. P. and Pohl, E. A. (2017) 'Small sample reliability growth modeling using a grey systems model', Quality Engineering, 29(3), pp. 455–467.

Teece, D. J., Pisano, G. and Shuen, A. (1997) 'Dynamic capabilities and strategic management', Strategic Management Journal, 18(7), pp. 509–533.

Thaduri, A. et al. (2012) 'Two-stage design of experiments approach for prediction of reliability of optocouplers', International Journal of Reliability, Quality and Safety Engineering, 19(02), p. 1250007.

Tian, Z., Wu, B. and Chen, M. (2014) 'Condition-based maintenance optimization considering improving prediction accuracy', Journal of the Operational Research Society, 65(9), pp. 1412–1422.

Tobias, P. A. and Trindade, D. C. (2012) 'Chapter 9: Alternative Reliability Methods', in Applied Reliability. 3rd edn. CRC Press LLC, pp. 320–321.

Tomsky, J. (1982) 'Regression models for detecting reliability degradation', Proceedings - Annual Reliability and Maintainability Symposium, pp. 283–245.

Tsai, T.-R. et al. (2016) ‘Optimal Two-Variable Accelerated Degradation Test Plan for Gamma Degradation Processes’, IEEE Transactions on Reliability, 65(1), pp. 459–468.

Tseng, S.-T., Balakrishnan, N. and Tsai, C.-C. (2009) ‘Optimal Step-Stress Accelerated Degradation Test Plan for Gamma Degradation Processes’, IEEE Transactions on Reliability, 58(4), pp. 611–618.

Tsui, K. L. et al. (2015) ‘Prognostics and health management: A review on data driven approaches’, Mathematical Problems in Engineering, 2015, p. 17.

US MIL-HDBK-217F (1991) MIL-HDBK-217F, Military Handbook, Reliability Prediction of Electronic Equipment. US Department of Defense.

Vencl, A. and Rac, A. (2014) ‘Diesel engine crankshaft journal bearings failures: Case study’, Engineering Failure Analysis. Elsevier Ltd, 44, pp. 217–228.

Viertl, R. (1981) ‘A note on a lifetime model’, Microelectronics Reliability, 21(3), pp. 745–748.

Wan, F. et al. (2014) ‘Data analysis and reliability estimation of step-down stress accelerated degradation test based on Wiener process’, in 2014 Prognostics and System Health Management Conference (PHM-2014 Hunan). Zhangiiaijie, China: IEEE, pp. 41–45.

Wang, D. et al. (2017) ‘Nonlinear-drifted Brownian motion with multiple hidden states for remaining useful life prediction of rechargeable batteries’, Mechanical Systems and Signal Processing. Elsevier Ltd, 93, pp. 531–544.

Wang, L. et al. (2013) ‘A Bayesian reliability evaluation method with integrated accelerated degradation testing and field information’, Reliability Engineering and System Safety. Elsevier, 112, pp. 38–47.

Wang, P. et al. (2009) ‘Bayesian Reliability Analysis With Evolving, Insufficient, and Subjective Data Sets’, Journal of Mechanical Design, 131(11).

Wang, S. P. and Shi, J. (2006) ‘Accelerated Life Testing under Variable Synthetic Stresses for Hydraulic Pump’, Materials Science Forum, 505–507, pp. 1165–1170.

Wang, X. et al. (2016) ‘Remaining useful life prediction based on the Wiener process for an aviation axial piston pump’, Chinese Journal of Aeronautics. Chinese Society of Aeronautics and Astronautics, 29(3), pp. 779–788.

Wang, X. and Xu, D. (2010) ‘An Inverse Gaussian Process Model for Degradation Data’, Technometrics, 52(2), pp. 188–197.

Wang, Z. and Zhou, H. (2009) ‘A general method of prior elicitation in Bayesian reliability analysis’, Proceedings of 2009 8th International Conference on Reliability, Maintainability and Safety, ICRMS 2009, (2), pp. 415–419.

Weaver, B. P. and Meeker, W. Q. (2014) ‘Methods for planning repeated measures accelerated degradation tests’, Applied Stochastic Models in Business and Industry, 30, pp. 658–671.

Wedeven, L. D. and Ludema, K. C. (2012) ‘Chapter 6: Lubrication Fundamentals’, in Totten, G. E. and De Negri, V. J. (eds) Handbook of Hydraulic Fluid Technology. 2nd edn. Taylor and Francis Group, LLC, pp. 258–302.

Williams, J. A. and Hyncica, A. M. (1992) ‘Mechanisms of abrasive wear in lubricated contacts’, Wear, 152, pp. 57–74.

World Pumps (2016a) ‘Life-cycle costs concerns major part of purchasing’, World Pumps, pp. 16–17.

World Pumps (2016b) ‘UK pump market forecast 2016–2019’, World Pumps, pp. 32–33.

Wu, T. H. et al. (2008) ‘Journal Bearing Wear Monitoring via On-Line Visual Ferrography’, Advanced Materials Research, 44–46, pp. 189–194.

Wu, Y.-F. and Lewins, J. D. (1992) ‘Monte Carlo studies of engineering system reliability’, Annals of Nuclear Energy, 19(10–12), pp. 825–859.

Wu, Z. and Huang, N. E. (2009) ‘Ensemble Empirical Mode Decomposition: A Noise-Assisted Data Analysis Method’, Advances in Adaptive Data Analysis, 01(01), pp. 1–41.

Xia, T. et al. (2018) ‘Recent advances in prognostics and health management for advanced manufacturing paradigms’, Reliability Engineering & System Safety. Elsevier Ltd, 178(June), pp. 255–268.

Xin, Q. (2011) ‘Friction and lubrication in diesel engine system design’, in Diesel Engine System Design. Woodhead Publishing Limited, pp. 651–758.

Xu, A. and Tang, Y. (2012a) 'Objective bayesian analysis for linear degradation models', Communications in Statistics - Theory and Methods, 41(21), pp. 4034–4046.

Xu, A. and Tang, Y. (2012b) 'Objective Bayesian analysis for linear degradation models', Communications in Statistics - Theory and Methods, 41(21), pp. 4034–4046.

Xu, H.-Y. and Fei, H.-L. (2007) 'Planning Step-Stress Accelerated Life Tests With Two Experimental Variables', IEEE Transactions on Reliability, 56(3), pp. 569–579.

Xue, X. et al. (2014) 'An improved ensemble empirical mode decomposition method and its application to pressure pulsation analysis of hydroelectric generator unit', Proceedings of the Institution of Mechanical Engineers, Part O: Journal of Risk and Reliability, 228(6), pp. 543–557.

Yan, R., Gao, R. X. and Chen, X. (2014) 'Wavelets for fault diagnosis of rotary machines: A review with applications', Signal Processing. Elsevier, 96(PART A), pp. 1–15.

Yan, W.-A. et al. (2013) 'Empirical Bayesian estimation of Wiener process with integrated degradation data and life data', in 2013 International Conference on Quality, Reliability, Risk, Maintenance, and Safety Engineering. IEEE, pp. 183–188.

Yang, G. (2013) 'Heuristic degradation test plans for reliability demonstration', IEEE Transactions on Reliability, 62(1), pp. 305–311.

Yang, G. and Zaghati, Z. (2006) 'Accelerated life tests at higher usage rates: A case study', in 2006 Proceedings of Annual Reliability and Maintainability Symposium. Newport Beach, California USA: IEEE, pp. 313–317.

Yang, M. (2009) Modelling and analysis of pressure pulsations in hydraulic components and systems with particular reference to pump fault diagnosis. University of Bath.

Yang, M., Edge, K. A. and Johnston, D. N. (2008) 'Condition monitoring and fault diagnosis for vane pumps using flow ripple measurement', in Johnston, D. N. and Plummer, A. R. (eds) Fluid Power and Motion Control (FPMC2008). Centre for Power Transmission and Motion Control, Bath, UK.

Yang, Q. and Wang, J. (2015) 'Multi-Level Wavelet Shannon Entropy-Based Method for Single-Sensor Fault Location', Entropy, 17, pp. 7101–7117.

Yang, T.-Y. and Leu, L.-P. (2008) 'Multi-resolution analysis of wavelet transform on pressure fluctuations in an L-valve', International Journal of Multiphase Flow, 34, pp. 567–579.

Ye, Z.-S. et al. (2014) 'Accelerated Degradation Test Planning Using the Inverse Gaussian Process', IEEE Transactions on Reliability, 63(3), pp. 750–763.

Yeh, T.-M., Pai, F.-Y. and Yang, C.-C. (2010) 'Performance improvement in new product development with effective tools and techniques adoption for high-tech industries', Quality & Quantity, 44, pp. 131–152.

Yu, D., Cheng, J. and Yang, Y. (2005) 'Application of EMD method and Hilbert spectrum to the fault diagnosis of roller bearings', Mechanical Systems and Signal Processing, 19, pp. 259–270.

Yu Fan and Li, X. (2012) 'An ADT life prediction method based on the wavelet-packet band energy', in Proceedings of the IEEE 2012 Prognostics and System Health Management Conference (PHM-20120. Beijing: IEEE, pp. 1–6.

Zaharia, S. M. and Morariu, C. O. (2015) 'Reliability analysis for gears using accelerated testing through Monte Carlo simulation', 2(V), pp. 19–28.

Zaludova, A. H. and Zalud, F. H. (1985) 'New Development in Accelerated testing', in Proceedings of the 20th EOQC Conference: quality and development. Estoril, Portugal: APQ - Praca das Industias, pp. 10–24.

Zaretsky, E. V. (1987) 'Fatigue criterion to system design, life, and reliability', Journal of Propulsion and Power, 3(1), pp. 76–83.

Zarzycki, E. P. (2015) Submission 1: Project Proposal: How to Predict the Onset of Wear-out for a Heavy-Duty Diesel Engine Lubrication Pump in a Vehicle Engine Environment? University of Warwick.

Zarzycki, E. P. (2016) Submission 2: Gear Pump Wear Concept Model: How to Predict the Onset of Wear-out for a Heavy-Duty Diesel Engine Lubrication Pump in a Vehicle Engine Environment? University of Warwick.

Zarzycki, E. P. (2017a) Submission 3: The Feasibility of a Pump Wear Monitoring Technique Using Pump Pressure Ripple. University of Warwick.

Zarzycki, E. P. (2017b) Submission 4: The Design and Test of an Accelerated Degradation Test to Estimate the Life of a Gear Pump in Heavy-Duty Diesel Engine Lubrication Pump in a Vehicle Engine Environment. University of Warwick.

Zarzycki, E. P. (2018a) Submission 5: The Reliability Estimation of a Gear Pump Using Step-Stress Accelerated Degradation Test Data. University of Warwick.

Zarzycki, E. P. (2018b) Submission 6: The Simulated Degradation and Reliability Estimation of a Lubrication Gear Pump in a Heavy-Duty Diesel Engine Truck. University of Warwick.

Zhang, H., Yuan, H. and Li, P. (2015) 'Estimation method for extremely small sample accelerated degradation test data', in 2015 First International Conference on Reliability Systems Engineering (ICRSE). IEEE, pp. 1–5.

Zhang, J.-R. et al. (2011) 'Optimization of the test stress levels of an ADT', in 2011 Proceedings of Annual Reliability and Maintainability Symposium. Lake Buena Vista, FL, USA: IEEE, pp. 1–6.

Zhang, L. et al. (2010) 'Time-frequency representation based on time-varying autoregressive model with applications to non-stationary rotor vibration analysis', Sadhana - Academy Proceedings in Engineering Sciences, 35(2), pp. 215–232.

Zhang, P. et al. (2011) 'A Survey of Condition Monitoring and Protection Methods for Medium-Voltage Induction Motors', IEEE Transactions on Industry Applications, 47(1), pp. 34–46.

Zhang, Z.-X. et al. (2016) 'Planning Repeated Degradation Testing for Products with Three-Source Variability', IEEE Transactions on Reliability, 65(2), pp. 640–647.

Zhang, Z. et al. (2018) 'Degradation data analysis and remaining useful life estimation: A review on Wiener-process-based methods', European Journal of Operational Research. Elsevier B.V., 271(3), pp. 775–796.

Zhu, L., Wang, Y. and Fan, Q. (2014) 'MODWT-ARMA model for time series prediction', Applied Mathematical Modelling. Elsevier Inc., 38, pp. 1859–1865.

Zhu, Y. and Elsayed, E. A. (2013) 'Design of accelerated life testing plans under multiple stresses', Naval Research Logistics, 60(6), pp. 468–478.

Zio, E. (2013) The Monte Carlo Simulation Method for System Reliability and Risk Analysis. Springer London.

Appendix A. Manual Valve Gauge Repeatability and Reproducibility

A gauge repeatability and reproducibility (Gauge R&R) study is a statistical tool used to assess the variation in a measurement. The source of variation may include the setting of test parameters and the differences between operators. In the feasibility stage, the automated valve used to set the restriction was found to be problematic, with insufficient resolution in step changes and susceptibility to hysteresis. Therefore, a manually operated valve was used that could reproduce setting the test parameters. Although the manual valve had no position feedback, the control was significantly improved and finite. This section demonstrates the accuracy level achieved as required in ISO 10767-1:2015 (ISO, 2015). The procedure was to stop the pump (0 rpm) after each measurement, reset the valve to fully open before restarting the pump (1020 rpm), set the valve to the desired pressure setting (5E5 Pa) and then record the measurement again. In this project, there is only one operator and the study is categorised as a Type 1 Gauge Study. A minimum of 28 measurements were required to satisfy the 95% confidence ($\alpha = 0.05$).

The results plotted for pump speed, outlet pressure, inlet temperature and flow are plotted from Figure A-1 to Figure A-4 all meet the requirements of ISO 10767-1:2015 (ISO, 2015). Setting the capability limits to the acceptable tolerance outputs a gauge capability (C_g) close to 1 which is ideal.

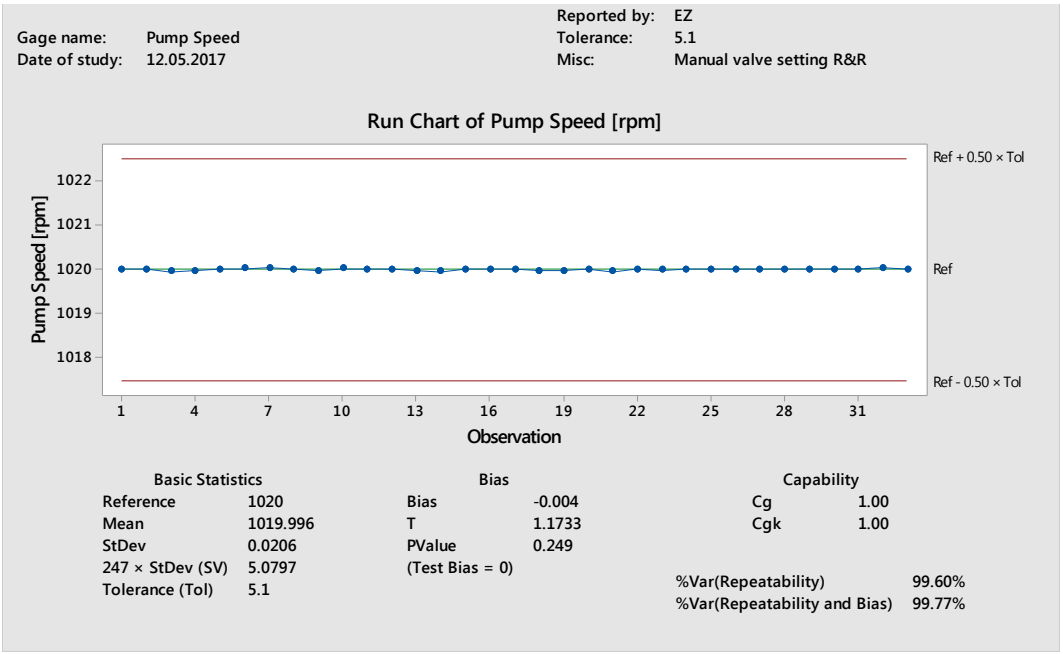

Figure A-1 Pump speed manual valve setting gauge R&R.

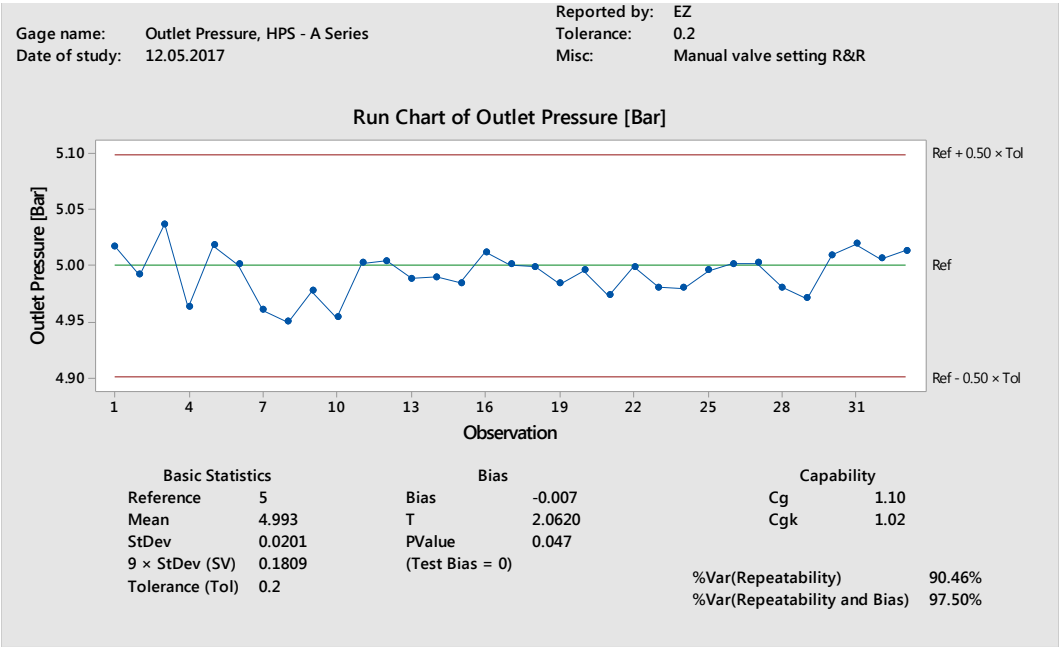

Figure A-2 Outlet pressure manual valve setting gauge R&R.

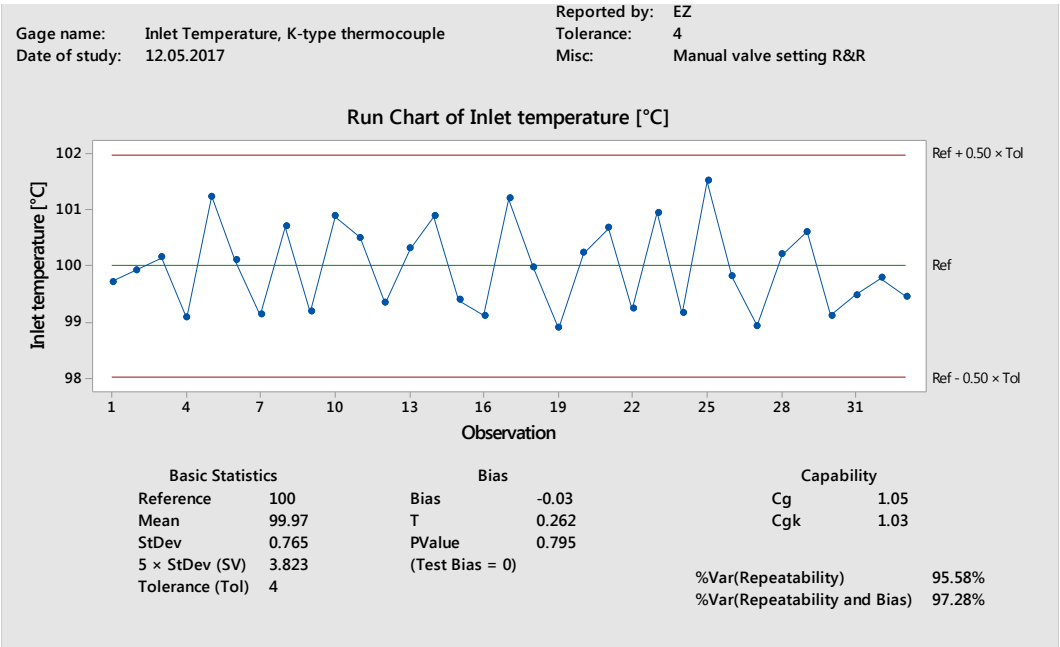

Figure A-3 Inlet temperature manual valve setting gauge R&R.

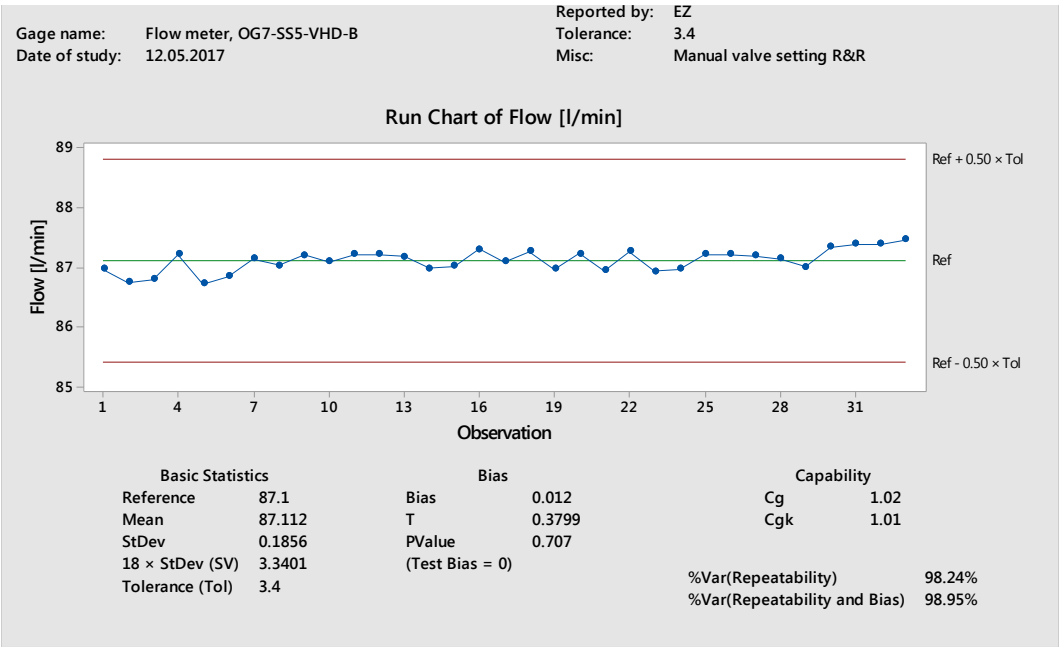

Figure A-4 Flow rate manual valve setting gauge R&R.

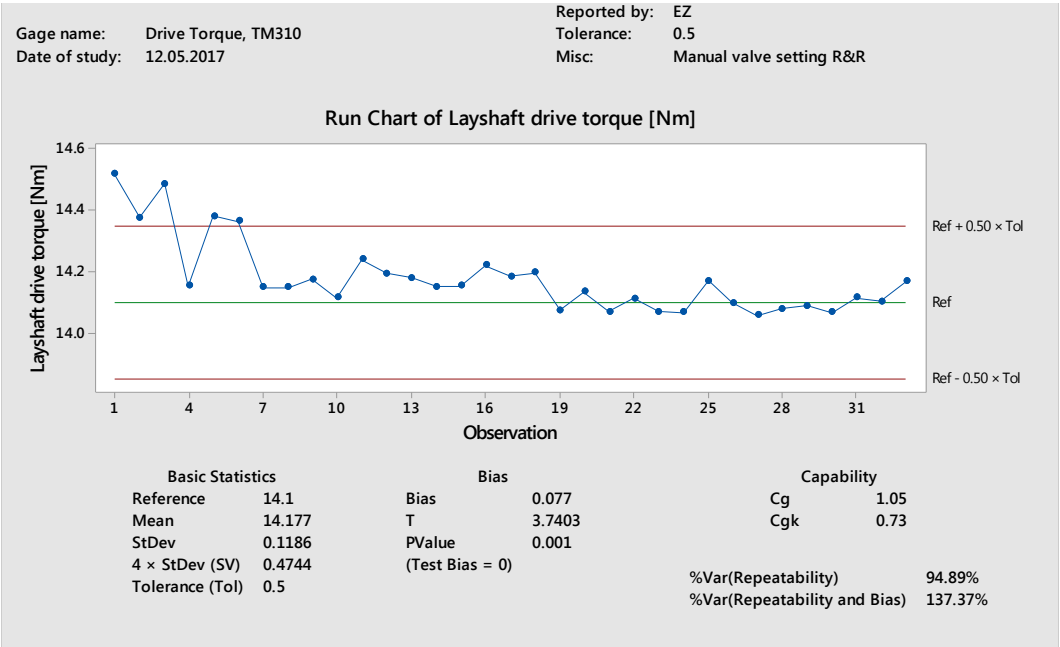

Figure A-5 Layshaft drive torque manual valve setting gauge R&R.

Although there is no tolerance requirement in ISO 10767-1:2015 (ISO, 2015), exploring the lay shaft drive torque measurements in Figure A-5 show a trend that appears related to the gauge R&R process. There is a settled period after 7 measurements and it is hypothesised that the reduction of torque as the number of measurements increases is related to the cooling of the driveline components during the stop-start operation. This is of no issue for the project

because during the test the first outlet valve will be locked in position and there will no need to stop and start the pump. To prove this, each pressure ripple measurement is accompanied by recording the performance measurements. The initial pump values before test are plotted as a gauge R&R study as shown in Figure A-6 to Figure A-10. Revisiting the drive torque in Figure A-10, the repeated measurement process shows no trend in the data as observed in the manual valve gauge R&R. Additionally, (compared to the initial feasibility study of manually setting the valve), the lower speed outputs lower flows and pressures, thus the tolerance band is narrowed. This is particularly important for the outlet pressure where 5 of the recordings are out of tolerance. However, the standard deviation of 0.011E5 Pa and the standard error of mean of ±0.002 (as shown in Table A-1) are within tolerance proving the measurement system acceptable.

Table A-1 Gauge R&R Summary.

Variable	Mean	SE Mean	StDev	Minimum	Maximum
Pump Speed [rpm]	746.8	0.067	0.401	746.0	747.0
Flow [l/min]	71.7	0.031	0.184	71.2	71.9
Outlet Pressure [x10^5 Pa]	0.74	0.002	0.011	0.71	0.77
Inlet Temperature [°C]	106.1	0.017	0.100	105.8	106.2
Layshaft Drive Torque [Nm]	3.26	0.005	0.029	3.16	3.32

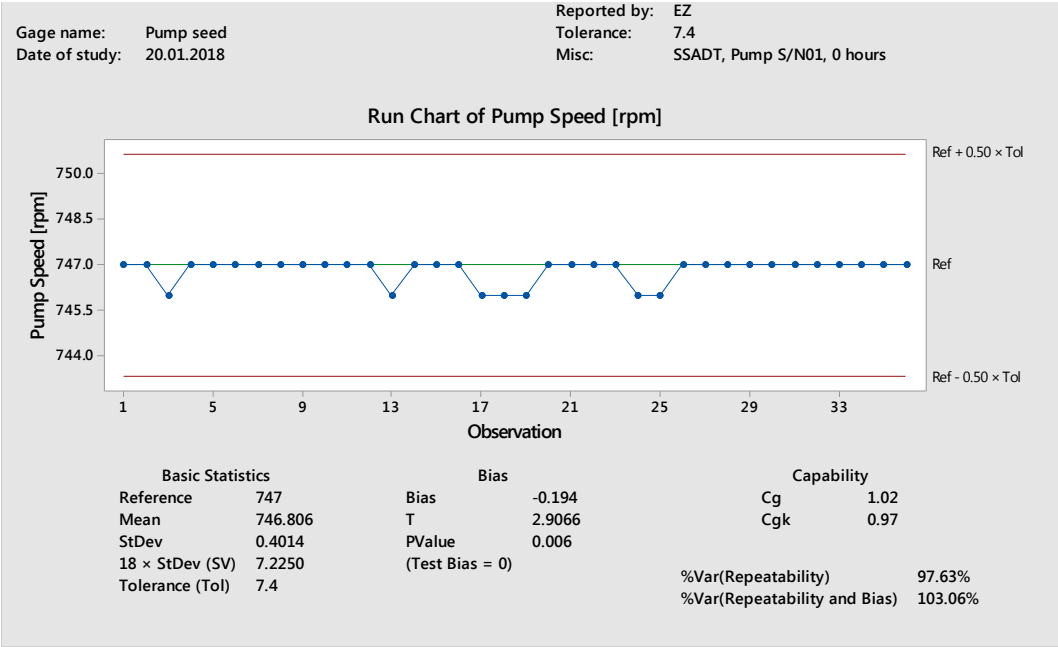

Figure A-6 Pump speed SSADT, Pump no.1, 0 hours gauge R&R.

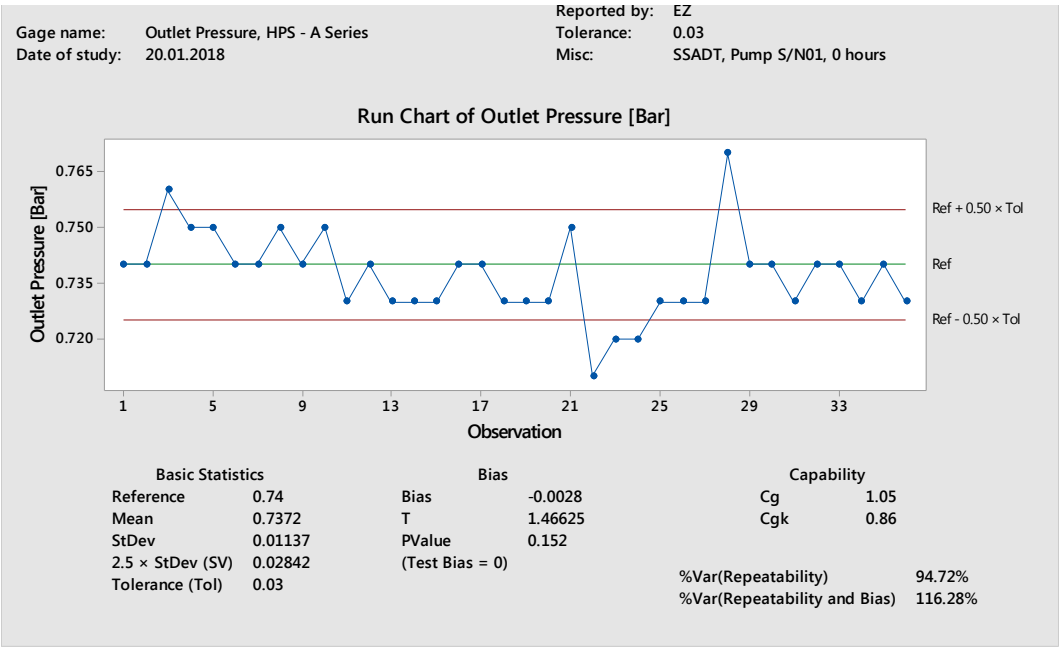

Figure A-7 Outlet pressure SSADT, Pump no.1, 0 hours gauge R&R.

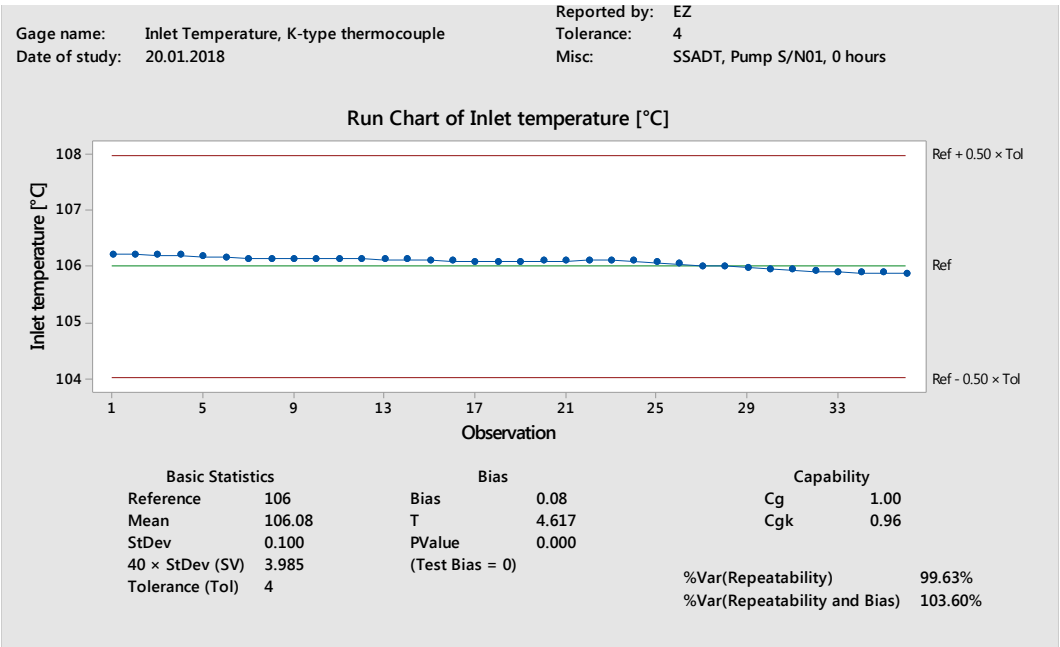

Figure A-8 Inlet temperature SSADT, Pump no.1, 0 hours gauge R&R.

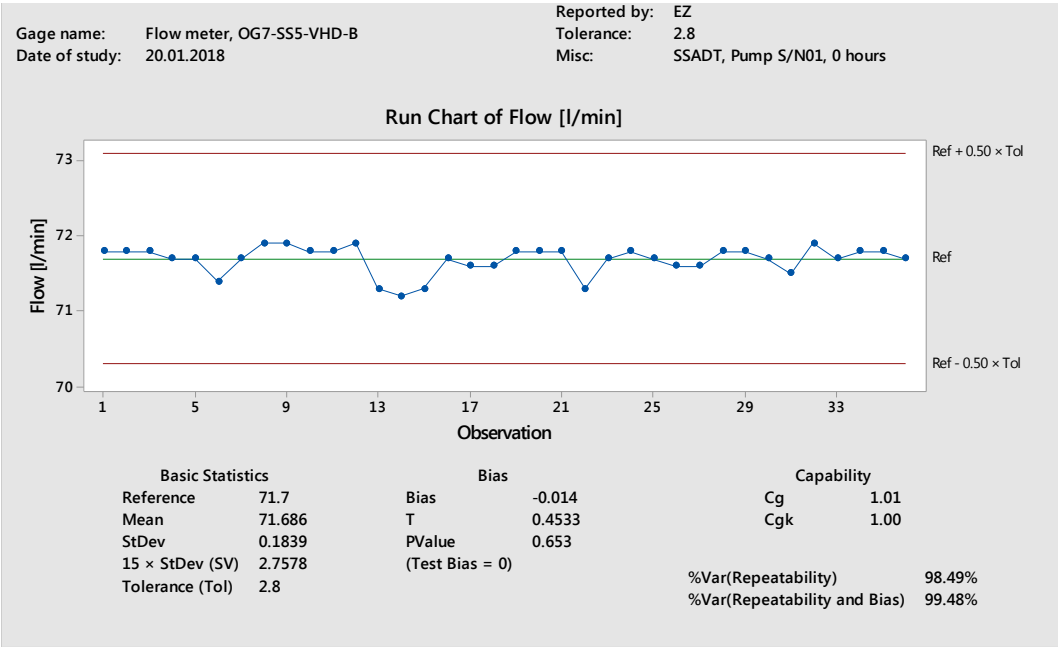

Figure A-9 Flow rate SSADT, Pump no.1, 0 hours gauge R&R.

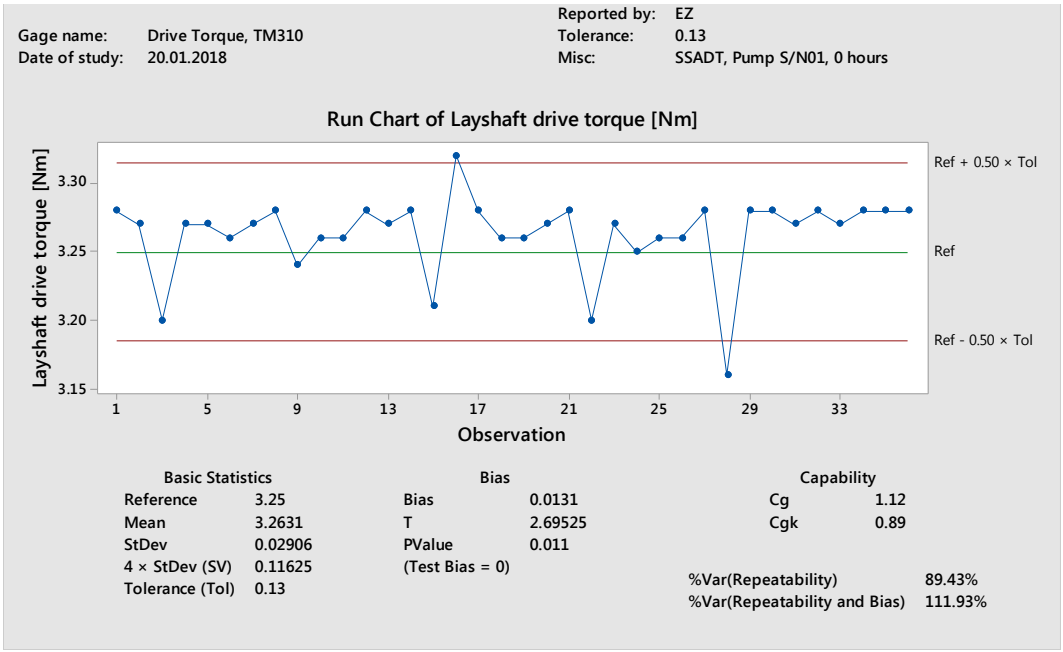

Figure A-10 Layshaft drive torque SSADT, Pump no.1, 0 hours gauge R&R.

Appendix B. Pseudo Failure Times (PFT)

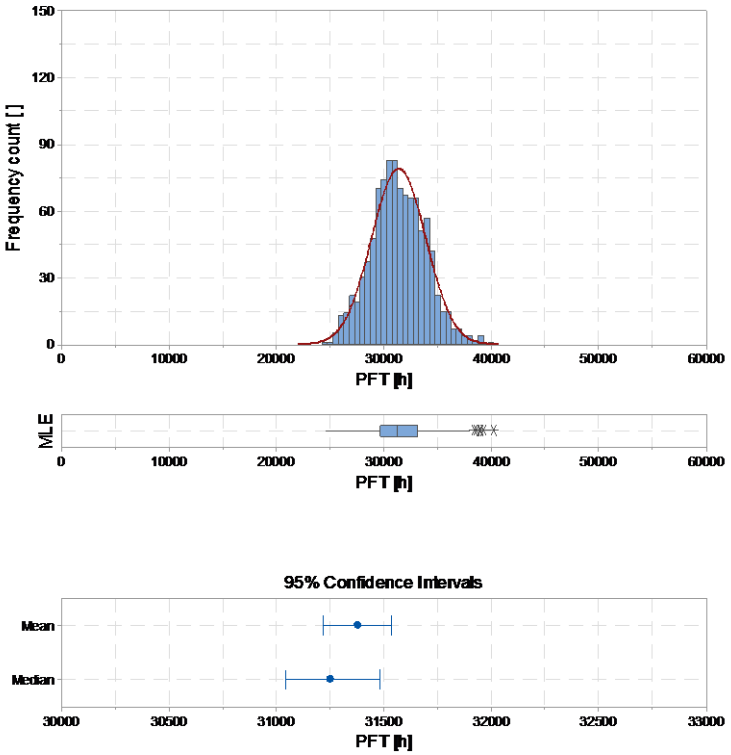

Anderson-Darling Normality Test	
A-Squared	0.53
P-Value	0.174
Mean	31376
StDev	2522
Variance	6361762
Skewness	0.156648
Kurtosis	0.039477
N	1000
Minimum	24576
1st Quartile	29662
Median	31248
3rd Quartile	33111
Maximum	40183
95% Confidence Interval for Mean	
31220	31533
95% Confidence Interval for Median	
31041	31484
95% Confidence Interval for StDev	
2416	2638

Figure B-1 Cycle 04, MLE, PFT, Summary statistics, n = 1000, Normal 95% CI.

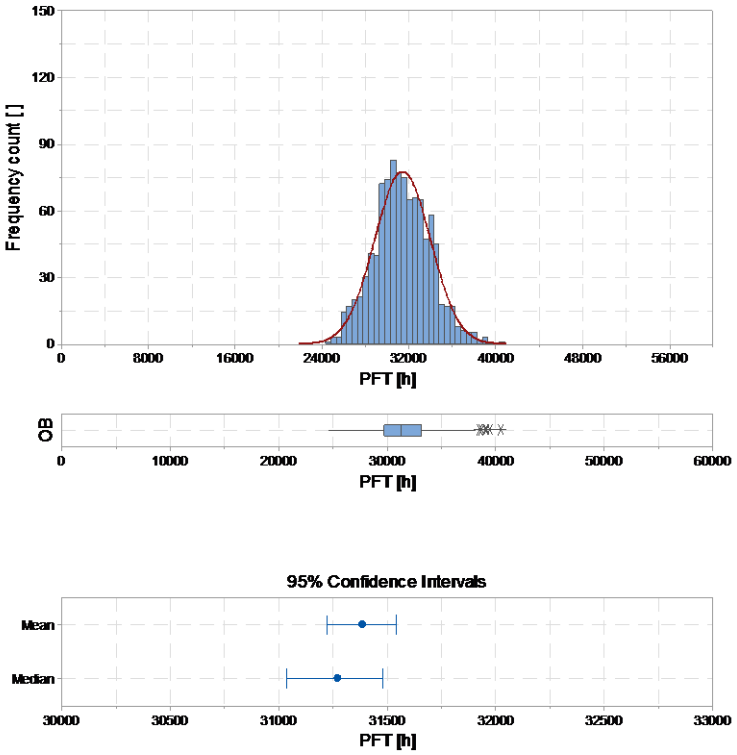

Anderson-Darling Normality Test	
A-Squared	0.53
P-Value	0.179
Mean	31380
StDev	2570
Variance	6603070
Skewness	0.161929
Kurtosis	0.030858
N	1000
Minimum	24566
1st Quartile	29645
Median	31268
3rd Quartile	33142
Maximum	40392
95% Confidence Interval for Mean	
31221	31540
95% Confidence Interval for Median	
31037	31479
95% Confidence Interval for StDev	
2462	2688

Figure B-2 Cycle 04, OB, PFT, Summary statistics, n = 1000, Normal 95% CI.

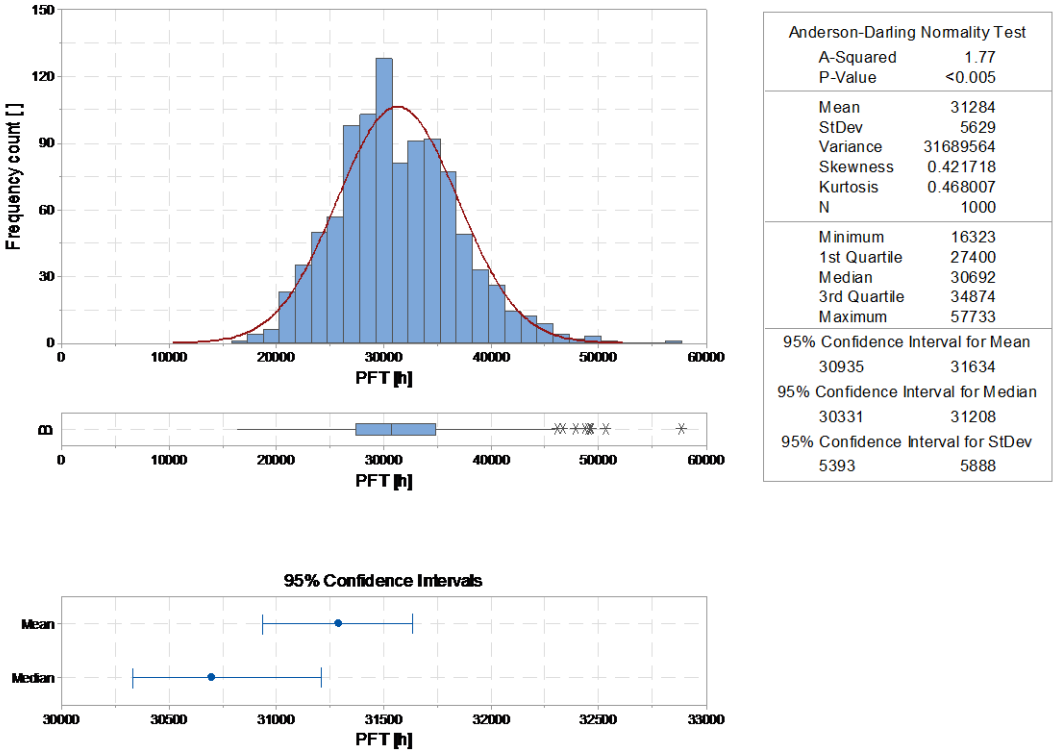

Figure B-3 Cycle 04, BU, PFT, Summary statistics, n = 1000, Normal 95% CI.

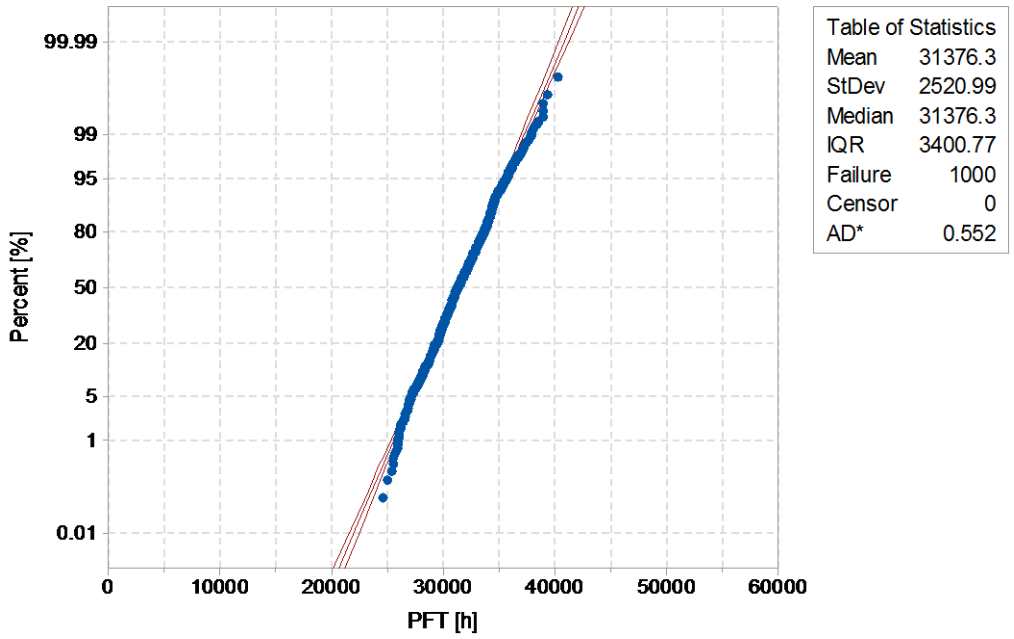

Figure B-4 Cycle 04, MLE, PFT, Normal probability plot, n = 1000, Normal 95% CI.

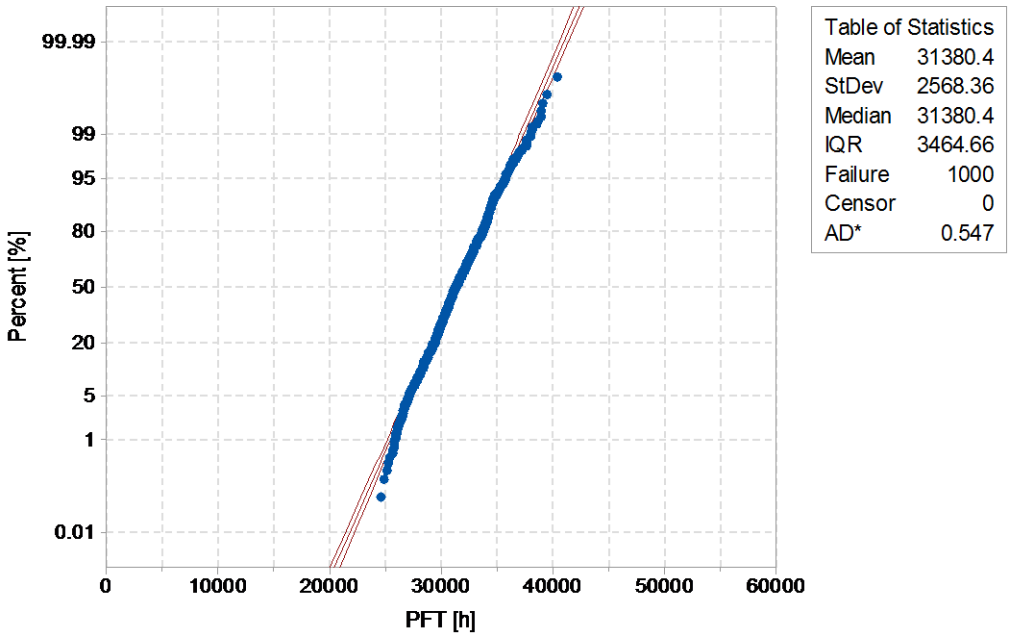

Figure B-5 Cycle 04, OB, PFT, Normal probability plot, n = 1000, Normal 95% CI.

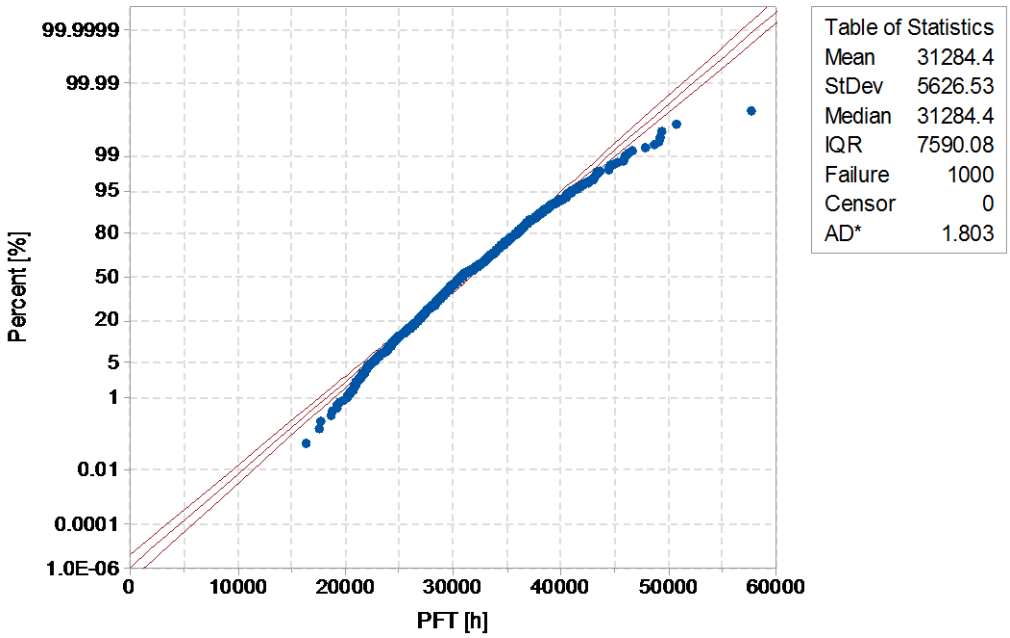

Figure B-6 Cycle 04, BU, PFT, Normal probability plot, n = 1000, Normal 95% CI.